Morphogenesis at the shoot Apical Meristem

Ursula Citlalli Abad Vivero

Numéro National de Thèse : 2017LYSEN088

THESE de DOCTORAT DE L'UNIVERSITE DE LYON
opérée par
l'Ecole Normale Supérieure de Lyon

Ecole Doctorale N° 340
Biologie Moléculaire, Intégrative et Cellulaire (BMIC)

Spécialité de doctorat : Biologie du Développement, Biologie des Plantes
Discipline : Sciences de la Vie

Soutenue publiquement le 08/12/2017, par :
Ursula Citlalli ABAD VIVERO

Morphogenesis at the Shoot Apical Meristem

La morphogenèse au sein du méristème apical caulinaire

Devant le jury composé de :

Mme. Angela HAY, Group Leader, MPI for Plant Breeding Research, Köln	Rapporteure
Mme. Naomi NAKAYAMA, Group Leader, University of Edinburgh, Edinburgh	Rapporteure
M. Olivier HAMANT, Directeur de recherche, Ecole Normale Supérieure de Lyon	Examinateur
M. François PARCY, Directeur de recherche, Université de Grenoble Alpes-CNRS	Examinateur
M. Jan TRAAS, Directeur de recherche, Ecole Normale Supérieure de Lyon	Directeur de thèse

Summary

The process of morphogenesis is driven by cell division and expansion, which are controlled in a differential manner among cell types and tissues. In plants, the above ground organs are continuously produced by the shoot apical meristem (SAM), where the initiation of new primordia is triggered by the local accumulation of the plant hormone auxin. We study the process of morphogenesis in the inflorescence of *Arabidopsis thaliana*, where flowers are formed in a regular pattern from the SAM.

The DNA-binding auxin response factor ARF5/MP plays a central role in the initiation of flowers. After its activation, it induces the expression of LEAFY, AINTEGUMENTA and AINTEGUMENTA-LIKE6 transcription factors necessary for the specification of floral identity and proliferative growth. However, at the cellular level, the initiation of lateral outgrowths depends on regional differences in growth. In plant cells, these processes are regulated via modifications of the cell wall. Auxin and its downstream targets are also involved in these processes, by activating changes in the dynamics of the cortical microtubules, which result in changes in growth direction. Auxin also slightly reduces wall rigidity prior to organ outgrowth in the SAM, which results in changes in growth rate. This is correlated with the transcriptional activation of a number of cell wall modifying genes.

Thus, auxin signaling regulates primordium initiation by integrating the activation of a transcriptional regulatory network and both the stiffness and anisotropy of the cell wall, which directly influence the rate and direction of growth.

The findings of this thesis provide evidence indicating that the mechanisms of organ initiation at the SAM involve feedbacks where changes in the local properties of the cell wall influence the molecular regulation of the transcriptional regulatory network. Our results suggest that this might require the influence from other hormones, different from auxin, that funnel the initiation of lateral outgrowths.

Résumé

Le phénomène de morphogenèse est le fruit de la division des cellules et de leur expansion, qui sont controllées de façon différentielle selon les types cellulaires et les tissus. Dans le cas des plantes, le méristème apical caulinaire (MAC) produit de façon continue les organes aériens à partir de primordia qui sont initiés suite à l'accumulation locale d'une hormone végétale, l'auxine. Pour étudier le processus de formation des organes aériens, nous utilisons l'inflorescence d'*Arabidopsis thaliana*, dont les fleurs sont mises en place selon un patron régulier à partir de cellules dérivées de cellules souches. Au cours de ce processus, ARF5/MP – un facteur de réponse à l'auxine se liant à l'ADN – joue un rôle central. Une fois activé, il induit l'expression des facteurs de transcription LEAFY, AINTEGUMENTA et AINTEGUMENTA-LIKE6, qui sont nécessaires pour la spécification de l'identité florale et pour la croissance prolifération.

A l'échelle cellulaire, des excroissances latérales sont initiées suite à des hétérogénéités locales de croissance. Dans les cellules végétales, ces différences sont dues à des modifications de la paroi cellulaire impliquant l'auxine et ses cibles, qui induisent des variations dans la dynamique des microtubules corticaux résultant en des changements de direction de croissance. Dans une moindre mesure, l'auxine diminue la rigidité des parois cellulaires préalablement à la formation d'un nouvel organe, conduisant à des changements de taux de croissance. Ceci est corrélé à l'activation transcriptionnelle de nombreux gènes qui sont impliqués dans les modifications de la paroi. Ainsi, la voie de signalisation de l'auxine régule l'initiation des primordia en intégrant d'une part l'activation d'un réseau de régulation transcriptionnelle et, d'autre part, la rigidité et l'anisotropie de la paroi cellulaire, impactant directement le taux et la direction de croissance.

Cette thèse soutient l'idée selon laquelle l'initiation des organes dans le MAC repose sur des boucles de rétroaction là où des changements locaux de propriétés de la paroi cellulaire influent sur le réseau moléculaire. Il est probable que d'autres hormones soient nécessaires afin de canaliser l'initiation des organes.

Acknowledgements

I would like to thank Naomi Nakayama, Angela Hay, François Parcy and Olivier Hamant for reviewing this thesis. Also thanks to my thesis committee, who guided me through my PhD, Patrick Laufs and Olivier Hamant. I am especially grateful to Jan Traas my thesis director, who gave me academic support as well as to Massimiliano Sassi, who assisted in supervising me and answering my questions.

To all the members of the Meristem and Mechanodevo teams, I extend my gratitude to those with whom I worked in the past and that are no longer in the lab and those who are still in the RDP. A special thanks to Amélie who gave me a lot of support in this last part of the thesis. Thanks to Léa who helped me a lot with the summary. To all my lab mates Laia, Mar, Roberta, Massi, Carlos, Jazmin, Ana, Chie, Kateryna, Antoine et tous les copains du foyer, who offered me their friendship and their support both academic and personal. I thank to all the members of the RDP, who through their work and motivation provide the best conditions to work in this laboratory.

I want to express my gratitude to my family, Pilli, Papo, Bin, Naye y familia (Emmanuel, Andres y choquinho(a)), quienes siempre me han apoyado en todos los aspectos de mi vida. Gracias por estar conmigo y ofrecerme su amor incondicional. Gracias tambien a mi familia extendida, Gise, Juan y Jimena, quienes tambien me ofrecen su carino y consejo. A mis amigos, que aun a la distancia siguen cercanos y me reciben siempre con una sonrisa.

Gracias a mi Uke, que es el que mas me aguanta y del que mas aprendo en muchos aspectos. Gracias port tu compania, tu apoyo y tu carino.

Finally, I want to thank anyone who I could have forgotten to mention, to all those who have somehow shared this project with me.

Table of Contents

List of Abbreviations

ABP1	AUXIN BINDING PROTEIN 1
AG	AGAMOUS
AGL	AGAMOUS-LIKE
AGO10	ARGONAUTE 10
AHK	ARABIDOPSIS HISTIDINE KINASE
AHP	ARABIDOPSIS HISTIDINE PHOSPHOTRANSFERASE
AIL6/PLT3	AINTEGUMENTA-LIKE6/PLETHORA3
ANT	AINTEGUMENTA
AP1	APETALA1
AP2/ERF	APETALA2/ETHYLENE RESPONSE FACTOR
ARF	AUXIN RESPONSE FACTOR
ARR	ARABIDOPSIS RESPONSE REGULATOR
AS1	ASYMMETRIC LEAVES 1
AT	ACETYLTRANSFERASE
AUX/IAA	AUXIN/INDOLE ACETIC ACID
BAS1	PHYB ACTIVATION TAGGED SUPRESSOR 1
BAK1	BRI1-ASSOCIATED RECEPTOR KINASE 1
BES1	BRI1-EMS-SUPRESSOR1
BIM1	BES1 INTERACTING MYC-LIKE1
BIN2	BRASSINOSTEROID INSENSITIVE 2
BKI1	BRI1 KINASE INHIBITOR
BOP1	BLADE ON PETIOLE
BRI1	BRASSINOSTEROID INSENSITIVE1
BRM	BRAHMA
BSK1	BRASSINOSTEROID-SIGNALING KINASE 1
BSU1	BRI1-SUPPRESSOR 1
BZR1	BRASSINAZOLE RESISTANT1
CAL	CAULIFLOWER
CESA	CELLULOSE SYNTHASE A
CDG1	CONSTITUTIVE DIFFERENTIAL GROWTH1
CKX	CYTOKININ DEHYDROGENASE/OXIDASE
CLV3	CLAVATA3
CMT	CORTICAL MICROTUBULES
CPD	CONSTITUTIVE PHOTOMORPHOGENIC AND DWARF
CRF2	CYTOKININ RESPONSE FACTOR 2
CSI1/POM2	CELLULOSE SYNTHASE INTERACTING
CSC	CESA COMPLEX
CSLC	CELLULOSE SYNTHASE-LIKE
CUC1	CUPSHAPED COTYLEDON 1
DREB2A	DRE-BINDING PROTEIN 2A
DWF4	DWARF4

ER	ERECTA
EXPA	A-TYPE EXPANSIN
FD	FLOWERING LOCUS D
FER	FERONIA
FIL	FILAMENTOUS FLOWER
FT	FLOWERING LOCUS T
GH	GLYCOSIDE HYDROLASES
GT	GLYCOSYLTRANSFERASES
GRF9	GROWTH-REGULATING FACTOR 9
HD-ZIP III	HOMEODOMAIN LEUCINE ZIPPER CLASS III
HEC1	HECATE 1
HG	HOMOGALACTURONANS
HTA13	HISTONE H2A 13
IAA	INDOLEACETIC ACID
IPT	ISOPENTENYLTRANSFERASE
IWS1	INTERACT WITH SPT6 1
JLO	JAGGED LATERAL ORGANS
KAN	KANADI
KNAT1	KN1-LIKE IN ARABIDOPSIS THALIANA 1
KTN1	KATANIN
LBD	LATERAL ORGAN BOUNDARIES DOMAIN
LFY	LEAFY
LOB	LATERAL ORGAN BOUNDARIES
LOG	LONELY GUY
LRR	LEUCINE-RICH REPEAT RECEPTOR KINASES
LSH4	LIGHT-DEPENDENT SHORT HYPOCOTYL 4
MBD	MICROTUBULE-BINDING DOMAIN
MAP4	MICROTUBULE-ASSOCIATED PROTEIN 4
MP	MONOPTEROS
MT	METHYLTRANSFERASES
NAC	NAM-ATAF1/2-CUC2
NPA	N-1-naphthylphthalamic acid
NUC	NUCLEAR CAGE
PDF1	PROTODERMAL FACTOR 1
PI	PISTILLATA
PID	PINOID
PIN1	PIN-FORMED1
PHB	PHABULOSA
PHV	PHAVOLUTA
PME	PECTIN METHYL ESTERASE
PMEI	PECTIN METHYL ESTERASE INHIBITOR
PUP	PURINE PERMEASE
REV	REVOLUTA
RG	RHAMNOGALACTURONAN

RIC1	ROP-INTERACTIVE CRIB MOTIF-CONTAINING PROTEIN 1
RLP44	RECEPTOR-LIKE PROTEIN 44
RLK	RECEPTOR-LIKE KINASE
ROP6	RHO-LIKE GTPASE FROM PLANTS 6
SEP	SEPALLATA
SOC1	SUPPRESSOR OF OVEREXPRESSION OF CO 1
SPK1	SPIKE
SPL10	SQUAMOSA PROMOTER BINDING PROTEIN-LIKE 10
STM	SHOOT MERISTEM LESS
SVP	SHORT VEGETATIVE PHASE
SWI/SNF	SWITCH/SUCROSE NONFERMENTING
SYD	SPLAYED
THE	THESEUS
TIR1/AFB	TRANSPORT INHIBITOR RESISTANT1/AUXIN SIGNALING F-BOX
TMK	TRANSMEMBRANE KINASE
TMO3	TARGET OF MONOPTEROS
TOC1	TIMING OF CAB EXPRESSION1
TPL	TOPLESS
VIP1	VIRE2-INTERACTING PROTEIN1
WAK	WALL-ASSOCIATED KINASES
WUS	WUSCHEL
XET	XYLOGLUCAN ENDOTRANSGLUCOSYLASES
XTH	XYLOGLUCAN ENDO-TRANSGLUCOSYLASE/HYDROLASE
XXT	XYLOGLUCAN XYLOSYL-TRANSFERASES
YAB	YABBY

Glossary of Terms

activator	a short-ranging substance that promotes its own production and the synthesis of its antagonist
anisotropy	the existence of directions with distinctive properties
anisotropic growth	growth with a maximal and minimal direction
canalization	a valley in Waddington's epigenetic landscape that represents a cluster of similar trajectories
complex system	a system made of many elements that exhibits emerging global properties not directly predictable from the properties of the individual components
crosstalk	specific interactions between components of more than one pathway
emergent property	a feature that is characteristic of system-level dynamics that cannot be attributed to any of its components
epigenetic landscape	visual depiction of a set of developmental choices that is faced by a cell in the embryo
elastic deformation	reversible extension of the cell wall
feedback regulation	control mechanism that uses the consequence of a process to regulate the rate at which the process occurs
feed-forward loop	a biochemical pattern in a transcription network , a three-gene pattern, composed of two input transcription factors, one of which regulates the other, both jointly regulating a target gene
hydrogel	network of polymer chains that are hydrophilic, they are highly flexible due to their significant water content
inhibitor	rapidly difussing antagonist of an activator, it slows down the production of the activator or catalyzes its decay
lateral inhibition	strategy for emphasizing differences between inputs, a chemical inhibitor diffusing faster through neighboring cells prevents the accumulation of the activator creating a zone of lateral inhibition
microtubule anisotropy	indicates a dominant microtubule orientation over a population of microtubules
morphogen	a diffusible signal that acts at a distance to regulate pattern formation in a dose- dependent manner

phyllotaxis	the pattern at which new leaf and flower primordia emerges
plastic deformation	irreversible extension of the cell wall
plastochron	interval between the initiation of two consecutive primordia
self-organization	evolution of a system into an organized form in the absence of external pressures
strain	deformation of an object induced by stress, corresponds to growth rate in living organisms
stiffness	the extent to which an object resists deformation
stress	force applied on a surface normalized by the surface area upon which it is exerted
stress anisotropy	stress with maximal and minimal directions
tensile strength	the resistance of a material to breaking under tension
yield threshold	level of stress that needs to be applied to a structure to induce an irreversible deformation
wall creep	cell wall extension that involves the breaking of hydrogen bonds between cell wall polymers

Introduction

1. Generalities of pattern formation and morphogenesis in multicellular organisms

One of the most fundamental questions in biology is that of biological pattern formation: how do the individual cells of a multicellular organism differentiate and how is this related to the overall structures and shapes that arise during development? In this first part of the introduction I will present the main theories that have addressed the problem of biological pattern formation and that have largely influenced modern developmental biology.

1.1. On Growth and Form

In 1917 D'Arcy Thompson published an extensive study on growth and form during development. He hereby underlined the fact that biological form is the consequence of physical processes and mechanical forces (Thompson, 1917). Thompson eloquently described form as a direct product of growth, and emphasized that growth and form are inseparably associated. According to his view the form of an organism is determined by its rate of growth in various directions. "Every growing organism; and every part of such a growing organism, has its own specific rate of growth, referred to this or that particular direction; and it is by the ratio between these rates in different directions that we must account for the external forms of all save certain very minute organisms".

On Growth and Form is Thompson's most famous work containing its most influential ideas. In the book, he offers a descriptive explanation of the shapes of various parts of multicellular organisms. These descriptions were more than anything else mathematical descriptions. Due to his preference for mathematical and biophysical concepts, but most likely also because ideas about molecular regulation were not known at that time, Thompson did not invoke biochemical explanations for his thesis. In this way, he excluded any explanation for the function of such shapes. Since then, the elaboration of biological knowledge has made it possible to address the question of pattern formation not only as a consequence of biophysical forces, but also in terms that consider biochemical signaling and downstream molecular regulation.

Regardless of the limitations (McClung, 1942), Thompson's ideas provided an important basis for shaping modern developmental biology, and have gained renewed interest. I will now present a number of concepts that have focused more on biochemical regulation.

1.2. Reaction-diffusion model

The assembly of basic physical laws served Alan Turing to propose a key explanation for the formation of biological patterns (Turing, 1952). Turing's hypothesis was that patterns in biological tissues can arise from simple chemical processes that can be described precisely and mathematically. He suggested "a system of chemical substances, which he termed morphogens, reacting together and diffusing through a tissue, is adequate to account for the main phenomena of morphogenesis".

The essential feature of the reaction-diffusion model proposed by Turing is that a small perturbation in the concentration of two substances, initially distributed homogeneously can become spatially distributed heterogeneously given the differences in their diffusion properties and cross-regulation. Over time, the theory of Turing of biological pattern formation was further developed by Gierer and Meinhardt, who introduced to the reaction-diffusion model, the role of autocatalysis in conjunction with lateral inhibition (Gierer and Meinhardt, 1972; Meinhardt and Gierer, 2000). They proposed that one of the two substances is a short-range "activator", a chemical that can make more of itself; the other one a long-range "inhibitor", slows the production of the "activator". Each of these substances acts on itself as well as the other. This dynamical interaction between the morphogens allows the mechanism to become self regulated and endows the ability to produce spontaneously a pattern when starting from a uniform field of cells. The system could be illustrated as follows (Figure 1a). (i) Molecular fluctuations of the morphogens, will cause some cells to accumulate slightly higher levels of activator. (ii) The activator self-regulation will increase its concentration enhancing also the production of the inhibitor. (iii) The activator positive feedback stabilises its own levels. (iv) However, since the inhibitor diffuses faster, it will increase its level in neighbouring cells, preventing the accumulation of the activator, creating a zone of "lateral inhibition" where no new peaks of activator can form (v) The whole system dynamically changes until a regular array of peaks and valleys is formed across the whole field of cells (Green and Sharpe, 2015).

In principle such a reaction-diffusion system can account for many patterning events. This could be the case, for example, for the patterning of digits during limb development in mouse embryos. This mechanism depends on the feedback loop between Wnt and Bmp signaling and the transcription factor Sox9 (Figure 1b)(Newman and Frisch, 1979; Raspopovic et al., 2014). Another example of a potential reaction-diffusion based mechanism is the left-right patterning of the early vertebrate embryo (Figure 1c). The distinction between the left and right side of the body is driven by the interaction between the protein Nodal, the activator, and Lefty 2, the repressor. Their interaction creates a broad gradient that allows cells to distinguish in which side of the embryo they are. Nodal-Lefty network forms spontaneously from an initial maternal bias through local auto-activation and long range inhibition (Green and Sharpe, 2015). In plant systems, probably the best example of a mechanism potentially based on reaction-difussion is phyllotaxis, which describes the pattern at which new leaf and flower primordia emerge (Meinhardt, 1994). Various patterns can be created depending on the range of activation and inhibition, either an alternating (distichous), 90° rotated (decussate) and even spiral (Meinhardt, 1996). Later on Kuhlmeier and collegues discovered that actively transported auxin is the instructive signal determining the induction and positioning of lateral organs. Although in this example, patterning is not through an inhibitor but through a redistribution of an activator by transport (see also below). Good evidence for an activator – inhibitor system also exists for the initiation of leaf hairs (Hulskamp, 2004).

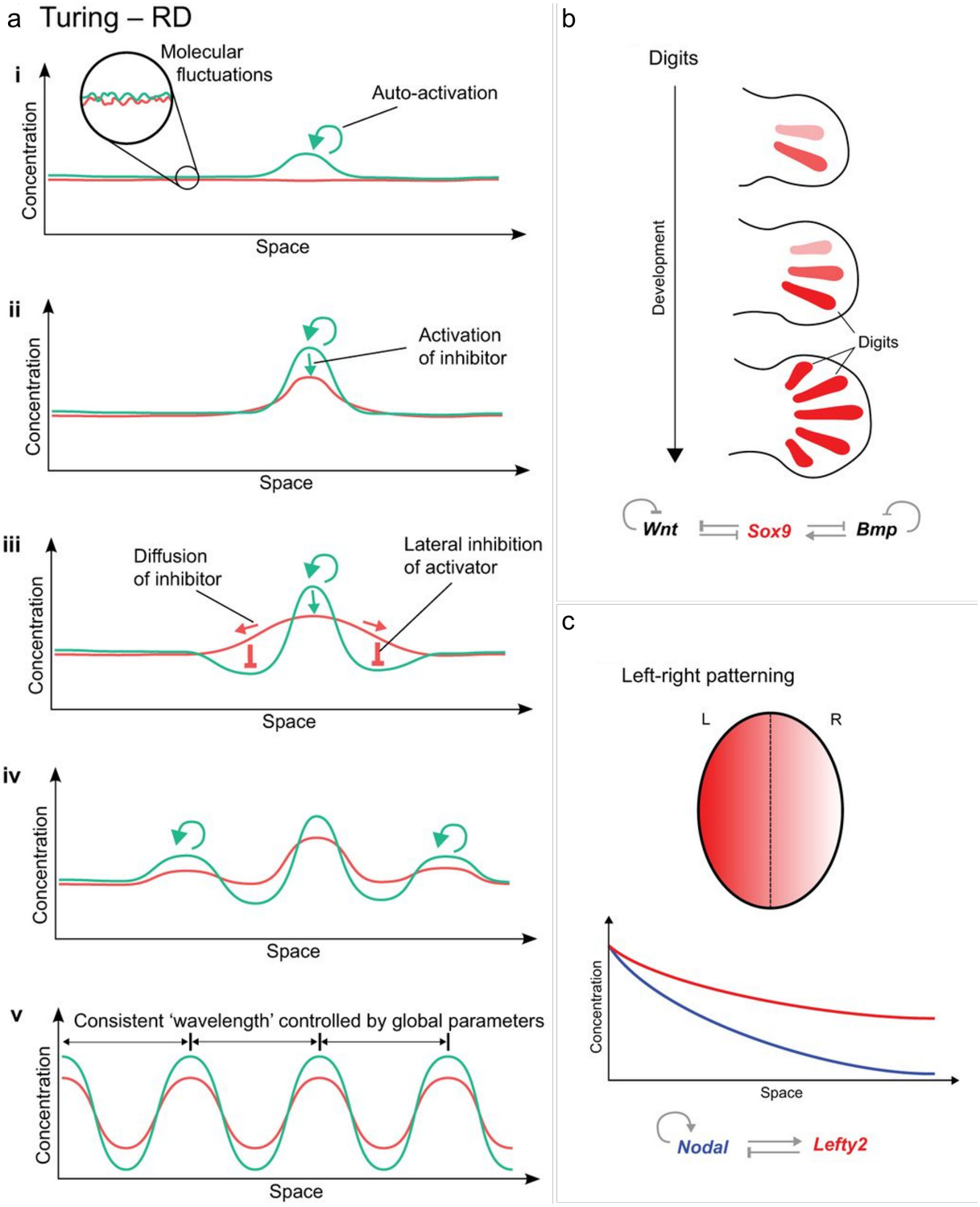

Figure 1. The principles of reaction-diffusion and examples of real patterning systems (adapted from Green and Sharpe, 2015).

(a) Morphogen fluctuation generates higher levels of activator, lower and more diffuse inhibitor levels. Although the inhibitor fails to repress the activator, it prevents the activator region from growing and imposes a zone of "lateral inhibition". The system dynamically changes until it reaches an equilibrium.

(b) Mouse limb buds are created as a Turing pattern guided by a feedback loop between the signalling of Wnt and Bmp and Sox9.

(c) Mouse embryo body sides, left (L) and right (R) are dictated by a RD system, which include Nodal and Lefty.

1.3. Positional-information model

Another notable contribution to the concept of pattern formation was the notion of morphogen concentration and gradients proposed by Wolpert. In his aim to understand how more complex patterns were constructed from earlier tissue heterogenities, he proposed that differences in morphogen concentration across space could be enough to define different positions. In the gradient model there is a fixed source of morphogens. The morphogens leave this site by diffusing within the tissue. Since they are also degraded, they will form a concentration gradient (Wolpert, 1969, 1971). Cells that are responsive to the morphogen interpret the local concentration, whereby different threshold concentrations would hereby give different reponses (Ashe and Briscoe, 2006; Kondo et al., 2009; Kondo and Miura, 2010).

The positional information concept explains how a prior asymmetry results in a graded distribution of a morphogen, and how cells use this distribution to acquire different identities. This concept is commonly illustrated with a French Flag pattern (Figure 2a), in which the field of cells are divided into three different regions of cell fates (red, white and blue). After the interpretation of the morphogen threshold levels (T1, T2), cells react differently to these concentrations and adopt diverse fates. It has been proposed that the development of the *Drosophila* embryonic segments is based on a positional information system (Figure 2b and c). Each stripe is defined independently by its unique anterior-posterior position in a succession of local concentration gradients of the gap genes. Differences in morphogen concentration at each position of the field provide distinct inputs to the gap gene network, which convert the smooth spatial differences into more discrete molecular patterns. This more complex molecular pattern of gap genes then provides the positional information for the next level of gene regulation, the segment polarity genes, which are each expressed as a series of stripes (Figure 2b and c) (Green and Sharpe, 2015).

Both, Turing's reaction-difussion and Wolpert's positional information models are able to explain biological patterns. The key feature that differentiates a reaction-difussion system from a positional information system is that the gradient is self-organized through the dynamics of the activator-inhibitor pair, unlike the positional information concept, which explains how a prior asymmetry is converted into a specific pattern. Therefore, the two

processes rather than mutually exclusive may be complementary and could function together as regionalizing mechanisms (Green and Sharpe, 2015).

A number of morphogens have been well described in animals (Wolpert, 2011). The first one discovered was the concentration gradient of Bicoid (Bcd) protein in *Drosophila*, which patterns embryo segmentation (Driever and Nusslein-Volhard, 1988; Frigerio et al., 1986). On the other hand, in plants the morphogen concept has remained a subject of debate. The signaling molecules closest to this concept are hormones. Particularly, auxin fulfils the characteristics of a morphogen, since it functions in diverse patterning events in a concentration-dependent manner and directly regulates target cells (Benkova et al., 2009; Bhalerao and Bennett, 2003; Sabatini et al., 1999).

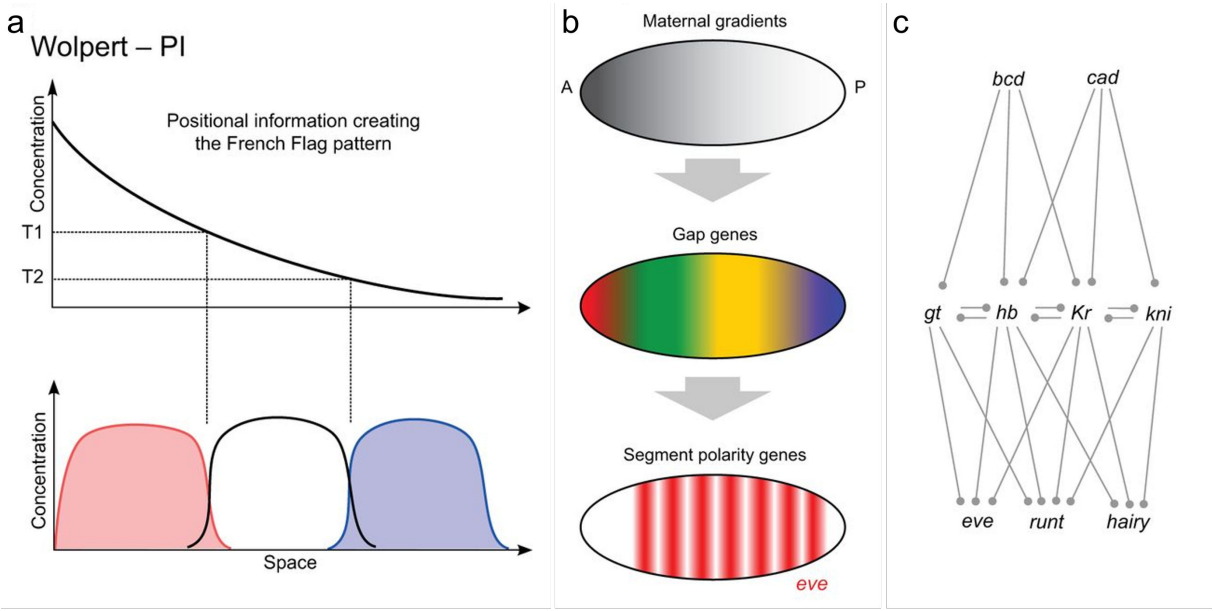

Figure 2. The principles of positional information and examples of real patterning systems (adapted from Green and Sharpe, 2015)
(a) The concept of positional information arises from molecular asymmetries that result in the graded distribution of a morphogen, cells make use of this information to acquire different cell fates, represented in the scheme by the three different colours.
(b) Initial asymmetries in the anterior-posterior axis of the early *Drosophila* embryo result in the graded distribution of morphogens that in turn regulate the expression of the gap genes providing the positional information for the segment polarity genes, expressed as a series of stripes.
(c) Differences in the concentration of the morphogens Bicoid and Caudal across the embryo inputs the gap genes network (*giant*, *hunchback*, *Krüppel*, and *knirps*). In turn, the complex interactions among gap genes create molecular patterns of expression of the segment polarity genes (*even-skipped*, *runt*, *hairy*).

1.4. Epigenetic landscape

A third theory worth to mention, is the epigenetic landscape concept proposed by Conrad Waddington. At the time he started to develop his ideas, the Mendelian laws of heredity were well accepted. Waddington agreed with the distinction between the individual's physical appearance, or the phenotype and the hereditary information contained in the germ cells and passed to the next generation, better known as the genotype. He considered the phenotype as the result of the interrelations among genetic processes, their potentialities and constraints, and the external environment.

Waddington studied the development of embryonic cells triggered by given stimuli, through a process he called induction. He proposed a hypothesis in which he emphasized the importance of the reacting tissue, in the sense that change occurs not only because cells receive a particular signal, but also because they have the 'potency' to react. In other words, cells react to different stimuli, biochemical or environmental, in a way allowed by their state at that time. With each new reaction, the cell might differentiate further into a state with more constraints or more possibilities and potentialities.

He argued that the various developmental pathways a cell might take follow an epigenetic path. Each step is defined by instructions in the genotype that interact to produce a system that moves along a trajectory. The diverse paths in development are protected or canalized by threshold reactions, providing stability and direction. Waddington illustrated this canalization concept, as a landscape, an epigenetic landscape formed by a series of ridges and valleys a cell can traverse on its way to a final tissue type (Waddington, 1956, 1957) (Figure 3a). The landscape thus represents the tendency of cells to pass from an immature stage to an adult and specified condition. The path of a cell would start from a totipotent state, passing via a pluripotent state to a lineage -committed state that leads it into one of many possible fates.

The steepness of the walls, represents the stability of the path. If the walls are very high, it is hard for the cells to escape from their developmental faith and even big mutational or environmental perturbations will not be able to bring the cell out of its path. The control of the steepness of the walls in turn depends on the underlying genetic landscape (Figure 3b). Importantly, not only genes and their products, but also gene-gene interactions and gene – environment interactions are in control of development. According to Waddington's ideas,

genes not only regulate, but they are also regulated by non-genetic factors (Van Speybroeck, 2002).

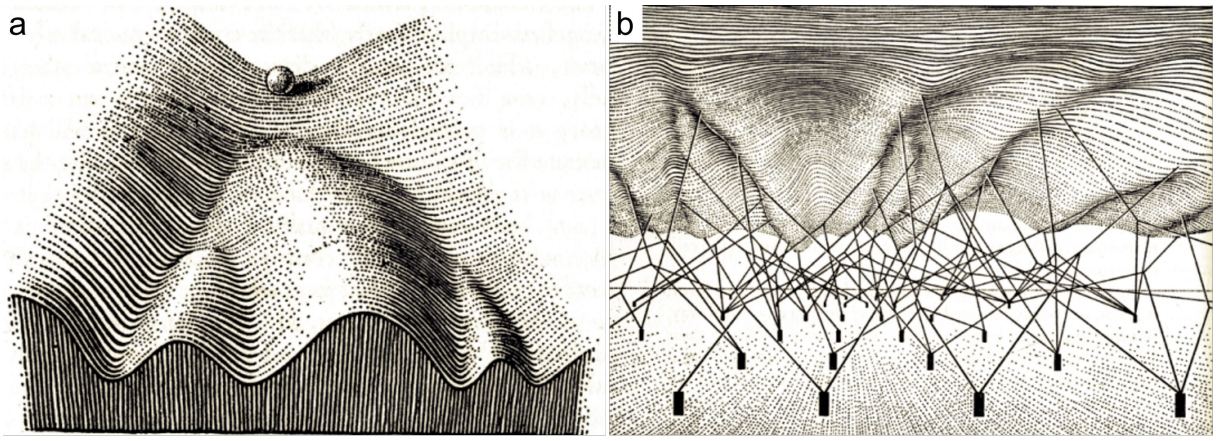

Figure 3. Waddington's epigenetic landscape (adapted from Waddington 1957).
(a) The classical view of an epigenetic landscape, in which the differentiation of cell in an embryo is illustrated as a pebble that begins at the top of a hill and rolls down the epigenetic landscape though a series of branching points that represent decision events. Cells evolve according to the same laws, but because of the existence of inducing signals, cells in different regions would follow different pathways and end up at different states of differentiation represented as valleys. The effect of these signals is restricted to reacting tissue and ultimately trigger the cells select one of a few possible developmental pathways.
(b) The genetic landscape underlying the architecture of the epigenetic landscape. The valleys are formed by tension on ropes attached to gene complexes represented as cylindrical pins stuck in the ground.

1.5. General concepts: some concluding remarks

According to these theories there are multiple factors directing pattern formation. The physical properties and form diversity in D'Arcy Thompson's theory, the self-organization and biochemical patterning in Turing patterns and the importance of the interaction of these factors at multiple scales. However, in order to understand pattern formation it is necessary to analyze how are these elements acting in concert. These interactions lead to the emergence of collective properties that cannot be deduced from adding up local behaviour. These are properties common to all multicellular organisms comprised under the concept of complex systems.

Plants as complex systems are hierarchically organized and composed by interactive elements: molecules assemble into cells, cells into tissues and organs. The interactions between the individual components and the multiple feedbacks between the diverse levels of organization are fundamental for pattern formation. Therefore, these systems can only be understood by analysing them at multiple scales, leading to the use of more interdisciplinary approaches. In addition, certain constraints imposed by the developing system might limit the possible final shapes. In plant development some specific emergent properties should be considered when studying pattern formation and morphogenesis. Of them I will speak in the following section.

2. Generalities of pattern formation and morphogenesis in plants

The generation of form in plants is distinguished by a number of specific features (Hernandez-Hernandez et al., 2012; Niklas, 2000; Niklas and Kutschera, 2009). First, plant architecture is characterized by an open and indeterminate ontogeny, with multiple growing points (or meristems) where cell proliferation persist continuously producing new tissues and organs (Esau, 1965). This characteristic relates to the sessile nature of plants. It provides them the opportunity to adjust to their external environment, adapting their shape and architecture in relation to it.

A notable characteristic of plant cells that highly influences development is the presence of a relatively rigid extracellular matrix, the cell wall. The presence of this cell wall provides plants with specific mechanical properties. As a result, morphogenesis must occur in the absence of cell migration. Therefore, cell expansion, cell division and, to a lesser extent, programmed cell death, are of major importance in plant morphogenesis (De Smet and Beeckman, 2011; Van Hautegem et al., 2015). Given that plant cells are immobilized they rely on mobile signals to trigger the local differences that guide tissue morphogenesis. A major category of these mobile signals is plant hormones, which largely control plant growth and development and represent excellent candidates for plant morphogens.

In what follows I will review the basic characteristics of plant development that define pattern formation in plants. I will firstly focus on the role of signaling molecules, hormones and their effect on establishing molecular expression patterns. Secondly, I will describe the role of the extracellular matrix in controlling growth patterns. A good amount of our knowledge in these topics has been obtained from the plant experimental system *Arabidopsis thaliana* (hereafter called *Arabidopsis*); therefore I will mainly focus on this species.

2.1. Molecular regulation: the role of hormones in plant development

As mentioned previously, positional information is perceived and transmitted via communication between different parts of the organism, locally and over long distances. This communication is based on the perception and production of mobile signals. In plants, the distribution and perception of hormones as instructive mobile signals of growth and development has been well established, involving in particular cytokinins, auxins,

gibberellins, brassinosteroids and strigolactones (Santner et al., 2009; Santner and Estelle, 2009; Wolters and Jurgens, 2009).

Major aspects of plant hormone synthesis, degradation, transport and signaling have been extensively studied. In what follows I will briefly summarize the role of hormones in controling gene regulation, in particular at the transcriptional level, where they play a central role (Nemhauser et al., 2006). I will hereby focus on auxins, cytokinins and brassinosteroids, which have major roles in development of the meristems and plant architecture and are a central focus of this thesis.

2.1.1. Auxin

Auxin is certainly one of the most important signals, affecting plant developmental processes at cellular, tissue and organ levels. It has been considered as the closest equivalent to morphogens in plants (Bhalerao and Bennett, 2003; Sabatini et al., 1999). During development, auxin differentially accumulates in different parts of the plant. Auxin gradients are fundamental in the regulation of many developmental processes. From the very early stages of development onwards, auxin accumulation and its graded distribution play fundamental roles in defining plant shape. Already after fertilization, the apical cell of the divided zygote is the site of auxin accumulation and activity. This is maintained this way until the 32-cell-embryo stage. Later on auxin distribution changes to establish the root pole and cotyledons (Friml et al., 2003). Another example of the importance of differential auxin distribution is the accumulation of auxin at the location of organ initiation, either at the root (Figure 4b)(Dubrovsky et al., 2008) or at the shoot (Figure 4c)(Heisler et al., 2005; Meinhardt, 2003). There are numerous examples about the role that auxin distributions and gradients play in the regulation of plant growth and development. But how does these specific distributions arise?

One mechanism for the differential distribution of auxin is attributed to its site of biosynthesis. The most common auxin in vascular plants is indole-3-acetic acid (IAA). IAA is synthesized by one tryptophan (Trp)-independent and four Trp-dependent pathways. Two of them, the tryptamine (TAM) pathway, and the indole-3-piruvic acid (IPA) pathway are most relevant for plant development. Rate-limiting enzymes for these pathways include the flavin monooxygenase-like enzymes of the YUCCA family and the Trp aminotransferase of

Arabidopsis (TAA) (Teale et al., 2006; Woodward and Bartel, 2005) (Figure 5a). Mutations of multiple *YUCCA* and *TAA* genes impair local auxin accumulation and result in severe developmental defects, in embryogenesis, leaf venation, and floral organ patterning, among others (Cheng et al., 2006, 2007; Stepanova et al., 2008).

Another major process controling auxin distribution is auxin transport. It has been well established that auxin moves directionally through plant tissues. From the sites of its synthesis it is transported to the whole plant (reviewed in (Peer et al., 2011). A long distance source-to-sink transport occurs by the loading of auxin into the phloem, from young biosynthetically active shoot tissues towards sink tissues (Figure 4a). Cell-to cell transport can also achieve auxin movement over both short and long distances. Cell-to-cell transport was predicted by the chemiosmotic model, based in the physicochemical properties of the auxin molecules (Goldsmith, 1977; Raven, 1975; Rubery and Sheldrake, 1974). Auxins are weak acids, and their ability to penetrate through the membrane, depends on the pH. The plant's apoplastic pH is approximately 5.5. Under this conditions it is predicted that only a small but signficant fraction (17%) of auxin molecules are proton-associated (HA). Although protonated auxin freely diffuses from the apoplast into the cytoplasm, 83% of the auxin pool remains unavailable for diffusion in its dissociated form. Once in the cytoplasm where pH is approximately 7, the equlibrium of the auxin shifts to the anionic, dissociated form. In this circumstances auxins cannot diffuse across the cell membrane, hence the active transport of auxin is required. Indeed, three main families of transmembrane proteins provide means of active auxin transport in and out of the cell, across the plasma membrane: i) the AUX1/LIKE AUX1 (AUX1/LAX) auxin influx permeases, ii) the P-glycoproteins of the ATP-Binding Cassette family B (ABCB/PGP) efflux transporters, and iii) the PIN-FORMED (PIN) auxin efflux carriers reviewed in (Zazimalova et al., 2010) (Figure 5b). Among them, mainly PIN-mediated transport seems to contribute to polar auxin transport (PAT), which is essential for defining differential auxin distribution (Weijers et al., 2005).

PINs are plant specific proteins with a predicted secondary structure of five transmembrane helices at the N and C terminus (Galweiler et al., 1998; Krecek et al., 2009; Paponov et al., 2005) linked by an intracellular hydrophilic loop that influences protein localization and activity (Bennett et al., 2014; Dhonukshe et al., 2010; Huang et al., 2010). *Arabidopsis* PIN family consists of eight members, PIN1-8. PIN1, 2, 3, 4 and 7 localize preferentially in the

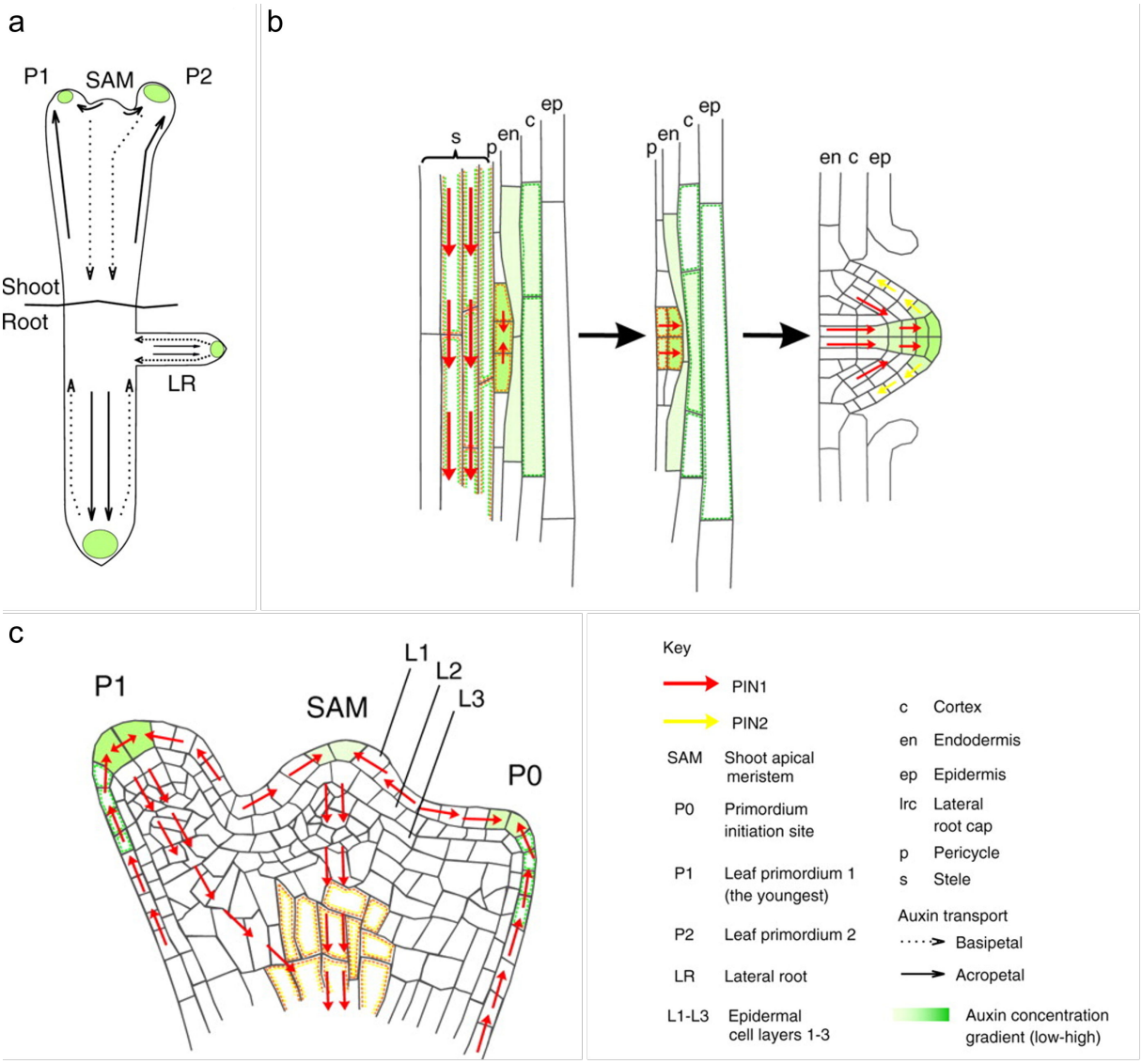

Figure 4. Auxin graded distribution in root and shoot morphogenesis (Petrasek and Friml, 2009).
(a) Directional flow of auxin in the shoot and root of *Arabidopsis*. The accumulation of auxin at the location of organ initiation (green) is maintained by flow towards root and shoot apices (solid arrows). Reverse flow towards root and shoot basis (dashed arrows).
(b) Auxin transport in the developing lateral root. Auxin maxima specify the founder cells in the pericycle, subsequent coordinated divisions form the lateral root primordium. PIN1 and PIN2 facilitate the transport of auxin that enables the development of the primordia.
(c) Auxin transport in the shoot apical meristem in developing primordia (P1 and P2). Auxin is transported through the epidermis layer L1 by the activity of PIN1, maintaining an auxin maxima at the organ primordium tip. From there, a basipetal transport route is established through the interior of the primordium, marking the future vasculature tissues.

plasma membrane (Adamowski and Friml, 2015; Petrasek et al., 2006; Wisniewska et al., 2006); PIN5 and 8 localization has been reported at the endoplasmic reticulum (Dal Bosco et al., 2012; Ding et al., 2012; Mravec et al., 2009); whereas there are still doubts regarding the localization and function of PIN6 (Nisar et al., 2014). Plasma membrane localized PINs often display polar cellular localization, which notably correlates with the directional flow of auxin and therefore have also been used to deduce such fluxes (Benkova et al., 2003; de Reuille et al., 2006; Friml et al., 2002a; Galweiler et al., 1998; Wisniewska et al., 2006). The auxin transport ability of PINs has been shown in *Arabidopsis* and heterologous systems (Petrasek et al., 2006; Yang and Murphy, 2009; Zourelidou et al., 2014). The positioning of PINs is highly dynamic. It is crucial to the production of organs during development (Blilou et al., 2005; Friml et al., 2003; Heisler et al., 2005; Reinhardt et al., 2003) and to the modulation of patterns of growth and development in response to the environment, for example in gravitropism (Friml et al., 2002b). After their transcription, PINs are either retained in the endoplasmic reticulum (ER) or translocated through the Golgi Apparatus (GA) to the plasma membrane (Matheson et al., 2006). PINs undergo continuous shuttling between the plasma membrane and the intracellular compartments by rounds of internalization (endocytosis) and polar recycling (exocytosis). These processes together are known as consitutive endocytic cycling (Dhonukshe et al., 2010; Dhonukshe et al., 2008; Geldner et al., 2001; Kleine-Vehn et al., 2011). According to current models, the regulation of PIN trafficking is based on their phosphorylation status, determined by the action of the PINOID (PID) and other AGC3 kinases and the antagonistic action of PP2A/PP6 phosphatases (Figure 5b) (Benjamins et al., 2001; Michniewicz et al., 2007). Unphosphorylated PINs are recycled to the plasma membrane by the ADP-ribosylation factor-guanine nucleotide exchange factor (ARF-GEF) GNOM. Phosphorylated PINs result in GNOM-independent recycling to the opposite plasma membrane (Dhonukshe et al., 2007; Geldner et al., 2001; Kleine-Vehn et al., 2008). Monoubiquitination of PINs induces their endocytosis, which occurs via clathrin-coated vesicles and requires the actin cytoskeleton. Subsequently, polyubiquitination labels PIN proteins for degradation (Leitner et al., 2012). The post-translational modifications of PINs, ubiquitination and phosphorylation, provide an entry point for various external signals, for example gravity (Abas et al., 2006; Friml et al., 2002b) or light (Ding et al., 2011; Michniewicz et al., 2007; Willige et al., 2013). Thereby the abundance of PINs in the plasma membrane or their polarity can be modified in reponse to external signals. Several hormones (auxin included) may influence directly or indirectly the transcription of *PIN*s (Bishopp et al., 2011a; Dello Ioio et al., 2008; Hacham et al., 2012; Liu et al., 2013; Zhang et al., 2011) or

influence their abundance (Crawford et al., 2010; Hacham et al., 2012; Willige et al., 2011). Experimental evidence partially combined with modelling approaches suggests that auxin itself provides feedback regulation on its own distribution influencing transcription, turnover, and plasma membrane localization of PIN proteins (Heisler et al., 2005; Stoma et al., 2008).

Besides production and transport, auxin perception and downstream signaling have also been extensively studied in a range of developmental processes. Auxin is first perceived via one or more receptors that initiate a signaling cascade that translates the auxin concentration into diverse cellular behaviors. Mainly two auxin receptor systems have been described, involving respectively the TRANSPORT INHIBITOR RESISTANT1/AUXIN SIGNALING F-BOX (TIR1/AFB) complexes (Dharmasiri et al., 2005a; Dharmasiri et al., 2005b; Kepinski and Leyser, 2005) and AUXIN BINDING PROTEIN 1 (ABP1) (Woo et al., 2002) (Figure 5c). From these, the best characterized is the TIR1/AFB pathway that regulates auxin responses within the nucleus (Calderon Villalobos et al., 2012; Chapman and Estelle, 2009; Dharmasiri et al., 2005a; Kepinski and Leyser, 2005; Parry et al., 2009) (Figure 6a). At low auxin concentrations the transcriptional repressors AUXIN/INDOLE ACETIC ACID (Aux/IAAs) negatively regulate auxin signalling. Aux/IAAs carry out their repressor activity by binding to the DNA-binding AUXIN RESPONSE FACTOR (ARF) proteins (Guilfoyle and Hagen, 2007; Kim et al., 1997), and recruiting the transcriptional co-repressors of the TOPLESS (TPL) family to ARF-bound promoters (Ke et al., 2015; Szemenyei et al., 2008). This prevents the ARF mediated transcription of auxin responsive-genes (Figure 6a). At high auxin concentrations, auxin interacts with TIR1 or other AFBs (Dharmasiri et al., 2005a). The binding of auxin occurs within an internal pocket formed from the binding between the F-box protein and the Aux/IAA, forming a complex TIR1/AFB-auxin-Aux/IAA that targets Aux/IAA for ubiquitination and degradation via the 26S proteasome (Figure 6a) (Calderon Villalobos et al., 2012). Once Aux/IAA are degraded, ARF proteins can either activate or repress auxin responsive genes (Chandler, 2016). More than 50 genes encoding *ARF* and *Aux/IAA* have been identified in the *Arabidopis* genome (Vernoux et al., 2011). Differential expression of each of these players provides combinatorial possibilities for auxin-dependent gene regulation (Chapman and Estelle, 2009). Large-scale analyses of the AUX/IAA-ARF network have been performed in order to try to understand the distribution and perception of auxin signaling; for instance, in the shoot apex of *Arabidopsis* (Vernoux et al., 2011). Through a combination of expression data, a set of molecular interactions, mathematical

modelling and auxin signaling sensors, Vernoux et al., (2011) have described a key role for local auxin signaling in the regulation of the shoot apex patterning.

Notably auxin functional specificity can be generated at different levels. For instance, at the level of protein-DNA interactions, by the presence of cis regulatory elements in auxin-responsive genes. At the level of chromatin-level it has been shown that ARF5/MP transcriptional regulation requires chromatin state changes target loci. Aux/IAA repressors of auxin signalling together with co-repressors of the TPLs family and the repressive chromatin regulator histone deacetylase HDA19, prevent the expression of ARF5/MP regulated genes (Long et al., 2006; Szemenyei et al., 2008). Local accumulation of auxin, drives Aux/IAA degradation, as well as the dissociation of TPL and HDA19. This in turns leaves ARF5/MP free to recruit the SWITCH/SUCROSE NONFERMENTING (SWI/SNF) chromatin-remodeling complexes, SPLAYED (SYD) or BRAHMA (BRM). SWI/SNF complex unlock the repressed chromatin state at ARF5/MP target loci, which also increases chromatin accessibility for additional transcription factors. In contrast, in the absence of auxin, Aux/IAAs promote chromatin closure by recruiting TPL transcriptional co-repressors to ARF-bound promoters (Wu et al., 2015).

ABP1 was the first auxin-binding protein described in the literature. Its binding capacity was demonstrated by physiological and structural studies (Hesse et al., 1989; Woo et al., 2002). ABP1 localizes mainly to the ER, but a small portion is likely secreted to the cell wall where it is assumed to be active (Sauer and Kleine-Vehn, 2011). Described physiological responses linked to ABP1 are initiated on the outside of the plasma membrane, this requires that the signal is passed into the cell. This role is supposedly accomplished by plasma membrane-localized proteins TRANSMEMBRANE KINASE (TMK) or SPIKE (SPK1) (Lin et al., 2012; Xu et al., 2014), which were reported to transfer auxin signal inside the cell via the RHO OF PLANTS (ROP)-GTPases and the ROP INTERACTIVE CRIB motif-containing (RIC) proteins. ROP-RIC systems regulate endocytosis/exocytosis of PIN proteins on the plasma membrane, thus controlling auxin fluxes. In leaf pavement cells, for example, two ROP-RIC downstream pathways have been described (Fu et al., 2005; Xu et al., 2010). The ROP2-RIC4 pathway acts in the lobe outgrowth through the stabilization of cortical actin microfilaments and further inhibition of PIN1 endocytosis (Nagawa et al., 2012; Xu et al., 2010). The ROP6-RIC1 pathway inhibits the indentation outgrowth by the activation of the microtubule severing protein KATANIN (KTN1), which promotes the bundling of cortical microtubules in

the necks, and further inhibits PIN1 and PIN2 endocytosis (Chen et al., 2012b; Fu et al., 2009; Lin et al., 2013). In the root, ABP1 was reported to control cell cycle entry by regulating the D-type CYCLIN/RETINOBLASTOMA pathway and the PLETHORA (PLT) gradients (Tromas et al., 2009). Although a number of non-transcriptional responses mediated by ABP1 have been reported (Chen et al., 2012a; Chen et al., 2015; Chen et al., 2012b; Lin et al., 2012; Nagawa et al., 2012; Wu et al., 2011; Xu et al., 2014; Xu et al., 2010) the function of ABP1 as an auxin receptor has remained unclear. The recent isolation of two *Arabidopsis abp1* mutants with no obvious phenotypes raised strong questions (Gao et al., 2015). Although ABP1 inactivation by inducible antibody- and antisense-based lines present strong phenotypes not caused by ABP1 down-regulation, which might suggest redundancy (Michalko et al., 2016).

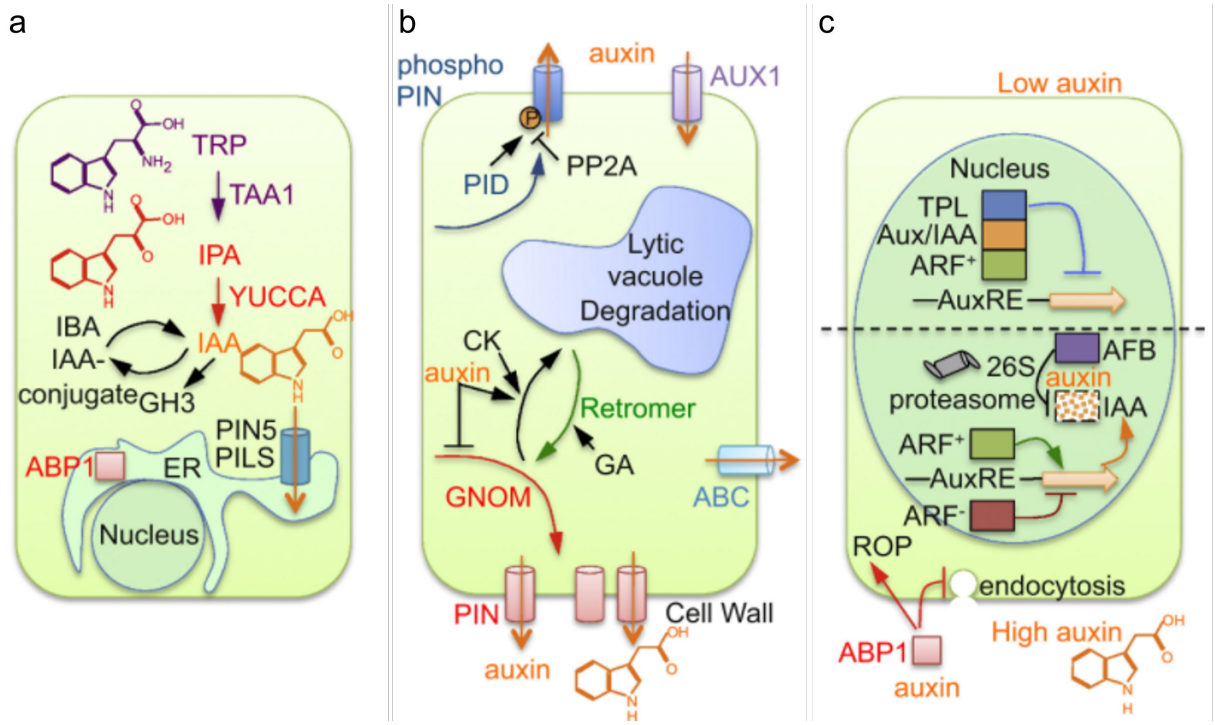

Figure 5. Underlying processes of auxin differential distribution (Finet and Jaillais, 2012).
(a) Auxin biosynthesis and storage as inactive conjugates, which involves enzymes of the GH3 family. Intracellular homeostasis of auxin provided by ER localized PINs and PIN-LIKE proteins (PILS) (Barbez et al., 2012).
(b) Polar auxin transport depends on influx (AUX/LAX) and efflux carriers (PIN and ABCB/PGP) that promote the uptake and release of auxin to the apoplast. The endocytic trafficking and polar recycling of PINs is illustrated. Hormonal regulation of these pathways include auxin feedback regulation, cytokinin control over PIN endocytosis (Marhavy et al., 2011), and gibberellin regulation of PIN trafficking to lytic vacuoles (Willige et al., 2011)
(c) Auxin perception and signalling

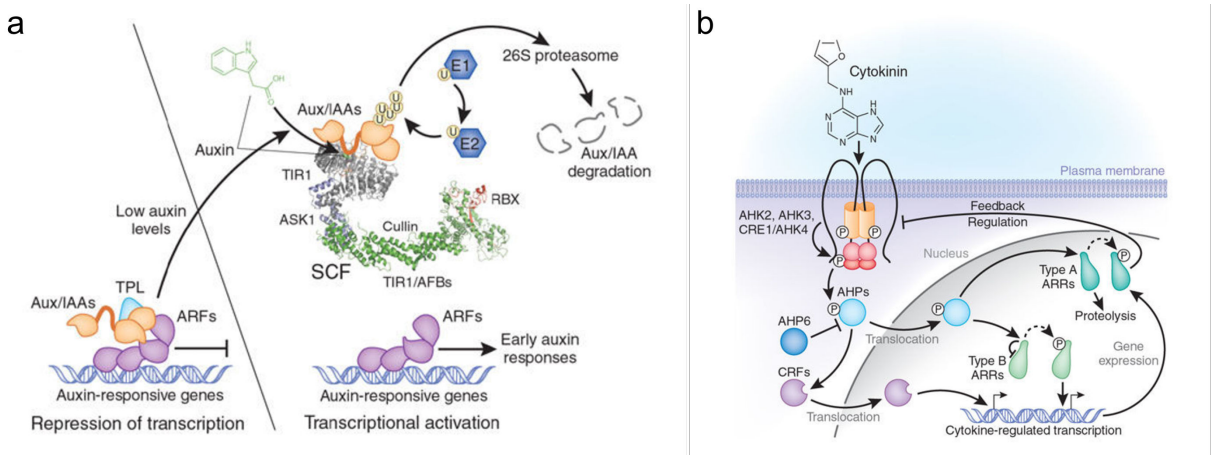

Figure 6. Auxin and cytokinin transduction pathways (adapted from Santner 2009).
(a) At low auxin (left) transcription of auxin-responsive genes is prevented by Aux/IAAs. At high auxin (right) the F-box receptor TIR1/AFBs bind auxin and enhances its affinity for Aux/IAAs, promoting their ubiquitination and degradation, ARFs are released to initiate transcription of auxin-responsive genes.
(b) Cytokinin is perceived by the plasma membrane localized receptors AHK. A series of phosphorelay steps follow the AHK activation, which lead the activation and nuclear translocation of the AHP proteins. Once inside the nucleus AHP transfer the phosphoryl group to ARR proteins. CRF proteins are also activated by cytokinin and act as activators of cytokinin-regulated transcription

2.1.2. Cytokinins

Cytokinins are known for their ability to promote cytokinesis, hence their name. Cytokinins are adenine derivatives carrying either an isoprene-derived or an aromatic side chain (Mok and Mok, 2001). Great diversity exists among the predominant CKs between plant species (Sakakibara et al., 2006). Major derivatives present in *Arabidopsis* are *trans*-zeatin (tZ), and isopentenyladenine (iP) types. The initial step of CK synthesis is catalyzed by isopentenyltransferases (IPTs), which use ADP, ATP and tRNA as isoprenoid acceptors (Kakimoto, 2001; Takei et al., 2001). In higher plants two pathways for the synthesis of tZ coexist. The iP nucleotide-dependent pathway catalyzed by the cytochrome P450 monooxygenases CYP735A and the nucleotide-independent pathway, catalysed by the CK riboside 5'-monophosphate phosphoribohydrolase, LONELY GUY (LOG) (Kurakawa et al., 2007; Kuroha et al., 2009; Tokunaga et al., 2012; Zurcher and Muller, 2016) Additionally steady-state levels of active CKs are determined by the rate of conjugation and degradation. Active CKs, the free bases, are modified into ribosides and ribotides by O-glycosylation. Modified cytokinins can be activated when needed and seem to be the major long-range transport forms in plants (Zurcher and Muller, 2016). CYTOKININ DEHYDROGENASE/OXIDASE (CKX) proteins catalyse the degradation of CKs; they act by cleaving the CKs side chains. Genes encoding cytokinin degradation and synthesis proteins are widely expressed and active both in the shoot and the root (Nordstrom et al.,

2004). Regulation over the synthesis of CKs depends on the differential expression of the basic elements of its metabolism *IPT*s, *CKX* and *CYP735A*. CKs homeostasis is fine-tuned by other hormones and external factors, such as nitrogen availability (Sakakibara et al., 2006).

The signaling of CKs initiates by its perception by the membrane-bound *Arabidopsis* HISTIDINE KINASE (AHK) proteins, which serve as CKs receptors (Heyl et al., 2012). Binding of cytokinin to AHK proteins triggers a phosphorelay, in which a phosphoryl group is transferred from a His residue into an Asp residue within the kinase domain of the receptor. Afterwards, the phosphoryl is transmitted to a His residue of an *Arabidopsis* HISTIDINE PHOSPHOTRANSFERASE (AHP) protein. The previous is true for AHP1-5. AHP6 differs, since it cannot accept an activated phosphoryl group, which makes it unable to perform the phosphorelay (Mahonen et al., 2006). The role of AHP6 is, however, important, since it performs an inhibiting role over cytokinin signaling by competing with the "true" AHPs and contributes to confine the CKs signaling domains (Besnard et al., 2014; Bishopp et al., 2011b). AHP1-5 proteins continuously translocate to the nucleus enabling the phosphorylation of *Arabidopsis* RESPONSE REGULATOR (ARR) proteins. According to C-terminal differences, the family of ARRs has been classified into type –A –B and C (D'Agostino et al., 2000). Type-B ARRs have a transcription factor domain for DNA binding, once phosphorylated type-B ARRs as DNA-binding transcription factors activate transcription of cytokinin-regulated genes (Kiba et al., 1999; Mason et al., 2004). Type-A ARRs lack the transcription factor domain and instead act as negative regulators of cytokinin by attenuating the signal (Brandstatter and Kieber, 1998; D'Agostino et al., 2000; Rashotte et al., 2003). Transcription of type-A ARRs is under the direct regulation of type-B ARRs (Figure 6b). Type-C ARRs are less characterized, although they might have roles as modulators, since their ectopic expression affects cytokinin signaling (Kiba et al., 2004).

Sites of cytokinin synthesis do not necessarily coincide with the sites of perception, suggesting the transport of cytokinins (Zurcher et al., 2013). Long distance transport of tZ-type cytokinins occurs from the root to the shoot via the xylem, whereas iP-type cytokinins move through the phloem from the shoot to the root (Bishopp et al., 2011b). Cell-to-cell transports of cytokinins seem to be mediated by the PURINE PERMEASE (PUP) proteins (Burkle et al., 2003).

The components involved in cytokinin biosynthesis, degradation and phosporelay signaling, are encoded by multigene families (Muller and Sheen, 2007). The diverse but specific expression patterns of these components, suggest a broad range of cytokinin functions. Physiological functions of cytokinins include male and female gametophyte development, root and shoot apical meristem maintenance and development, as well as vasculature development and nodule organogenesis (Zurcher and Muller, 2016).

2.1.3. Brassinosteroids

Brassinosteroids (BRs) are steroidal hormones that play a major role in promoting cell expansion and proliferation (Hardtke et al., 2007; Nakaya et al., 2002). Brassinolide (BL) is the most biologically active BR among more than 50 natural BRs (Fujioka and Yokota, 2003). The biosynthesis of BRs involves parallel and highly branched pathways (Fujioka and Yokota, 2003). The initial step is the formation of campestanol (CN) from campesterol (CR). For this step, two branches have been proposed, the early C-22 oxidation, and the late C-22 oxidation. In *Arabidopsis* the early C-22 oxidation appears to be the major BR biosynthetic pathway (Fujita et al., 2006). Two main pathways have been identified for the biosynthesis of BL from campestanol, the early and late C-6 oxidation pathways (Ohnishi et al., 2009). In the early C-6 oxidation pathway, C-6 oxidation occurs ahead of C-22 hydroxylation. While in the late C-6 oxidation pathway, C-22 hydroxylation takes places before C-6 oxidation (Chung and Choe, 2013). A number of the genes relevant for brassinosteroids biosynthesis or signaling have been cloned taking advantage of BR-deficient mutants. Features such as dwarfism, dark-green and curled leaves, reduced fertility and delayed senescence, are characteristic of these mutants. When grown in the dark, such mutants are de-etiolated with short hypocotyls and open cotyledons (Clouse et al., 1996; Li et al., 1996; Szekeres et al., 1996).

Two different enzymes can perfom the initial modification of CR. The cytochrome P450 monooxygenase (CYP90B1) DWARF4 (DWF4) (Choe et al., 1998); and the cytochrome P450 monooxygenase (CYP90A1) CONSTITUTIVE PHOTOMORPHOGENIC AND DWARF (CPD)(Szekeres et al., 1996). DWF4 acts as a C-22-hydroxylase, whereas CPD functions as a C-3 dehydrogenase (Ohnishi et al., 2012). Depending on the availability of substrates and enzymes, the biosynthesis of BL progresses via either DWF4- or CPD-mediated pathways. Interestingly, both DWF4 and CPD can act on multiple substrates,

constituting multiple biosynthetic parallel pathways. Nevertheless, the overall flux of the BR biosynthetic pathway seems to be determined by the activity of DWF4 (Chung and Choe, 2013). The expression of BR- biosynthetic genes is primarily regulated at the transcriptional level. Interestingly the expression of several biosynthetic genes is subject to feedback regulation from the BRs signaling pathway (Bancos et al., 2002; He et al., 2005; Mathur et al., 1998).

BRs are widely distributed throughout plant tissues, although the active forms seem to accumulate mostly in young growing regions undergoing active cell division and elongation. BRs do not seem to undergo long-distance transport; in contrast they appear to be synthesized and function in the same tissue or even the same cell (Bishop et al., 1996; Shimada et al., 2003; Symons and Reid, 2008). BRs synthesis seems to take place in the endoplasmic reticulum, while its perception is located at the exterior cell surface. Thus movement of BRs is more likely to occur within and between neighbouring cells (Symons and Reid, 2008).

BRs receptors have been described in *Arabidopsis* as plasma membrane localized leucine-rich repeat receptor kinases (LRR), BRASSINOSTEROID INSENSITIVE1 (BRI1) and its two homologues BRL1 and BRL3 (Li and Chory, 1997). The kinase activity of BRI1 is activated following the binding of BR (Kinoshita et al., 2005; Wang et al., 2001). Upon perception of BRs by BRI1, the inhibitory protein BRI1 KINASE INHIBITOR (BKI1) is phosphorylated and dissociated from BRI1(Jaillais et al., 2011; Wang and Chory, 2006). BRI1 is then free to interact with BRI1-ASSOCIATED RECEPTOR KINASE 1 (BAK1) (Nam and Li, 2002), leading to the autophosphorylation and transphosphorylation between the kinase domains of BRI1 and BAK1 (Wang et al., 2008). Activated BRI1 is able to phosphorylate BRASSINOSTEROID-SIGNALING KINASE 1(BSK1) and CONSTITUTIVE DIFFERENTIAL GROWTH1 (CDG1) kinases (Kim et al., 2011; Tang et al., 2008). Subsequently, phosphorylated BSK1 and CDG1 bind and phosphorylate BRI1-SUPPRESSORS1 (BSU1) phosphatase (Kim et al., 2011; Kim et al., 2009). Phosphorylated BSU1 inactivates by dephosphorylation the GSK3-like kinase BRASSINOSTEROID INSENSITIVE 2 (BIN2) (Kim and Wang, 2010). Activated BIN2 phosphorylates transcription factors BRASSINAZOLE RESISTANT1 (BZR1) and BZR2 (hereafter called BRI1-EMS-SUPRESSOR1 (BES1)) (Wang et al., 2002; Yin et al., 2002). Phosphorylated BZR1 and BES1 are retained in the cytoplasm via the activity of 14-3-3 proteins (Gampala et al., 2007; Vert and Chory, 2006). Thus, under high BR levels, inactivation of BIN2 by BSU1

leads to the dephosphorylation and activation of BZR1 and BES1 (Tang et al., 2011). Unphosphorylated BZR1 and BES1 are free to move into the nucleus and bind the promoter of their target genes (He et al., 2005; Sun et al., 2010; Yin et al., 2005; Yu et al., 2011). The activation of BR signaling requires histone modifications and additional interacting transcription factors, among them, BES1 INTERACTING MYC-LIKE1 (BIM1) and INTERACT WITH SPT6 1 (IWS1) (Figure 7)(Li et al., 2010; Yin et al., 2005; Yu et al., 2008).

A number of target genes of BZR1 and BES1 have been identified, revealing diverse molecular links. Noteworthy, the activity of BZR1 is responsible for the transcriptional regulation of BR biosynthetic genes, such as *DWF4* and *CPD* (Kim et al., 2006; Wang et al., 2002). When activated, BZR1 binds to the BR-responsive elements of the promoter sequence of *DWF4* and *CPD* and repress their transcription (He et al., 2005). BES1 might also repress *DWF4* and *CPD* transcription to attenuate BR responses in a feedback loop, but this mechanism is primarily dependent on the repression and de-repression of transcription by BZR1 (Yu et al., 2011). Additional targets of BRs signaling are related with cell wall modification (Xie et al., 2011) and cellular transport, in agreement with BRs effects on cell expansion and growth. Not surprisingly, BR signaling converges substantially with other hormonal and environmental signals, such as light and GA signaling (Guo et al., 2013; Zhu et al., 2013). Of special relevance for this thesis are the interactions with auxin signaling, which I will examine next.

2.1.4 Hormonal crosstalk. The case of auxin and brassinosteroids

Multiple hormones are at play during plant growth and development. Their specific functions, however, are sometimes difficult to define, in particular because extensive crosstalk and signaling integration among growth regulating hormones has been demonstrated (Nemhauser et al., 2006). For instance, cell proliferation is regulated by cytokinins and auxin, while, cell expansion is under the control of auxin, BRs and gibberellins. More recently, a role of BRs in cell proliferation has been identified (Hardtke et al., 2007; Nakaya et al., 2002). Antagonistic relationships between cytokinin and auxin have also been described in much detail. This relationship seems to keep a balance between cell proliferation and differentiation, especially during embryogenesis and during shoot and root meristem development (Barkoulas et al., 2007; Dinneny and Benfey, 2008; Muller and Sheen, 2008).

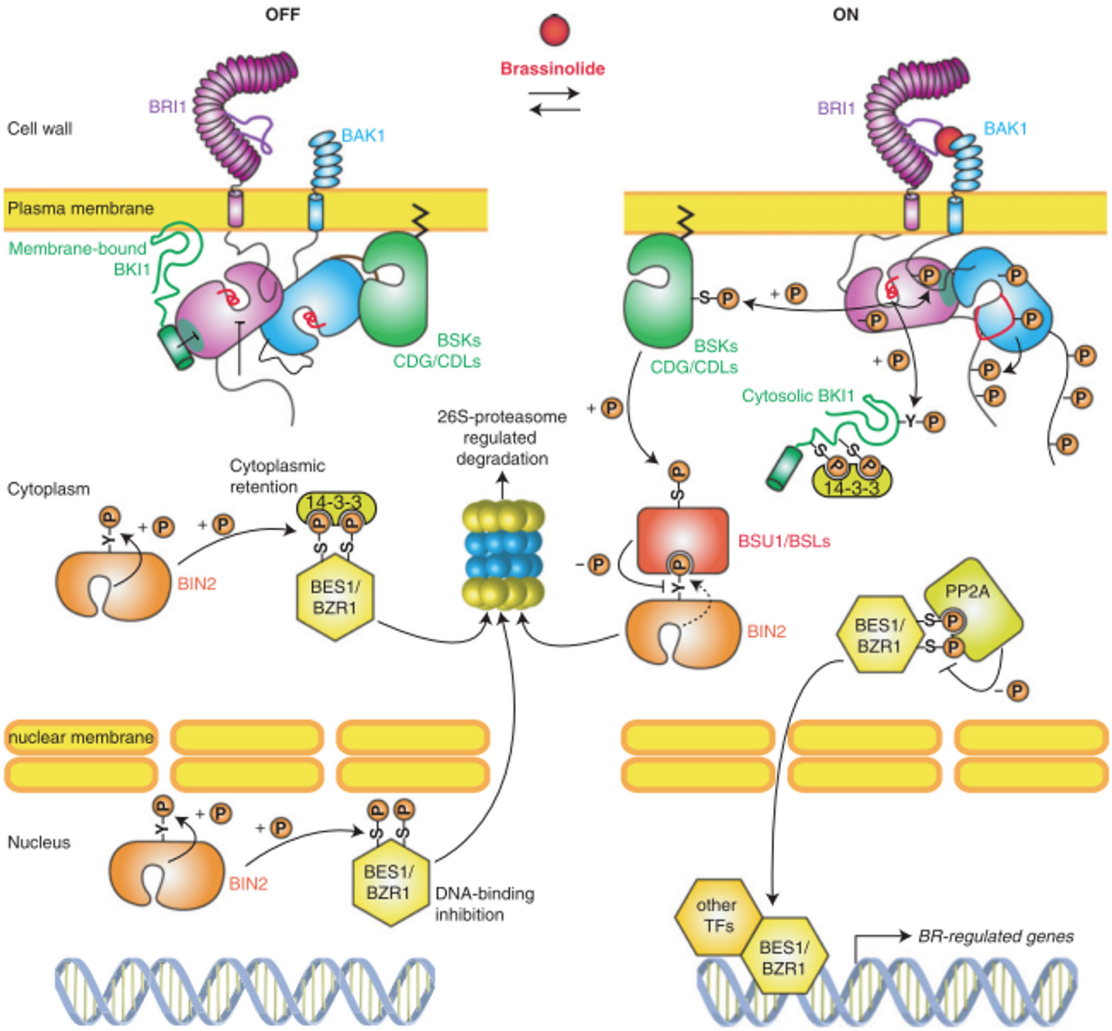

Figure 7. Brassinosteroids signal transduction pathway (adapted from Belkhadir and Jaillais, 2014)
OFF stands for inactive pathway, whilst ON portrays the active pathway. In the presence of Brassinolide, BRI1 kinase phosphorylates BKI1 and in turn interacts with BAK1. A series of phosphorelay steps follows; firstly the phosphorylation and activation of BSK1 and CDG1 kinases, which then leads to the phosphorylation of BSU1 phosphatase. BSU1 dephosphorylates and inactivates BIN2, allowing the nuclear translocation of BZR1 and BES1 transcription factors. Once inside the nucleus BZR1 and BES1 are able to bind the promoter of their target genes aided in certain cases by other transcription factors.

Here I will focus on auxin and BRs, which modulate cell expansion and proliferation and because of their relevance for this thesis. In the following paragraphs I will describe some of the evidence that suggests molecular interactions between auxin and BRs signaling pathways.

Physiological assays of cell elongation have provided the first evidence of the interaction between auxin and BRs. In these assays segments of hypocotyls were promoted to elongate by the application of auxin or BRs. The asymmetrical application of auxin or BRs both triggered bending of the root or hypocotyl, mimicking the tropic response normally achieved by the local accumulation of auxin. This similarity in the responses triggered by both hormones, i.e. elongation by directional expansion as well as certain tropic responses, suggested interaction between the two hormone pathways. (Clouse et al., 1993; Clouse and Sasse, 1998; Zurek et al., 1994).

The close relationship between auxin and BRs very likely reflects several levels of cross-regulation. One possibility is that auxin and BRs control cell elongation through different cellular mechanisms. In this case the signaling pathways and mechanisms used by each hormone can be independent from each other and the interaction is at the level of the physical properties of the system. This can happen without any interaction between the hormone signaling pathways. In addition, interference between the two hormone signaling pathways (Mundy et al., 2006) can be at the biosynthesis level, the components of the signaling pathways might interact, or the signaling pathways might share components (Hardtke, 2007).

In the first case, it has been found that among the targets of BZR1 and BES1 there are genes involved in auxin biosynthesis, transport and signaling (Bao et al., 2004; Kim et al., 2007; Nakamura et al., 2004; Sun et al., 2010; Yu et al., 2011). In turn, there is evidence indicating that auxin regulates BR biosynthesis (Chung et al., 2011; Scacchi et al., 2009) and signaling (Sakamoto et al., 2013).

Nevertheless, the hypothesis which has more support is that auxin and BR pathways converge at the level of common target genes (Hardtke et al., 2007; Nemhauser et al., 2004). Transcriptomic studies identified significant overlap of genes that respond to external application of auxin with genes that respond to external application of BR (Goda et al., 2004; Goda et al., 2002; Mussig et al., 2002; Nemhauser et al., 2004; Yin et al., 2002). Notably, genes repressed by auxin are usually repressed by BRs, while auxin-induced genes are also

BR-induced, indicating that the two hormone pathways affect gene expression in a coordinated manner (Hardtke, 2007). Many of these genes are synergistically induced by the simultaneous application of these hormones (Chung et al., 2011; Goda et al., 2004; Mouchel et al., 2006; Nemhauser et al., 2006; Vert et al., 2008). Moreover, expression changes in response to auxin require intact BR biosynthetic and signaling pathway and vice versa (Hardtke, 2007; Nakamura et al., 2006b). Although, no direct interactions between ARFs and BES1/BZR1 have been demonstrated, it has been suggested that auxin and BR responses are mediated by a combination of specific cis-regulatory elements (Walcher and Nemhauser, 2012). For instance, a Hormone Up at Dawn (HUD)-type E-box combined with a nearby auxin-responsive element variant has been identified as a target for BES1 and MP. Interestingly, their binding can be enhanced by treatment with either hormone (Chandler et al., 2009). BES1 has been shown to interact with IWS1 protein which promotes transcriptional elongation (Li et al., 2010). This could suggest a model where BES1 boosts the response to auxin (Walcher and Nemhauser, 2012).

Both auxin and BR modulate cell expansion and proliferation, therefore ultimately their regulation must feed into cellular effectors of growth. In plant cells, growth results from the irreversible plastic yielding of the cell wall to the internal turgor pressure. Thus, the structural elements of the cell wall as well as the underlying cytoskeleton might be targets of auxin-BR regulation. Nevertheless, evidence in this regard is scarce. At least partially, BR signaling seems to affect the rearrangement of the cortical microtubules, just as auxin signaling does (Catterou et al., 2001; Takahashi et al., 1995). In addition, both auxin and BR also induce the expression of genes encoding for cell wall associated proteins (Yin et al., 2002).

In order to have a clearer idea of how growth could be regulated, we need to take a closer look at the cell wall. In the next section I will cover this aspect and present the structural components of the cell wall that make growth possible.

2.2. The cell wall in plant development and morphogenesis

In most prokaryotes, algae, fungi and plants, cells are enclosed by a stiff extracellular matrix or cell wall. Plant cell walls fulfil a wide range of biological roles; they provide support, act as defensive barrier, as conduits for information and as source of signaling molecules and developmental cues. Cell walls can be quite diverse in their composition, depending on the

developmental stage, the cell type, and the plant species. Most cell walls are viscoelastic fibre composites based on a load-bearing network, infiltrated with matrix polymers.

Primary cell walls, the type of wall surrounding cells that are dividing and/or expanding, are laid down during cytokinesis. They are mainly constituted by cellulose microfibrils embedded and cross-linked into a viscous matrix of pectin and hemicellulose chains (Figure 8a). Although growing cells have relatively thin but flexible walls (less than 1μm), they are able to resist the extremely high turgor pressure that pushes on the plasma membrane. Turgor pressure can reach up to 1 MPa (Beauzamy et al., 2015), but as long as it does not exceed a certain threshold, coined yielding threshold, it only leads to a reversible elastic deformation of the cell wall. (Cosgrove, 2005; Wolf et al., 2012a). Growth occurs when the turgor pressure exceeds the yielding threshold causing the matrix elements to break and the wall to expand in a non reversible manner (plastic deformation) (Ali et al., 2014). This plastic deformation is in principle accompanied by cell wall synthesis.

Since plant cells usually do not move relative to one another growth patterns are entirely defined by local cell expansion. The rate of cell wall expansion can be equivalent in all directions of the cell, in which case expansion is considered isotropic. On the contrary, when the rate of cell wall expansion in one direction differs from the rate in other directions, expansion is anisotropic. It is the integration of the local expansions which will allow the plant to reach its particular size and shape (Baskin, 2005).

Although, plant cell growth depends on both turgor pressure and cell wall mechanics, I will mostly consider the role of cell wall througout this work. Cell wall expansion implies a constant modification of the cell wall properties, for instance, through wall loosening followed by synthesis and insertion of new wall materials. To better understand plant cell growth, we will need to take a look at the composition of the primary cell wall and the roles that these elements play during cell expansion.

2.2.1. Cellulose microfibrils as cell wall load-bearing elements

Cellulose is a paracrystalline polysaccharide, whose primary structures are unbranched β1, 4-linked glucan chains, synthesized in parallel at the cell surface by CELLULOSE SYNTHASE

A (CESA) COMPLEXES (CSC) (Schneider et al., 2016). In *Arabidopsis*, the *CESA* gene family has 10 members (Richmond and Somerville, 2000). *CESA1, CESA3*, and *CESA6* are preferentially expressed in expanding tissues (Desprez et al., 2007; Doblin et al., 2002), while *CESA4*, *CESA7*, and *CESA8* have proven roles in the secondary cell wall thickening in xylem (Scheible et al., 2001; Taylor et al., 2003; Taylor et al., 2000). The remaining *CESA2*, *CESA5*, *CESA9*, and *CESA10* genes are poorly understood but might have certain redundancy with other *CESAs* (Desprez et al., 2007; Persson et al., 2007). According to the current model each CESA protein can synthesize one β1, 4- linked glucan chain. In *Arabidopsis*, the association of three CESA proteins into heterotrimeric CSC facilitates the interaction of dozens of these glucan chains in such a way that they associate to form fibrils of undefined length and shape (Figure 8b)(Cosgrove, 2014; Desprez et al., 2007; Persson et al., 2007). The regulation of CSC activity remains ill defined. However, phosphorylation might play a role in their motility and might also regulate their activation (Sanchez-Rodriguez et al., 2017).

Cellulose microfibrils provide tensile strength to the wall and regulate the degree of expansion. They are usually oriented transversely to the growth axis of elongation, which has been considered to underlie the anisotropy of expansion (Bashline et al., 2014; Baskin and Jensen, 2013; Green, 1962; Ivakov and Persson, 2013). Remarkably, a good amount of evidence indicates that cellulose microfibrils align with cortical microtubules (CMT). It has been noticed that upon transport of the CSC to the cell surface, they are inserted in the plasma membrane close to the CMT (Gutierrez et al., 2009). There, the CMT direct the track of CSC affecting the deposition of cellulose microfibrils (Figure 8a)(Baskin et al., 2004; Chan et al., 2010; Emons et al., 2007; Paredez et al., 2006; Sanchez-Rodriguez et al., 2012). The most direct link between the synthesis machinery of cellulose microfibrils and microtubules is via the protein CELLULOSE SYNTHASE INTERACTING (CSI) 1/POM2 (Bringmann et al., 2012; Gu et al., 2010; Li et al., 2012), although a number of additional proteins have been described (see Landrein and Hamant, 2013). Disruption of the CMT via microtubule-depolymerizing drugs, such as oryzalin alters the alignment of cellulose microfibrils (Baskin et al., 2004; Corson et al., 2009). Notably, disruption of the synthesis of cellulose using the cellulose synthesis inhibitor isoxaben, results in disorganized CMTs in tobacco culture cells (Fisher and Cyr, 1998) and pollen tubes (Lazzaro et al., 2003), suggesting the presence of a mutual feedback relationship between CMTs and cellulose microfibril deposition (Figure 8b).

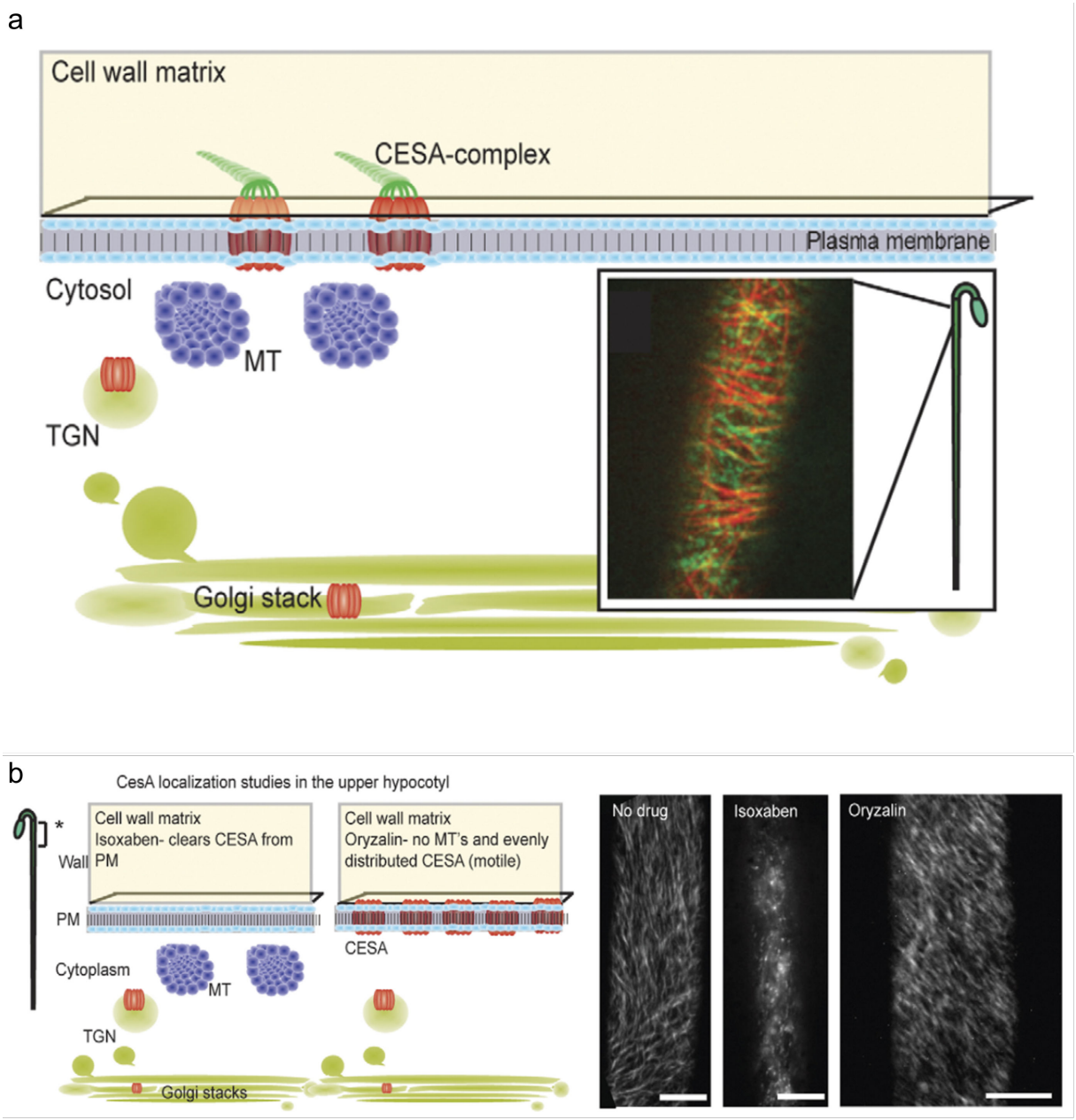

Figure8. Cellulose synthesis at the plasma membrane (adapted from (Mutwil et al., 2008))
(a) The CESA complex (red) is transported from the Golgi to the plasma membrane via exocytosis. Cellulose microfibrils are synthesized directly in the plasma membrane. During this process the synthesis machinery is guided by the cortical microtubules (blue). The inset shows a YFP-tagged CESA6 (green) and a CFP-tagged tubulin (red).
(b) Studies of cellulose biosynthesis inhibition performed in the upper hypocotyl. Treatment with isoxaben targets cellulose synthesis, while treatment with oryzalin targets MT. The summary of the observations during the drug treatments is displayed on the left, while on the right the time average images of YFP-CESA6 are displayed.

Thus, CMTs are crucial for growth anisotropy, since they orient the cellulose microfibrils. But how are CMT orientations controlled? A recent hypothesis proposes that CMT respond and align in the direction of maximal stress in the cell wall (Landrein and Hamant, 2013; Uyttewaal et al., 2012). The force patterns, ultimately generated by the turgor pressure, depend on different factors, including the geometry of the cells and tissues as well as local differences in growth rate. Mechanical stress is of great relevance since it allows the cell to sense and adapt its mechanical status. This involves a feedback loop in which microtubules affect morphogenesis through oriented cellulose deposition and anisotropic growth, which in turn defines global mechanical stress patterns that influence microtubule orientation. I will come back to this topic later, after introducing the other elements of the cell wall, which also play a role in the expansion of the cell wall. The complexity of the cell wall, involving many different polysaccharides and hundreds of proteins exceeds the scope of this work. Thus the description of the cell wall will only be partial.

2.2.2. Hemicelluloses and their role in cell wall architecture

Hemicelluloses are a heterogeneous group of polysaccharides, initially defined as those cell wall polysaccharides that do not solubilize in water or chelating agents but in the presence of aqueous alkali. Under this definition, the term hemicelluloses would include xyloglucan, glucomannan, mannan, xylan, arabinoxylan and arabinogalactan. Alternatively hemicelluloses are defined chemically as cell wall polysaccharides structurally homologous to cellulose characterized by β-1-(1-4)- linked backbones of sugars in equatorial configuration. This definition includes xyloglucans, glucomannans, mannans, xylans, arabinoxylans, but not arabinogalactans (Scheller and Ulvskov, 2010). A number of enzymes involved in hemicelluloses biosynthesis have been identified (Cantarel et al., 2009).

Xyloglucans (XyG) are the most abundant hemicelluloses of primary cell walls of eudicots. They are composed of β-(1-4)-glucan backbone substituted with α-(1-6)-xylosyl residues in a regular pattern, and occasional galactosyl or fucosyl residues (Figure 9a)(Park and Cosgrove, 2015). The β-(1-4)-glucan backbone of XyG is synthesized at the Golgi by glucan synthases members of the cellulose synthase-like (CSLC) family of proteins (Cocuron et al., 2007). Most XyG have backbone substitutions, that can reach very complex branching patterns (Fry et al., 1993). Their biosynthesis involves the activity of a number of glycosyltransferases,

including β-(1-4)-glucan synthase (Cocuron et al., 2007), α-fucoyltransferse (Perrin et al., 1999), β-galactosyltransferase (Levy et al., 1991; Madson et al., 2003), and α-xylosyltransferses (Faik et al., 2002)(Figure 9b). *Arabidopsis* contains seven genes encoding XyG xylosyltransferases (XXT). Of these, xylosyltransferase activity has been demonstrated for XXT1, XXT2 and XXT5 (Cavalier and Keegstra, 2006; Faik et al., 2002; Zabotina, 2012; Zabotina et al., 2008). Yet, although the double *Arabidopsis* mutant *xxt1 xxt2* has no detectable levels of XyG (Cavalier et al., 2008; Park and Cosgrove, 2012a), it has only a minor phenotype (Cavalier et al., 2008; Park and Cosgrove, 2012a; Xiao et al., 2016). Two possibilities were discussed by the authors to explain the absence of strong phenotypes in the complete lack of XyG. They suggest that an aberrant form of XyG might be present in the *xxt1 xxt2* that could not be detected by their methods. They also suggest that the lack of XyG might be compensated either by an altered β-glucan backbone able to function in a similar fashion to XyG, or by modification of other components (i.e. pectin cross-linking) of the cell wall. This unexpected result opened new questions, which contribute to the reexamination of the role of XyG in primary cell wall.

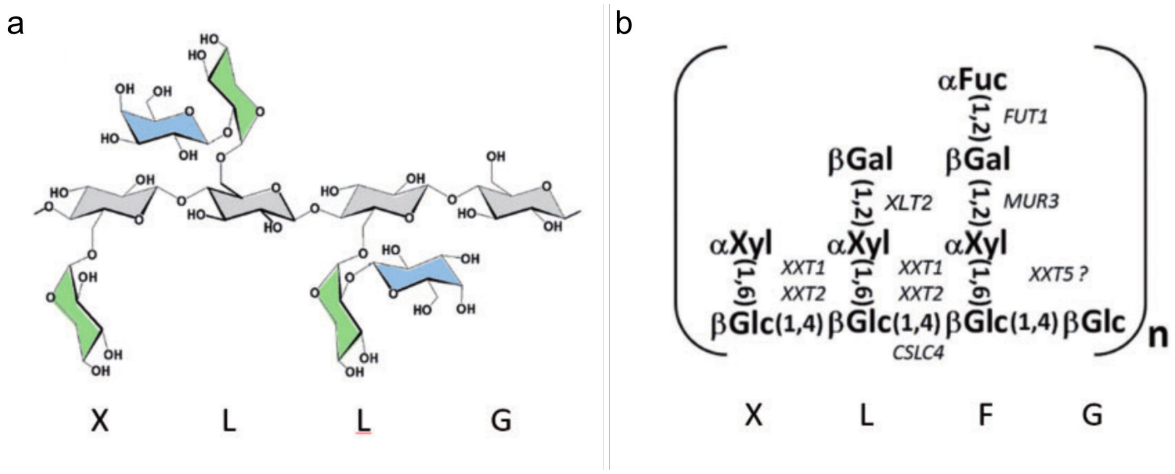

Figure 9. Xyloglucan structure (adapted from Park and Cosgrove, 2015)
(a) Structure of XLLG oligosaccharide, showing the β-(1-4)-glucan backbone (gray) with side chains, xylose (green) and galactose (blue).
(b) XLFG oligosaccharide with its pattern of linkages with the associated glycosyl transferases indicated in upper case letters.

It has been suggested that the most important role of XyG was to coat cellulose microfibrils and tether them together, thus reinforcing the load-bearing properties of the cell wall. (Scheller and Ulvskov 2010). However, our understanding about the nature of the interaction between cellulose and XyG is evolving and other models have been proposed. In contrast to

the “tethered network” model, which suggests that most of the microfibrilar surface is coated with XyG (Figure 10a), nuclear magnetic resonance (NMR) analyses of *Arabidopsis* cell walls indicated that the interactions between XyG and cellulose are limited (Dick-Perez et al., 2011; Wang et al., 2012). Additional tests of the tethered network model based on biochemical changes induced by substrate-specific endoglucanases (Park and Cosgrove, 2012b) led to the hypothesis that the sites where cell walls are loosened are probably digested by an enzyme with both xyloglucanase and cellulase activity. This model, coined the “biomechanical hotspot model”, proposes the existence of a limited number of cellulose-cellulose junctions, which are attached together by XyG. These XyGs would keep the microfibrils together, prevent their aggregation and limit enzymatic accessibility to these biomechanical hotspots (Figure 10b)(Park and Cosgrove, 2012b). These sites which would be the location of cell wall loosening during growth could also be the targets of another set of wall loosening proteins named expansins, which will be discussed in the next paragraph.

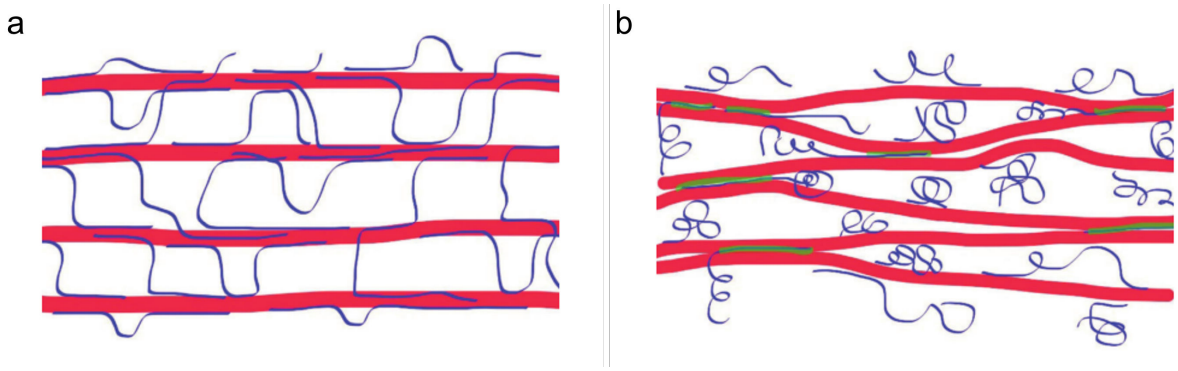

Figure 10. Two models of primary cell wall structure (adapted from Cosgrove 2016)
(a) The “tethered network” model suggests that the cellulose microfibrils (red) are well separated by xyloglucans (blue), whose role is to fasten the microfibrils resulting in a load-bearing network.
(b) The “biomechanical hotspot” model proposes a mixture of xyloglucan-cellulose (green) to be in charge of the limited cellulose-cellulose connections. These sites, the biomechanical hotspots, have limited enzymatic accessibility and may be subject to the loosening activity of expansins

Expansins are pH-dependent wall-loosening proteins (McQueen-Mason et al., 1992). Although, no clear enzymatic activity has been reported yet for expansins, a number of studies support their ability to induce selective wall loosening that enables irreversible extension, or “wall creep” and wall relaxation (Cosgrove et al., 2002; McQueen-Mason and Cosgrove, 1995). Plant expansins are divided into four families (Kende et al., 2004) of which α-expansins (EXPAs), and β-expansins (EXPBs) have different biological roles (Cosgrove, 2015; Sampedro and Cosgrove, 2005).

In addition to expansins, other enzymes (e.g. glycoside hydrolases (GH)) have been considered as wall loosening. Such is the case of the GH16 or xyloglucan endotransglucosylase/hydrolases (XTH), encoded by a large multigene family. After XTHs were discovered they were considered as wall-loosening enzymes, but with time, experiments showed they have limited ability to induce cell wall creep. This entailed to hypothesize that the effect of XTHs in cell loosening is minimal, but that they are likely involved in the remodelling an turnover of XyG during the formation of the primary wall and after cell elongation (Cosgrove, 2016a). Among the XTHs, the xyloglucan endotransglucosylases (XETs) seem to perform a wall-strengthening action by cutting XyG backbones and bind them to chains that are already part of the wall network (Thompson and Fry, 2001).

Another group of enzymes that might cause wall expansion are the GH9s, also called endoglucanases or cellulases. In plants, 11 distinct clades of GH9s have been reported, which seem to have roles in cell wall modification during diverse processes. One of the best studied GH9 is a membrane-associated endoglucanase named KORRIGAN, which is part of the synthesis machinery complex of cellulose microfibrils and therefore influences the organization of cellulose in the wall (Vain et al., 2014). Despite the efforts it is not conclusive whether GH9 enzymes are able to directly loosen the cell wall.

2.2.3. Pectins and their role in cell wall expansion

Pectins, like hemicelluloses, are complex and heterogeneous polysaccharides. They are characterized by chains of galacturonic acid molecules linked at their 1 and 4 positions. There are three major types: homogalacturonans (HG), rhamnogalacturonans I (RG-I), and rhamnogalacturonans II (RG-II). Distinct combinations of these polysaccharide residues covalently bind and produce different pectin molecules (Atmodjo et al., 2013).

Pectin polysaccharides are produced in the Golgi and later on deposited in the cell wall. Given that specific enzymes are needed to catalyse the formation of each glycosidic linkage and modification, at least 67 transferases are required for the synthesis of pectins. These include, glycosyltransferases (GTs), methyltransferases (MTs) and acetyltransferases (ATs) (Mohnen, 2008).

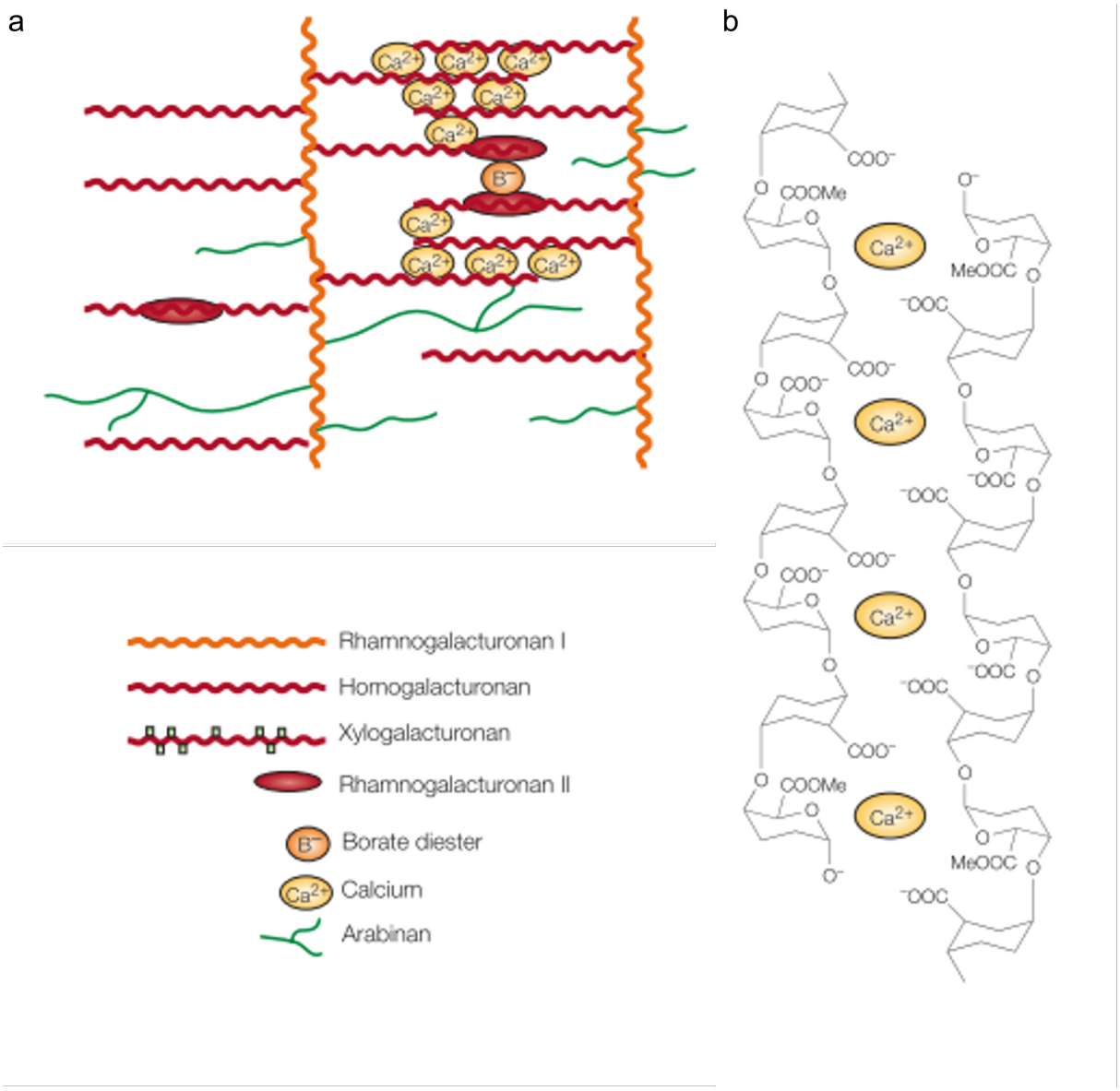

Figure 11. Formation of pectin networks (adapted from Cosgrove, 2005)
(a) Pectin domains covalently crosslink each other, thay also formlinkages involving boron and calcium.
(b) Homogalacturonana form stiff gels through Ca^{2+} mediated crosslinking of its carboxyl groups.

Pectins possess the ability to bind to other pectins, as well as to cellulose and hemicellulose. This allows the formation of structures with hydrogel characteristics. HGs have the ability to form multiple intermolecular bonds in the presence of calcium cations. Prior to crosslinking they should be 'activated' via the removal of the methyl group that protects them from the action of lyases. Demethyl-esterified pectin then acquires the capacity to create big aggregates known as 'egg boxes' (Figure 11). Specialized enzymes, pectin methyl-esterases (PMEs), are in charge of this process. In counteraction, PME-inhibitors (PMEIs) modulate the activity of PMEs. 66 PMEs and 69 PMEIs have been identified so far in the *Arabidopsis* genome

(Levesque-Tremblay et al., 2015). The PME/PMEI system is potentially very important, since the degree and pattern of demethyl-esterification might strongly influence biomechanical properties of the cell wall (Ali and Traas, 2016; Peaucelle et al., 2011a). Indeed, modifications in the level of PME or PMEI can strongly affect plant development (see also below).

2.2.4. Cellulose/xyloglucan and pectin act together during morphogenesis

Pectins, like hemicelluloses, interact with cellulose microfibrils to assemble the cell wall. This complex network allows for many potential sites where loosening and expansion can be initiated. But how are the assembly and rearrangements of these elements coordinated in order to produce cell expansion? As earlier mentioned, the expansion of plant cells results from the interaction between the turgor pressure inside the cells and the irreversible expansion of the viscoelastic wall that surround plant cells. Turgor pressure is the product of the osmotic force, which is equal in all directions or isotropic, whereas morphogenetic processes require anisotropic growth, which consequently relies on the cell wall properties. It is widely accepted, that the orientation of the cellulose microfibrils, controlled by the microtubules underlies anisotropic growth (Baskin and Jensen, 2013). Recently it has been proposed that changes in pectin configurations can trigger anisotropic organogenesis even prior to changes in cellulose orientation. This has been reported for the epidermal cells of *Arabidopsis* hypocotyl, where AFM analyses indicated that the walls that preferentially expand during elongation (the longitudinal anticlinal walls) experience softening previous to the initiation of anisotropic elongation (Peaucelle et al., 2015). This led to suggest a two-step mechanism for anisotropic plant cell growth (Figure 12) (Bidhendi and Geitmann, 2016). This might also be true for other tissues, such as the shoot apex, where a reduction in the elastic modulus detected by AFM precedes organogenesis (Milani et al., 2011; Peaucelle et al., 2011a).

Either way, cellulose microfibrils as well as hemicelluloses and pectins, interact and contribute altogether to control cell expansion (Cosgrove, 2014). The integration of the local expansions of all the growing regions gives an organ its characteristic shape. How this orchestrated expansion is regulated during morphogenesis remains poorly understood.

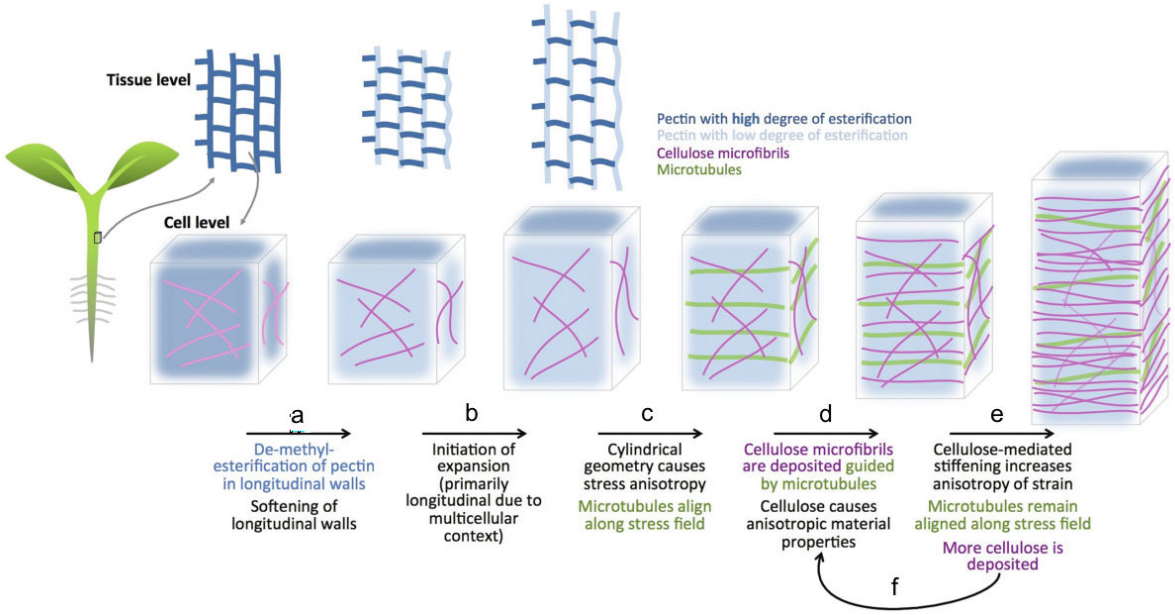

Figure 12. Two-step mechanism for anisotropic plant cell growth (adapted from Bidhendi and Geitmann, 2016)
(a) Longitudinally oriented cell walls soften through pectin de-methyl-esterification.
(b) The differential mechanical properties of the longitudinal and transverse walls triggers expansion of longitudinal walls.
(c) The newly generated geometry causes stress anisotropy and further microtubule alignment in the direction of maximal stress.
(d) The deposition of cellulose microfibrils following microtubule orientation causes the longitudinally walls to become anisotropically reinforced.
(e) The increase in stress anisotropy feedbacks into the orientation of microtubules.
(f) The further deposition of cellulose microfibrils following microtubules alignment reinforces wall anisotropy.

In the previous sections we have seen that a molecular network involving a set of hormones governs morphogenesis in plants. This network interferes with cell wall composition and structure which in turn defines local growth rates and directions, driven by turgor pressure.
In this thesis I have studied the link between molecular regulation and cell wall remodelling at the shoot apical meristem. In section 3 of this introduction I will therefore review a number of aspects concerning this structure.

3. Pattern formation and morphogenesis at the shoot apical meristem

The shoot apical meristem (SAM) located at the tip of the growing shoot contains a group of non-differentiated stem cells. These cells continuously generate organs at the meristem flanks while maintainig themselves via asymetrical cell divisions. The lateral organs emerge following a continuous and precise pattern, called phyllotaxis (Figure 13c). The type of organ generated from the SAM depends on the developmental phase. I will focus here on the SAM in *Arabidopsis* which, as a typical dicotylenous plant produces leaves and side branches during the vegetative phase and flower primordia during the reproductive phase.

Functional domains in the SAM of *Arabidopsis* are defined by specific histological features and gene expression profiles. In what follows, I will review the SAM functional domains and the molecular pathways that underlie them.

3.1. Shoot Apical Meristem set-up during the embryonic stage

During embryogenesis, a number of stereotypic cell divisions set up the basic polarity and patterning of the plant body plan. Through this process only a very rudimentary plant is formed, that displays an apical-basal axis of polarity and perpendicular to it, a radial pattern of concentric tissues. After the first two rounds of cell divisions, the determination of shoot and root domains is separated (Haecker et al., 2004). At the globular stage the SAM is specified at the top of the axis of polarity (Sarkar et al., 2007). Although the molecular organization characteristic of the vegetative SAM is not yet established at this stage, it develops gradually during embryogenesis (Lau et al., 2012; ten Hove et al., 2015).

3.2. Shoot Apical Meristem functional domains

The SAM is a dome-shaped structure (Figure 13). At its summit, in the central zone (CZ), resides the pool of stem cells. Surrounding the CZ lays the peripheral zone (PZ), consisting of small cells that frequently divide but are still undifferentiated. Underneath the PZ, the rib zone (RZ) can be distinguished, characterized by a group of cells that mainly contribute to the formation of the central tissues of the shoot axis (Figure 13a). Superimposed to this zonation, a layered organisation can be distinguished. From outside to inside, the L1 and L2 layers are

composed cells that generally divide perpendicular to the surface by this means forming two different sheets of clonally distinct tissue. The L1 gives preferentially rise to the epidermis, while the L2 largely contributes to the sub-epidermal tissues. The underlying L3 cells divide in apparently random directions and generate the internal tissues of lateral organs (Figure 13b).

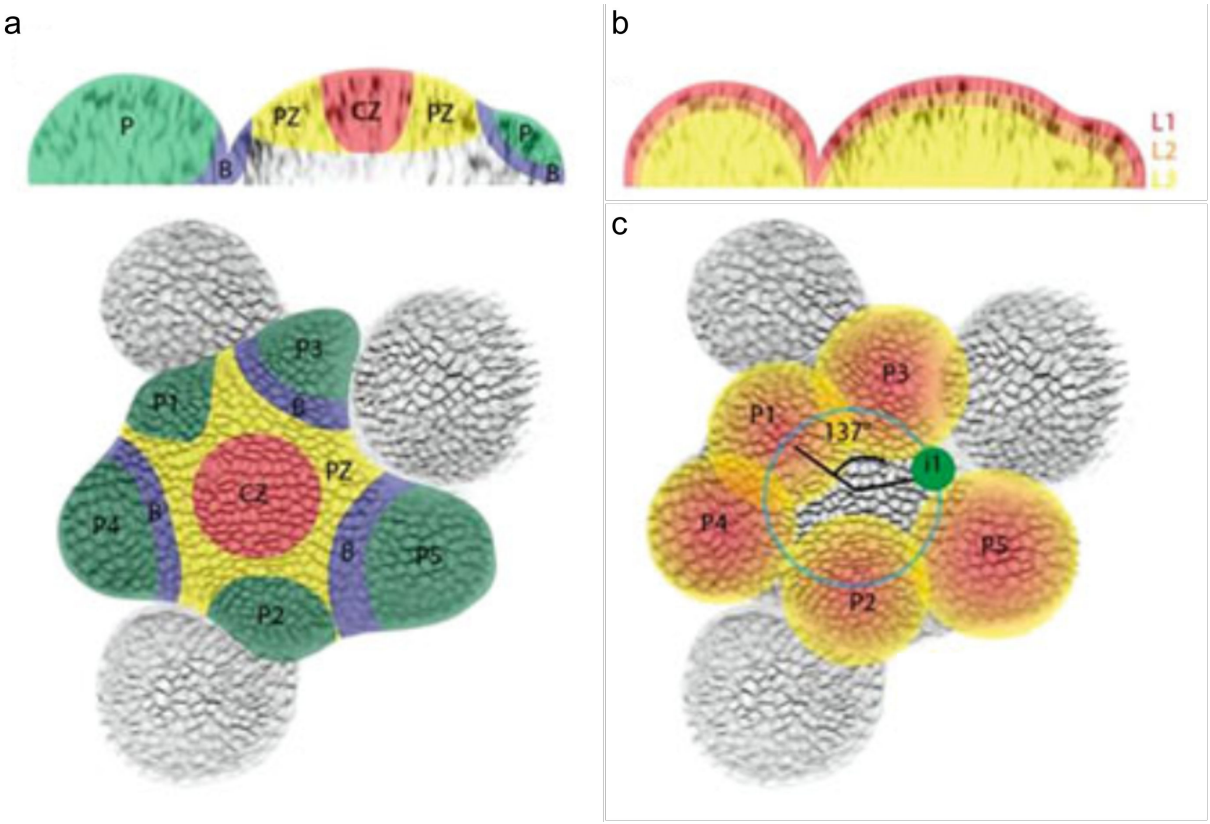

Figure 13. Structural and functional organization of the SAM of *Arabidopsis* adapted from (Landrein and Vernoux, 2014)
(a) Top and orthogonal views showing the structural zonation of the SAM: central zone (CZ), peripheral zone (PZ), primordia (P), and boundaries (B).
(b) Orthogonal view of the SAM showing the organization into layers.
(c) Primordia spaced according to a regular pattern of phyllotaxis. In *Arabidopsis* phyllotaxy is spiral. P5 indicates the oldest primordium and P1 the youngest. Successive organs are separated by an angle close to 137.5°. The position at which the next primordium (i1) will be initiated.

3.2.1. The Central Zone and the maintenance of a group of undifferentiated stem cells

Optimal functioning of the SAM requires a balance between the indeterminate growth at its centre and the production of lateral organs at the flanks. Local maintenance of stem cells is provided by a well-described feedback regulation, orchestrated by the homeodomain transcription factor WUSCHEL (WUS). *WUS* expression is restricted to a small region of the

SAM better known as the organizing centre (OC) located underneath the stem cells (Baurle and Laux, 2005; Laux et al., 1996; Mayer et al., 1998). The WUS protein migrates into the overlying cells, where it binds to the promoter of *CLAVATA3* (*CLV3*) to positively regulate its expression (Brand et al., 2002; Daum et al., 2014; Yadav et al., 2011; Yadav and Reddy, 2012). *CLV3* encodes a peptide that diffuses from the stem cells to the underlying cell layer, where it binds to the leucine-rich repeat-like kinase (RLK) CLV1 (Clark et al., 1997; Ogawa et al., 2008) or to a receptor complex formed by the receptor-like protein CLV2, and CORYNE, which is a serine/threonine kinase localized at the plasma membrane (Jeong et al., 1999; Muller et al., 2008). Through this interaction the CLV signalling components negatively regulate *WUS* expression, by this means restricting the size of the OC (Mayer et al., 1998; Yadav et al., 2011). In turn, CLV3 signaling is also regulated by WUS, since it directly represses *CLV1* (Busch et al., 2010). This interaction establishes a negative feedback loop with the potential to dynamically adjust the size of the stem-cell population and the OC, thus contributing to meristem homeostasis (Figure 14a)(Soyars et al., 2016). Transcriptomic analysis of the *Arabidopsis* shoot meristem indicated that genes activated by WUS are specific to the stem cells, whereas those repressed are mostly expressed in differentiating cells of the PZ (Busch et al., 2010; Yadav et al., 2009; Yadav et al., 2013). More recently the transcription factor HECATE 1 (HEC1), which promotes stem cell proliferation, was described as negatively regulated by WUS. Absence of HEC1 in the OC is necessary for stem cell maintenance, since it can uncouple the WUS-CLV feedback turning stem cells into organizer cells (Schuster et al., 2014).

Parallel to the WUS-CLV pathway, the class I KNOTTED1-like homeobox (KNOX) protein family performs key roles in the maintenance of stem cell homeostasis in *Arabidopsis* (Endrizzi et al., 1996; Long et al., 1996). In *Arabidopsis*, this family includes *SHOOT MERISTEM LESS* (*STM*), *Kn1-like in Arabidopsis thaliana 1*(*KNAT1*)/*BREVIPEDICELLUS* (*BP), KNAT2* and *KNAT6*, with partially overlapping expression patterns in the SAM (Hay and Tsiantis, 2010). *STM* expression can be distinguished all throughout the shoot meristem except for the organ primordia (Long et al., 1996). STM prevents stem cell differentiation by suppressing the expression of organ-specific regulators in the CZ such as *ASYMMETRIC LEAVES 1* (*AS1*) and *AS2*. In turn, the MYB transcription factor AS1 and the LBD transcription factor AS2 seem to create an AS1/AS2 complex that represses *KNAT1* and *KNAT2* in the lateral organ primordia (Byrne et al., 2000; Lodha et al., 2013). Additionally, *BLADE ON PETIOLE* (*BOP1*) and *BOP2*, which encode BTB/POZ domain proteins,

negatively regulate *KNAT1*, *KNAT2* and *KNAT6*. *KNOX* genes. Both WUS and STM regulate meristem formation independently from each other but in a complementary manner. WUS contributes non-cell-autonomously with stem cell specification at the meristem summit, at the CZ. STM prevents differentiation through the meristem dome including the CZ and the PZ and at the same time is required to promote cell division in the PZ (Lenhard et al., 2002).

Hormonal balance contributes to the establishment and maintenance of the meristem domains (Figure 14a and b)(Shani et al., 2006). The synthesis and action of cytokinin is necessary for the maintenance of an undifferentiated pool of stem cells in the centre of the meristem. In *Arabidopsis* the biosynthetic enzyme LOG4 is expressed in the epidermal layer of the shoot meristem, while the expression of the cytokinin receptor AHK2 and AHK4 is localized to the organizing centre (Chickarmane et al., 2012). WUS positively regulates cytokinin signalling by directly repressing transcription of the negative regulators, *ARR7* and *ARR15* (Jasinski et al., 2005; Leibfried et al., 2005). In turn, cytokinin signaling directly activates *WUS* expression (Zhang et al., 2017), generating a positive feedback loop, which contributes to maintain and even re-establish the stem cell pool (Adibi et al., 2016; Chickarmane et al., 2012; Gordon et al., 2009). Moreover, this mechanism seems to be buffered by members of the ERECTA (ER) receptor kinase family that regulate cell homeostasis by preventing an excessive increase of cytokinin in the SAM (Uchida et al., 2013). In addition, STM activates cytokinin biosynthesis, via the positive regulation of *IPT7* and represses gibberellin activities in the meristem (Jasinski et al., 2005; Leibfried et al., 2005). I will discuss auxin and its crucial role in lateral organ initiation (Heisler et al., 2005) in section 4.1.

In addition, two pathways of miRNAs have been implicated in maintaining the position of stem cells at the shoot apical meritem. First, miR394, produced at the L1, difusses downwardly and acts as a positive stem cell cue by maintaining the expression of *CLV3* (Knauer et al., 2013). The second miRNA pathway involves miR165/miR166, which targets mRNAs of CLASS III HOMEODOMAIN LEUCINE ZIPPER (HD-ZIP III). miR165/166 are sequestered in the provasculature surrounding the meristem by ARGONAUTE 10 (AGO10) also known as ZWILLE (ZLL) (Zhu et al., 2011). This allows the expression of *HD-ZIP III* genes in the meristem and promotes its maintenance (Liu et al., 2009b). Interestingly, this pathway seems to be relevant for shoot meristem maintenance only in the *Arabidopsis* accession *Landsberg erecta* (*Ler*), in which *zll* mutants display stem cell exhaustion (Tucker et al., 2013).

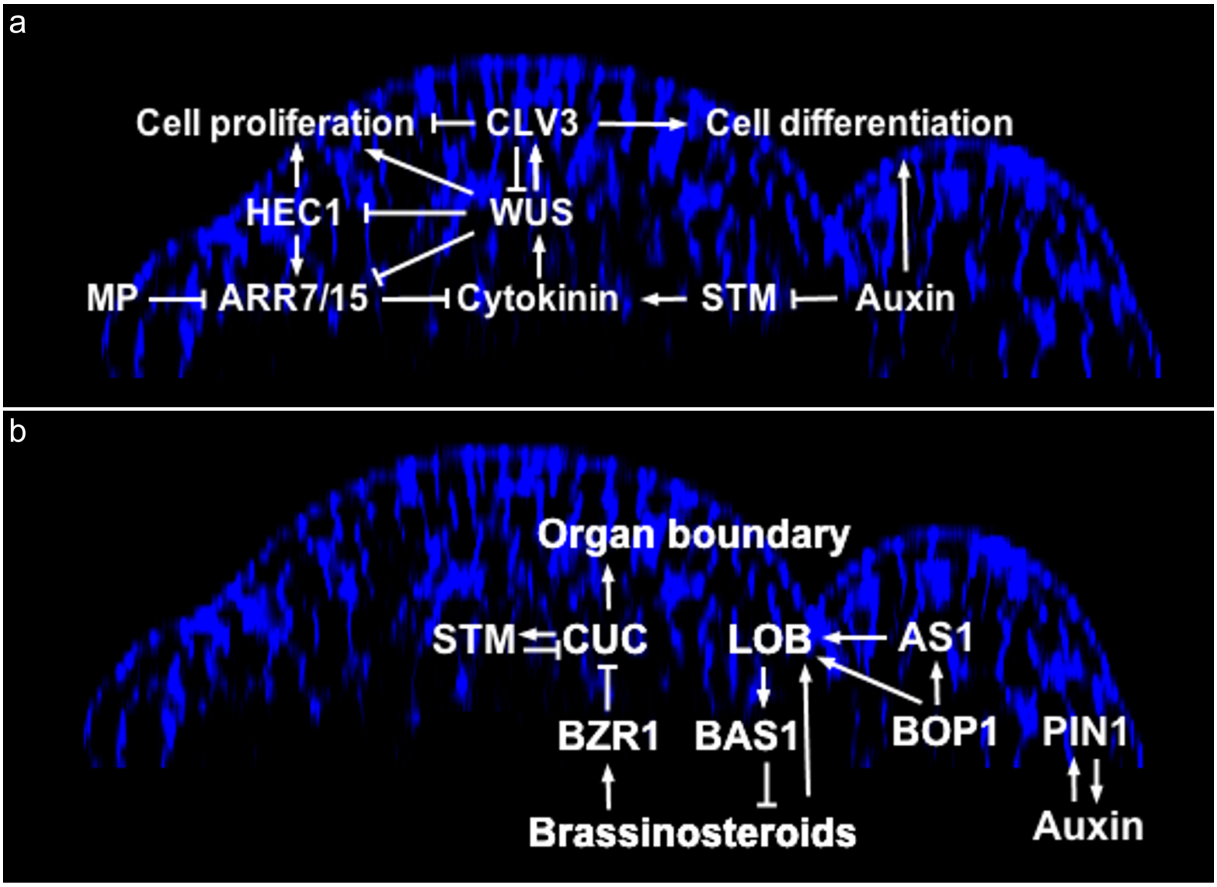

Figure 14. The maintenance of the stem cell niche and the initiation of lateral organs
(a) WUS expressed in the organizing centre moves to induce *CLV3* in the stem cells. CLV3 represses in turn *WUS*. WUS inhibits cell proliferation in the organizing centre and differentiation in the peripheral zone. WUS modulates stem cell non-cell autonomously by directly repressing HEC1 and by promoting CLV3 expression. WUS also integrates CK signaling inputs, which are positively influenced by MP and negatively by HEC1 through the regulation of A-type ARRs,
(b) The demarcation of the meristem-to-organ-boundary requires brassinosteroid signalling. The boundary genes CUC1 and LOB are tightly interconnected with this signaling pathway. By regulating the BR catabolic gene BAS1, LOB creates a minimum in BR levels and allows the expression of CUC1, which is alleviated from BZR1 repression, and can specify the boundary domain.

3.2.2. The Peripheral Zone and the generation of organ primordia : the inflorescence meristem

The initiation of organ primordia occurs at the flanks of the SAM at a certain distance from the pool of stem cells in the PZ. In *Arabidopsis* one of the first requirements for organ initiation, either leaf or flower, is the down-regulation of *STM* gene expression in the organ founder cells (Jackson et al., 1994; Long and Barton, 2000; Long et al., 1996). This occurs before the primordium is recognizable as a bulge in the meristem, in the incipient primordium also known as I1/P0 ("P" refers to the plastochron stage, time interval between the initiation of two consecutive primordia (Green et al., 1970)). There are a number of processes in common with the vegetative meristem and the inflorescence meristem. Since the main focus of this thesis is on the morphogenesis in the inflorescence meristem, I will hereby focus on the generation of organ primordia in this meristem.

At the inflorescence meristem of *Arabidopsis*, the sites of incipient primordia and high auxin levels are coincident with the expression of *ARF5/MONOPTEROS* (*MP*) (Vernoux et al., 2011). Downstream of MP in the incipient primordia, the transcriptional regulation of a group of targets has been identified (Figure 15a)(Wu et al., 2015; Yamaguchi et al., 2013). These include the LEAFY (LFY) transcription factor, which is necessary and sufficient for specification of floral identity (Liu et al., 2009a; Weigel et al., 1992) and two members of the APETALA2/ETHYLENE RESPONSE FACTOR (AP2/ERF) family, i.e. AINTEGUMENTA (ANT) and AINTEGUMENTA-LIKE 6/PLETHORA3 (AIL6/PLT3), which are expressed in all organ primordia throughout the plant (Elliott et al., 1996) and have critical roles in proliferative growth of the flower (Krizek, 1999; Mizukami and Fischer, 2000). ANT and AIL6 also contribute to the auxin dependent activation of *LFY* in parallel with MP (Yamaguchi et al., 2016). Additional targets of MP in the flower primordia include: *AHP6, TARGET OF MONOPTEROS 3* (*TMO3*) and *FILAMENTOUS FLOWER* (*FIL*) (Wu et al., 2015). *AHP6* encodes a negative regulator of cytokinin signaling (Besnard et al., 2014), *TMO3* was firstly described as a target of MP during embryo development (Schlereth et al., 2010) and encodes a cytokinin response factor (CRF) (Rashotte et al., 2006); whereas *FIL* encodes a member of the YABBY family of transcription factors.

After the apical extension of the flower primordium (P1), once a cleft is form between the SAM and the primordium (P2), the polarity genes acquire differential adaxial/abaxial

expression (Husbands et al., 2009). Although most of our knowledge on the acquisition of organ polarity is based on *Arabidopsis* leaf, it is clear that the mutually exclusive mechanisms dictating adaxial/abaxial polarity in floral primordia echoes those established for leaves. The acquisition of organ polarity is a gradual process and initially relies on positional information supplied from the meristem (Kuhlemeier and Timmermans, 2016). Prior to organ initiation the *HD-ZIP III* genes, *REVOLUTA* (*REV*), *PHABULOSA* (*PHB*) and *PHAVOLUTA* (*PHV*), are preferentially expressed at the tip of the meristem. Upon primordium initiation, the expression of these genes extends into the incipient primordium (McConnell et al., 2001), where they become restricted to the adaxial side by the post transcriptional regulation of mir166 (Yao et al., 2009). Upon organ initiation KANADI (KAN) proteins relocalize to the abaxial side of the lateral organ, where they restrict the expression *AS2*. Thus AS1-AS2 activity becomes adaxialized and in turn polarizes the expression of additional components (Husbands et al., 2015; Lin et al., 2003). In addition to the *KAN* genes, *YABBY* (*YAB*) genes including *FIL*, *YAB2*, *YAB3* and *YAB5* in *Arabidopsis* (Husbands et al., 2009), promote abaxial polarity, along with *ARF3* and *ARF4* (Eshed et al., 2001; Siegfried et al., 1999). The spatial restriction of some adaxial / abaxial determinants is regulated via small RNA pathways (Husbands et al., 2009). For instance, miR166, expressed at the abaxial side, promotes the cleavage of HD-ZIPIII mRNA, restricting the expression of these genes in the adaxial side; while in opposition, tasiARFs expressed at the adaxial developing primordia moves abaxially to target *ARF3* and *ARF4* restricting the expression of these genes in the abaxial side (Figure 15b)(Chitwood and Timmermans, 2010).

In *Arabidopsis* the demarcation of boundaries between cells expressing *STM* and those lacking its expression is a requirement for the initiation of organ primordia. These boundaries, which separate lateral organs from the adjacent meristem, are characterized by low cell division rates and specific patterns of gene expressions (Aida et al., 1997; Breuil-Broyer et al., 2004; Reddy et al., 2004; Takada et al., 2001). In addition to its regulating role in the meristem, STM functions in the specification of this boundary domain. In *Arabidopsis* the NAM-ATAF1/2-CUC2 (NAC) family of transcription factors, CUPSHAPED COTYLEDON 1 (CUC1), CUC2 and CUC3 control the formation of organ boundaries in the shoot (Aida et al., 1997; Aida et al., 1999; Vroemen, 2003). *STM* and *CUC* regulate each other's expression all throughout development (Hibara et al., 2006; Spinelli et al., 2011; Vroemen, 2003). Since the expression of *CUC* genes overlaps with the slowly dividing cells of the boundaries, it has been thought that CUC proteins might repress growth and inhibit differentiation in the

boundary regions (Aida et al., 1997; Breuil-Broyer et al., 2004; Souer et al., 1996; Takeda et al., 2011). Downstream targets of CUC proteins include *LIGHT-DEPENDENT SHORT HYPOCOTYL 4* (*LSH4*) and *LSH3,* which are directly activated by CUCs and supress organ inititation in the boundary (Takeda et al., 2011). Additional described regulators of boundary formation include certain members of the family of transcription factors LATERAL ORGAN BOUNDARIES DOMAIN (LBD) (Shuai et al., 2002), for instance, JAGGED LATERAL ORGANS (JLO). Its expression is firstly detected at the sites of organ initiation, where JLO seems to act as positive regulator of the expression of *STM* and *BP* (Borghi et al., 2007), thereby promoting the exit of these cells from a meristematic state. Once organs are established, the expression of JLO gets restricted to the boundary (Rast and Simon, 2012). A second LBD member involved in boundary specification is LATERAL ORGAN BOUNDARIES (LOB), which regulates the boundary region by restricting the accumulation of brassinosteroids. LOB was suggested to directly activate *PHYB ACTIVATION TAGGED SUPRESSOR1* (*BAS1*), which encodes a brassinosteroid-inactivating enzyme. In turn *LOB* expression is regulated by brassinosteroids, by this means creating a feedback loop to modulate the local accumulation of brassinosteroids (Bell et al., 2012). As already discussed, brassinosteroids have proven functions in cell expansion and proliferation, hence low brassinosteroid activity in the boundary likely reduces cell expansion and division. In addition, the brassinosteroid transcription factor BZR1 directly represses the expression of *CUC* genes (Gendron et al., 2012), thus low brassinosteroid activity in the boundary zone also allows the induction of *CUC* genes (Figure 14b).

In addition to the regulatory gene network involved in the establishment of the boundary, a characteristic feature of boundary zones is low auxin concentrations and signaling. In contrast, organ initiation is closely correlated with the accumulation of auxin. Contrary to the meristem, the incipient primordium has a high auxin to cytokinin ratio, high levels of giberellic acid and likely high brassinosteroid activity (Tsuda et al., 2014). Auxin depletion from the boundary and accumulation in the incipient primordia induces organ initiation by restricting the expression of *CUC* and *KNOX* genes (Furutani et al., 2004; Vernoux et al., 2000). I will further discuss the role of auxin as positive regulator of organ primordia in the inflorescence meristem in the next section.

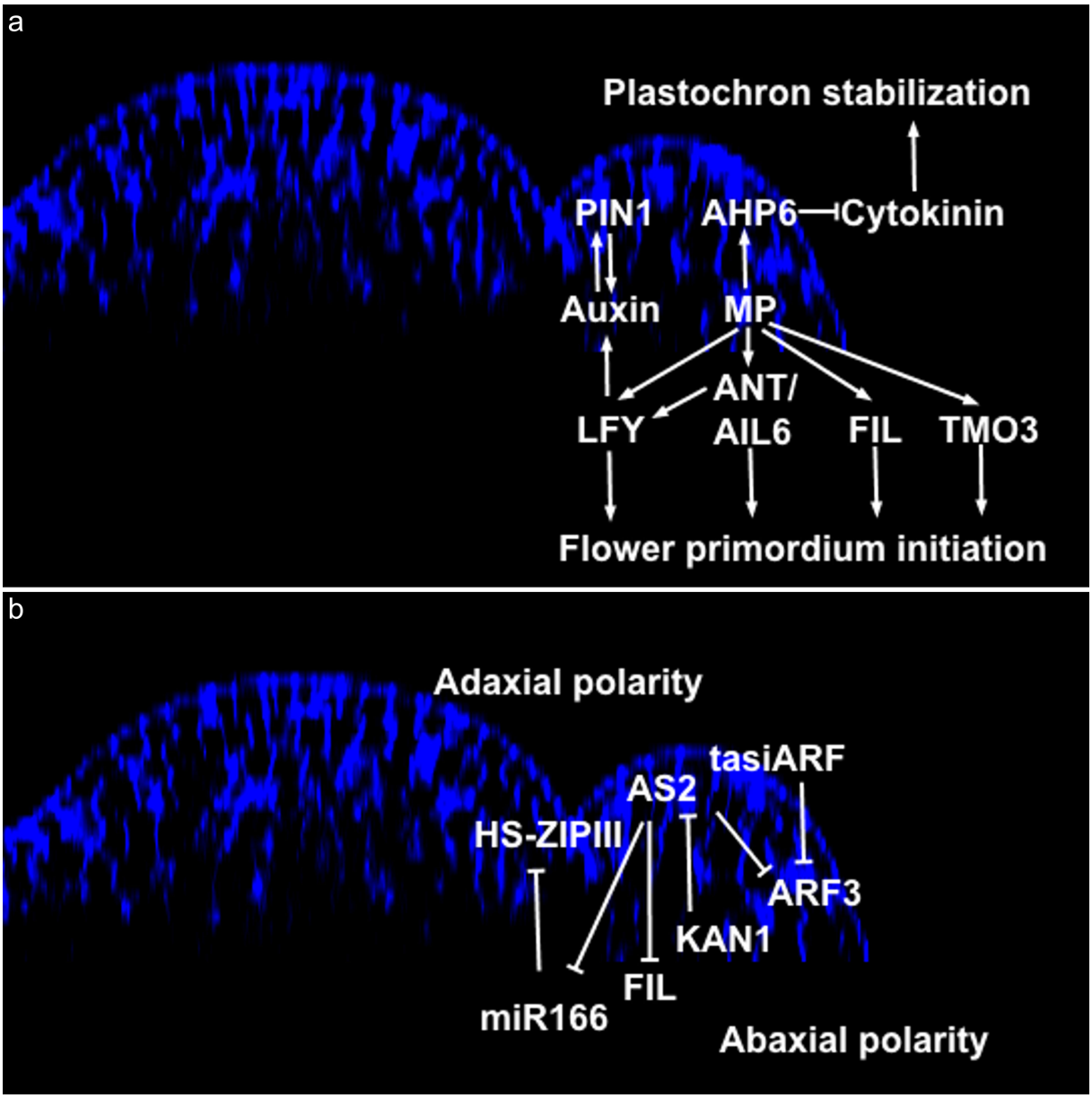

Figure 15. The initiation of flower primordia and the acquisition of organ polarity.
(a) The initiation of lateral organs is determined by the auxin/PIN1 feedback loop. Downstream of auxin, MP regulates the expression of LFY, ANT, AIL6, FIL and TMO3 transcription factors, which altogether promote flower primordium initiation. MP also regulates AHP6 expression, which allows the spatiotemporal establishment of cytokinin signalling, thereby stabilizing the plastochron.
(b) HD-ZIP III genes are restricted to the adaxial side by the inhibition of miR166. KAN proteins become active on the abaxial side of the primordium, they directly repress AS2 confining its activity to the adaxial side.

4. Flower initiation as model system to understand plant morphogenesis

The SAM initially gives rise to vegetative organs, but at some point the SAM makes the transition to reproductive development. The transition from the vegetative phase to the reproductive phase, called the floral transition, is marked by the conversion of the shoot apical meristem into an inflorescence meristem. This event is characterized by several physiological changes; the elongation of the stem, the acceleration of cell division, and the formation of flowers in the flanks of the shoot apex (Kwiatkowska, 2006; Steeves and Sussex, 1989).

The floral transition is the culmination of a complex interaction of multiple environmental and endogenous inputs. Ultimately, these inputs promote the activation of a group of genes termed floral pathway integrators. In *Arabidopsis* the main integrator is *LEAFY* (*LFY*), which not only confers flower mersitem identity, but also plays a central role in controlling the identity of individual floral organs (Parcy et al., 1998). This gene is already weakly expressed during the vegetative phase in leaf primordia and a dramatic increase in its expression is necessary for the floral transition (Blazquez et al., 1997; Hempel et al., 1997; Li et al., 2013). Two genes termed flowering time genes *FLOWERING LOCUS T* (*FT*) and *SUPPRESSOR OF OVEREXPRESSION OF CO 1* (*SOC1*) also known as *AGAMOUS-LIKE 20* (*AGL20*) are also strongly implicated in the transition from producing leaves to the production of flowers.

Flower primordia start as new meristems, which in turn will form the successive floral organs, often arranged in concentric whorls. The characteristic features that underlie the initiation of flower primordia at the flanks of the inflorescence meristem, will be described in this section paying special attention to the role of auxin and the cell wall.

4.1. The molecular regulation of flower initiation: a central role for auxin

There is strong evidence coming from work on several plant species, that auxin is concentrated at specific locations at the meristem periphery, where it induces organ initiation (Bayer et al., 2009; de Reuille et al., 2006; Heisler et al., 2005; Reinhardt et al., 2000; Reinhardt et al., 2003; Vernoux et al., 2011). The accumulation of auxin is possible through the activity of PIN membrane transporters, which often show polar localization. Since neighbouring cells frequently show a coherent distribution of these proteins, they can generate

fluxes of auxin through the tissues, causing the formation of auxin maxima at certain places and auxin depletion at others (Murray et al., 2012; Reinhardt et al., 2000; Reinhardt et al., 2003; Sassi and Vernoux, 2013). Via immunological studies the localization of PIN1, the founding member of the family of PIN efflux carriers, has been determined in the surface layers of the SAM (Benkova et al., 2003; Reinhardt et al., 2003). Cell membranes carrying PIN1 in the epidermis seem to be preferentially oriented toward the incipient primordia, coinciding with the sites of high intracellular auxin (Benkova et al., 2003; Brunoud et al., 2012; de Reuille et al., 2006; Heisler et al., 2005; Reinhardt et al., 2003; Vernoux et al., 2011). Subsequently, upon bulging of the organ primordium, the polarity of PIN1 reverses at the boundary and is then directed towards the center of the SAM. Since both the organ and meristem itself continue to act as auxin sinks, a low auxin domain is created that corresponds to the boundary region (Wang et al., 2014). As discussed above, it was proposed that these low auxin levels permit the activation of the CUC genes.

The precise cellular mechanisms by which the coordination of auxin transport between cells occurs is not entirely understood, but two general classes of theoretical models have been proposed to explain the patterns at the meristem surface: flux-based and concentration-based models (van Berkel et al., 2013). Flux based-models were the first to be proposed and are based on the hypothesis that cells experiencing the flux of auxin in a certain direction will increase their capacity to transport the hormone in that direction (Rolland-Lagan and Prusinkiewicz, 2005; Sachs, 1981). In this type of models small auxin fluxes through the membrane may be amplified by the polar localization of PINs, which point in the direction of the original flux (Alim and Frey, 2010; Feugier et al., 2005). Concentration-based models suggest that cells are able to sense the concentration of auxin and direct its transport towards the neighbouring cell with the highest auxin level (Jonsson et al., 2006; Smith et al., 2006). Both models can explain the patterns of PIN polarity at the meristem surface, but only the flux based model is capable of reproducing also the behaviour of PIN induced fluxes in the internal tissues (Bayer et al., 2009; Merks et al., 2007; Stoma et al., 2008). Nevertheless, it remains unclear which precise cellular mechanism directs PIN allocation in the SAM.

The presence of PIN1 is essential for the transport of auxin in the meristem. Reduction of auxin transport has been reported in the loss-of-function mutant *pin-formed 1* (*pin1*) (Bennett et al., 1995; Okada et al., 1991). The *pin1* phenotype is striking, with most of the effects observed at the level of flower initiation. Impaired auxin transport in the inflorescence results

in the formation of naked inflorescence stems, which are unable to initiate flower primordia (Okada et al., 1991; Vernoux et al., 2000). In a similar manner, impairment of auxin transport by polar auxin transport inhibitors, such as *N*-1-naphthylphthalamic acid (NPA) and 2, 3, 5-triiodobenzoic acid (TIBA), results in defects in the formation of lateral primordia in the shoot apex (Grandjean et al., 2004; Okada et al., 1991). Notably, the local application of auxin on the naked inflorescence apex of *pin1* mutants and NPA treated plants restores the initiation of lateral primordia (Reinhardt et al., 2000).

The transient accumulation of auxin feeds into a complex network of molecular regulators, which has been relatively well characterized. As already mentioned, the core machinery of auxin-dependent gene regulation comprises the ARFs and their binding partners the Aux/IAA. At the inflorescence meristem of *Arabidopsis*, the sites of incipient primordia and high auxin levels are coincident with the expression of *ARF5/ MP* and a range of other *ARF*s (Vernoux et al., 2011). *MP* is very strongly expressed, and like *pin* mutants, *monopteros* (*mp*) mutants, are unable to initiate flower primordia (Hardtke and Berleth, 1998; Odat et al., 2014; Przemeck et al., 1996). The naked meristem of *mp* are unresponsive to externally applied auxin (Reinhardt et al., 2003), which indicates that auxin signaling largely triggers flower primordium initiation via ARF5/MP (Przemeck et al., 1996).

In the incipient primordia auxin activated MP acts at several levels. As mentioned in the previous section, MP induces the expression of a number of direct targets ultimately leading to the initiation of flower primordium (Figure 15a). Cell division and growth is promoted via the activation of expression of *ANT* and *AIL6*. The peripheral fate and the abaxial polarity is promoted via the activation of *FIL*. Finally, floral identity is promoted via the activation of *LFY* (Wu et al., 2015; Yamaguchi et al., 2013). In addition, MP induces the expression of *AHP6,* which encodes a negative regulator of cytokinin signaling that diffuses to neighbouring initium to prevent the initiation of new floral primordia (Besnard et al., 2014). MP also represses in the central region of the shoot apex two negative regulators of cytokinins, *ARR7* and *ARR15* (Zhao et al., 2010), and in the incipient primordia MP induces the expression of the cytokinin response factor (CRF) TMO3/CRF2 (Rashotte et al., 2006), thus promoting cytokinin responses in incipient flower primordia. Additional feedbacks and feed-forward loops come into action during flower primordium initiation. For instance, ANT and AIL6 both induce *LFY,* and LFY in turn reinforces auxin transport (Li et al., 2013; Yamaguchi et al., 2016; Yamaguchi et al., 2013; Yamaguchi et al., 2014). AIL/PLT genes

contribute to control the transport and synthesis of auxin (Pinon et al., 2013; Prasad et al., 2011). While MP orients non-cell autonomously the polarity of PIN1, thereby facilitating a positive feedback loop (Bhatia et al., 2016).

Once established and after an initial growth phase, the flower primordium acquires meristematic features. This includes the expression of *WUS* and *CLV3* and the establishment of an organizing center and a stem cell niche (Figure 16a)(Gruel et al., 2016). The identity of the floral primordia relies on the activity of LFY, which later on also plays a role in controlling the identity of individual floral organs (Parcy et al., 1998). In the flower meristem, LFY positively regulates the expression of the MADS-domain transcription factors APETALA1 (AP1) and its homolog CAULIFLOWER (CAL) (Kempin et al., 1995). AP1 together with SHORT VEGETATIVE PHASE (SVP) and AGL24 MADS-domain transcription factor specify floral identity and maintain the flower meristem in a meristematic state during the early stages of the flower (de Folter et al., 2005). After establishment of the floral meristem, the patterning of the flower is activated with the upregulation of the floral homeotic genes (reviewed in (O'Maoileidigh et al., 2014; Wils and Kaufmann, 2017). Typically, angiosperm flowers are characterized by sterile perianth organs in the outer whorls, followed by reproductive organs in the inner whorls. According to the classical ABC model, floral organ identities are specified by functional gene classes (Causier et al., 2010; Haughn and Somerville, 1988). In *Arabidopsis*, sepal identity specification is mediated by A-class protein AP1 combined with E-class proteins SEPALLATA1-4. Petal identity is defined by AP1 together with the B-class proteins AP3, PISTILLATA (PI), and SEP proteins. Stamens are specified by the C-class protein AGAMOUS (AG) with AP3 and PI, while carpels are specified by AG and SEP complexes (Honma and Goto, 2001) (Figure 16a).

As we have already seen, MP signalling activates diverse developmental processes during flower primordium inititation. It directs the specification of floral fate, cell proliferation and growth, the establishment of organ polarity, and cytokinin responses. Nevertheless, is not clear how the activation of these transcriptional regulators influence the physical events behind the shape changes that lead to the emergence of the flower primordia. In the following section I will address this issue including some putative targets of these transcription factors.

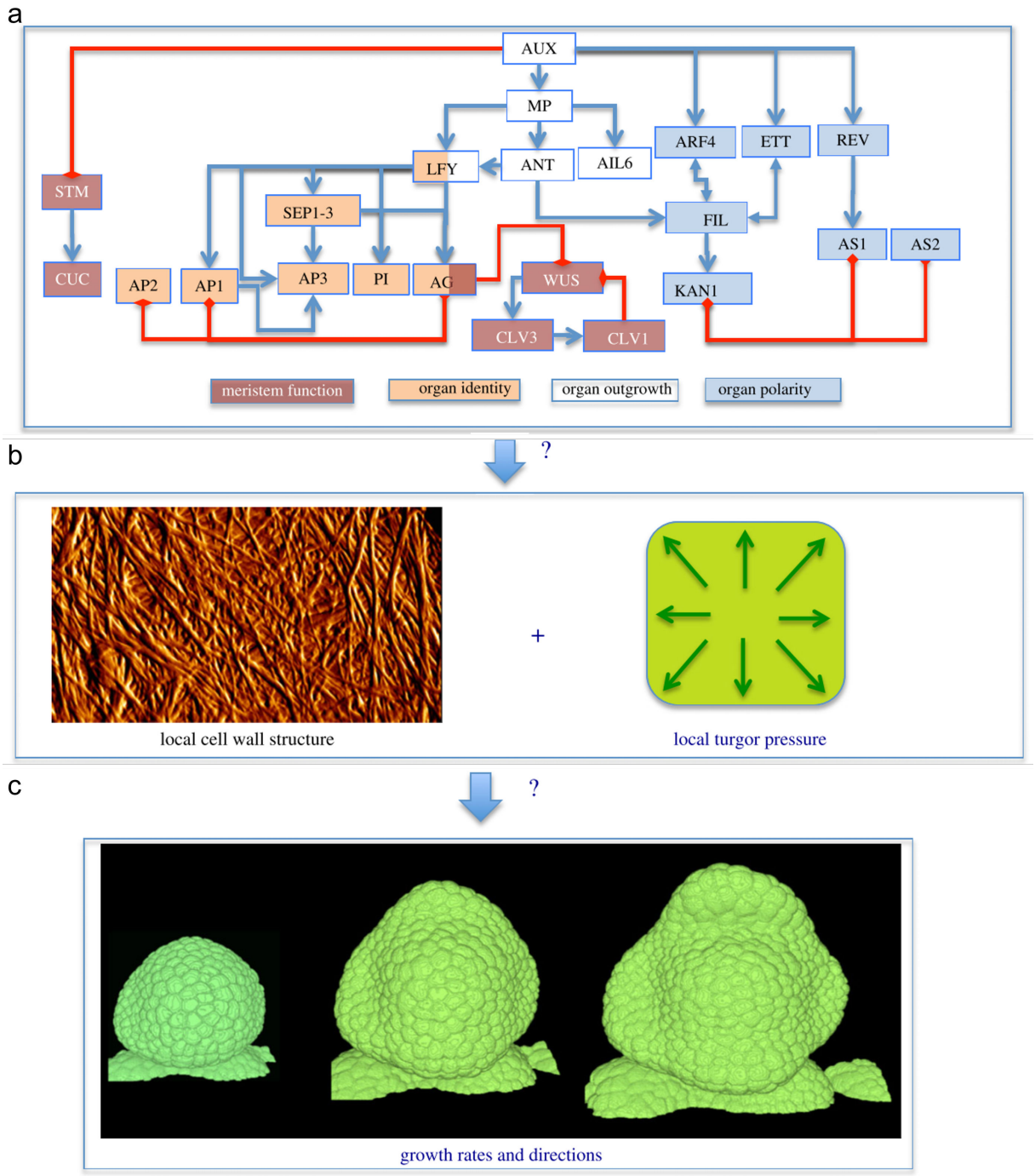

Figure 16. General concept of floral morphogenesis (adapted from (Abad et al., 2017))
(a) Auxin activates a molecular network of transcriptional regulators associated with diverse developmental processes, such as cell or organ identity, cell proliferation and growth, organ polarity.
(b) The molecular network must interfere with the cell wall mechanical properties in order to influence growth. Cellulose microfibrils in a meristematic cell wall as viewed with atomic force microscopy (left) Modifications in the cell wall make it yield to the turgor pressure at different rates and directions (right).
(c) The changes in shape, here illustrated by an *Arabidopsis* growing flower bud.

4.2. The physical regulation of flower initiation: a central role for the cell wall

As we have seen, the mechanochemical state of the cell wall is a fundamental link between molecular growth regulation and the effective shape evolution of the tissue (Figure 16b). Therefore to control morphogenesis, the above mentioned genetic network controlling flower primordium initiation should somehow modulate the synthesis or remodelling of the cell wall. In the two following subsections I will give an overview of the state of the art on this topic at the onset of my thesis.

4.2.1. Control of growth anisotropy the dialog between mechanical forces and the cytoskeleton

Several studies have focused on the regulation and role of wall anisotropy during organ initiation (Baskin, 2005; Uyttewaal et al., 2012). As the microfibrils themselves cannot be visualized directly *in vivo*, these studies looked at microtubule dynamics, which are guiding cellulose deposition (Bringmann et al., 2012; Gutierrez et al., 2009; Li et al., 2012; Paredez et al., 2006). An important feature of the growing meristem is that the outer (surface) wall seems to be loadbearing (Beauzamy et al., 2015; Kierzkowski et al., 2012; Milani et al., 2011; Savaldi-Goldstein et al., 2007). This hypothesis is supported by the fact that this wall is much thicker than the inner walls (typically 200-250 nm versus 80-120 nm in the *Arabidopsis* inflorescence according to our own unpublished results). This feature also represents an important advantage for experimentation, as the outer cells are easy to visualize *in vivo* using standard confocal microscopy.

Careful analysis of microtubule dynamics at the meristem, have revealed stereotypic behaviour and supracellular arrangements of the CMT arrays (Figure 17a)(Burian et al., 2013; Hamant et al., 2008; Sampathkumar et al., 2014; Uyttewaal et al., 2012). At the tip of the SAM microtubules are highly dynamic, showing isotropic arrangements. Towards the flanks of the meristematic dome and along the stem, microtubules show more anisotropic arrangements, perpendicular to the apical-basal axis, in particular along organ boundaries (Burian et al., 2013; Hamant et al., 2008). How microtubule orientation is coordinated at the supra-cellular level is not understood. However, as the microtubules seem to align along the predicted force fields at the meristem surface, it was proposed that the cells are somehow able to sense these forces and to reorganize their cytoskeleton and reinforce their walls accordingly

(Figure 17b)(Hamant et al., 2008; Uyttewaal et al., 2012). Would such a mechanism be sufficient to generate the morphodynamics seen *in vivo*? To address this and other questions, several authors have turned to mechanical models in the form of virtual tissues (Ali and Traas, 2016). Mechanical models where a feedback between mechanical forces and the cytoskeleton were simulated were able to reproduce typical morphological structures, such as cylindrical stems or an outgrowing primordium (Hamant et al., 2008). It is important to note that this is a typical example of self-organization: cells locally react to a mechanical signal, which more globally leads to particular shapes of the entire cell population. Later studies have further supported the hypothesis, that a feedback between mechanics and microtubules might play an important role in morphogenesis (Hervieux et al., 2016; Sampathkumar et al., 2014).

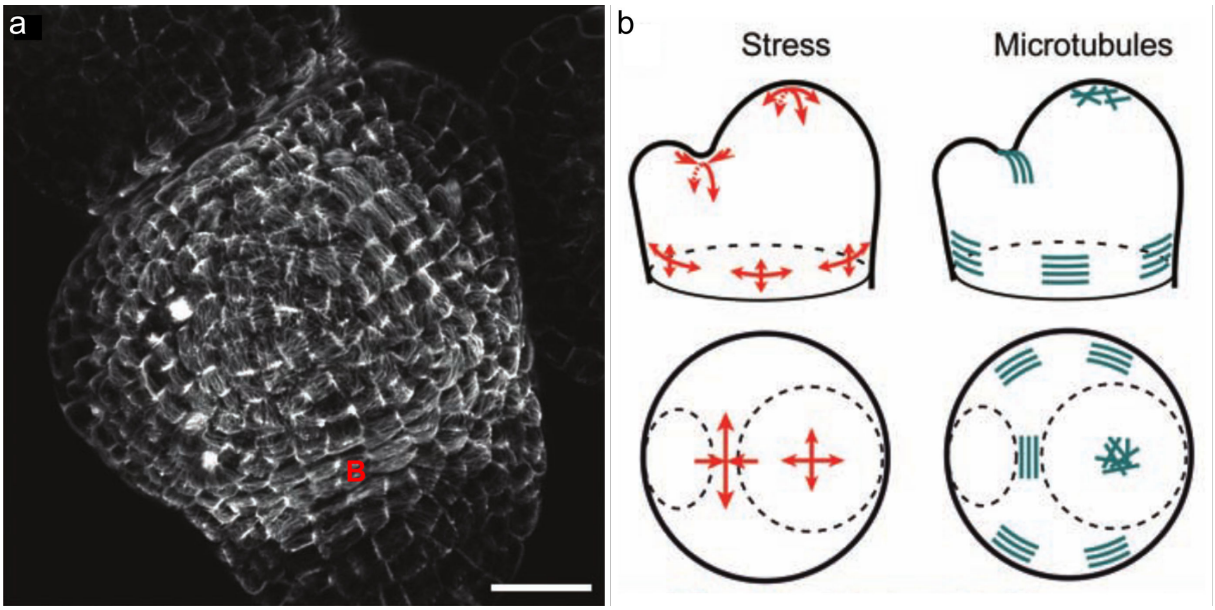

Figure 17. The mechancical feedback between stress and microtubule orientation in the SAM (adapted from Hamant et al., 2008)
(a) Patterns of cortical microtubules in the SAM as visualized following the expression of p35S::GFP-MBD fluorescent marker. The arrays of microtubules at the apex do not show a clear orientation, especially in comparison with the organ boundaries (B).
(b) As a result of the geometry of the SAM, which results from local differences in growth, mechanical stresses are produced. At the apex of the meristem the mechanical stress is equivalent in all directions, or isotropic; whereas in the meristem-to-organ boundary, the direction of stress is anisotropic, given the differential growth of contiguous regions (red). Cortical microtubule alignment follows the direction of maximal stress (green).

4.2.2. Control of growth rate: cell wall remodeling proteins

As indicated above, the transcriptional regulators act in principle not only on wall anisotropy but also on wall synthesis rate and stiffness. Many of the known cell wall-modifying proteins target the matrix molecules in which the cellulose microfibrils are embedded. As discussed earlier, these can be roughly divided in three subcategories, (i) pectin modifying enzymes such as pectin methyl esterases (PMEs) or pectin methyl estherase inhibitors (PMEIs), (ii) enzymes targeting the hemicellulose chains such as xyloglucan endotransglycosylase/hydrolases (XTHs) and (iii) expansins which possibly target hydrogen bond between hemicelluloses (Wolf et al., 2012a). Little is known about the precise molecular regulation of these cell-wall modifying proteins, but many of them can be found among the published potential targets of many transcription factors (Krizek et al., 2016; Peaucelle et al., 2011a; Yadav et al., 2009).

What is the precise function of these wall modifying proteins? Whereas many mutants perturbed in wall synthesis have been described, very few of them have been characterized at the level of the SAM. Nevertheless, experiments where the activities of some of these modifying enzymes are manipulated show their potential importance in organ formation at the shoot apex. For instance, local applications of expansins on SAMs of tomato induce the formation of ectopic leaf-like organs (Fleming et al., 1997). More recently, the possible roles of PMEs and PMEIs in organ formation at the inflorescence meristem of *Arabidopsis* have been explored (Peaucelle et al., 2011a; Peaucelle et al., 2008; Peaucelle et al., 2011b). These enzymes control the stiffness of the pectin matrix. Antibodies recognizing specific modifications in pectins chains indicate that specific meristematic zones, in particular organ boundaries, are likely to have a stiffer pectin matrix. Interestingly, overproduction of PMEI completely inhibits organ formation at the shoot apex, whereas local applications of PME induces extra flowers.

These experiments point to a scenario where matrix molecules are stiffened or loosened at sites where growth has to be respectively inhibited as in organ boundaries or increased as in organ primordia. Several attempts have been made to test this hypothesis using atomic force microscopy (AFM) to measure the local stiffness of the walls. Depending on the thickness of the AFM probes used, different results were obtained. Thicker probes (1-5 μm) indicated that

the inner walls became more elastic at the moment of organ initiation. However, when very small probes (10 nm) were used to measure only the supposedly limiting outer wall, relatively minor differences were observed, not exceeding a reduction of 20-50 % in stiffness in the very young initium (Peaucelle et al., 2011a; Sassi et al., 2014).

5. Concluding remarks and Objectives of the thesis

As we have seen the production of patterns, relies on multiple factors: the physical properties and mechanical forces of the system (Thompson, 1917), its intrinsic system of chemical substances (Turing, 1952) with its particular properties (e.g. diffusion, reaction, autocatalysis, lateral inhibition (Gierer and Meinhardt, 1972; Meinhardt and Gierer, 2000)), the interpretation of this chemical system by the responsive tissue (Wolpert, 1969, 1971) as well as the properties of the tissue which makes it responsive but resilient at same time (Waddington, 1956, 1957). In principle, these factors and their interactions are able to coordinate the production of multiple diverse and reproducible shapes.

Pattern formation in plants relies on certain aspects of their cell biology. Plant cells remain glued together through their cell walls. As a result, morphogenesis is basically a matter of localized cell growth largely through cell wall modifications. As in animals, cell-cell communication is essential to establish the local differences that guide tissue morphogenesis. Cell communication (chemical and physical) feeds into molecular regulation, which then controls cell wall modifications. Although this general scenario is well accepted, it is not clear at all how this functions.

Through this thesis I have studied patterning in plants. I have used the shoot apical meristem of *Arabidopsis* as a system of study and the initiation of lateral organs from the inflorescence meristem as the patterning event. The structure and function of the molecular networks orchestrating flower primordium initiation are quite well understood. The initiation of new organs is determined by the local accumulation of auxin, which exerts its function by activating the expression of a group of transcription factors. Each of them related with the activation of diverse developmental processes. An oversimplified view of this process is that auxin activates ARF5/MP, which directly regulates the transcription of *LFY*, *ANT* and *AIL6* whose activities ultimately lead to the initiation of flower primordium (Wu et al., 2015; Yamaguchi et al., 2013). However how this molecular network interferes with cell wall structure to direct the intiation of flower primordia remains unclear.

To gain insight into the patterning event of flower primordium initiation in *Arabidopsis*, I have studied three different aspects:

(i) I firstly addressed the role of cell wall anisotropy in the initiation of organ outgrowth and how this relates with the local accumulation of auxin and the patterns of CMT organization;
(ii) secondly, I studied the function of cell wall remodeling and its coupling to CMT organization;
(iii) finally, I explored the transcriptional control of organ initiation by analyzing the canonical ARF5/MP-regulated pathway and how it could be linked to cellular anisotropy via feedback.

Chapter I

An Auxin-Mediated Shift toward Growth Isotropy Promotes Organ Formation at the Shoot Apical Meristem in *Arabidopsis*

Ursula Abad, Massimiliano Sassi, and Jan Traas

Summary

To control morphogenesis, spatiotemporal patterns of gene expression somehow must interfere with the mechanical properties of the individual cells of developing organs and tissues, ultimately resulting in different growth patterns. Nevertheless, the characterization of the mechanisms that link gene activities to cell behaviors remain to be defined. We study the process of morphogenesis in the shoot apical meristem, a group of undifferentiated cells where complex changes in growth rates and directions drive the formation of new organs in a periodic and continuous manner (Murray et al., 2012; Sassi and Vernoux, 2013). Here, we show that the plant hormone auxin plays an important role in this process by interfering with wall anisotropy via the regulation of cortical microtubule dynamics. We propose that to induce growth isotropy and organ outgrowth, auxin interferes with the cortical microtubule-ordering activity of a network of proteins, including ROP6/RIC1 and KATANIN. Moreover we provide evidence that the microtubule rearrangements occuring during organ initiation require the auxin regulated transcription factor MONOPTEROS/AUXIN RESPONSIVE FACTOR 5.

This chapter describes the results that are directly related to my contribution to our publication in Current Biology (Sassi et al., 2014), see annex 1. I mainly contributed to the characterization of the cortical microtubule-ordering pathway. I performed the crosses and the isolation of the transheterozygous mutant *abp1-1s/abp1-5*, *abp1-1s/abp1-5 35S::GFP-MBD* and *bot1-7 abp1-5*. The characterization of wild type and these mutants as well as the *rop6-1, ric1-1 and pin1-6 bot1-7* were done in collaboration with Massimiliano Sassi. In addition, the chapter contains my unpublished results regarding the role of MP/ARF5. The crosses, isolation and characterization of the mutants *arf5-1 bot1-7* and the *arf5-1 PDF1::mCitrine-MBD* were done by myself as well as the analyses of these data. The *PDF1::mCitrine-MBD* fluorescent line was produced by Thomas Stanislas.

Introduction

A specific requirement for the initiation and positioning of organs in the SAM of *Arabidopsis* is the local accumulation of the hormone auxin (IAA). This is achieved at the meristem surface, via the PIN-FORMED1 (PIN1) auxin efflux carrier (Benkova et al., 2003; Heisler et al., 2005; Reinhardt et al., 2000; Reinhardt et al., 2003). The importance of auxin transport is clearly illustrated by the phenotype of *pin1* loss-of-function mutants, which form naked inflorescence meristems, unable to initiate flower primordia (Okada et al., 1991). This phenotype is also obtained by chemical treatments using inhibitors of auxin transport such as N-1-naphthylphthalamic acid (NPA). This and additional evidence indicate that auxin accumulation is indispensable for the initiation of lateral organs (Kuhlemeier, 2017; Reinhardt et al., 2000; Reinhardt et al., 2003). However, how auxin precisely functions in this process remains unclear.

To induce organ outgrowth, auxin has to modify directly or indirectly growth rates and growth directions which in plants largely rely on the mechanical properties of the cell wall. Previous studies have pointed to the importance of wall remodeling and elasticity at the SAM, via wall-loosening proteins (Fleming et al., 1997; Peaucelle et al., 2008). Auxin is thought to promote primordia formation, at least in part through this process (Murray et al., 2012; Sassi and Vernoux, 2013). However, this represents a rather one-sided view of the contribution of wall mechanics to organogenesis.

Here, we will focus on mechanical anisotropy, another essential property of the wall which mainly depends on the orientation of cellulose microfibrils and plays a central role in defining growth directions (Bashline et al., 2014; Baskin and Jensen, 2013; Ivakov and Persson, 2013). The deposition of the cellulose microfibrils is controlled by the cortical microtubules (CMT), which guide the cellulose synthesis complexes, controlling the orientation of the cellulose microfibrils (Bringmann et al., 2012; Gutierrez et al., 2009; Paredez et al., 2006). Consequently, the organization of the CMT has been used as proxy to predict the direction of the cellulose microfibrils and the anisotropy of the cell wall. We show here that auxin interferes with CMT organisation during organ initiation at the SAM. We present evidence that this involves a pathway depending on ROP6 as well as its partners RIC1 and KATANIN.

Results

Transgenic plants, expressing the green fluorescent protein (GFP) fused to a microtubule-binding domain (MBD) of the microtubule-associated protein 4 (MAP4), both under the expression of the Cauliflower mosaic virus (CaMV) promoter 35S (35S::GFP-MBD), permit the analysis of microtubules dynamics by live imaging. Since it has been considered that the epidermal L1 layer is rate limiting for growth, analyses of the cytoskeleton have been mainly focusing on this layer (Kierzkowski et al., 2012; Reinhardt et al., 2003; Savaldi-Goldstein et al., 2007). Notably, the naked meristems of plants grown on NPA (Hamant et al., 2008), exhibited supracellular, circumferential alignments of CMT at the periphery of the meristem and the stem. This orientation is thought to impose cell expansion in one main direction, along the vertical axis. In other words, in the absence of auxin transport plants are forced to grow in one main direction because of the anisotropic arrangement of the CMT of the individual cells (Hamant et al., 2008). This implies that to induce a lateral organ, auxin has to break this radial symmetry. How this occurs is not known.

To address this issue we set up an experimental system in which we could follow the dynamics of CMT from an anisotropic pin-shaped SAM. We grew *Arabidopsis* plants bearing the 35S::GFP-MBD transgene on NPA-containing medium, which prevents the formation of flowers. Subsequently, we treated the naked SAM with IAA, which induced changes in the organization of CMT across the SAM of 35S::GFP-MBD plants (Figure 1d and e). Already within the first 24hr following the treatment, the anisotropy of the CMT at the peripheral zone of the SAM was lost (Figure 1e). Notably, these changes in the organization of CMT preceded the production of lateral outgrowths, clearly visible after 72hr from the initial treatment with IAA (Figure 1d). After 96hr of treatment, a characteristic ring-like outgrowth emerging from the peripheral zone could be distinguished.

Discrete regions displaying disorganized CMTs were also observed in the SAM of soil-grown plants, i.e. in the presence of an active auxin transport and preexisting lateral organs. These regions displayed substantially different GFP-MBD patterns, compared to highly anisotropic organ boundaries (Hamant et al., 2008), and produced visible organ primordia 24 hr later (Figure 1a and b) (Hamant et al., 2008). The appearance of these regions correlates in time and space with peaks of high auxin activity indicated by the auxin-signalling synthetic

reporter DR5::VENUS-N7 (Figure 1c). These results suggest that in normal untreated meristems changes in CMT anisotropy coincide with auxin maxima and precede organ outgrowth at the SAM. It has been shown for other tissues, that auxin (IAA) induces rapid changes in the orientation of microtubules in growing cells (Bergfeld et al., 1988; Nick et al., 1990).

The previous findings suggested a correlation between three events, all taking place in the periphery of the SAM: the creation of local auxin maxima, the reorganization of CMT, and the formation of lateral outgrowths. The relationship between these three events was further explored by addressing whether the reorganization of CMT could be instrumental in the formation of lateral outgrowths. To do so, plants with impaired auxin transport were first exposed to the microtubule depolymerizing drug oryzalin. Since high global oryzalin treatments lead to complete loss of CMT polymerization (Corson et al., 2009; Hamant et al., 2008), local treatments of this drug were applied. These treatments are performed by local application in the periphery of the SAM of lanolin paste emulsified with oryzalin. *pin1* mutants or NPA grown plants treated locally with oryzalin initiated the production of lateral outgrowths already after 72hrs from the local treatment with oryzalin.

We next altered CMT dynamics by using the *bot1-7* mutant allele of *KATANIN1* (*KTN1*). *KTN1* encodes a microtubule-severing protein that promotes bundling and ordered alignment of CMT patterns (Bichet et al., 2001; Burk and Ye, 2002; Stoppin-Mellet et al., 2006). Importantly, the modulation of CMT orientation via KTN1 has been linked to an auxin signaling pathway (Lin et al., 2013; Xu et al., 2014; Xu et al., 2010).

bot1-7 plants grown on NPA, are more prone to initiate lateral outgrowths and to produce flowers than wild type (WT) plants grown in the same conditions (Figure 1f). Notably, the double mutant *pin1-6 bot1-7* reestablished the formation of lateral outgrowths (Figure 1g). Thus, in auxin transport-depleted backgrounds, the *bot1-7* mutation replicates the effect of auxin treatments on CMT organization and organ initiation. Relevantly, auxin treatments were not able to further affect CMT in *bot1-7* SAMs. This suggests that (1) at low auxin concentrations, KTN1 leads to the formation of a pin, and (2) KTN1 is no longer able to maintain a pin in the presence of high auxin levels.

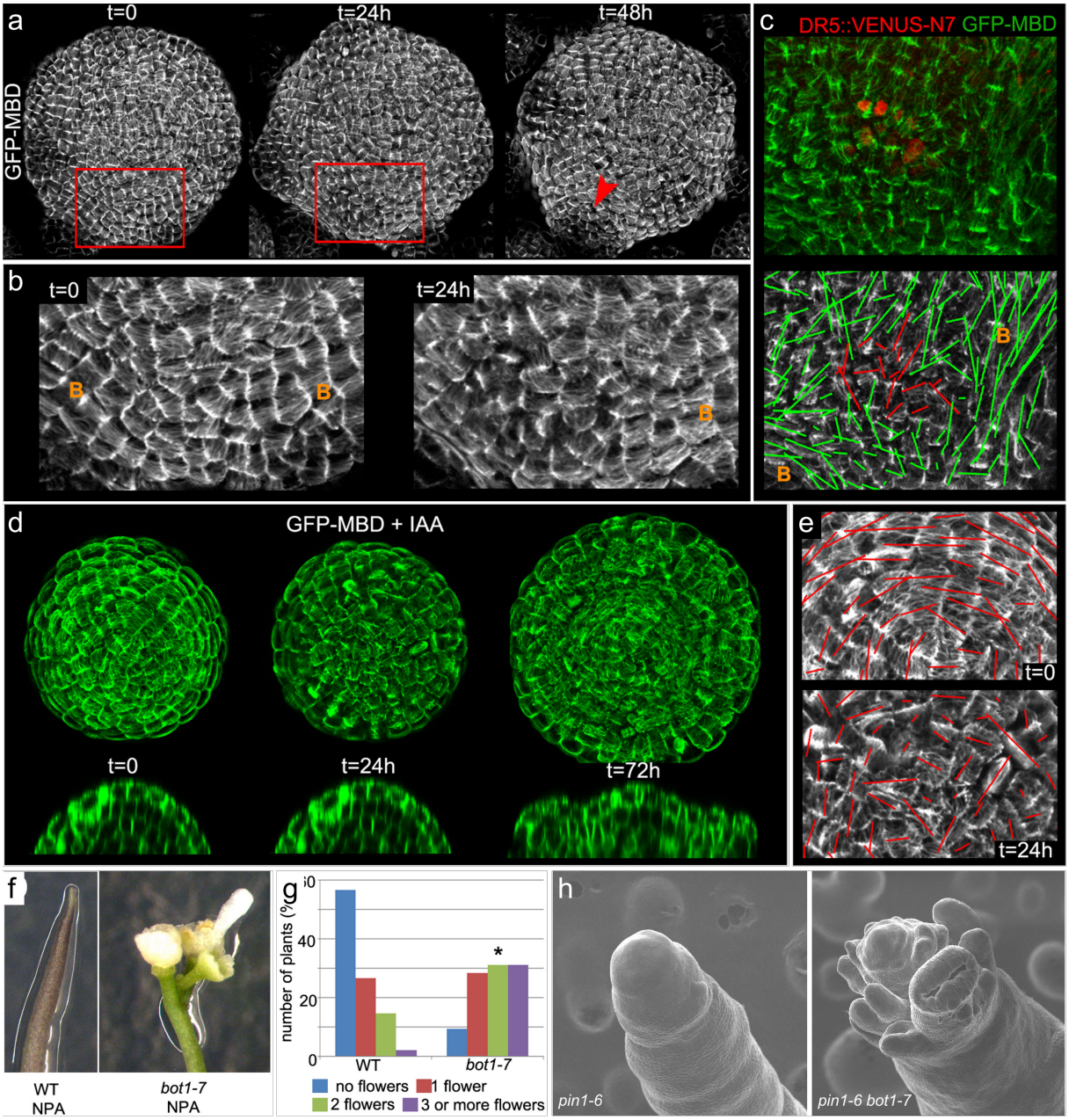

Figure 1. Auxin disrupts CMT organization at the SAM before organ outgrowth

(a) SAM of 35S::GFP-MBD plants grown on soil, time course showing the formation of a flower primordium (arrowhead).

(b) Detailed CMT organization in the regions highlighted in red in (a) at t=0 and t=24. B, boundaries.

(c) Spatiotemporal overlap between CMT disorganization and peaks of auxin activity. Upper panel shows CMT as visualized with the 35S::GFP-MBD marker (green), the incipient primordium presents DR5::VENUS-N7 (red). Lower panel shows the CMT measurements of the regions with (red) and without (green) expression of DR5::VENUS-N7. Those with expression display more disorganized CMT patterns compared to highly anisotropic boundaries (B)

(d) Surface projections of a 35S::GFP-MBD SAM treated with IAA to induce organ formation

(e) CMT organization of the SAM shown in (d) before (t=0) and after (24=hr) the initial application of IAA. The red lines are a representation of the of the CMT anisotropy. The direction and length of the lines indicate the average orientation and the anisotropy of the CMT in each cell. Notice that orientations are more random and the length of the lines shorter at t=24 in comparison with t=0.

(f) *bot1-7* mutation promote the formation of organs in absence of auxin transport. Shoot apices of NPA-grown WT and *bot1-7* plants. Notice the spontaneous formation of flower in *bot1-7*.

(g) Quantifications of the phenotypes displayed in (f).

(h) *bot1-7* mutation promotes the formation of outgrowths (right) in an otherwise naked *pin1-6* background (left)

Together, these results confirm the connection between local auxin maxima in the SAM, the reorganization of CMT, and the formation of lateral outgrowths. They suggest a causal relationship of these three events. Local auxin accumulation at the periphery of the SAM leads to the loss of CMT anisotropy, which results in a shift toward an isotropic state. As a result, the formation of lateral outgrowths is promoted. This points to a causal link between loss of CMT anisotropy and organogenesis. Importantly, *bot1-7* replicates auxin treatments, suggesting that somehow the microtubule-severing activity of KTN1 might control the link between auxin and the loss of CMT anisotropy.

A ROP6-RIC1 signaling pathway is involved in the initiation of primordia in the SAM

To investigate the nature of the molecular pathway through which auxin could regulate the disorganization of CMT in the SAM, we opted to explore described pathways active in other tissues. It has been reported that in leaf epidermal pavement cells, auxin regulates the organization of CMTs into parallel arrays via a ROP signaling pathway. In this tissue, the RHO-LIKE GTPASE FROM PLANTS 6 (ROP6) and its effector ROP-INTERACTIVE CRIB MOTIF-CONTAINING PROTEIN 1 (RIC1) promote MT ordering by activating a KTN1-based MT severing mechanism. Hereby RIC1 directly binds KTN (Chen et al., 2015; Fu et al., 2005; Fu et al., 2009; Lin et al., 2013; Xu et al., 2010).

To assess further the role of KTN1 and the ROP6-RIC1 pathway in the reorientation of CMT in the SAM we ascertained the expression of *ROP6* and *RIC1* in the shoot apex by qRT PCR. Both *ROP6* and *RIC1* were expressed at the shoot apex, although at different levels. If both genes are involved in the activation of KTN, we would expect similarities between the phenotypes of *bot1* and *rop6* or *ric1* mutants. We therefore next determined the capacity of *rop6-1* and *ric1-1* mutant alleles in the production of organs in absence of auxin transport. *rop6-1* and *ric1-1* mutants grown on NPA medium displayed increased organ formation (*rop6-1*: 86%, n = 146; *ric1-1*: 68%, n = 210) in comparison with the WT (36% n = 174)(Figure 2a and b). Next, in order to determine the organization of CMT we generated *rop6-1* mutants bearing the microtubule marker 35S::GFP-MBD. This allowed us to determine the organization of CMTs following auxin treatments in r*op6-1* mutants. We treated NPA grown r*op6-1* 35S::GFP-MBD and *ric1-1* 35S::GFP-MBD with IAA as in previous experiments. This did not induce changes in CMT organization at the tissue level

and led only to a minor decrease of cellular CMT anisotropy in *rop6-1* mutants in comparison with the WT (Figure 2c -f). This indicated that auxin is no further able to reorganize the CMTs on NPA in the absence of ROP6 and RIC1, suggesting they are part of the same pathway

In contrast ROP6 and RIC1 overexpressing lines grown on NPA exhibited decreased formation of organs when compared to WT plants (Figure 2b). In particular, ROP6 overexpression significantly reduced organogenesis. Instead of the 38% (n=169) of wild type plants able to produce flower primordia, only 20% (n=121) of the ROP6 overexpressing lines were able to do so. Altogether, these results suggested that microtubule organisation is an important parameter in organ initiation. They are also pointing towards a scenario where auxin would act on mechanical anisotropy via a ROP-based pathway.

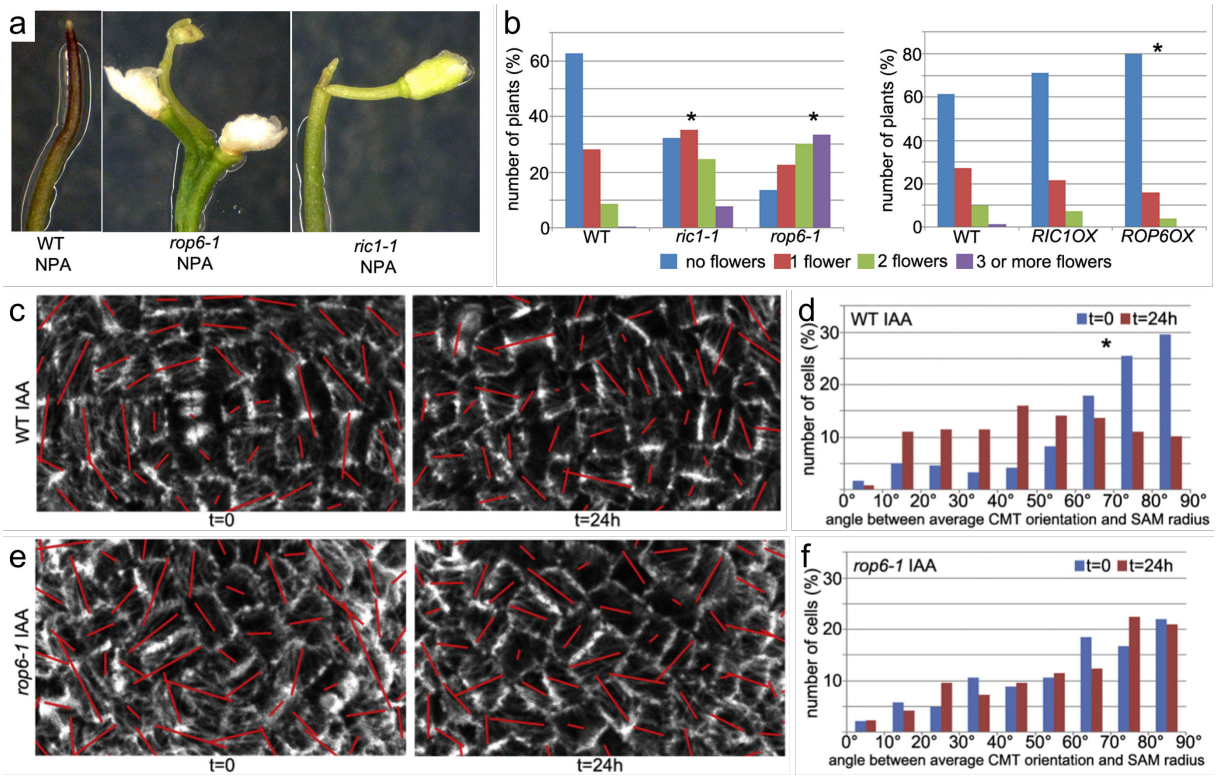

Figure 2. ROP6 and RIC1 regulate organ formation and auxin responsiveness of CMTs at the SAM
(a) Shoot apices of NPA-grown WT, *rop6-1* and *ric1-1* plants. Notice the spontaneous formation of flowers in *rop6-1* and *ric1-1*
(b) Quantification of the phenotypes of NPA-grown WT, *ric1-1* and *rop6-1* (left) and *RIC1OX* and *ROP6OX*
(c) CMT organization in cells of the shoot apex of WT plants before (t=0) and after (t=24hr) IAA
(d) Supracellular organization of CMT quantification of (c).
(e) CMT organization in cells of the shoot apex of *rop6-1* plants before (t=0) and after (t=24hr) IAA treatment
(f) Supracellular organization of CMT quantification of (e).

The ABP1-KTN1 pathway is involved in the initiation of primordia in the SAM

The ROP6-RIC1 signalling pathway that promotes the MT-severing activity of KTN1 is activated by auxin in pavement cells (Fu et al., 2005; Xu et al., 2014; Xu et al., 2010). The extracellular receptor AUXIN BINDING PROTEIN 1 (ABP1) and its functional partner transmembrane receptor-like kinases are reported to act upstream of this activation (Fu et al., 2005; Xu et al., 2014; Xu et al., 2010), although this is still a matter of debate (see discussion below). Thus, we investigated the role of ABP1 in the reorientation of CMTs at the SAM. Described *abp1* knockout mutants are embryo lethal (Chen et al., 2001). We therefore used the viable *abp1-5* allele, which contains a point mutation (H94Y) in the auxin-binding pocket of the protein that reduces the affinity of ABP1 to auxin (Robert et al., 2010; Xu et al., 2010). We firstly determined the capacity of *abp1-5* mutants to produce organs in absence of auxin transport. *abp1-5* mutants grown on NPA displayed significantly enhanced organogenesis compared to WT plants (Figure 3a and b). Next, in order to assess the organization of CMT we used the *abp1-5* mutants bearing the microtubule marker 35S::GFP-MBD (a gift from J. Friml). The naked meristem of *abp1-5* mutants displayed minor alterations in the supracellular circumferential CMT organization at the SAM periphery compared to the WT (Figure 3c and e). In addition, *abp1-5* mutants were still able to respond weakly to auxin-induced CMT reorganization and lateral outgrowth formation, although to a lesser extent than the WT (Figure 3c-f).

To gain additional understanding into ABP1 function, we generated a transheterozygous mutant by crossing homozygous *abp1-5* mutant plants with heterozygous *abp1-1s/ABP1* plants, which bears one copy of the T-DNA insertional knock-out allele *abp1-1s* (Tzafrir et al., 2004). We maintained only one allele *abp1-1s* given the lethality of its phenotype. The heteroallelic combination *abp1-1s/abp1-5* was not lethal for the mutant plants. Notably, when grown on NPA *abp1-1s/abp1-5* mutant plants displayed enhanced formation of lateral outgrowths compared with the parental *abp1-5* (Figure 3a and b). More random orientations of CMTs were also observed in *abp1-1s/abp1-5* 35S::GFP-MBD in comparison with *abp1-5* 35S::GFP-MBD (Figure 3e and g). Importantly, auxin-induced CMT reorganization and lateral outgrowth formation was completely abolished in the *abp1-1s/abp1-5* mutant background, comparable to *bot1-7* mutants (Figure 3e-h). The above is in line with the

hypothesis that ABP1 and KTN1 belong to the same signalling pathway in charge of reorganizing the CMT in the SAM and regulating the formation of lateral outgrowths.
Finally, we produced *bot1-7 abp1-5* double mutant plants and searched for additive phenotypes. Coherently with our hypothesis, no additional phenotypes could be distinguished as *bot1-7 abp1-5* grown on NPA display organ initiation phenotypes similar to those observed in the parental *bot1-7*.

Together, our results suggest that in the absence of local auxin accumulation, a network of interacting proteins, including KTN1, ROP6/RIC1 and ABP1, keep CMT arrays at the SAM periphery in an anisotropic state. We suggest that this network inhibits the spontaneous formation of lateral outgrowths, and when active it leads to the formation of a pin-shaped stem. Conversely, in the presence of high auxin levels, these molecules are no longer able to maintain CMT anisotropy, which results in a shift toward an isotropic state, in principle this could be sufficient for the formation of lateral outgrowths.

The auxin response factor ARF5/MONOPTEROS is required for microtubule reorganization at the SAM

The ROP-based signaling pathway does in principle not require transcription. We note, however, that the reorganization of CMT partially overlaps with the activation of the auxin transcriptional reporter DR5::VENUS-N7 (Figure1c). Auxin induced transcriptional responses are regulated by transcription factors of the AUXIN RESPONSE FACTOR (ARF) family (Chapman and Estelle, 2009). In the SAM, ARF5/MONOPTEROS (MP) is the main ARF required for flower formation (Guilfoyle and Hagen, 2007; Hardtke and Berleth, 1998; Przemeck et al., 1996; Yamaguchi et al., 2013). Auxin-activated MP directly induces the expression of a number of transcription factors that contribute to the formation of the flower primordium (Wu et al., 2015; Yamaguchi et al., 2013). These targets activate diverse developmental processes, floral fate specification, cell proliferation, cell growth as well as tissue and cell polarity.

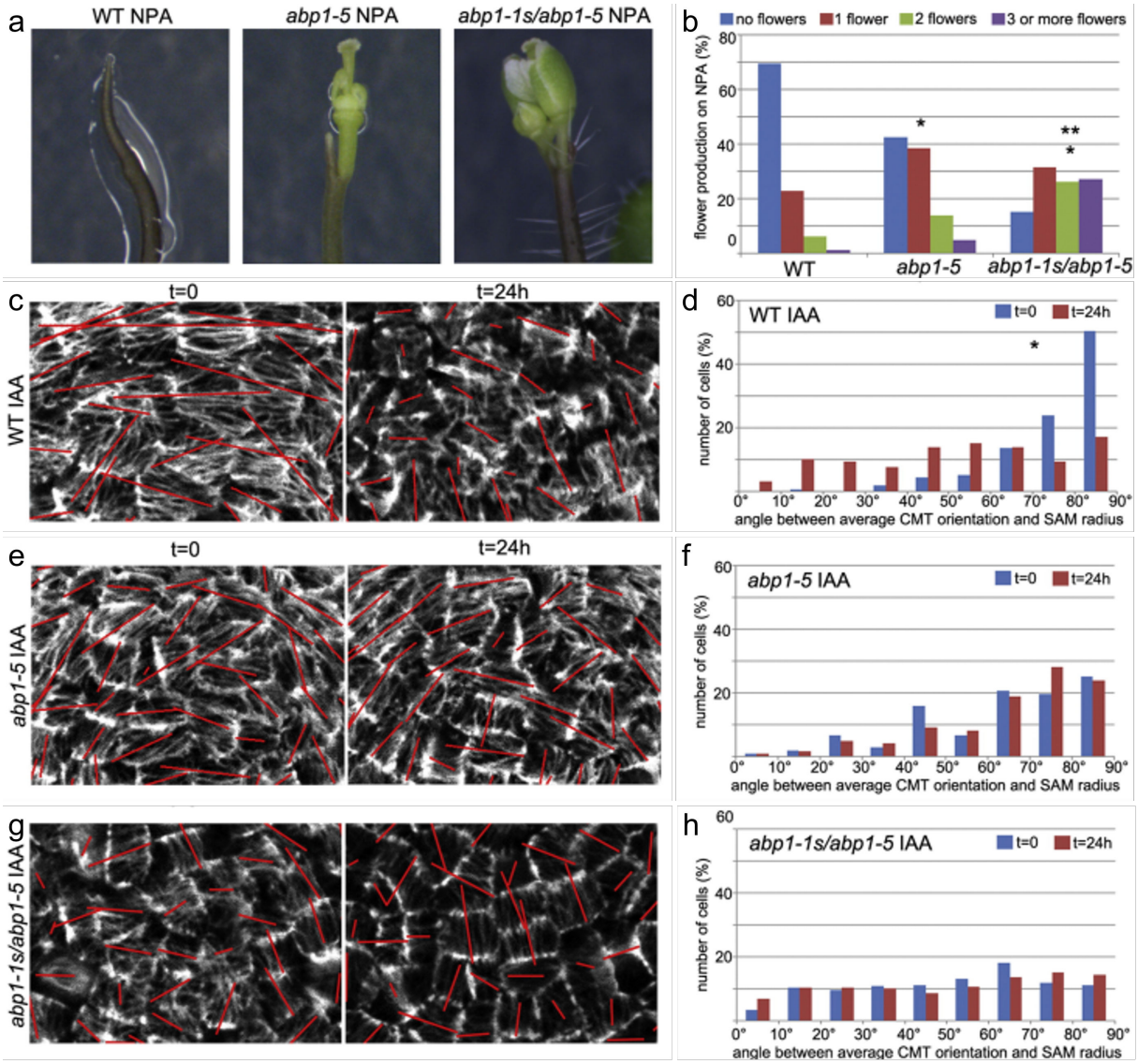

Figure 3. ABP1 regulates organ formation and auxin responsiveness of CMTs at the SAM
(a) Shoot apices of NPA-grown WT, *abp1-5* and *abp1-1s/abp1-5* plants.
(b) Quantification of the phenotypes in (a). Mutant vs WT: *p < 0.01; *abp1-5* vs *abp1-1s/abp1-5*: **p < 0.01.
(c) CMT organization in cells of the shoot apex of WT plants before (t=0) and after (t=24hr) IAA treatment
(d) Supracellular organization of CMT quantification of WT plants in (c).
(e) CMT organization in cells of the shoot apex of *abp1-5* plants before (t=0) and after (t=24hr) IAA treatment
(f) Supracellular organization of CMT quantification of *abp1-5* plants (e).
(g) CMT organization in cells of the shoot apex of *abp1-1s/abp1-5* plants before (t=0) and after (t=24hr) IAA treatment
(h) Supracellular organization of CMT quantification of *abp1-5* plants (g).

To gain insight into the connection between the reorganization of CMT and auxin induced transcriptional responses we analyzed the mutant allele *arf5-1*, which has a T-DNA insertion in the eighth exon of *ARF5/MP*, the sequence that encodes part of the DNA-binding domain (Odat et al., 2014). *arf5-1* homozygous plants display a rootless phenotype due to their inability to establish an embryonic root (Figure 4a). Seeds of mp/*arf5-1* mutants do germinate, however, and can be induced to form adventitious roots allowing the production of shoots. These shoots fail to produce flowers, resulting in the formation of naked pin-like stems (Figure 4b, c and f). We wondered, whether this pin-like phenotype was also correlated with transversely organized CMTs. In order to understand this, we introgressed a genetic construct of a fluorescent microtubule marker expressed only in the epidermal layer under the control of the promoter of the PROTODERMAL FACTOR 1 (PDF1::mCitrine-MBD) into fertile heterozygous *arf5-1* mutants. By analyzing the CMT organization of *arf5-1* PDF1::mCitrine-MBD plants, we detected circumferential supracellular CMT alignments at the periphery of the meristem and the stem, as observed in *pin* meristems after auxin transport has been impaired (Figure 4c). Since ARF5/MP is insensitive to auxin, these results suggest that the effect of auxin on CMT organization during organ initiation requires auxin dependent transcriptional input.

If MP regulates the reorganization of CMT that triggers the initiation of lateral outgrowths, it would suffice to change the dynamics of the CMT in the shoot apex to initiate lateral outgrowths even in the *mp/arf5* mutant. This hypothesis was tested inducing the disorganization of CMT in homozygous *arf5* mutants. As in our previous experiments, we firstly used oryzalin to induce the local disorganization of CMTs in the shoot apices. We initially tested the *arf5-2* allele of *MP/ARF5*, which carries a T-DNA insertion at the 3' end of the coding region (Odat et al., 2014). Homozygous *arf5-2* displayed incomplete penetrance of the rootless phenotype, allowing seedlings to form an embryonic root and grow easily on soil, however all plants are sterile (Donner et al., 2009). The lack of lateral organs in the shoot apex of homozygous *arf5-2* was observed in 12 out of 17 apices. Naked SAMs of homozygous *arf5-2* treated locally with oryzalin developed lateral outgrowths in 6 out of 7 apices, which were already visible 96 hr after the initial treatment (Figure 4d and e). Note that, as previously reported (Reinhardt et al., 2003), local applications of auxin on naked pin-like meristems of *arf5-2* were not able to initiate lateral outgrowths.

In order to confirm these observations, we used the strong mutant allele *arf5-1* to generated a *mp/arf5-1 bot1-7* double mutant where CMT organisation was genetically destabilised. *arf5-1 bot1-7* double homozygous mutants displayed a high number of lateral outgrowths around the SAM (80%, n=15) when compared to the parental *arf5-1* (0%, n=30) (Figure 4d and f).

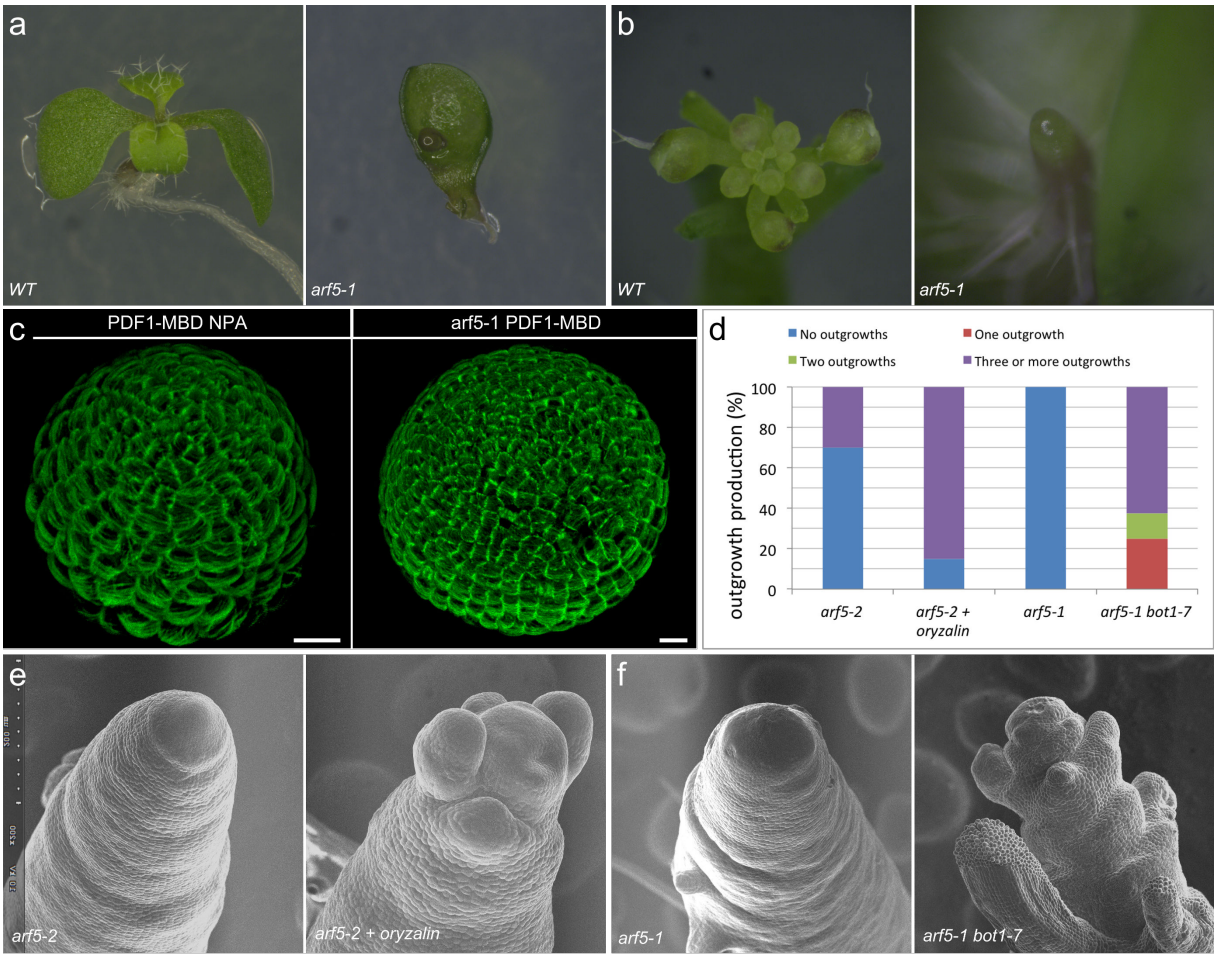

Figure 4. ARF5/MP regulates microtubule organization in the SAM
(a) WT and *arf5-1* mutant seedlings 10 dag, notice the lack of root in the mutant.
(b) Dissected WT inflorescence and naked *arf5-1* inflorescence.
(c) CMT organization in cells of pin-like meristems impaired in auxin transport (PDF1::mCitrine-MBD plants grown on NPA) and *arf5-1* PDF1::mCitrine-MBD homozygous plants.
(d) Quantification of phenotypes shown in (e) and (f).
(e) Local oryzalin applications (right) promote the formation of lateral outgrowths in *arf5-2* SAMs (left) already visible after 96 hr after the treatment.
(f) *bot1-7* mutation promotes the formation of lateral outgrowths (right) in otherwise naked *arf5-1* background (left).

Discussion

Here we provide evidence for a scenario where auxin interferes with the cortical cytoskeleton to induce organ initiation. We propose that in the absence of auxin accumulation, a network of interacting proteins, possibly including KTN1, ROP6 and RIC1 keeps microtubular arrays at the SAM in an anisotropic state. This is sufficient to inhibit lateral outgrowth, leading by default to the formation of a pin-shaped stem. In the presence of high auxin levels, these molecules are no longer able to maintain CMT anisotropy, which induces a shift toward isotropic cell walls. As a result, organ outgrowth is promoted (Figure 5).

A signaling pathway known to control CMT downstream of auxin was first described for epidermal pavement cells. In this system, plasma membrane localized ROP6 directs the parallel alignment of cortical microtubules. This is done through the activation of the ROP6 effector protein RIC1. ROP6 and RIC1 in turn activate the KTN1-mediated detachment of branched microtubules, thus promoting the organization of CMT into parallel arrays (Chen et al., 2015; Lin et al., 2013). Thus, the ROP6/RIC1 signaling pathway plays an important role in controling microtubule organisation and lateral cell expansion (Fu et al., 2005). It should be noted, however, that mutations in ROP6 and RIC1 have little phenotypic effects on plants grown on soil. This might suggest functional redundancy with other ROP and/or RIC proteins expressed in the meristem (e.g. ROP4 and ROP10).

We also obtained indications, that the activation of this ROP pathway might involve ABP1. There is evidence, that the binding of auxin to ABP1 directly activates ROP6 (Xu et al., 2014; Xu et al., 2010) and thus induces microtubule rearrangements. In addition the model of a ROP-based cytoplasmic auxin signaling pathway able to regulate the orientation of CMT, has been demonstrated by other groups using multiple mutant alleles encoding members of the TRANSMEMBRANE KINASE (TMK) subfamily of receptor-like kinases (*tmk1*, *2*, *3*, *4*), which could work as a link between ABP1 and ROP proteins (Xu et al., 2014). Although a number of studies suggest that auxin might directly act on a cellular ABP1 signaling pathway, recent work describing *Arabidopsis abp1* null mutant alleles with no obvious growth or developmental phenotypes have shed doubt on such a scenario (Gao et al., 2015). It was shown for example that the embryo lethal phenotype of *abp1-1* and *abp1-1s* is caused by disruption of the tightly-linked neighboring gene, *BELAYA SMERT/RUGOSA2* (*BSM/RUG2)*,

suggesting that the role of ABP1 during early embryogenesis might not be essential (Dai et al., 2015; Michalko et al., 2015; Michalko et al., 2016). Michalko et al; 2015b however, report strong effects of partial knock-downs of ABP1 activity. In addition, other proteins with overlapping functions might be involved. The precise function of ABP1, therefore, remains an open question.

Although our results point at a direct cellular signaling response to auxin, we also have obtained evidence that the reorganization of CMTs depends on transcriptional regulation. As we have seen, *arf5* mutants display phenotypes reminiscent of *pin1* phenotype. We show, that these apices are also characterized by ordered circumferential CMT patterns at the periphery of the SAM that force the tissue to grow in one single direction. Although auxin is no longer effective, if is sufficient to disorganize CMTs at the periphery of the *mp/arf5* SAM, to induce lateral outgrowths (Figure 5).

Several genes encoding for IQ67-domain (IQD) proteins have been identified as ARF5/MP targets (Moller et al., 2017). In plants, IQD proteins are the largest class of targets of the calcium (Ca^{2+}) ion sensor calmodulin (CaM). 33 members form *Arabidopsis thaliana* IQD family. Most *Arabidopsis* IQD members are aligned along microtubules, and additionally often localize to the cell nucleus or to membranes to recruit CaM or other calcium sensors (Burstenbinder et al., 2017b). IQD functions are mostly unknown, links with microtubule arrangements are strongly supported by the altered MT organization and plant growth phenotypes in *IQD* gain-of-function lines. Bürstenbinder and colleagues suggested that auxin-dependent regulation of *IQD*s might restrict their local abundance in specific tissues in order to control growth via control of the MT (Burstenbinder et al., 2017a).

Although the reorientation of CMT at the SAM is instrumental for the initiation of lateral organ outgrowths, cell wall remodeling and changes in cell wall stiffness also play a role (Braybrook and Peaucelle, 2013; Peaucelle et al., 2011a; Peaucelle et al., 2008; Peaucelle et al., 2015). AFM measurements of the outer wall of auxin-treated SAMs grown on NPA indicated a reduction of rigidity in the induced lateral outgrowths, which become slightly softer than the apex. According to the analyses the changes in stiffness did not exceed 30% and indicated that a major reduction in the outer wall rigidity does not occur during organ initiation. Modelling approaches showed that such relatively modest reductions in stiffness would on their own be insufficient to induce organ initiation. (Sassi et al., 2014). Relevantly,

simulations also showed that the combination of limited loosening with a shift to wall isotropy would lead to increased growth rates. This theoretical analysis therefore suggests that the anisotropy-to-isotropy shift could promote organ formation by amplifying the effect of relatively minor reductions in the outer wall rigidity at the SAM.

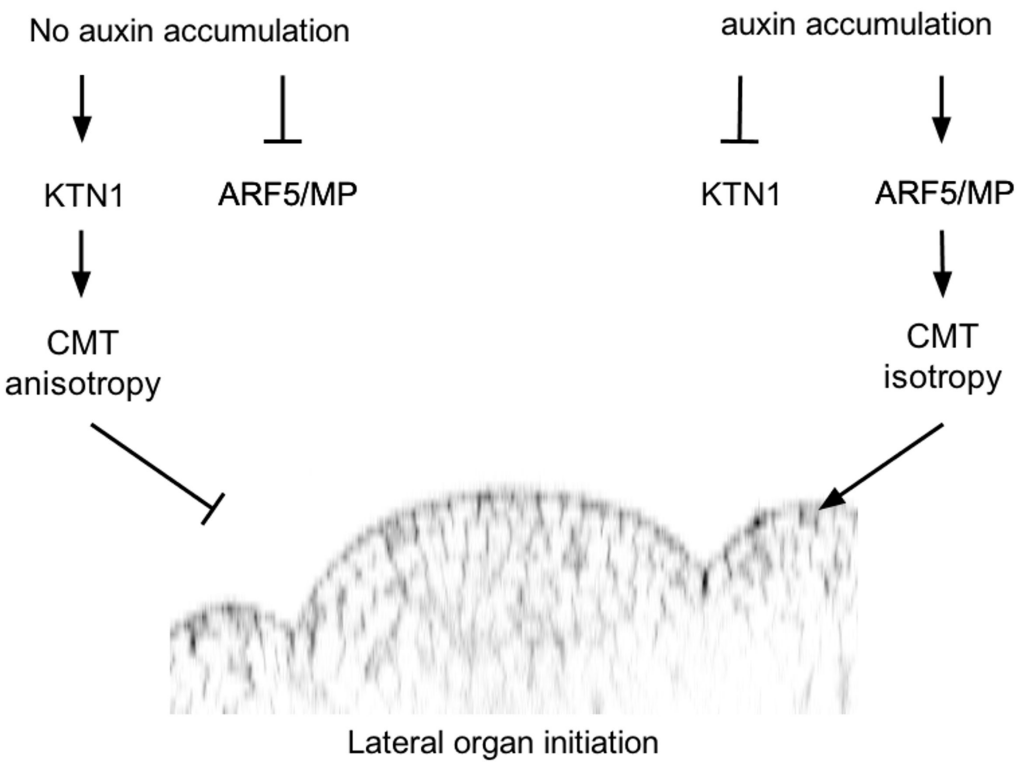

Figure 5. Graphical summary of our working hypothesis about the mechanisms leading to lateral organ initiation in the SAM. A KTN1-mediated pathway maintains an anisotropic expansion of cells under no auxin accumulation (left). This mechanism inhibits lateral organ initiation. In contrast, auxin accumulation (right) prevents the KTN1-mediated pathway, but activates an ARF5/MP-dependent pathway, which facilitates the reorientation of CMT. This mechanism in addition with cell wall loosening (not shown) trigger a shift towards isotropic expansion resulting in lateral organ initiation.

Conclusion and Perspectives

In summary, we have obtained evidence that auxin plays a role in the formation of new organs, by locally interfering with the properties of the cell wall. On one side the hormone interferes with cortical microtubule (CMT) dynamics, thereby inducing changes in growth direction. This shift to isotropic growth would signficantly enhance the slight reductions in cell wall stiffness induced during organ formation and thus allow the initiation of new growth axes. Our current working hypothesis proposes that the molecular mechanism by which auxin triggers the initiation of new growth axes includes on one side an auxin signaling via KTN1-mediated pathway and a MP-dependent pathway. According to our results the MP-dependent pathway facilitates the reorientation of CMT towards an isotropic expansion through a yet unknown mechanism.

Experimental procedures

Plant material and Genetic Analysis

Arabidopsis thaliana ecotypes Columbia-0 (Col-0) and Wassilewskija-2 (Ws-2) were the wild types seeds used in this study. Transgenic lines and mutants used in this work were for the most part previously described. *pin1-1* (introgressed in Col-0) (Sassi et al., 2012), *pin1-6* (Vernoux et al., 2000), *35S::GFP-MBD* (Marc et al., 1998); *bot1-7 35S::GFP-MBD* (Uyttewaal et al., 2012), *ric1-1* and *RIC1 OX* (Fu et al., 2005), *rop6-1*, and *ROP6 OX* (Fu et al., 2009), *abp1-5* (Xu et al., 2010), *abp1-1s* (NASC accession N16148), *arf5-1* (Przemeck et al., 1996), *arf5-2* (Donner et al., 2009), *DR5::VENUS-N7* (Heisler et al., 2005). The *PDF1::mCitrine-MBD* was kindly provided by Thomas Stanislas. The *DR5::VENUS-N7 35S::GFP-MBD*, *rop6-1 35S::GFP-MBD*, *ric1-1 35S::GFP-MBD*, *abp1-5 35S::GFP-MBD, pin1-6 bot1-7*, *arf5-1 bot1-7* and *arf5-1 PDF1::mCitrine-MBD* lines were generated by crossing and further PCR selection. Growth conditions were previously described (Hamant et al., 2008)

Growth Conditions and Treatments

For napthylphtalamic acid (NPA) treatments, plants were sown in petri dishes with a medium adapted for *Arabidopsis* (Duchefa) containing NPA to a final concentration of 10μM. To induceorgan formation plants were treated in petri dishes with 1mM IAA liquid solution for 3 h after imaging the t=0 time point and again the next day after imaging the t=24h time point. No other IAA was added after the 24h time point until the completion of the experiment. Lanolin paste for local SAM treatments was prepared as follows: 1 volume of chemical stock solution (3x concentrated) was added to 2 volumes of melted (55°C) lanolin and thoroughly mixed until the formation of a homogenous emulsion. The con centration of the stocks was 3mM for IAA and 666 μg/ml for oryzalin. Local applications were made with a pipette tip under a binocular. After lanolin application, plants were kept in humid conditions in a transparent plastic box for 4 days before further analyses. Equal amounts of DMSO were used for untreated controls. For adventitious root formation, seeds were surface-sterilized and germinated on MS medium. After germination, homozygous *arf5-1* seedlings were identified by the rootless phenotype. Mutant plants were wounded below cotyledons as earlier described (Berleth and Jurgens, 1993), then transferred to MS medium supplemented with the synthetic auxin 1-naphthaleneacetic acid (NAA) to a final concentration of 10μM and kept on these plates for 7 days, when they were transferred to free MS medium free of NAA to allow the elongation of the root. Plants were either kept in plates or transplanted to soil after rooting.

Microscopy

Confocal microscopy was carried out with a Zeiss LSM700 upright microscope equipped with 40x water immersion lens. Live imaging of NPA pins was carried out directly in petri dishes, after submerging plantlets in water. SAMs of plant grown on soil were imaged as previously described (Fernandez et al., 2010) or in whole mount preparations. Briefly, for whole mount preparations plants were grown on soil in flat vessels until bolting. After the removal of older flower buds to expose the SAM surface, plants were imaged with a droplet of water between the objective and the SAM surface. Plants were kept in humid transparent boxes for all the duration of the experiments to prevent SAM desiccation. Scanning electron microscopy was carried out with a Hirox SH-3000 table-top SEM on fresh plant material at -40°C, with an accelerating voltage of 5kV. Images of SAMs treated with lanolin paste were taken with a Leica MZ12 stereomicroscope equipped with a Leica DFC320 camera.

Image analyses

Image processing for PDF1::mCitrine-MBD was carried out with the ZEN software (Zeiss) using the 3D transparent projection. For MT visualization in 35S::GFP-MBD, confocal stacks were further processed with MerryProj (de Reuille et al., 2006) to obtain the projection of MTs on the L1 layer. Measurements of MT organization were carried out with the MT plug-in for ImageJ (Uyttewaal et al., 2012). Briefly, for each meristem cell contours were inferred from the original confocal stack (loaded onto the FIJI release of ImageJ; http://fiji.sc/Fiji) and further saved in a single Region Of Interest (ROI) file. The ROI file was then overlaid on the corresponding MerryProj-derived image and used as template to measure MT organization with the MT plug-in as previously described (Uyttewaal et al., 2012). Supracellular organization of MT in the SAM was assessed with FIJI by calculating the angle between the radius of the SAM and the average MT orientation from each cell as obtained by MT plug-in. Graphs and statistics were obtained with Microsoft Excel software.

Chapter II

A transcriptional coupling between microtubule-driven growth isotropy and cell wall remodeling promotes organogenesis at the shoot apex in *Arabidopsis*

Alessia Armezzani, Ursula Abad, Olivier Ali, Laetitia Vachez, Amélie Robin, Ann'Evodie Sallee, Antoine Larrieu, Ewa Mellerowicz, Nobu Nishikubo, Ludivine Taconnat, Virginie Battu, Teva Vernoux, Jan Traas, Massimiliano Sassi.

Summary

The shoot apical meristem (SAM) of higher plants plays a central role in the establishment of architecture, as it continuously generates new tissues and organs through complex changes in growth rates and directions of its individual cells. Plant cell growth is driven by the internal turgor pressure and largely depends on the cell walls, which provide external support and allow cell expansion through synthesis and structural changes. A previous study revealed the importance of growth isotropy in organ outgrowth, which involves disorganization of the cortical microtubules. Nevertheless, our results and those of others indicate that cell wall loosening is required in order to have proper organ outgrowth (Fleming et al., 1997; Peaucelle et al., 2011a; Peaucelle et al., 2008). We show here that this disorganization is tightly coupled to the transcriptional control of genes involved in wall loosening via pectin and hemicellulose modifications. Transcriptomic analysis combined with *in situ* hybridization identified a set of cell wall-remodeling genes, which are active in the SAM during organ formation. Interestingly, some of these wall-loosening genes are induced when microtubules are disorganized and cells shift to isotropic growth. Mechanical modeling shows that this coupling has the potential to compensate for reduced growth rates induced by the isotropic deposition of microfibrils in the organ primordium. Reciprocally, cell wall loosening induced by different treatments or altered cell wall composition promotes a disruption of microtubule alignment. Our data thus indicate the existence of a regulatory module involved in organ outgrowth, linking microtubule arrangements to cell wall remodeling. Although the transcriptional regulators involved in this module remain to be identified, an enhanced yeast 1-hybrid screen suggests that the cell wall modifying genes investigated here are the targets of multiple transcription factors and signaling pathways.

The following chapter corresponds to the manuscript that was recently submitted. I participated in the scientific discussions leading to this article. Experimentally, I verified the expression of wall-loosening genes by qRT-PCR following auxin induction. In collaboration with, Laetitia Vachez, Amélie Robin, and Ann'Evodie Sallee, we set up and performed the whole mount RNA *in situ* hybridizations. I produced the crosses and participated in the isolation of the mutants *xxt1 xxt2 PDF1:: mCitrine-MBD*, and the line expressing *DR5::VENUS-N7* in the *pin1-6 bot1-7* background. In addition to the manuscript, I have also incorporated, the results of the eYIH assay in this chapter, which was done in the Proteomics

Core Facility of UC Davis. I have performed the analyses of the eYIH with inputs from Jan Traas.

Introduction

The control of shape during growth of multicellular organisms is a fundamental, yet poorly understood process. We address this issue here in plants where in most species morphogenesis entirely depends on the local rates and directions of cell expansion (Coen et al., 2004; Sassi et al., 2014). This is because plant cells usually do not migrate or rapidly change shape during development, as in animals (Coen et al., 2004; Kicheva and Briscoe, 2010) while cell death in principle does not play an important role. For this reason, plants represent an excellent model to investigate the mechanisms that determine the architecture and shape of multicellular organisms.

Plant growth depends largely on the control of the cell wall, which surrounds most cells and counteracts the high internal turgor pressure. The wall in higher plants is largely composed of relatively stiff cellulose microfibrils that are cross-linked by matrix of polysaccharides such as hemicelluloses and pectins. In order to grow, cells have to expand their cell walls irreversibly, making them yield to the internal pressure. It is therefore thought that molecular regulation controls morphogenesis for a large part by affecting the local biochemical composition and arrangements of the cell wall polysaccharides (Braybrook and Jonsson, 2016).

A plethora of cell wall remodeling and synthesizing proteins have been identified. The precise number of synthesizing proteins is not known, but it is thought that hundreds of enzymes may be involved in this process (Yang et al., 2016). In addition, several multigene families encode proteins likely involved in modifying the existing bonds, thus affecting the mechanical properties of the wall. The best known of these so-called remodeling proteins include (i) the pectin methyl esterase (PME) family and their inhibitors (PMEIs), which control the assembly and mechanical properties of the pectin matrix, (ii) the xyloglucan endo-transglucosylase/hydrolase (XTH) and (iii) the A-type expansin (EXPA) families both supposed to act on the mechanical properties of the hemicellulose matrix (Braybrook and Jonsson, 2016; Cosgrove, 2016a, b). In addition, some XTH enzymes might also interfere with the interactions between hemicellulose and cellulose.

The remodeling of pectin and hemicellulose polysaccharides in principle modifies cell wall stiffness and has thereby the potential to modulate growth rates (Braybrook and Jonsson,

2016; Cosgrove, 2016a, b). Although pectins and hemicelluloses have also been associated with the control of growth anisotropy (Peaucelle et al., 2015), growth directions are largely determined by the presence of cellulose microfibril arrays in the cell wall. The polymers can be deposited in highly ordered arrays, restricting cell expansion along their axis (Baskin, 2005; Paredez et al., 2006). The orientation of the cellulose microfibrils themselves is controlled by cortical microtubules (CMTs), which guide the movement of the cellulose synthase (CesA) complexes across the plasma membranes (Bringmann et al., 2012; Paredez et al., 2006). Although the exact mechanisms underlying microtubule orientation are not known, several components of the Rho Proteins of Plants (ROP) signaling pathway seem to be involved. Indeed, mutations in ROP6 and ROP INTERACTING PROTEIN AND CRIB MOTIF-CONTAINING PROTEIN 1 (RIC1) affect microtubule organization at the shoot apex, and influence organ formation (Sassi et al., 2014). RIC1 itself directly interacts with KATANIN1 (KTN1) a microtubule associated protein required for microtubule severing and bundling (Lin et al., 2013). Accordingly, mutations in *KTN1* also affect organ initiation (Sassi et al., 2014; Uyttewaal et al., 2012).

In summary, to control growth directions and growth rates at the level of the cell wall, the regulatory molecular networks can act on two sets of parameters: (i) the composition and the structure of the wall and (ii) the orientation of the cellulose microfibrils, mainly via microtubule dynamics. However, the coordination of these processes as well as their relative contributions to morphogenesis, are not understood.

The shoot apical meristem (SAM) of *Arabidopsis thaliana* represents an ideal system to address these questions. As it harbors the stem cells, the SAM continuously generates new tissues and organs at the shoot tip, which involves complex changes in cell growth directions and in cell growth rates (Braybrook and Peaucelle, 2013; Peaucelle et al., 2011a; Sassi et al., 2014). Organ formation at the SAM is initiated by the accumulation of the hormone auxin in discrete foci at the periphery of the meristem (Benkova et al., 2003; Reinhardt et al., 2000; Reinhardt et al., 2003). Auxin is concentrated at the site of organ initiation by an active transport mechanism relying on the action of the PIN-FORMED 1 (PIN1) efflux carrier (Okada et al., 1991; Reinhardt et al., 2003; Vernoux et al., 2000).

Several studies have pointed at the importance of wall remodeling downstream of auxin during morphogenesis at the meristem. The local application of expansins can induce organ

formation, whereas induced changes in the degree of pectin methylation can induce or inhibit organogenesis (Braybrook and Peaucelle, 2013; Fleming et al., 1997; Peaucelle et al., 2011a; Peaucelle et al., 2008). Mutations directly or indirectly affecting pectin composition also affect morphogenesis. Likewise, the *xxt1*/*xxt2* mutant, that has greatly reduced xyloglucan (a hemicellulose) levels, shows abnormal plant architecture. It remains nevertheless unclear how wall composition is regulated during organ formation.

In a recent study we showed that high auxin concentrations at organ initia cause the disorganization of microtubules and we proposed that a shift to isotropic growth, through the isotropic deposition of microfibrils, plays a major role in organ formation. This shift could act in synergy to relatively modest changes in wall stiffness observed during organ formation (Sassi et al., 2014). Although both wall loosening and wall isotropy seem to be involved, their relative importance and their coordination during organogenesis remain to be established.

To address this question, we investigate the roles of microtubule dynamics and wall remodeling during morphogenesis at the SAM. For this purpose, we identified genes encoding XTHs, EXPAs, PMEs and PMEIs strongly expressed at the shoot meristem. We show that the transcription of the genes can be activated through changes in microtubule dynamics. Conversely, interfering with wall loosening promotes changes in microtubule organization. We propose that this tight coupling between cytoskeleton organization and cell wall remodeling plays a central role in coordinating growth during organ initiation at the SAM.

Results

Disorganizing the cortical microtubules increases growth rates *in vivo* but not *in silico*

Previous work suggested a central role for the organization of cortical microtubules in organ outgrowth (Sassi et al., 2014). To bulge out, cells in a primordium must initially grow more rapidly than the surrounding cells, in particular the boundary cells (Kwiatkowska, 2004; Kwiatkowska and Dumais, 2003). The partial restoration of organ formation observed in the *pin1-6 bot1-7* double mutant (Sassi et al., 2014) (Figure 1), suggests that disorganized CMTs are sufficient to cause this increase in growth rates. This is in line with the observation that the local disorganization of microtubules using the drug Oryzalin (ORY) also causes the induction of local outgrowths (Sassi et al., 2014). If we accept that the disorganization of microtubules primarily affects cellulose deposition, a shift to the isotropic distribution of microfibrils must also lead to outgrowth and an overall increase in growth rates. This leads to the somewhat counterintuitive hypothesis that not only microfibril density but also their orientation has the potential to affect global growth rates. In other words, the experimental results indicate that, at identical microfibril density, cells with an isotropic wall would grow faster than cells with anisotropic walls.

To explore this hypothesis, we performed mechanical simulations of a growing meristematic dome (Figure 2). These simulations were conducted with a dedicated numerical framework, where specific values of the mechanical wall parameters (stiffness, wall synthesis rates and yielding thresholds) and turgor pressure can be set in each cell (Boudon et al., 2015; Sassi et al., 2014). Growth is implemented through a strain-based law, stating that directional (plastic) expansion of the cell wall is proportional to its elastic stretching minus a given threshold (Boudon et al., 2015). We assumed the reversible mechanical behavior of the cell wall to be linear elastic. Since elastic strain results from the combination of the elastic properties and turgor-induced mechanical stress, we reasoned that a change from anisotropic to isotropic microfibril deposition would reduce stiffness in certain directions and increase it in others, leading to directional changes in growth. Considering a growing tissue where microfibril deposition is highly anisotropic, we indirectly changed the growth dynamics of an embedded, small group of cells by making their microfibril deposition isotropic (Supplemental Model Description, see annex 2). Based on the experimental observations, we expected that these

isotropic cells would grow faster than the otherwise anisotropic environment. However, simulations following this scenario showed a reduction in growth rate of about 20-25% in the isotropic domain (Figure 2a, see annex 2 for quantified output). Similarly, even when all the cells at the periphery of the virtual dome are made isotropic, growth rate is reduced by roughly 30% (Figure 2b, see annex 2 for quantified output). In fact, increased growth rates in primordium cells could only be obtained in simulations where this directional shift was combined with a reduction in the amplitude of the stiffness tensor, mimicking a decrease in the cellulose deposition rate or a loosening of the cell wall matrix. Accordingly, we observed that at least a 30% decrease of rigidity amplitude is needed for the initium zone to expand faster than its surroundings (Figure 2a, annex 2). In this context, it is important to note that we did observe relatively minor and variable reductions in stiffness at the wild type shoot apex in outgrowing organ primordia, not exceeding 50% (Sassi et al., 2014). Thus, in contrast to experimentation, simulations predict that isotropy alone is not able to increase cell growth rates. In fact, a shift to isotropic microfibril orientation would rather slow down growth unless it would be coupled to reductions in wall rigidity. This suggests that also *in vivo* the shift to isotropic growth must somehow lead to changes in wall stiffness. We therefore looked more in detail at regulators involved in cell wall remodeling, in particular those with the potential to modify cell wall stiffness.

A previous study investigating the role of wall synthesis in SAM morphogenesis did not reveal particular changes in the amount of cellulose correlating with organ initiation (Yang et al., 2016), Wightman personal communication). In addition, no strong overall transcriptional upregulation of genes encoding CesAs was found in outgrowing organs (Yang et al., 2016, Wightman personal communication, our own unpublished data). We therefore focused our attention on modifications of the cell wall matrix, more in particular we looked at four gene families, which have been associated with modifications in the wall matrix: pectin modifying enzymes (PMEs and PMEIs) and enzymes potentially targeting the hemicellulose matrix (XTHs and EXPAs).

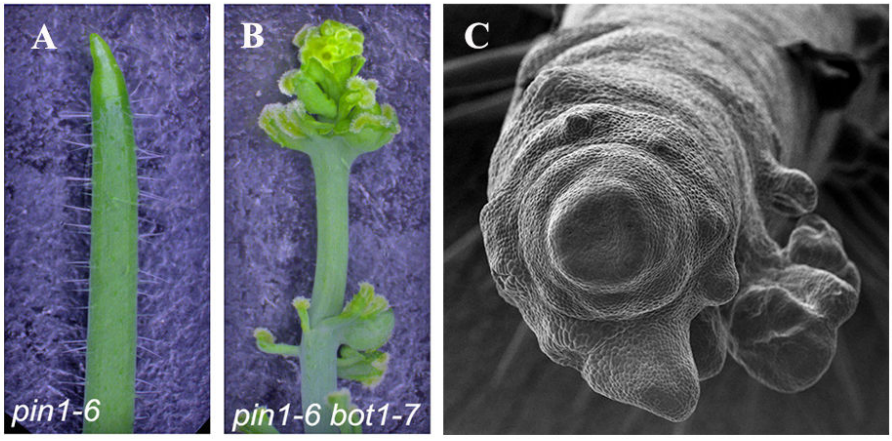

Fig 1. Restoration of organ formation in the *pin1-6 bot1-7* double mutant. The *pin 1-6* mutant normally forms a naked stem with no or very few lateral organs (A). This is in contrast to the *pin1-6/bot 1-7* double mutant, which produces many lateral outgrowths (B, C)

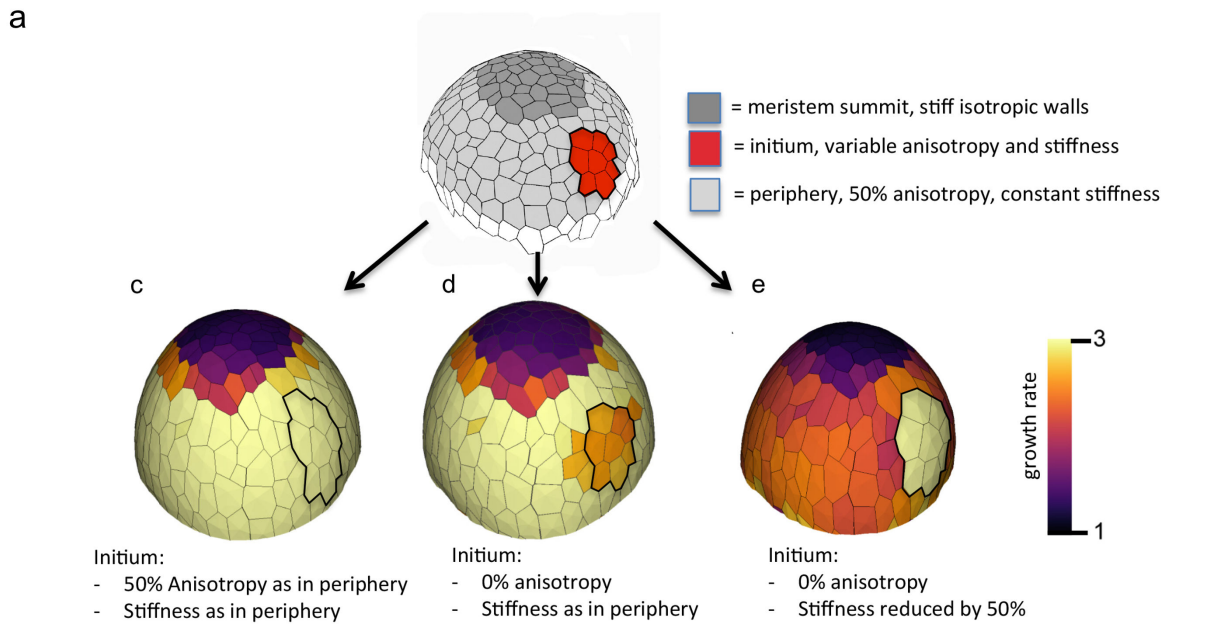

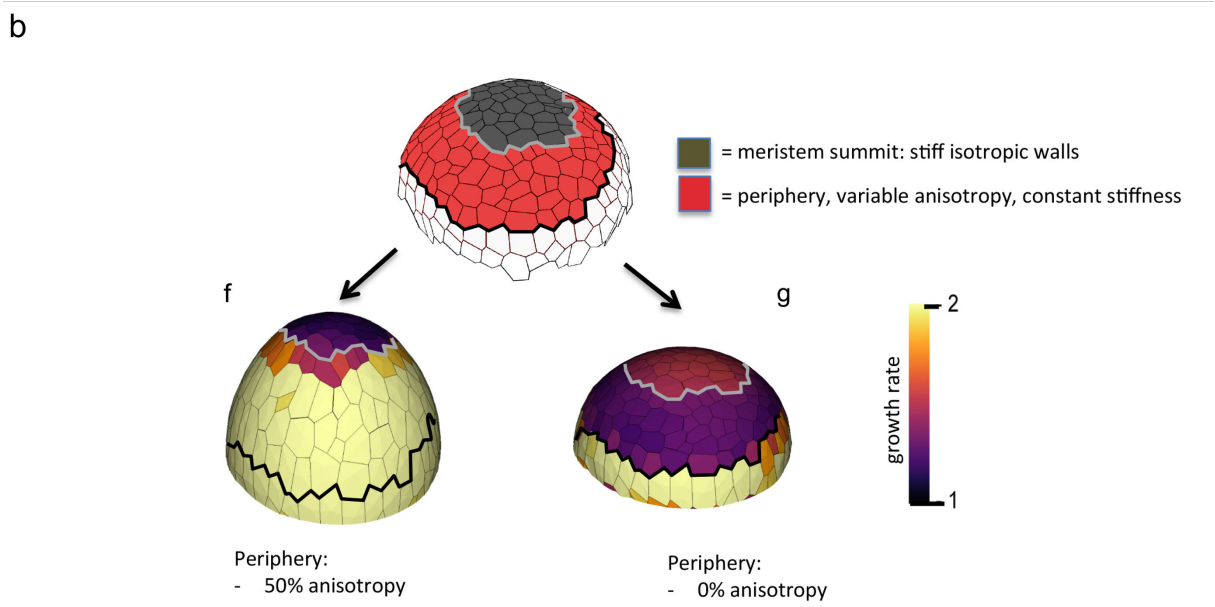

Figure 2. Influence of mechanical properties on cell expansion.
The structure used to perform the various simulations is a 2D shell tiled with polygonal cells. Each cell is composed of several triangular first order finite elements. The meshes are generated from a segmented 3D confocal stack of images from a pin meristem. See annex 2 for details. (a) and (b) show the structure at the beginning of the simulations. (c), (d), (e), (f) and (g) show the structure after 100 steps of growth simulation based on different hypotheses. The relative growth rate is color-coded.
In (a) a set of initium cells is defined (red zone) which can have variable levels of anisotropy and stiffness. The cells at the summit (dark grey in (a) and (b)) are very stiff and grow very slowly. The periphery has a constant stiffness and 50% anisotropy.
(c) When the primodium cells have the same stiffness and anisotropy as the peripheral cells, all cells grow at the same rate.
(d) When the cells in the primordium are made isotropic, but stiffness remains as in the periphery, the primordium grows more slowly than the surrounding periphery.
(e) When both anisotropy and stiffness are reduced, the primordium cells grow quicker than the surrounding cells.
In (b) the dome has only a peripheral zone with variable mechanical properties
(f) The peripheral cells are anisotropic, (g) when cells are made isotropic, growth rate is reduced

Identification of candidate cell wall-remodeling genes involved in organ initiation

In a first step, the expression of these cell wall related genes was investigated by exploiting an RNAseq analysis conducted on dissected inflorescences on which only a minimal segment of stem and the flowers up to stage 2/3 were left. The results allowed us to identify a set of abundantly expressed candidate genes (Figure 3 A and B; Table S1). Transcripts belonging to all four families were identified in the samples. In particular genes encoding XTHs were abundantly expressed. Genes encoding PMEIs, PMEs, and EXPAs were less expressed, but nevertheless more abundantly than the cellulose synthases for example. We next investigated the expression patterns of these genes through *in situ* hybridization. Of the 31 most abundantly expressed genes tested (Table S1 for list of tested genes), 16 were detectable in our hands (see Figure S1 for a complete set of results).

The most abundantly expressed *PMEI*'s (*PMEI AT5G62350*, *PMEI3*; Figure 3C; Table S1) were detected in the outgrowing primordia, mainly in the outer cell layers of the fast expanding floral organs (Figure 3C). These zones of high *PMEI* activity correlated with high labeling of the JIM5 antibody, interacting with partially or entirely de-methyl esterified pectins (Figure S1, see also Krizek 2015). The third *PMEI*, *AT1G14890*, was homogenously expressed at the meristem.

PME5 (33% of the PME transcripts) had a spotted expression pattern reminiscent of cell cycle-related genes as was reported previously (Peaucelle et al., 2011b) (Figure 3C). *PME3* (14 % of the PME transcripts) was weakly and homogeneously expressed throughout the SAM. The other *PME*s could not be detected.

We next investigated the putative xyloglucan remodeling genes (*XTH*s and *EXPA*s). The RNA-seq analysis identified a number of such genes expressed at the shoot apex (Table S1). *In situ* hybridization confirmed that 8 *XTH* and 4 *EXPA* genes were expressed at the detectable level in apical tissues (Figure 3C, Figure S2). Interestingly, three *XTH*s (*XTH9*, *XTH4* and *XTH22*) and three *EXPA*s (*EXPA6*, *EXPA15*, and *EXPA4*) represented the large majority of the transcripts in each family (Figure 3A, Table S1). Importantly *XTH9*, *XTH4* and *EXPA15* were strongly expressed at the shoot apex and clearly detected in the outgrowing primordia. *EXPA15* showed the most restricted pattern, mainly limited to what is the future

floral meristem, excluded from the cryptic bract zone. *XTH9* and in particular *XTH4* were expressed in the meristem, the expression decreased in the very young flower meristem, then it increased very strongly in the flower primordia as soon as they started to grow out. Two other highly active genes, *EXPA4* and *EXPA6*, were homogenously expressed, while *XTH22* was mainly expressed in the vascular tissues and in the differentiating epidermis. Taken together, these data suggest that three genes associated with hemicellulose remodeling (*XTH4*, *XTH9* and *EXPA15*) are highly expressed during the early stages of primordium formation.

The organ-specific expression of these three remodeling genes is somewhere downstream of the auxin accumulation that triggers organ initiation. Indeed, RNA *in situ* hybridizations showed that their expression was substantially reduced when compared to the WT in *pin1-6* apices, where auxin doesn't accumulate (Figure S2). Moreover, exogenous application of auxin at the flank of the SAM could restore the organ-specific expression of these genes in a *pin1-6* background (Figure S2). Importantly, these effects of auxin on gene expression can take up to several days, indicating that they are largely indirect.

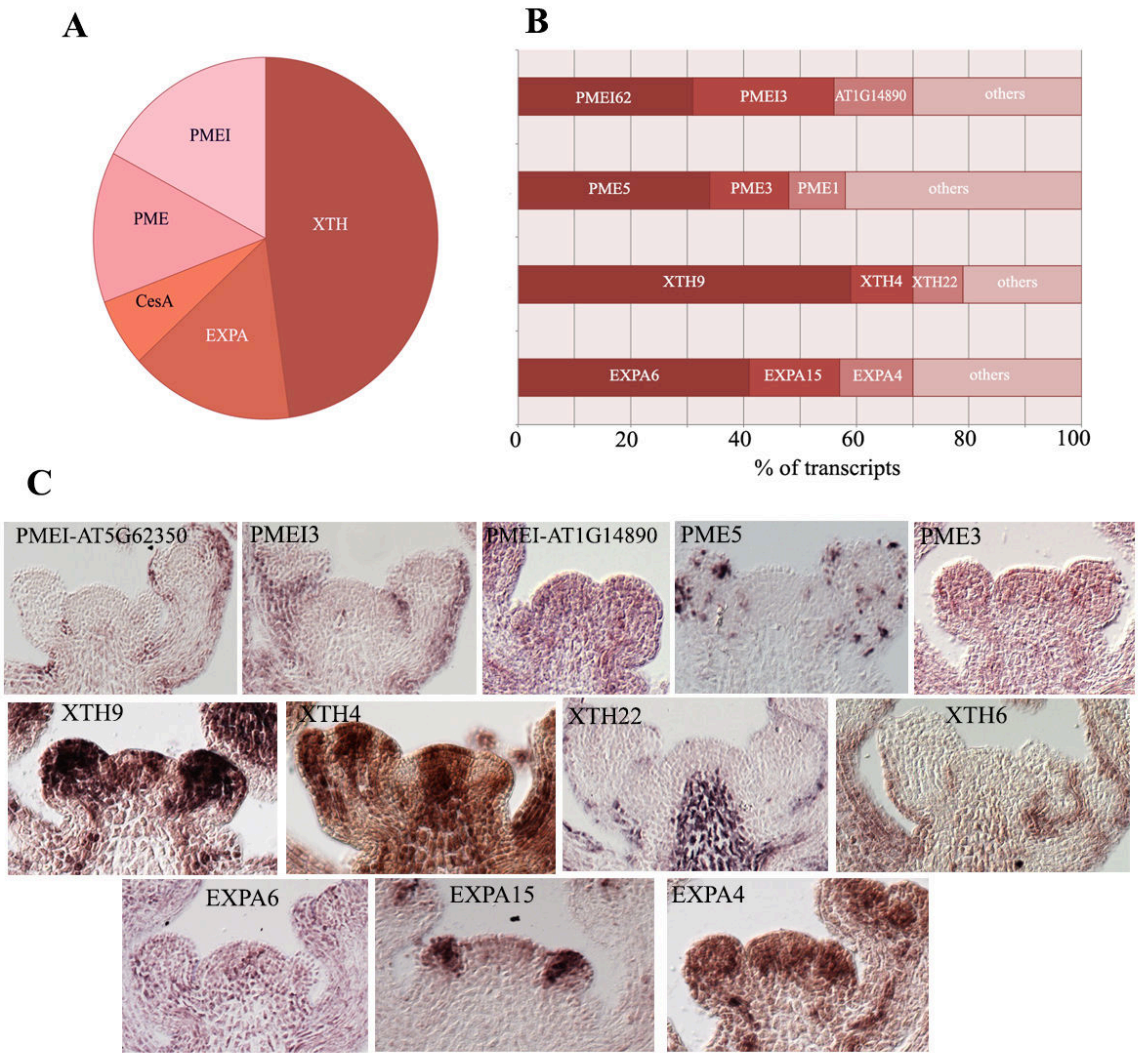

Figure 3. Cell wall composition and organ initiation. (A, B) Results from RNAseq of the shootapex (meristem and young flower primordia). (A) shows the relative abundance of major wall remodelling genes (XTHs, EXPAs, PMEIs and PMEs compared to CesA). Note the high relative expression levels of the XTH genes.
In B the relative amounts of the most abundant transcripts within each family are shown. For each family, the three most abundantly expressed genes produce between 58% (PMEs) and 78% (XTHs) of the transcripts of that family.
(C) shows the in situ hybridizations of the most abundantly expressed genes.

Figure 4. Disruption of CMT anisotropy promotes the expression of pectin and xyloglucan modifiers.
Expression patterns of XTH9, EXPA15 and PME3 in *pin1* mutants and *pin1 bot* mutants. Note the upregulation of all three genes in the outgrowths of the double mutant. PME 5 shows a punctuate pattern, probably cell cycle stage specific. Its labeling throughout the meristem is also a control for background noise, which remains low.

Perturbing cortical microtubule dynamics promotes the expression of wall remodeling genes

We next assessed whether the strongly expressed remodeling genes targeting pectins and hemicelluloses could be related to the increased growth rates observed in isotropic outgrowths, induced when microtubules become disorganized. To this end, we analyzed the expression of representatives of the *PME*, *XTH* and *EXPA* families in the *pin*/*bot* double mutant. In order to obtain a more global view of the expression in the irregularly shaped dome of this mutant, we used whole mount RNA *in situ* hybridizations. This showed that *PME3, XTH9* and *EXPA15* were specifically expressed in the outgrowths compared to the surrounding tissues (Figure 4). We confirmed this information for *XTH9* after ORY treatment and observed that, 4 days after application, *XTH9* was clearly expressed in ORY-induced outgrowths (not shown). In conclusion, the results suggest that the disruption of microtubule alignments also cause the transcriptional activation of three types of wall remodeling genes. The existence of this link between wall isotropy and wall loosening provides a plausible explanation for the increased growth rates induced by the disruption of microtubule organization, not predicted by the simulations.

An Enhanced Yeast-One-Hybrid suggests multiple regulation of wall remodeling genes

The specific expression patterns of some of the cell wall genes as well as their transcriptional activation after perturbations of the cytoskeleton raised questions regarding their upstream regulation. In this context, in particular *XTH9*, *EXPA4* and *EXPA15* represented interesting candidates for further analysis. In order to gain some insight into the identity of upstream regulators, we carried out an Enhanced yeast-one-hybrid (eYIH) assay. eYHI assays have been used in several systems to identify transcription factor-DNA interactions at a large-scale. They allow the production of transcriptional network models and the generation of hypotheses about gene regulation (Deplancke et al., 2004; Gaudinier et al., 2011; Reece-Hoyes et al., 2011a; Reece-Hoyes et al., 2011b). In plants, eYHI assays have been useful tools to generate large-scale models of interaction networks involved in developmental processes such as the synthesis of the secondary cell wall (Taylor-Teeples et al., 2015), or the establishment of the root ground tissue (Sparks et al., 2016).

For the eYIH assay, we prepared baits for *XTH9,* and the two *EXPA* genes, which show contrasting expression, *EXPA4* and *EXPA15*. All the baits used for the eYIH assay contained portions of the 2000bp sequences immediately upstream of the translational start site, except for *XTH9* bait, for which the intergenic region of 1386bp was used instead. The three promoters were Gateway cloned to the reporter genes *lacZ* and *HIS3*. In this system the expression of the reporter genes is activated when a TF interacts with the promoter bait. For the screen, a complete collection of 2000 *Arabidopsis* TFs was fused to a transcription activation domain and used as prey (Pruneda-Paz et al., 2014).

A total of 31 TFs (1.55% from the complete collection) were found to potentially regulate with the *XTH9* promoter fragment used, 97 TF (4.85%) were found to bind to the *EXPA4* promoter fragment, and 23 TF (1.15%) to the *EXPA15* promoter fragment (Table S4). The high numbers of *EXPA4* interactors might reflect the homogeneous expression of this gene when compared to the other two. One TF characterized as a B3 domain protein encoded by At5g38490 displayed potential binding to the three cell wall loosening genes. *XTH9* and *EXPA15,* both up regulated in the organ outgrowth, share only one putative upstream regulator, the MYB-related transcription TRFL10 (At5g03780). *EXPA4* and *EXPA15* showed potential co-regulation by the HISTONE H2A 2 (HTA2); whereas *EXPA4* and *XTH9* share 11 potential regulators, which represent more than 10% of the TF that might be regulating *EXPA4* expression (Table S5). These included one additional B3 domain TF, the HISTONE 2A 13 (HTA13), the LOB DOMAIN-CONTAINIG PROTEIN 3 (LBD3) also known as ASYMMETRIC LEAVES 2-LIKE 9 (ASL9), as well as two C2H2-type zinc finger TFs. Four TFs of the plant specific BASIC PENTACYSTEINE (BPC) family were putative regulators of *EXPA4* and *XTH9*, thus ATBPC1, ATBPC4, ATBPC5 and ATBPC7. These results indicate complex regulation of *XTH9*, *EXPA15* and *EXPA4* expression.

Increasing cell wall extensibility promotes the disruption of CMT organization

The results obtained thus far led to a scenario, where auxin would perturb microtubule alignments, which then would (indirectly) feed back on the transcriptional activation of wall loosening enzymes. This explains why interfering with microtubule alignments does also lead to increased growth rates and the bulging out of the cells, even in the absence of auxin transport.

Previous studies, however, have shown that interfering with wall properties through the ectopic expression of pectin modifying enzymes or expansins can also cause outgrowths (Fleming et al., 1997; Peaucelle et al., 2008) This led us to ask whether wall loosening induced by pectin or hemicellulose modifiers can also cause changes in microtubule arrangements.

We therefore investigated the effects of perturbing the pectin polymers within the wall using external PME treatment. PMEs in principle reduce wall stiffness by affecting the pectin matrix, and thereby cause the ectopic formation of outgrowths at the SAM (Peaucelle et al., 2011a; Peaucelle et al., 2008). In our hands, PME treatments induced organ formation in 7 (31,8%) of the tested LTI6b expressing SAMs (n=22) (Figure 5A, Figure S3). A substantial radial enlargement of the SAM was observed in the majority of the population (14 or 63.6%), with 1 plant not responding to the treatment (4.5%, Figure S3). Regardless of the final effect in all responding meristems, PME treatments affected CMT organization in 35S::GFP-MBD within 48h (Figure 5B and C). In particular we observed that 24h after the beginning of the PME treatment most of the meristematic cells still displayed an anisotropic arrangement of CMTs, although in some plants the average CMT orientation shifted from circumferential to longitudinal (Figure 5B and C). At 48h after the treatment, the majority of the cells clearly displayed isotropic CMT arrangements. It must be pointed out that the disruption of CMT organization by PME is substantially slower and less abrupt compared to that induced by IAA in control experiments (Figure 5B and C) (Sassi et al., 2014).

We next tested whether perturbing wall remodeling genes potentially targeting the hemicellulose matrix would also affect microtubules and cause the formation of outgrowths in the absence of auxin transport. Unfortunately, single and double *xth4* and *xth9* mutants as well as *expa15* knockouts did not show any obvious phenotype (our unpublished results). We therefore focused our attention on the *xxt1*/*xxt2* double mutant. The *XXT1* and *XXT2* genes encode XyG xylosyl-transferases, which are both expressed at the shoot apex (Yang et al., 2016). Mutants lacking both genes have very little or no xyloglucans and form stunted plants, which are nevertheless able to produce lateral organs such as branches, leaves and flowers. In addition, certain cell walls of the mutant are more elastic and more extensible, whereas microtubule alignments are perturbed in certain tissues (Park and Cosgrove, 2012a; Xiao et al., 2016).

Under normal conditions on soil, the *xxt1*/*xxt2* mutant had a mild phenotype (Xiao et al., 2016). The primary inflorescence stem was not able to grow vertically; the meristems were smaller, while phyllotaxis was perturbed. On NPA a particular phenotype was observed. In our hands, 60-70% (n=100) of wild type plants grown on NPA form pin-like stems. This is at least partially because the microtubules maintain a highly anisotropic organization of cellulose deposition, thus promoting the formation of a cylindrical stem (Hamant et al., 2008; Sassi et al., 2014). Interestingly, when grown on NPA, a 40% (n=100) of the *xxt1*/*xxt2* mutants showed the formation of multiple spontaneous outgrowths (Figure 6A and J) very rarely seen in wild type plants. A double mutant line expressing PDF1::mCitrine-MBD in the L1 layer of the meristem showed that this phenotype on NPA went along with altered microtubule organization. In particular, the zone of isotropic microtubule arrays at the meristem summit was extended to a variable degree (Figure 6D-I). Outside this zone, the cells were able to align their microtubules in the circumferentially around the stem. This implies that the level of xyloglucans can influence microtubule alignment at the shoot apex. However, this is only apparent in the absence of auxin accumulation.

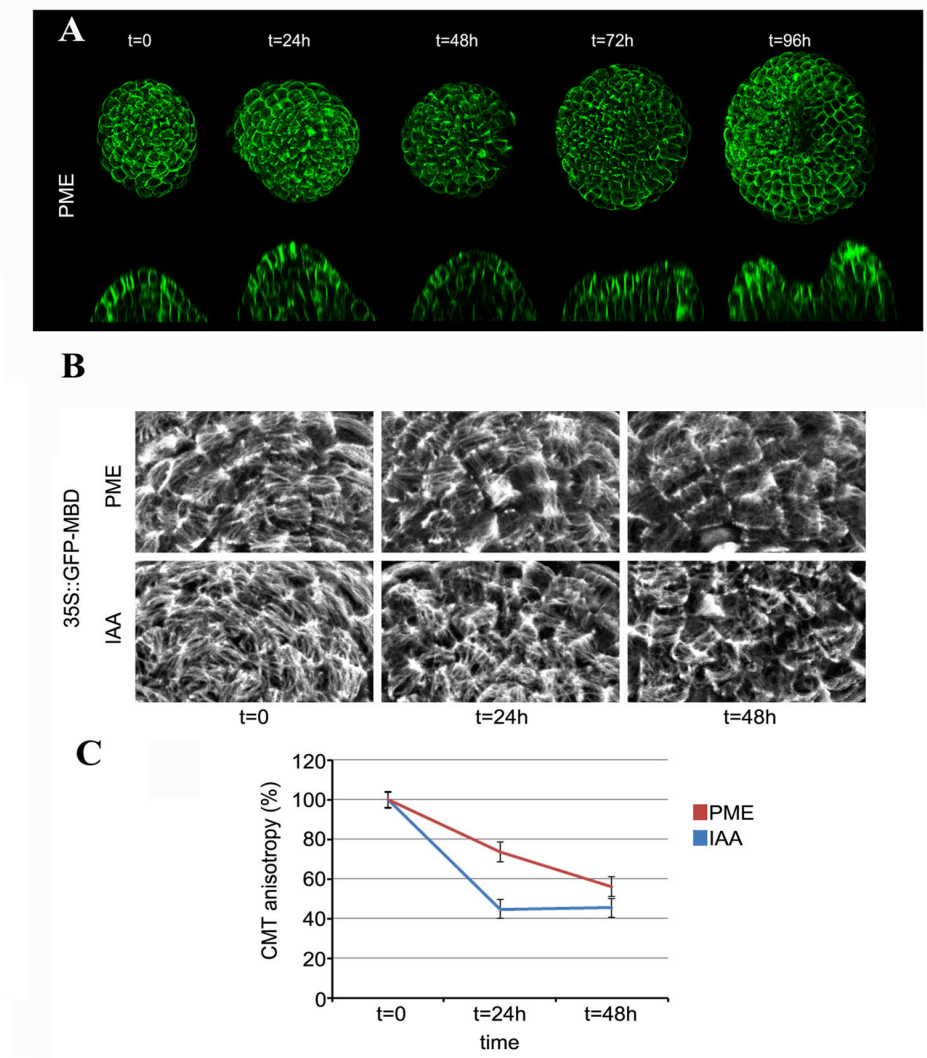

Figure 5. PME treatment promotes CMT isotropy in SAM cells.
(A) PME treatments effect on SAM morphogenesis. NPA-grown 35S::GFP-LTI6b plants were pictured before (t=0) and 96h after the beginning of the PME treatment. Top views (upper row) and longitudinal sections (bottom row) are shown. Whereas in most treatments PME caused a generalized swelling of the SAM, lateral outgrowths were formed in 7 out of 22 treated meristems. (B and C) PME treatments promote long-term disruption of CMT organization in SAM cells. (B) Details of SAM cells of NPA-grown 35S::GFP-MBD treated with PME (upper row) and IAA (lower row). (C) Relative quantification of CMT isotropy in SAM cells grown as in (B). In both cases the treatment leads to a reduction in anisotropy At least 140 cells were measured for each condition. Error bars represent SEM.

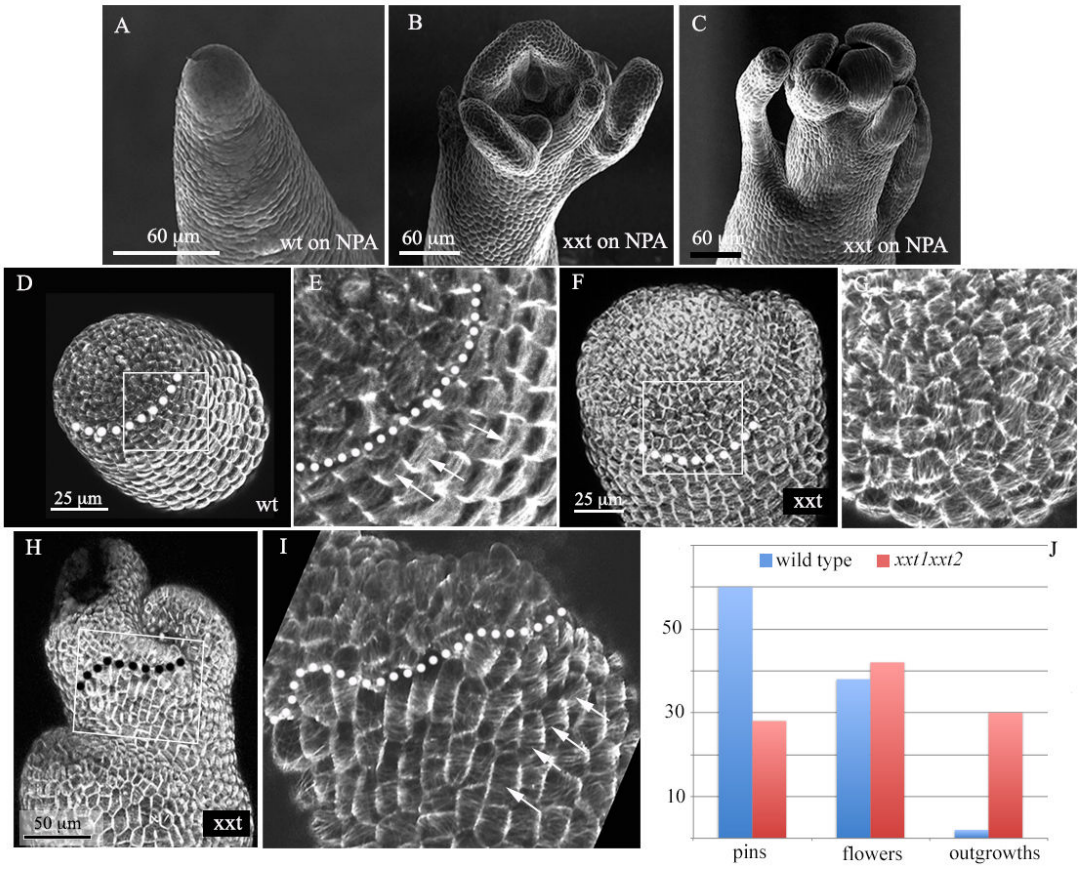

Figure 6. Effect of xxt1/xxt2 double mutation on organ production (A) SEM images depicting the SAM phenotypes of the xxt1xxt2 double mutant grown on NPA compared to the wild-type (Col-0). Overview (D) and detail (E) of a wild type meristem expressing MBD:GFP grown on NPA. The dotted line indicates the limit between the zone of isotropic microtubules (arrows in E) at the dome and the anisotropic beginning of the stem. (F-I) show two examples of the xxt1/xxt2 mutant. In both cases, the isotropic zone is extended (limits indicated by dotted lines), which is correlated with the formation of lateral outgrowths. Note that the cells are able to align their microtubules lower down (arrows in I). (J) shows quantification of phenotypes (%) in wild type and mutants on NPA, based on 100 individuals for each genotype. A majority of the wild type plants form naked pins, 28% form one or more flowers, while 2% form non defined outgrowths. In the mutant this percentage is much higher.

Discussion

Structural isotropy and lateral organ formation

Shape changes during morphogenesis in plants are achieved through the local isotropic or anisotropic yielding of the cell wall to the internal turgor pressure. In a previous study we highlighted the regulation of structural wall anisotropy during organ initiation at the shoot apical meristem (Sassi et al., 2014). The local accumulation of auxin destabilizes microtubule alignment, probably via a ROP-based signaling cascade. This supposedly causes a shift to isotropic microfibril deposition and consequently to isotropic growth and the formation of a new growth axis. Intuitively it seemed plausible that a group of structurally isotropic cells in an anisotropic environment would spontaneously bulge out. Our numerical simulations, however, showed that this is not the case. This comes from the fact that structurally isotropic walls expand more slowly than anisotropic walls if all other mechanical parameters are kept identical. This is probably because cell wall rigidity in a particular direction is not a linear function of the number of microfibers in that direction. Fibrils aligned in other, similar directions also contribute, generating a cooperative effect with a counter-intuitive consequence: when the structural anisotropy of the cell wall evolves, the average rigidity changes, although the number of fibrils remains constant. This change in wall stiffness in turn also affects growth rates (see Supplemental Model Description for detailed explanations). In our simulations this property led to decreased growth rates when the walls were made more isotropic.

Coupling anisotropy to wall loosening

The simulations left us with a contradiction: *in vivo*, isotropy seemed to be synonymous with increased growth rates and organ formation, while simulations and theory told us that the exact opposite should happen. We resolved this apparent contradiction by showing that in contrast to the simulations, where rigidity and anisotropy can be programmed independently, we were not able to separate both parameters experimentally. This is because a shift to isotropic growth *in vivo* also triggers an increase in wall loosening. At this stage it remains unclear how this transcriptional coupling functions. Our enhanced yeast one- hybrid assay showed that as many as 31 TFs have the potential to activate *XTH9* promoter, 23 to the

EXPA15 promoter and 97 to the *EXPA4* promoter (Abad and Traas unpublished), thus indicating that the regulation of cell wall loosening depends on many inputs.

Whatever the molecular basis, the coupling between wall loosening and isotropy could provide a mechanical module, which is essential for establishing the typical branched plant architecture. It remains to be seen if and how this coupling functions in other developmental contexts. Evidence exists suggesting that it could be widely activated during plant morphogenesis. A previous study identified a regulatory cross talk between microtubules and XTHs, which control petiole elongation in shaded plants downstream of auxin action (Sasidharan et al., 2014). Moreover, a recent cellular analysis of the *xxt1/xxt2* mutant, which shows a greatly reduced xyloglucan content, exhibited a loss of microtubule alignment in hypocotyls (Cavalier et al., 2008; Park and Cosgrove, 2012a; Xiao et al., 2016). It was also found that the expression of several microtubule-associated genes including MAP70-5 and CLASP as well as receptor genes such as HERK1 and WAK1 were changed in *xxt1 xxt2* mutants (Xiao et al., 2016). Together, these results indicate that the coupling between xyloglucan loosening and CMT organization is not restricted to the SAM but could be involved in the regulation of different developmental processes.

Organ initiation and the wall matrix

The cell wall matrix tethers the cellulose microfibrils together and the regulation of its composition is essential during organ development. A recent comprehensive analysis showed that the enzymes involved in hemicellulose synthesis play an important role throughout the meristematic apex (Yang et al., 2016). Our finding that several XTHs and EXPAs are very strongly upregulated in the rapidly outgrowing organs would suggest a prominent role for xyloglucan modifications, in line with the results of previous studies on organogenesis in tomato (Fleming et al., 1997; Reinhardt et al., 1998). Although mutants where XTH4 and 9 were knocked out show reduced XET activity (Mellerowicz et al unpublished), no strong phenotypes were observed under normal conditions in double mutants. Likewise, an EXPA15 knockout did not show any obvious effect. This probably reflects the extraordinary flexibility of the cell wall assembly and remodeling network. Nevertheless, the *xxt1/xxt2* mutant produced lateral outgrowths when auxin transport was inhibited, showing that the control of xyloglucan synthesis is at least partially responsible for the *pin* phenotype.

Several studies have also pointed at the importance of pectins in morphogenesis at the shoot apex. However, Yang and colleagues (Yang et al., 2016) did not find obvious differences in the degree of pectin methylation related to organ initiation at the SAM. We confirmed these results and found that PMEIs are much more strongly expressed in the more differentiating, expanding cells on the abaxial side of the organ primordia, whereas the expression of PMEs seems to be rather homogeneous at the meristem (see also: (Krizek et al., 2016)). We therefore would favor a hypothesis where the degree of pectin methylation is not subject to major changes during organ initiation. This does imply, however, that to remain constant, pectin properties would need to be regulated in a strict manner at the meristem. Accordingly, modifications in the degree of pectin methylation through overexpression of PMEs or PMEIs lead to extra outgrowths or to the inhibition of organ initiation (Peaucelle et al., 2011a; Peaucelle et al., 2008).

Conclusions and Perspectives

In conclusion, we provide evidence for the existence of a mechanical module at the shoot apex, which couples the transcriptional regulation of wall expansion to cellular anisotropy and show how this module might function during organ initiation. An important challenge will be to further unravel the coupling mechanisms and what signaling components and transcription factors are involved. More generally, it will be important to investigate how this coordination between wall loosening and anisotropy is modulated throughout plant development.

Experimental procedures

Plant material, growth conditions and chemical treatments

Arabidopsis thaliana plants of the ecotypes Columbia-0 (Col-0) and Wassilewskija-2 (Ws-2) were used as wild type. Transgenic lines and mutants used in this study have been previously described: 35S::LTi6b-GFP, 35S::GFP-MBD, *pin1-6* and *bot1-7/pin1-6* (Okada et al., 1991; Sassi et al., 2014). Plants were grown as previously described (Sassi et al., 2014). Napthylphthalamic acid (NPA), indole-3-acetic acid (IAA) and oryzalin (ORY) treatments were carried out as previously described (Sassi et al., 2014). Treatments with PME were

carried out as previously described (Peaucelle et al., 2008), with some modifications: plants were grown i*n vitro* on NPA plates until bolting, then they were transferred onto fresh NPA plates and imaged (t=0). Immediately after imaging, plants were submerged in a PME solution (1U/100µl in phosphate buffer pH=7) for 16h. Plants were imaged again at t=24h, and the treatment was repeated immediately after. No further treatments were applied until the end of the experiment.

Confocal live Imaging and image analyses.

Confocal imaging was carried out on a Zeiss LSM700 system as previously described (Sassi et al., 2014). SEM imaging was carried out on a Hirox SE-3000 system as previously described (Sassi et al., 2014). Analyses of CMT organization were carried out with FIJI software as previously described (Sassi et al., 2014).

RNA-Seq sample preparation and sequencing analysis

Ten dissected (to P5) Col-0 meristems were pooled for each biological replicate. RNA was extracted using the Arcturus PicoPure RNA extraction kit (ThermoFisher) according to the manufacturer's instructions. Libraries were prepared using the TruSeq Strand specific protocol following manufecturers instructions. The three RNA-seq libraries were sequenced using a HiSeq2000 Pair End 2x100bp at the Unité de Recherche en Génomique Végétale (Institute of Plant Sciences Paris-Saclay). The raw reads in fastq format were analyzed in house. We first assessed the quality of the reads using FastQC (http://www.bioinformatics.babraham.ac.uk/projects/fastqc). Reads were cleaned (quality threshold: 20, adaptors removed, and reads mapping to rRNA removed). Preprocessed reads were then mapped to the Col-0 reference genome using Bowtie 2 and TopHat and counted using HTSeq. TPM (Transcripts Per Kilobase Million) were calculated for each gene by dividing the raw number of reads to the length of the cDNA in kb, normalized to the number of reads per biological replicate in million reads. All raw and normalized data are available through the CATdb database (AU_XXXXXXX), (Gagnot et al., 2008) and from the Gene Expression Omnibus repository (Barrett et al., 2007) at the National Center for Biotechnology Information (GSE XXXXX).

Histochemistry

RNA in situ hybridization assays were performed as described previously (Ferrandiz and Sessions, 2008a, b). For whole-mount RNA in situ hybridization assays, untreated and treated (IAA or ORY) *pin1-6* meristems from soil-grown plants were processed as previously described (Rozier et al., 2014). At least three independent experiments for both assays were performed for each probe tested. Whole mount immunolabellings were carried out as previously described (de Reuille et al., 2006). Cell wall antibodies were obtained from the Plant Probes service at the University of Leeds, UK (http://www.plantprobes.net/index.php)

Quantitative reverse transcription PCR (qRT-PCR)

Total RNA was extracted using the Spectrum Plant Total RNA Kit (Sigma). Total RNAs were digested on-column with Turbo DNA-free DNase I (Ambion) according to the manufacturer's instructions. SuperScript VILO cDNA Synthesis Kit (Invitrogen) was used to reverse transcribe RNA. The quantitative reverse transcription PCR (qRT-PCR) was performed on a StepOne Plus Real Time PCR System (Applied Biosystems), using FastStart Universal SYBR Green Master (Rox) (Roche). Data were analyzed using the StepOne Software v2.2 (Applied Biosystems). TCTP gene has been used as reference. Expression levels of each target gene, relative to TCTP, were determined using a modification of the Pfaffl method (Pfaffl, 2001). Primers are listed in the Table S3.

Enhanced Yeast-One-Hybrid

The eYIH assays were performed as previously described (Gaudinier et al., 2011; Taylor-Teeples et al., 2015). Briefly, gene promoters (2000bp of upstream regulatory region from the translational start site, or the next gene) were cloned and recombined to reporter vectors pMW2 (Y1H *HIS3* reporter vector) and PMW3 (YIH *LacZ* reporter vector) (Brady et al., 2011). Interactions were called for transcription factors that activated at least one reporter assay. Primers used are listed in Table S3.

Author contributions

Conceptualization: M.S., J.T., A.A., O.A.; Software: O.A.; Investigation: M.S., A.A., L.V., A.E.S., U.A, A.L., V.B., LT; Resources: T.V.; Writing – Original Draft : M.S. and J.T. ; Visualization : M.S., O.A. and J.T. ; Supervision : AA, M.S. and J.T.; Funding Acquisition : J.T.

Acknowledgements

This work was funded by the ERC grant (MORPHODYNAMICS); we thank Olivier Hamant Françoise Moneger and Roberta Galletti for the critical reading of the manuscript.

Supplementary Material

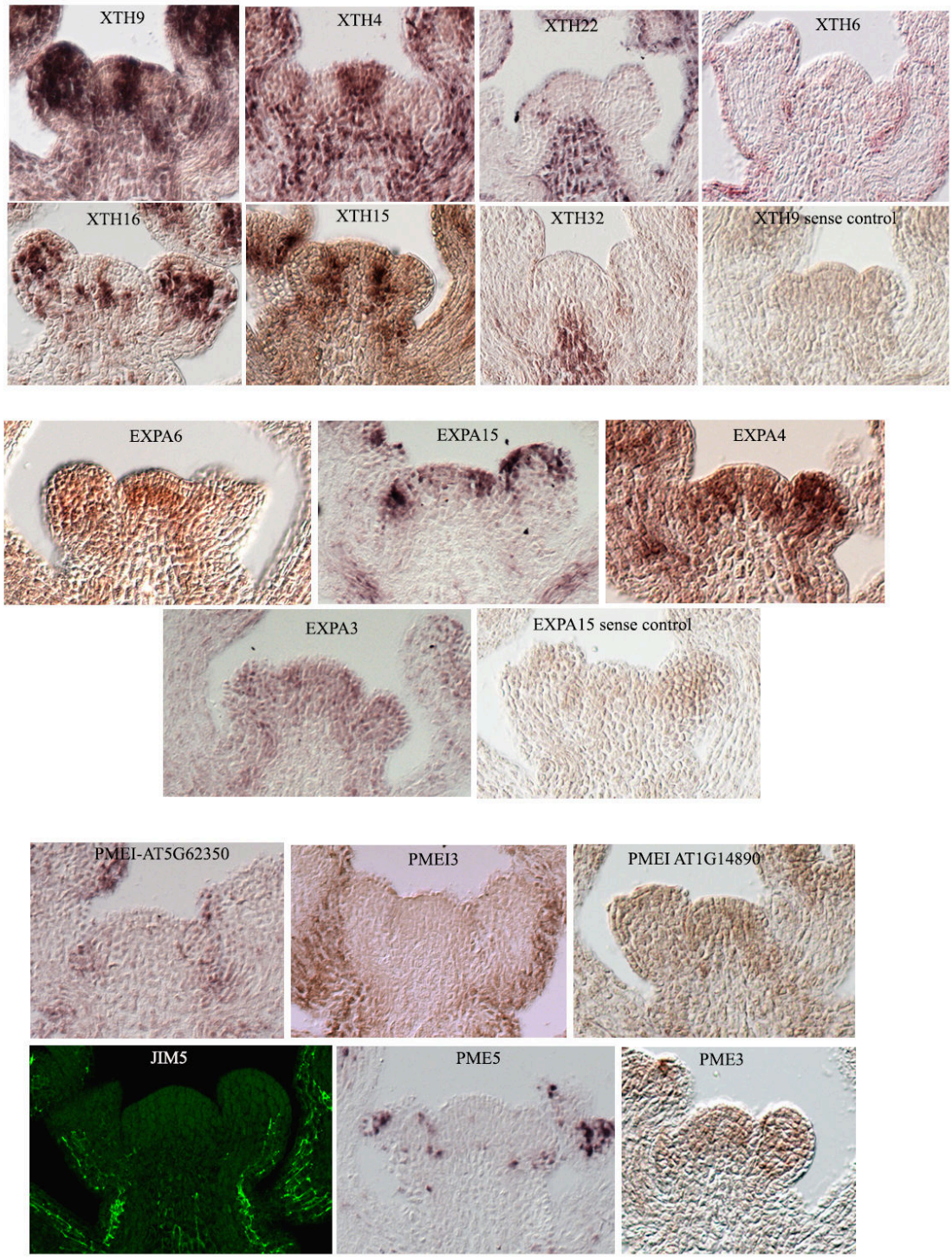

Figure S1 In situ hybridization showing the distribution of all detectable RNAs of the XTHs, EXPAs, PMEIs and PMEs. Note that the patterns of *PMEI-AT5G62350* and *PMEI3* match part of the domains labelled by JIM5 (bottom left image), which labels partially methyl-esterified epitopes of homogalacturonan and can also bind to un-esterified homogalacturonan.

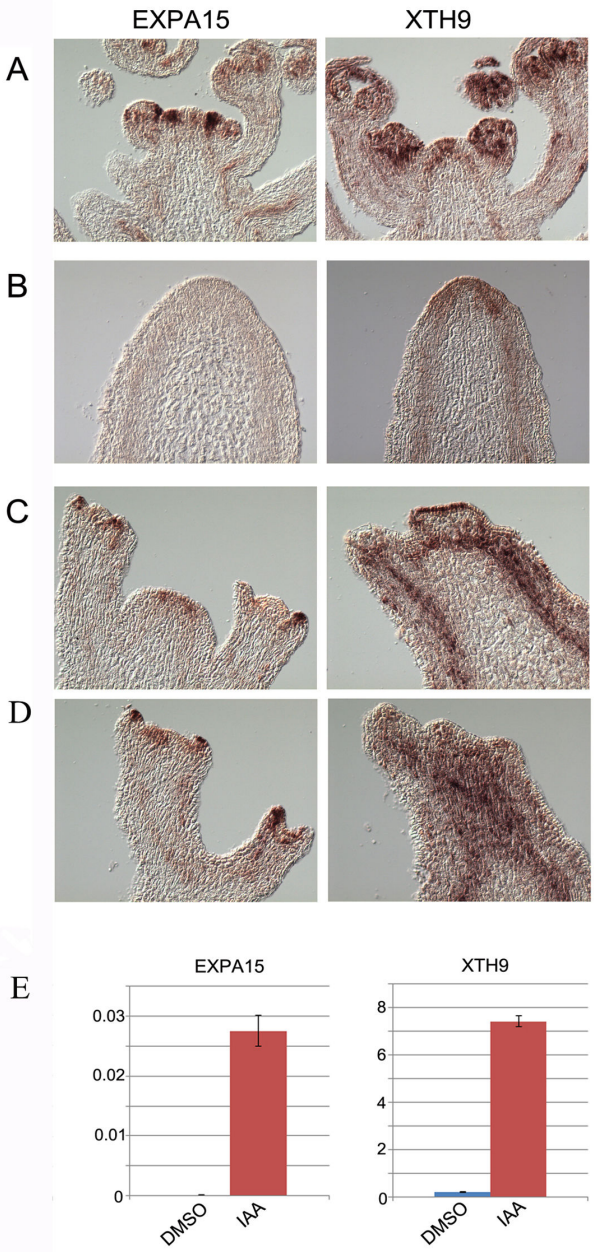

Figure S2 Induction of EXPA15 and XTH9 expression by auxin. (A-C)in RNA situ hybridization, (D) RTqPCR of *pin* mutants treated with DMSO (control) and IAA in lanolin paste. Row (A) shows normal patterns. In *pin* mutants (B and D) the expression levels of these genes are very low or barely detectable. After treatment with auxin, the two genes are again expressed in the induced lateral outgrowths. Note that the effects on EXPA15 and XTH9 are largely indirect.

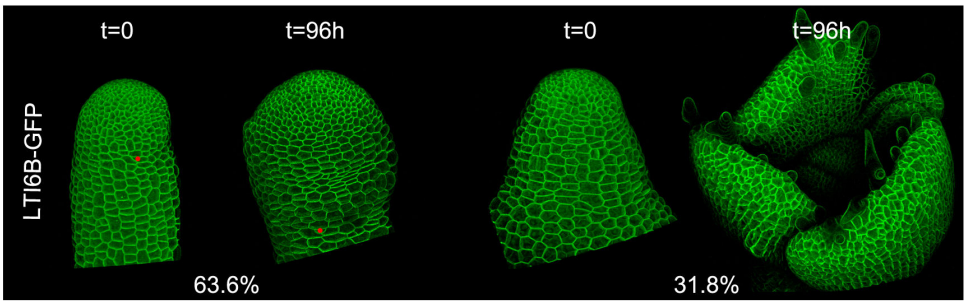

Figure S3. Effects of PME on organ production in pin-shaped meristems on NPA. Two thirds of the meristems swelled up but did not produce outgrowths (N=15/22), the remaining meristems formed organ like structures (N=7/22)

Table S1: results RNA seq, for XTHs, PMEs, PMEIs, EXPAs and CesAs. For normalized values taking into account the length of the RNAs, the TPM (Transcripts Per Kilobase Million has been calculated)
Summary

XTH9	59%
XTH4	11%
XTH22	9%
XTH6	7%
rest XTH	13%
EXPA6	41%
EXPA15	16%
EXPA4	13%
EXPA3	9%
EXPA20	6%
rest EXPAs	15%
CesA3	33%
CesA1	30%
CesA6	16%
CesA5	12%
CesA2	8%
rest CesA	1%
PME5	34%
ATPME3	14%
ATPME1	10%
ATPME31	6%
AT3G10720	5%
AT3G49220	5%
ATPME44	5%
rest PMEs	21%
AT5G62350	31%
AT5G20740	25%
AT1G14890	14%
ATC/VIF2	12%
AT2G01610	4%
rest	14%

Table S2: Primers used for *in situ* hybridization

GeneID	Primers used to amplify total cDNA sequence from TAIR cds
XTH9	XTH9_For : ATGGTCGGTATGGATTTGTTCAAATGTGTA
	XTH9_T7 Rev : TGTAATACGACTCACTATAGGGCCTACAAATGACGATGATGTT
XTH4	XTH4_For : ATGACTGTTTCTTCATCTCC
	XTH4_T7 Rev : TGTAATACGACTCACTATAGGGCTTATGCGTCTCTGTCCCTTT
XTH22	XTH22_For : ATGGCGATCACTTACTTGCTTCCTCTGTTT
	XTH22_T7 Rev : TGTAATACGACTCACTATAGGGCTGCAGCTAAGCACTCTTTAG
XTH6	XTH6_For : ATGGCTAAGATATATTCCCCTTCTTTTCCC
	XTH6_T7 Rev : TGTAATACGACTCACTATAGGGCTCAAGCACGACACTCGGGTG
XTH16	XTH16_For : ATGGGTCGAATCTTGAA
	XTH16_T7 Rev : TGTAATACGACTCACTATAGGGCTTAGACTCTAGACTTCCTAC
XTH15	XTH15_For : ATGGGTCCAAGTTCGAGCCTCACCACCATC
	XTH15_T7 Rev : TGTAATACGACTCACTATAGGGCTCAGACTCTGGACTTCTTGC
XTH32	XTH32_For : ATGGGTAACTCTTTGATCTCTC
	XTH32_T7 Rev : TGTAATACGACTCACTATAGGGCCTAACGCCAACATTCCGGCG
XTH28	XTH28_For : ATGGGTTTTATAACTCGATTTTTAGTTTTC
	XTH28_T7 Rev : TGTAATACGACTCACTATAGGGCTCATATCGACTCAGTTCGAG
XTH27	XTH27_For : ATGGAGACTCTGAGTCGTTTATTGGTTTTC
	XTH27_T7 Rev : TGTAATACGACTCACTATAGGGCTCATATCGACTCGGTTCCAT
XTH4 sense	XTH4_T7 For :TAATACGACTCACTATAGGGATGACTGTTTCTTCATCTCC
	XTH4_Rev : TTATGCGTCTCTGTCCCTTTTACATTCAGC
XTH9 sense	XTH9_T7 For : TAATACGACTCACTATAGGGATGGTCGGTATGGATTTGTT
	XTH9_Rev :CTACAAATGACGATGATGTTGGCACTCAAG
EXPA6	EXPA6 For : ATGGCAATGTTGGGCTTGGTTTTATCTGTT
	EXPA6 T7 Rev : TGTAATACGACTCACTATAGGGCTCAGACTCTGAAGTTCTTTC
EXPA15	EXPA15_For : ATGTTCATGGGTAAGATGGG
	EXPA15_T7 Rev : TGTAATACGACTCACTATAGGGCTTAACGGAATTGACGGCCGG
EXPA4	EXPA4_For :ATGGCTATTAAACTAGCAATTCTATTTACC
	EXPA4_T7 Rev : TGTAATACGACTCACTATAGGGCTTAAACCCTGAAATTCTTCC

EXPA3	EXPA3_For : ATGACGGCGACTGCGTTTAG
	EXPA3_T7 Rev : TGTAATACGACTCACTATAGGGCTCAGACTCGAAAGTTTTTGC
EXPA20	EXPA20_For : ATGGATTCTGGGCTTCAGCAACTCGCATTG
	EXPA20_T7 Rev : TGTAATACGACTCACTATAGGGCTCAGGAGTGGAACTGCTTTC
EXPA13	EXPA13_For : ATGCAACGGTTTCTTCTACCTTTACTCTTC
	EXPA13_T7 Rev : TGTAATACGACTCACTATAGGGCTCACGGAGTCTCGAATTGTT
EXPA10	EXPA10_For : ATGTGCAGGTTGTTAACACA
	EXPA10_T7 Rev : TGTAATACGACTCACTATAGGGCTTAACGGAACTGTCCACCGG
	EXPA10_For1 : ATGGGTCATCTTGGGTTCTT
EXPA1	EXPA1_For :ATGGCTCTTGTCACCTTCTT
	EXPA1_T7 Rev : TGTAATACGACTCACTATAGGGCTCAAGCACTCGAAGCACCAC
EXPA5	EXPA5_For : ATGGGAGTTTTAGTAATCTCGCTTCTCGTG
	EXPA5_T7 Rev : TGTAATACGACTCACTATAGGGCTTAATACCGAAACTGCCCTC
PME5	PME5 S: ATGGCGCAACTTACTAATTC
	PME5 AS: TGTAATACGACTCACTATAGGGCTTAAGCATCTCGAGGAGCGATC
PME3	PME3_For : ATGGCACCATCAATGAAAGAAATTTTTTCT
	PME3_T7 Rev :TGTAATACGACTCACTATAGGGCTCAAAGACCGAGCGAGAAGG
PME1	PME1_For : ATGGATTCAGTGAACTCCTTCAAAGGATAT
	PME1_T7 Rev : TGTAATACGACTCACTATAGGGCTTAAGATAGCTGATTGATCA
PME31	PME31_For : ATGGCAACGACTCGAATGGTTAGGGTTTCG
	PME31_T7 Rev : TGTAATACGACTCACTATAGGGCCTAAGCCGAATATGGTGTTT
PMEI 62350	PME62350_For : ATGGCAAAACAATATCTCTT
	PME62350_T7 Rev : TGTAATACGACTCACTATAGGGCTTAGTAAGTTTTAGCAAAGG
PMEI3	PMEI3_For : ATGGCTCCTACACAAAATCTCTTCCTTGTC
	PMEI3_T7 Rev : TGTAATACGACTCACTATAGGGCTCAAAGATGTACGTCGTGGG
AT1G14890	PMEI14890_For : ATGTTAACTCGAAACAAAGAAGAAATAAAC
	PMEI14890_T7 Rev : TGTAATACGACTCACTATAGGGCTTAGGCTCCATTGTTGGCGT
ATC/VIF2	AT5G64620_For : ATGGCTTCTTCTCTCATCTTCCTCCTCCTC
	AT5G64620_T7 Rev : TGTAATACGACTCACTATAGGGCTCATTCAACAAGGCGATCAA

Table S3. Primers used for qRT-PCR (Figure S3) and to amplify promoter regions for YIH assays

Primer name	Sequence (5'>3')	Use
TCTP-FW	GCTCAGCGAAGAAGATCAAGCTGTC	qRT-PCR
TCTP-RV	CCCTCCCCAACAAAGAATTGGAAG	qRT-PCR
EXPA15-FW	TAACGCTGGTGGTTGGTGTA	qRT-PCR
EXPA15-RV	CTGAGCAATGCGTTGAAAAA	qRT-PCR
XTH9-FW	GCTGGGCTATGGATCATTGT	qRT-PCR
XTH9-RV	TTCAAACCCAGCTCCAGAGT	qRT-PCR
EXPA4 Y1H F 1st	TGATGTCTTTGATGGTGGTGG	1st round promoter cloning Y1H
EXPA4 Y1H R 1st	TGGGACTAACCCATTGTGC	1st round promoter cloning Y1H
EXPA15 Y1H F 1st	GCAACACAGTCAAAGCATACTC	1st round promoter cloning Y1H
EXPA15 Y1H R 1st	GCCATGAACAGAGCACACC	1st round promoter cloning Y1H
XTH9 Y1H F 1st	ACTGAGGAATGGAAACTATTAGA	1st round promoter cloning Y1H
XTH9 Y1H R 1st	GCCTTCGTTGACACAATG	1st round promoter cloning Y1H
EXPA4 Y1H F 2nd	TTTTTTTTCAGCAAGAAGAAA	2nd round promoter cloning Y1H
EXPA4 Y1H R 2nd	TTTGTGTGTGAATTACTAGAAACAG	2nd round promoter cloning Y1H
EXPA15 Y1H F 2nd	CATACTCGAACCAACAGTAAAAA	2nd round promoter cloning Y1H
EXPA15 Y1H R 2nd	TTACTGCTTTAACTGTTTTCCCTAC	2nd round promoter cloning Y1H
XTH9 Y1H F 2nd	ACTGAGGAATGGAAACTATTAGA	2nd round promoter cloning Y1H
XTH9 Y1H R 2nd	TTTTTTTTTAACTTATCTCTCTAAATAA	2nd round promoter cloning Y1H

Table S4. Identified transcription factor-promoter interactions

TF AGI	TF Name	TF family	Target
AT1G61660	AT1G61660	BHLH	XTH9
AT1G26610	AT1G26610	C2H2	XTH9
AT2G26940	AT2G26940	C2H2	XTH9
AT1G16530	LBD3		XTH9
AT1G34390	ARF22	ARF	XTH9
AT4G35280	DAZ2	C2H2	XTH9
AT3G20670	HTA13	CCAAT	XTH9
AT1G19490	AT1G19490	bZIP	XTH9
AT5G59430	ATTRP1	MYB-related	XTH9
AT5G24050	AT5G24050	REM(B3)	XTH9
AT5G03780	TRFL10	MYB-related	XTH9
AT4G00210	LBD31	LOB/AS2	XTH9
AT2G17180	DAZ1	C2H2	XTH9
AT2G35550	ATBPC7/BBR	BBR-BPC	XTH9
AT5G38490	AT5G38490	REM(B3)	XTH9

AT5G64610	HAM1	C2H2	XTH9
AT1G50410	AT1G50410	SNF2	XTH9
AT2G45420	LBD18	LOB/AS2	XTH9
AT1G26590	AT1G26590	C2H2	XTH9
AT2G33550	AT2G33550	TRIHELIX	XTH9
AT2G41835	AT2G41835	C2H2	XTH9
AT5G44260	AtTZF5	C3H	XTH9
AT2G01930	ATBPC1/BBR	BBR-BPC	XTH9
AT5G15480	AT5G15480	C2H2	XTH9
AT3G46590	ATTRP2/TRFL1	MYB-related	XTH9
AT4G38910	ATBPC5BBR/BPC5	BBR-BPC	XTH9
AT1G02040	AT1G02040	C2H2	XTH9
AT3G53680	AT3G53680	PHD	XTH9
AT2G21240	ATBPC4/BBR	BBR-BPC	XTH9
AT1G24190	ATSIN3/SNL3	Orphans	XTH9
AT5G15020	SNL2	Orphans	XTH9
AT5G44160	NUC	C2H2	EXPA15
AT3G21270	ADOF2	C2C2-DOF	EXPA15
AT2G22430	ATHB6	HB	EXPA15
AT5G57660	ATCOL5	C2C2-CO-LIKE	EXPA15
AT2G34140	AT2G34140	C2C2-DOF	EXPA15
AT1G10480	ZFP5	C2H2	EXPA15
AT3G49940	LBD38		EXPA15
AT1G73870	AT1G73870	C2C2-CO-LIKE	EXPA15
AT1G68550	CRF10	AP2/EREBP	EXPA15
AT1G19860	AT1G19860	C3H	EXPA15
AT4G37780	ATMYB87	MYB	EXPA15
AT3G23230	AtERF98/AtTDR1	AP2-EREBP	EXPA15
AT5G10120	AT5G10120	EIL	EXPA15
AT3G03660	WOX11	HB	EXPA15
AT4G27230	HTA2	CCAAT	EXPA15
AT5G66770	AT5G66770	GRAS	EXPA15
AT5G03780	TRFL10	MYB-related	EXPA15
AT5G38490	AT5G38490	REM(B3)	EXPA15
AT1G51220	AtWIP5	C2H2	EXPA15
AT3G06220	AT3G06220	ABI3-VP1	EXPA15
AT1G05690	BT3	TRAF/TAZ	EXPA15
AT1G68800	BRC2/TCP12	TCP	EXPA15
AT4G22745	MBD1	MBD	EXPA15
AT5G06960	OBF5	BZIP	EXPA4

AT2G20880	AT2G20880	AP2/EREBP	EXPA4
AT2G21230	AT2G21230	BZIP	EXPA4
AT5G10140	FLC	MADS	EXPA4
AT1G47870	ATE2F2	E2F/DP	EXPA4
AT3G23240	ERF1	AP2/EREBP	EXPA4
AT4G27410	RD26	NAC	EXPA4
AT5G48250	AT5G48250	C2C2-CO-LIKE	EXPA4
AT1G14350	FLP	MYB	EXPA4
AT4G38960	AT4G38960	C2C2-CO-LIKE	EXPA4
AT5G08520	AT5G08520	MYB	EXPA4
AT2G44730	AT2G44730	TRIHELIX	EXPA4
AT1G04880	AT1G04880	ARID	EXPA4
AT2G26940	AT2G26940	C2H2	EXPA4
AT5G06950	AHBP-1B	BZIP	EXPA4
AT5G05410	DREB2A	AP2/EREBP	EXPA4
AT4G37260	MYB73	MYB	EXPA4
AT4G01120	GBF2	BZIP	EXPA4
AT2G40950	BZIP17	BZIP	EXPA4
AT1G51600	ZML2	C2C2-GATA	EXPA4
AT1G21910	DREB26	AP2/EREBP	EXPA4
AT3G61830	ARF18	ARF	EXPA4
AT1G16530	LBD3		EXPA4
AT1G76420	CUC3	NAC	EXPA4
AT1G56010	NAC1	NAC	EXPA4
AT2G45190	YAB1	C2C2-YABBY	EXPA4
AT5G63090	LOB		EXPA4
AT5G57390	PLT5	AP2/EREBP	EXPA4
AT1G76420	CUC3	NAC	EXPA4
AT1G12980	DRN	AP2/EREBP	EXPA4
AT1G77850	ARF17	ARF	EXPA4
AT2G24430	ANAC038/ANAC039	NAC	EXPA4
AT3G18400	NAC058	NAC	EXPA4
AT3G20670	HTA13	CCAAT	EXPA4
AT1G51060	HTA10	CCAAT	EXPA4
AT1G14685	ATBPC2	BBR-BPC	EXPA4
AT3G01890	AT3G01890	SWI/SNF-BAF60	EXPA4
AT2G40450	AT2G40450	TRAF	EXPA4
AT3G11100	AT3G11100	TRIHELIX	EXPA4
AT1G55650	AT1G55650	ARID	EXPA4
AT5G01860	AT5G01860	C2H2	EXPA4

AT4G39410	ATWRKY13	WRKY	EXPA4
AT2G02820	AtMYB88	MYB	EXPA4
AT4G03170	AT4G03170	ABI3-VP1	EXPA4
AT5G13780	AT5G13780	GNAT	EXPA4
AT4G12670	AT4G12670	MYB-related	EXPA4
AT3G12977	AT3G12977	NAC/NAM	EXPA4
AT5G48890	LATE	C2H2	EXPA4
AT5G66870	ASL1/LBD36	LOB/AS2	EXPA4
AT5G19650	ATOFP8	OFP	EXPA4
AT4G27230	HTA2	CCAAT	EXPA4
AT5G14170	BAF60/CHC1	SWI/SNF-BAF60	EXPA4
AT3G45150	TCP16	TCP	EXPA4
AT1G65620	AS2	LOB/AS2	EXPA4
AT5G60142	AT5G60142	ABI3-VP1/B3	EXPA4
AT3G14740	AT3G14740	PHD	EXPA4
AT5G24050	AT5G24050	REM(B3)	EXPA4
AT2G35550	ATBPC7/BBR	BBR-BPC	EXPA4
AT4G00238	AT4G00238	GeBP	EXPA4
AT3G63030	MBD4	zf-CW	EXPA4
AT5G07500	AtTZF6/PEI1	C3H	EXPA4
AT5G38490	AT5G38490	REM(B3)	EXPA4
AT1G05230	HDG2	HB	EXPA4
AT5G18090	AT5G18090	ABI3-VP1	EXPA4
AT3G25790	AT3G25790	G2-like	EXPA4
AT5G25190	ESE3	AP2-EREBP	EXPA4
AT3G12730	AT3G12730	G2-like	EXPA4
AT2G42430	ASL18/LBD16	LOB/AS2	EXPA4
AT2G45410	LBD19	LOB/AS2	EXPA4
AT3G27650	LBD25	LOB/AS2	EXPA4
AT1G75390	AtbZIP44	bZIP	EXPA4
AT2G01930	ATBPC1/BBR	BBR-BPC	EXPA4
AT4G00270	AT4G00270	GeBP	EXPA4
AT3G16160	AT3G16160	CPP	EXPA4
AT1G72570	AT1G72570	AP2-EREBP	EXPA4
AT2G40140	ATSZF2/CZF1/ZFAR1	C3H	EXPA4
AT4G00130	AT4G00130	GeBP	EXPA4
AT5G19790	RAP2.11	AP2-EREBP	EXPA4
AT5G15480	AT5G15480	C2H2	EXPA4
AT4G33280	AT4G33280	ABI3-VP1	EXPA4
AT4G38910	ATBPC5BBR/BPC5	BBR-BPC	EXPA4

AT5G05550	AT5G05550	TRIHELIX	EXPA4
AT4G34590	ATB2/AtbZIP11/GBF6	bZIP	EXPA4
AT2G30130	ASL5/LBD12/PCK1	LOB/AS2	EXPA4
AT4G03250	AT4G03250	HB	EXPA4
AT2G37520	AT2G37520	PHD	EXPA4
AT4G13480	AtMYB79	MYB	EXPA4
AT4G00390	AT4G00390	GeBP	EXPA4
AT1G66420	AT1G66420	GeBP	EXPA4
AT3G01530	ATMYB57	MYB	EXPA4
AT4G31615	AT4G31615	ABI3-VP1	EXPA4
AT3G53680	AT3G53680	PHD	EXPA4
AT5G52170	HDG7	HB	EXPA4
AT5G25470	AT5G25470	ABI3-VP1/B3	EXPA4
AT2G21240	ATBPC4/BBR	BBR-BPC	EXPA4
AT2G47850	AT2G47850	C3H	EXPA4
AT1G75530	AT1G75530	FHA	EXPA4

Table S5. Identified transcription factor–XTH9 promoter -EXPA4 promoter interactions

TF AG1	TF Name	TF family	Target
AT5G38490		REM(B3)	XTH9, EXPA4 and EXPA15
AT5G24050		REM(B3)	XTH9 and EXPA4
AT3G20670	HTA13		XTH9 and EXPA4
AT1G16530	LBD3		XTH9 and EXPA4
AT2G26940	AT2G26940	C2H2	XTH9 and EXPA4
AT5G15480	AT5G15481	C2H2	XTH9 and EXPA4
AT3G53680		PHD	XTH9 and EXPA4
AT2G35550	ATBPC7/BBR	BBR-BPC	XTH9 and EXPA4
AT2G01930	ATBPC1/BBR	BBR-BPC	XTH9 and EXPA4
AT4G38910	ATBPC5BBR/BPC5	BBR-BPC	XTH9 and EXPA4
AT2G21240	ATBPC4/BBR	BBR-BPC	XTH9 and EXPA4

Chapter III

Microtubule-driven growth isotropy affects the expression of genes involved in organogenesis at the shoot apex of *Arabidopsis*

Ursula Abad, Amélie Robin, Massimiliano Sassi, Jan Traas

Summary

In plants, the production of new tissues and organs is continuous and reflects the activity of meristems. All the aerial parts of the plants are generated by shoot apical meristems (SAMs). This involves the local accumulation of auxin orchestrating a series of events that ultimately result into the emergence of organs at the meristem flanks. Downstream of auxin, the genetic control of organ initiation is well established. Accumulating evidence indicates that auxin contributes to generate new axes of growth by interfering with the mechanical properties of cells although this remains poorly understood. Here we show that genetic and mechanical regulation of organ initiation might control and influence each other independently of auxin control. This coordination might involve additional signals, in particular brassinosteroids.

This last chapter contains my unpublished results regarding the link between microtubule-driven growth isotropy and the expression of the auxin/MP controlled genetic network. I played an important part in conceiving and carrying out most of the experiments. In collaboration with Amélie Robin, we performed the whole mount RNA *in situ* hybridizations. The treatments and analyses of the fluorescent reporter line *pLFY>GFP*, the *arf5-2 bot1-7* cross and the analyses of its phenotype were done in collaboration with Massimiliano Sassi. The eYIH assay was done by the Proteomics Core Facility of UC Davis. I have performed the analyses of the eYIH with inputs from Jan Traas.

Introduction

The generation of shape is a central question in developmental biology. Plants represent an excellent system to study this issue, due to their dynamic and continuous organogenesis. The aerial parts of the plant are produced by small groups of non-differentiated cells, the shoot apical meristems (SAMs). Here we study the initiation of new organs in the SAM of *Arabidopsis thaliana*. New organ primordia initiate at the accumulation points of the plant hormone auxin. It is widely accepted that auxin driven transcription activates the expression of a group of targets ultimately resulting in the initiation of organ primordia. A central role in this process is given to the DNA-binding auxin response factor AUXIN RESPONSE FACTOR/MONOPTEROS (ARF5/MP). After its auxin-dependent activation, ARF5/MP orchestrates a number of developmental processes notably by directing the expression of transcription factors involved in the specification of floral identity and proliferative growth, LEAFY (LFY), AINTEGUMENTA (ANT) and AINTEGUMENTA-LIKE6 (AIL6); organ polarity, FILAMENTOUS FLOWER (FIL) and cytokinin responses, TARGET OF MONOPTEROS (TMO3) (Wu et al., 2015; Yamaguchi et al., 2013).

Plant cells remain glued together through their cell walls, cell migration is not possible and plant morphogenesis is basically a matter of localized cell growth. Growth results from the irreversible, plastic yielding of the cell wall to the internal turgor pressure. This process implies the constant modification of the wall components, allowing changes in the rate and direction of growth. To induce organ outgrowth, the plant hormone auxin and its downstream targets therefore must play a central role in the regulation of the cell wall. There is evidence, that the initiation of organs at the sites of auxin accumulation at the SAM involves local changes in cell wall stiffness (Braybrook and Peaucelle, 2013; Kierzkowski et al., 2012; Peaucelle et al., 2011a; Qi et al., 2017; Sassi et al., 2014). Auxin accumulation also affects the dynamics of the cortical microtubules (CMT) and the anisotropic properties of the cell wall. The accumulation of auxin promotes the disorganization of ordered CMT arrays at the periphery of the SAM, activating changes in growth direction from anisotropic-to-isotropic. Cell wall loosening and isotropy act synergistically to promote the initiation of the lateral outgrowths (Sassi et al., 2014).

Although it is assumed that auxin signaling regulates primordium initiation by integrating transcriptional regulation and the control of cell wall mechanics, the connection between these two processes is still unclear. In addition, the mechanical status of the cell wall is not just a downstream target of auxin signaling. The local application of wall loosening proteins and microtubule disorganizing agents are both able to induce organ production (Fleming et al., 1997; Sassi et al., 2014; chapter 2), indicating the presence of some type of feedback. Here we present evidence that this feedback can even shortcut upstream auxin signaling. We propose a model where an auxin induced shift to isotropic growth - promoted in part by the reorientation of CMT - feeds back on the activation of the transcriptional regulatory network controlling flower initiation. Although the feedback mechanism itself remains elusive, our results indicate that organ initiation might involve multiple inputs, some of which might act in parallel to auxin. In particular, we further explore here the possible role of the brassinosteroid-signaling pathway.

Results

CMT disorganization promotes outgrowths that express developmental patterning genes

To obtain further information on the feedback mechanisms discussed above, we first analyzed the effects of changes in CMT dynamics on transcription factors involved in organ outgrowth. As an experimental system, we used plants impaired in auxin transport. This was achieved chemically by growing the plants on media containing N-1-naphthylphthalamic acid (NPA) or genetically by using *pin1* mutants (see material and methods). Under these conditions, plants are severely impaired in organ initiation, especially during the floral stage and produce naked stems characterized by their anisotropic growth sustained by the anisotropic microtubule arrangements. Lateral outgrowths can be induced in the system via the induction of changes in CMT dynamics, either by local oryzalin applications in lanolin paste or by using the *botero1-7* allele of *KATANIN1* (*KTN1*) (Sassi et al., 2014). Both approaches break down microtubule anisotropy at the periphery of the SAM.

We analyzed the expression patterns of three transcription factors with central roles in flower initiation, namely, *LFY*, *ANT*, *AIL6* as well as their upstream regulator *MP*. As previously

reported, the transcripts of these three genes accumulated in the incipient flower primordia of WT plants and at the periphery of *pin1-6* mutant apices (Vernoux et al., 2000; Yamaguchi et al., 2013) (Figure 1). We next analyzed the expression pattern of these genes in *pin1-6 bot1-7* double mutant plants. *pin1-6 bot1-7* SAMs characteristically display lateral outgrowths which can develop into flower like structures. We detected accumulation of transcripts of *LFY, ANT, AIL6* as well as *MP* in the lateral outgrowths of *pin1-6 bot1-7* double mutant, although at variable levels (Figure 1).

The variability in expression levels might be due to arrest of the lateral outgrowths, as not all of them continue to develop. Since the dynamics of gene expression in the outgrowths cannot be easily revealed by *in situ* hybridization, we analyzed in more detail *LFY* and *ANT* expression using fluorescent reporter lines *pLFY>GFP* and *pANT::erGFP* grown on NPA. We excluded *AIL6* and *MP* from this analysis given the lack of fluorescent reporter lines that faithfully reproduced their expression pattern.

To study gene expression dynamics in lines expressing fluorescent markers, we induced lateral outgrowths by local oryzalin applications. About 60% (n=30) of the plants react to oryzalin by producing defined bumps, which become visible in the binocular around 72hrs after application (Sassi et al., 2014). Differently from auxin-induced outgrowths, where *pLFY>GFP* was consistently expressed throughout (n=8), oryzalin-induced outgrowths expressed *pLFY>GFP* in irregular patches (n=17) (Figure 2a). However, *pANT::erGFP* expression was consistently detected in both auxin (n=14) and oryzalin-induced outgrowths (n=16)(Figure 2b).

To explore this further, we followed the expression dynamics of the p*ANT::erGFP* fluorescent reporter. We observed that *pANT::erGFP* expression was initiated already after 48h of the local oryzalin application (n=10). Later on, the expression of *ANT* expanded throughout the lateral outgrowths (Figure 3a).

Together these results suggest that microtubule disorganization in addition to promoting lateral outgrowths at the periphery of the SAM also induces the expression of the developmental patterning gene *ANT* and possibly of *LFY*, *AIL6* and *MP* although this remains to be confirmed.

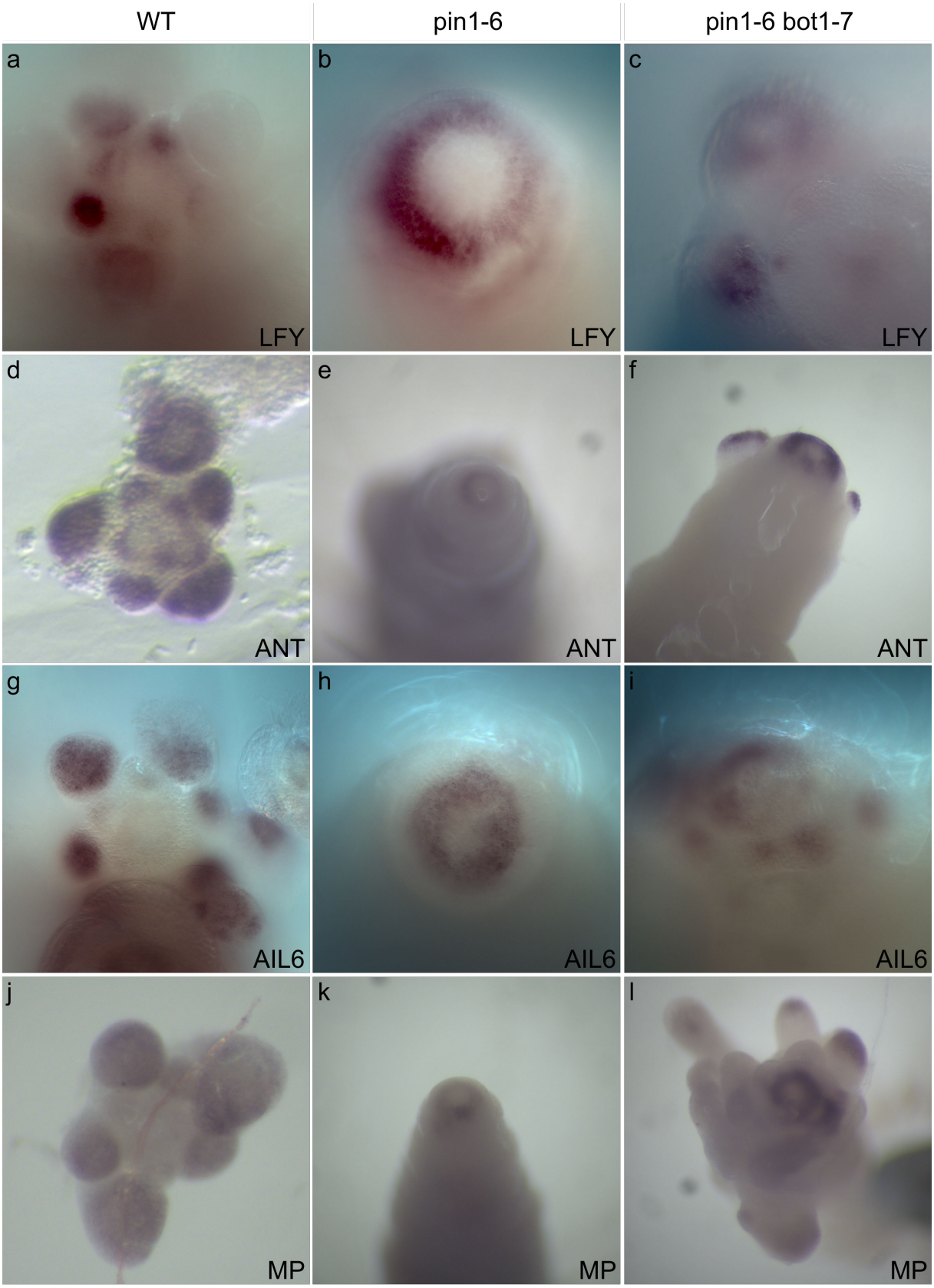

Figure 1. Disruption of CMT anisotropy promotes the expression of developmental patterning genes.
Expression pattern of *LFY* (a, b and c), *ANT* (d, e and f), *AIL6* (g, h and i) and *MP* (j, k, and l) detected by whole mount *in situ* hybridization in WT plants (a, d, g and j), *pin1-6* (b, e, h and k) and *pin1-6 bot1-7* (c, f, i and l) mutants.

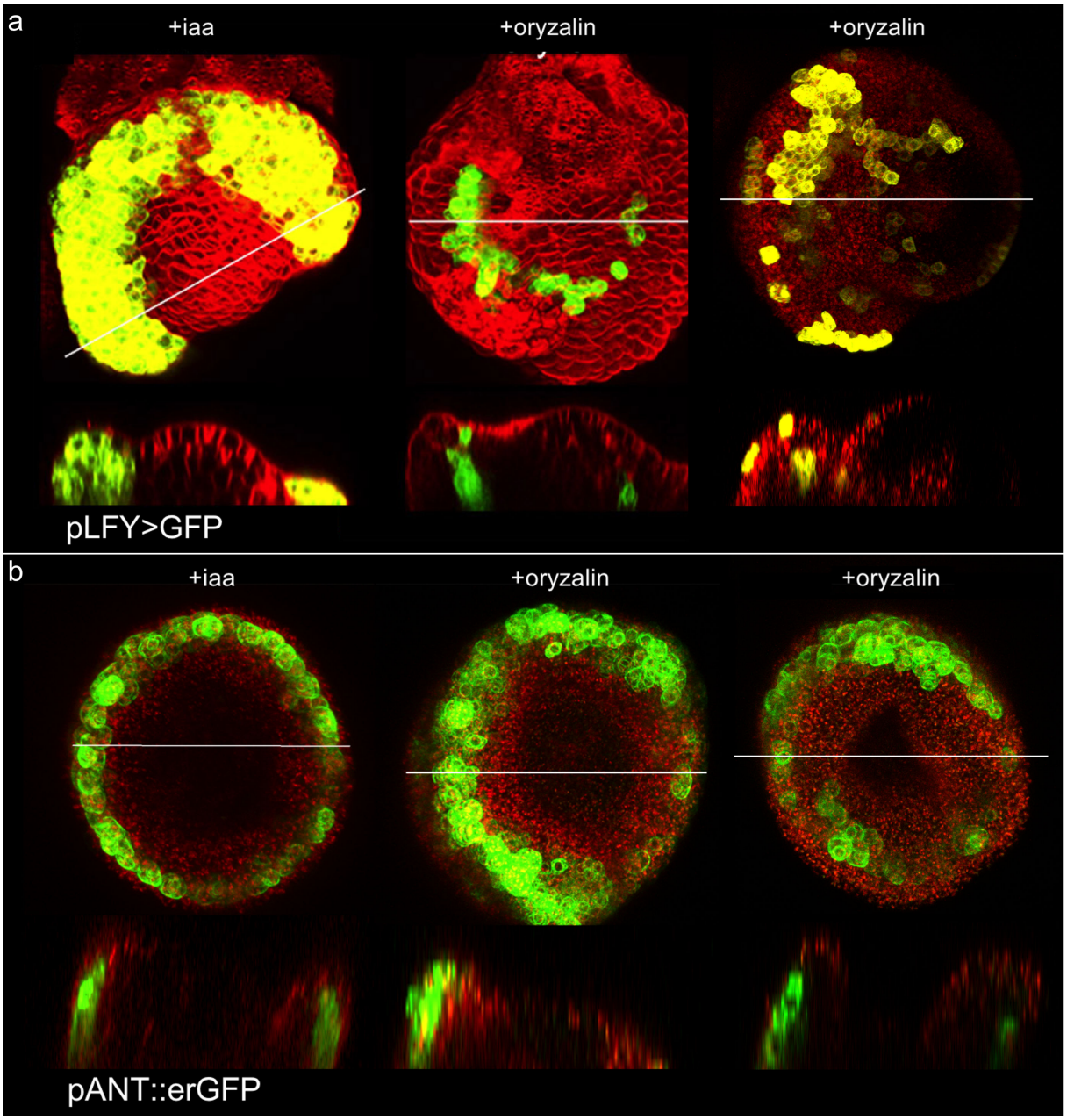

Figure 2. Microtubule disorganization induces differently *LFY* and *ANT* expression.
(a) pLFY>GFP expression in auxin-induced (+iaa) and oryzalin-induced outgrowths (+oryzalin)
(b) pANT::erGFP expression in auxin-induced (+iaa) and oryzalin-induced outgrowths (+oryzalin)

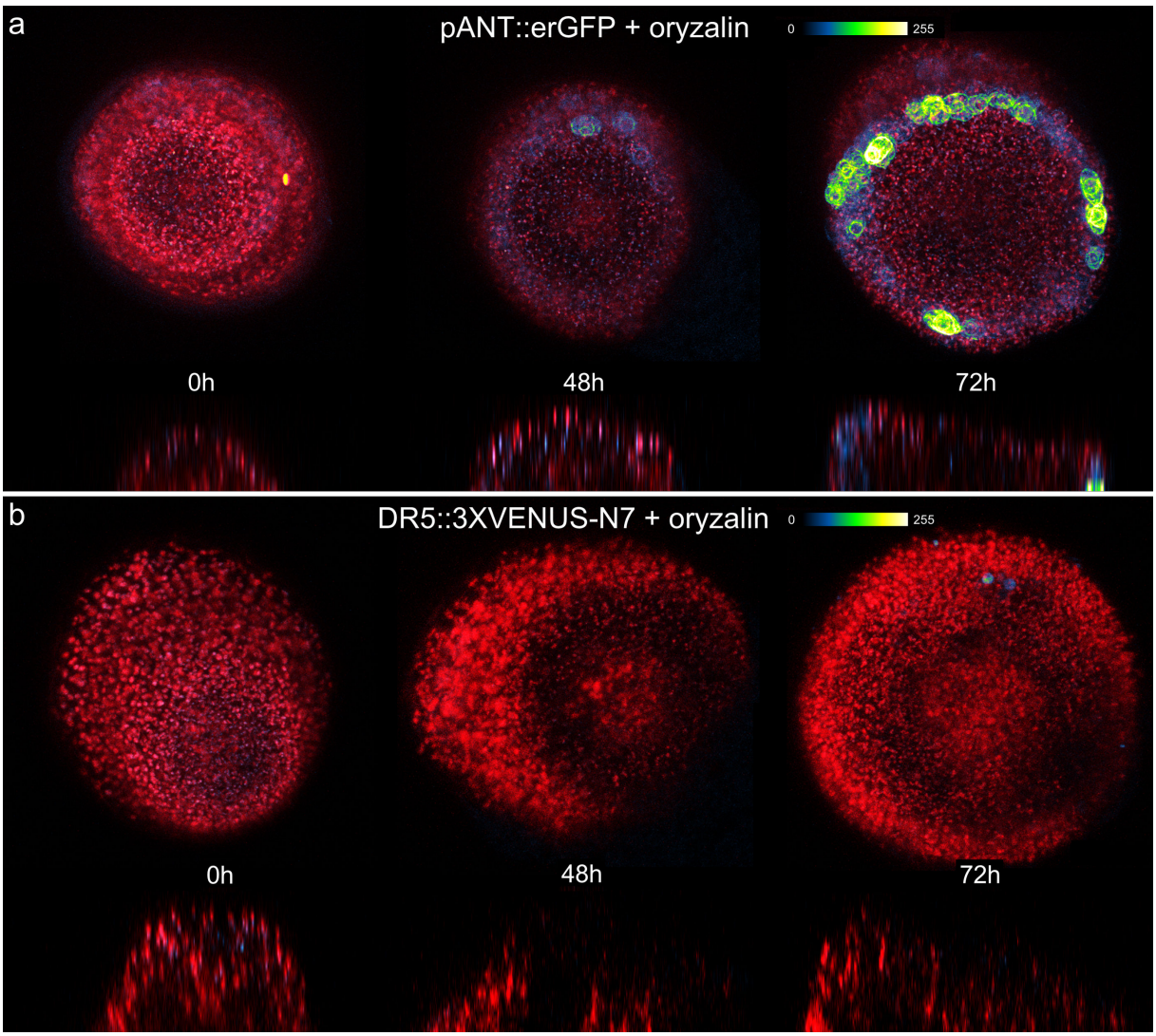

Figure 3. Microtubule disorganization induces *ANT* expression independently of auxin transcriptional regulation.
(a) NPA-grown pANT::erGFP plants showing *ANT* transcriptional activity before (0h) and after (48h) and (72h) local treatment with oryzalin.
(b) NPA-grown DR5::3XVENUS-N7 plants showing auxin-mediated transcriptional activity before (0h) and after (48) and (72h) local treatment with oryzalin.

CMT disorganization promotes outgrowths and *ANT* expression independently of the auxin master regulator MP

Only 6 out of 20 outgrowths in 5 *pin1-6 bot1-7* meristems accumulated MP transcripts; whereas 18 out of 21 outgrowths in 7 *pin1-6 bot1-7* meristems accumulated transcripts of *ANT*. This made us wonder if *ANT* could be activated independently of MP (Figure 1). To enquire this further, we tested the activation of the synthetic auxin-signalling reporter DR5::VENUS-N7 after oryzalin-induced microtubule disorganization. Although local oryzalin applications induced the production of lateral outgrowths (60%, n=24), these outgrowths did not show the activation of the fluorescent reporter (93%, n=14) (Figure 3b). In contrast, auxin-induced outgrowths systematically expressed the fluorescent DR5 reporter (100%, n=10) (Figure S1). These results suggest that the initiation of lateral outgrowths by growth isotropy may be independent of auxin transcriptional regulation.

To further explore whether the formation of lateral outgrowths following the disruption of CMT anisotropy occurs independently of MP, we examined the *MP* strong mutant allele *arf5-1*. These mutants display a phenotype reminiscent of *pin1*: they fail to form lateral flowers, which results in naked pin-like stems (Przemeck et al., 1996). As in *pin* mutants, they exhibit supracellular circumferential CMTs alignments that reinforce growth anisotropy via the parallel deposition of cellulose microfibrils (see chapter 1). Local disorganization of the CMT of *arf5-1* shoot apices, achieved by oryzalin treatments or by crossing with *bot1*-7, was able to restore the formation of lateral outgrowths (chapter 1, Figure 4a). These results were corroborated with a second weak mutant allele *arf5-2*, which was also crossed with *bot1-7*. Double mutants *arf5-2 bot1-7* enhanced the production of lateral outgrowths in comparison with the single mutants *arf5-2* (Figure 4b).

We used the double mutants *arf5-1 bot1-7* and *arf5-2 bot 1-7* to investigate if the expression of *ANT* could be induced independently of MP regulation. Indeed, lateral outgrowths produced in the double mutant *arf5-1 bot1-7* and *arf5-2 bot 1-7* correlated with the expression of *ANT* as detected by whole mount *in situ* hybridization (Figure 4). Together, these findings indicate that the initiation of lateral outgrowths in the SAM as well as the expression of *ANT* can be induced independently of MP transcriptional regulation.

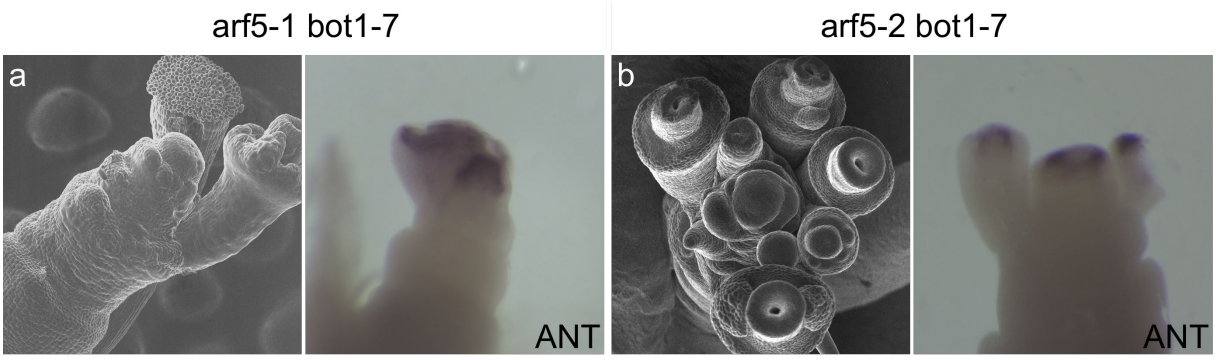

Figure 4. CMT disorganization promotes outgrowths that express the developmental patterning gene *ANT* even in the absence of MP regulation
Scanning electron micrograph images of *arf5-1 bot1-7* (a) and *arf5-2 bot1-7* apices (b). The right part of each panel shows the expression pattern of *ANT* detected by whole mount *in situ* hybridization.

Identification of putative *ANT* transcriptional regulators

The previous results suggested that during organogenesis, *ANT* expression could be regulated by transcription factors other than MP. To explore this further, we performed an Enhanced yeast one-hybrid (eYIH) assay in order to identify putative transcription factors regulating *ANT* during lateral outgrowth formation. Since ANT and AIL6/PLT3 are related transcription factors with partially overlapping roles in flower primordium initiation (Han and Krizek, 2016; Krizek, 2009; Krizek, 2015; Krizek et al., 2016; Yamaguchi et al., 2016), we included *AIL6* in our analyses. We prepared DNA baits of *ANT* and *AIL6* promoters that contained portions of 2000 bp sequences immediately upstream of the translational start site. These promoters were sufficient for expression in the meristem as confirmed by fluorescent reporters. The bait promoters were fused to the reporter genes l*acZ* and *HIS3* and screened against a complete collection of 2000 *Arabidopsis* transcription factors (TF) fused to a transcription activation domain and used as prey (Pruneda-Paz et al., 2014). As many as 42 TFs had the potential to bind *ANT* promoter (2.1% from the complete TF collection), whereas 105 TFs (5.25%) came up as putative regulators of *AIL6* (Table S1). Of these, five TF appeared to be potential common regulators of both genes; the SQUAMOSA PROMOTER BINDING PROTEIN-LIKE 10 (SPL10), the C2H2-like zinc finger family TF NUCLEAR CAGE (NUC), the Acyl-CoA N-acyltransferase with RING/FYVE/PHD-type zinc finger domain-containing protein encoded by AT3G53680, the DRE-binding protein 2A (DREB2A) and the NAC DOMAIN CONTAINING PROTEIN 4 (NAC4). Of these, only DREB2A and NAC4 are expressed in the inflorescence meristem at a relatively high level according to

public resources (Winter et al., 2007) and a high-throughput transcriptomic analysis (Mantegazza et al., 2014), which place them among the 30% transcripts with highest expression in the inflorescence meristem.

The candidates with the potential to bind to *ANT* promoter and that are highly expressed in the meristem (following the same criteria as above) included (Figure 5): the basic leucine zipper (bZIP) FLOWERING LOCUS D (FD), the histone H2A 13 (HTA13), the CCT motif-containing response regulator TIMING OF CAB EXPRESSION1 (TOC1), the class II homeodomain-leucine zipper ATHB4, the BTB/POZ domain-containing protein encoded by AT1G21780, the LOB DOMAIN-CONTAINING PROTEIN 18 (LBD18), the GROWTH-REGULATING FACTOR 9 (ATGRF9), the SIN3-LIKE 3 (ATSIN3) and two transcription factors involved in the brassinosteroid (BR) regulated gene expression pathway BRASSINAZOLE-RESISTANT 2 (BZR2) and INTERACT WITH SPT6 1 (IWS1). Notably, the eYIH screen did not show ARF5/MP as regulator of *ANT* promoter nor of *AIL6* promoters, probably due to the promoter fragments used.

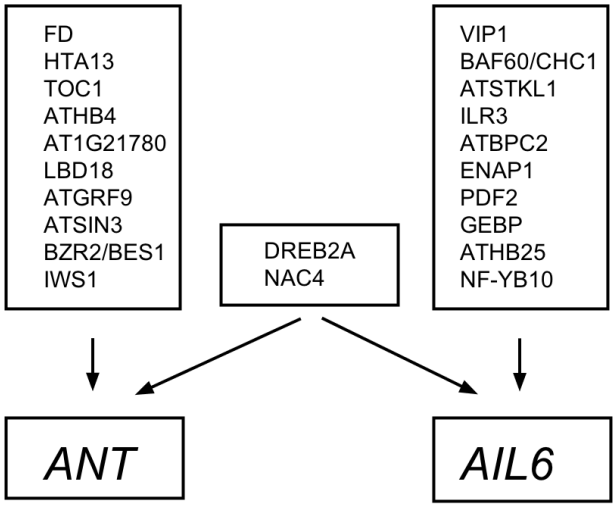

Figure 5. Putative regulators of *ANT* and *AIL6* transcription according to the eYIH screen. Only candidates expressed in the top 30% of all transcripts of the inflorescence meristem according to Mantegazza et al., (2014) are shown.

BZR2, also known as BRI1-EMS-SUPPRESOR 1 (BES1) and IWS1, represented two promising candidates identified in the eYIH screen based on the following criteria. First, BES1 and IWS1 interact to direct BR-regulated gene expression, thus they belong to the same

signaling pathway (Li et al., 2010). Second, both *BES1* is expressed in the incipient flower primordia of WT plants and in the lateral outgrowths of *pin1-6 bot1-7* (Figure 6). Third, BRs signaling in the shoot epidermis has a major role in facilitating shoot growth (Savaldi-Goldstein et al., 2007). Fourth, BRs might play important roles in cell wall anisotropy via the rearrangement of the cortical microtubules (Catterou et al., 2001; Takahashi et al., 1995) or in cell wall loosening via feedback regulation of pectin (Wolf et al., 2012b; Wolf et al., 2014), they might also induce the expression of genes encoding for cell wall associated proteins (Xie et al., 2011; Yin et al., 2002). Finally, evidence from *Arabidopsis* and rice suggest that high BR activity enhances cell proliferation and cell differentiation in the SAM, and antagonize boundary formation between organs including the SAM boundary (Arnaud and Laufs, 2013; Bell et al., 2012; Gendron et al., 2012; Tsuda et al., 2014).

To explore whether BR signaling could be involved in the formation of lateral outgrowths in the SAM, we tested if plants grown on NPA or *pin1* mutants were able to restore the initiation of lateral outgrowths following treatments with the BR 24-epi-brassinolide (EBL). Treatments with 100nM EBL induced lateral outgrowth formation in *pin1* mutants (11 out of 15 meristems tested) in comparison with DMSO treatment (2 out of 15) (Figure 4a). We next tested the induction of *ANT* expression following BL treatments. To this end we followed the expression pattern of NPA-grown fluorescent *pANT::erGFP* reporter. *ANT* transcriptional activity was increased already after 48h after treatment with EBL (4 out of 15 meristems) or 72h (increasing to 9 out 15 meristems) (Figure 4b), in contrast with DMSO treatment (1 out of 9 meristems). Together our results suggest that in addition to auxin, BR signaling can interfere with the cell mechanical properties that lead to organ initiation. BR signaling might even represent a link between microtubule-driven growth isotropy and the transcriptional activation of *ANT*.

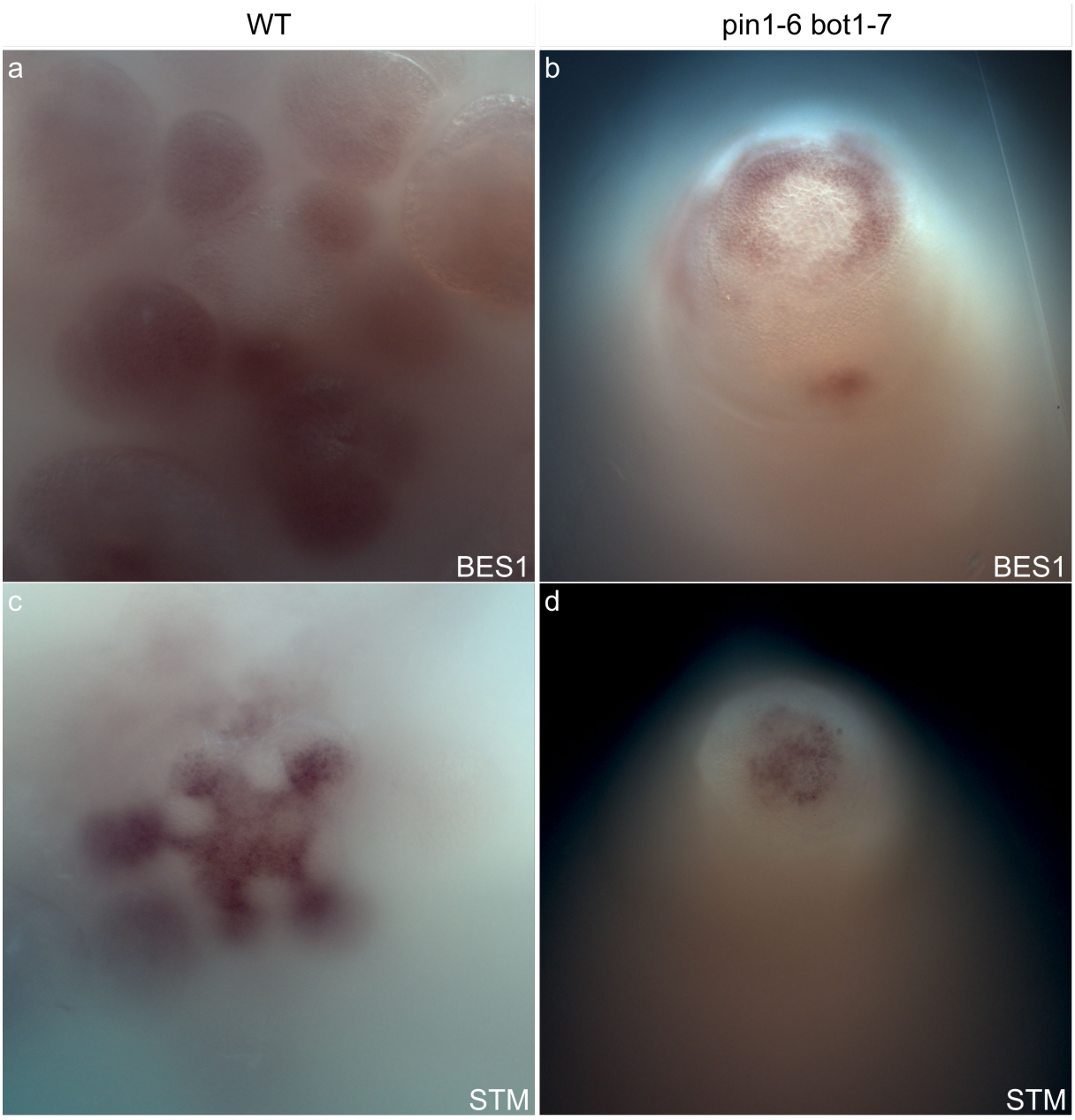

Figure 6. Disruption of CMT anisotropy promotes the expression of developmental patterning genes.
Expression pattern of *BES1* (a and b) and *STM* as control (c and d) detected by whole mount *in situ* hybridization in WT plants (a and c), and *pin1-6 bot1-7* (b and d) mutants.

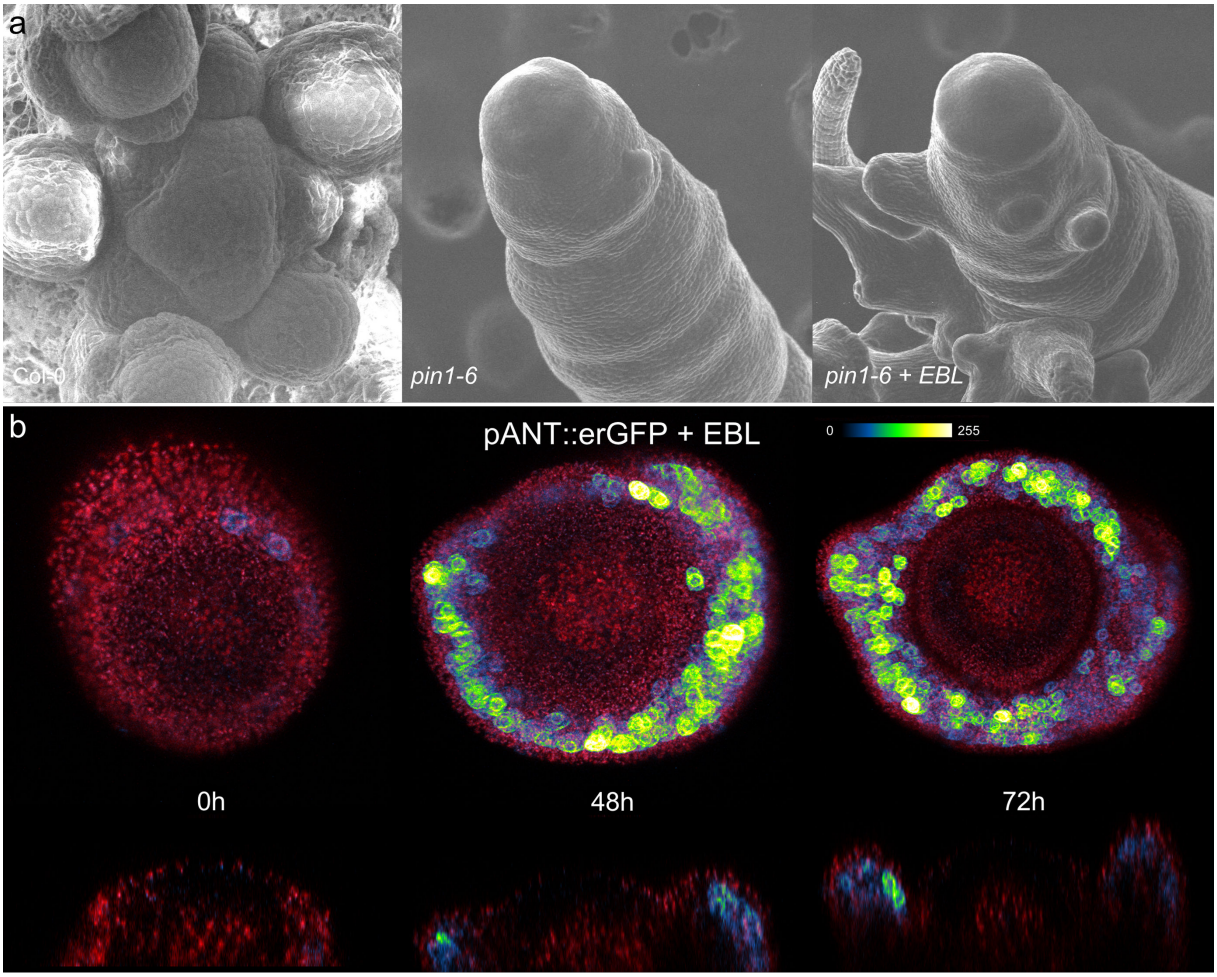

Figure 7. BRs signaling in the shoot apex might link CMT disorganization, lateral outgrowths and *ANT* expression

(a) Scanning electron micrograph images of WT apex, *pin1-6* and *pin1-6* one-week after treatment with EBL

(b) Expression pattern of NPA-grown fluorescent reporter plants pANT::erGFP showing *ANT* transcriptional activity before (0h) and after (48h) and (72h) of treatment with EBL.

Discussion

Microtubule disorganization triggers the transcriptional activation of *ANT*

The molecular pathway controlling flower primordium initiation in *Arabidopsis* has been relatively well characterized. The most widely accepted view proposes that auxin accumulates at precise sites of the SAM and triggers a molecular network largely via the activation of ARF5/MP (Wu et al., 2015; Yamaguchi et al., 2013) and its direct downstream targets. These downstream targets then directly or indirectly control cell wall modifications that lead to growth. Several observations, however, indicate that this view of a hierarchical regulatory chain is probably oversimplified. Our previous work (Sassi., et al 2014) proposed that auxin might also more directly act on the cytoskeleton organization and wall anisotropy via ROP signaling, indicating the existence of parallel signaling pathways. We show here also the existence of feedbacks from downstream elements, as the disorganization of the CMT arrays at the periphery of the *pin1* and *mp*/*arf5* SAMs, is sufficient to induce at least *ANT* expression, i.e. a direct target of MP high in the hierarchy of the molecular network. Importantly, we show here that *ANT* activation can occur independently from MP, suggesting additional layers of regulation.

Our eY1H analysis suggests that multiple TF and signaling pathways have the potential to regulate *ANT* and *AIL6*, most likely in parallel with MP (Figure 5, Table S1). Among the TF discovered as possible regulators of *ANT*, some are associated to precise signaling pathways. For example, FD that interacts with FLOWERING LOCUS T (FT) to promote flowering (Abe et al., 2005), TOC1 that is involved in the generation of circadian rhythms (Strayer et al., 2000) and ATHB4, which is involved in shade avoidance syndrome (Carabelli et al., 1993; Sorin et al., 2009) as well as in apical embryo development and meristem functions (Turchi et al., 2013). Other TFs are associated with broader aspects of transcriptional regulation, for example HTA13 and DREB2A. The latter, showed up as common regulator of *ANT* and *AIL6*. DREB transcription factors recognize the dehydration-responsive element sequence motif in the promoters of stress-inducible genes. DREB2A is specifically involved in responses to salinity, heat, drought and cold (Liu et al., 1998; Nakashima et al., 2000). Another putative common regulator is SPL10, that in conjunction with SPL11 and SPL12 redundantly controls the development of lateral organs and shoot maturation in the

reproductive phase (Shikata et al., 2009). More than 5% from the complete collection of transcription factors used for this study could potentially regulate *AIL6*. Among them we discovered the VIRE2-INTERACTING PROTEIN1 (VIP1), which is a mechano-sensitive transcription factor that localizes to the nucleus upon hypo-osmotic treatment (Tsugama et al., 2016a, b). Although the validity of the eY1H results still needs to be verified, these assays have proven to be strong tools for hypothesis generation as illustrated by Sparks et al., who in a recent report generated an eYIH-based model for the root ground tissue, of which they validated in planta many (>50%) of the interactions obtained by the assay (Sparks et al., 2016).

BES1 and IWS1, putative regulators of *ANT*, are associated to the BR signaling pathway. Since BR signaling has been associated with meristem function but its function remains poorly characterized, we chose to examine the possible role of this signaling pathway more in detail.

In general, BR signaling has been associated with cell expansion. Mutants impaired in BR production or signaling are dwarf, which seems to result from a reduced expansion of dividing and non dividing cells (Nakamura et al., 2006a; Nakaya et al., 2002; Savaldi-Goldstein et al., 2007). A limited number of studies have also revealed a role in patterning. BR signaling in the growing primordia of the SAM prevents the expression of genes associated with the boundary domain including the CUC genes (Bell et al., 2012; Gendron et al., 2012). Conversely, the boundary specific gene LATERAL ORGAN BOUNDARIES (LOB) inhibits the accumulation of BR in the organ boundaries (Bell et al., 2012). Interestingly, a similar regulation might be involved in the control of ovule primordia initiation (Cucinotta et al., 2014). Auxin-induced ANT promotes growth of ovule primordia, whereas CUC genes play a role in the establishment of the ovule primordia boundaries (Galbiati et al., 2013). In this model, *ANT* expression was detected to be regulated by BR signaling, as shown by qRT-PCR and ChiP-PCR experiments (Huang et al., 2013).

Our results further confirm a direct role of BR signaling in organ formation via the transcriptional regulation of *ANT*. This is not only suggested by the eY1H experiments, but also by the induction of *pANT::erGFP* after BR treatment of pin meristems and the localized expression of BES1 in the lateral outgrowths of *pin1-6 bot1-7*. To substantiate these results, *bri1-5* insensitive mutant (Noguchi et al., 1999) has been crossed with the *pin1-6 bot 1-7*

double mutant. If indeed CMT disorganization acts via BR regulation, we would expect that *bri1-5* suppresses lateral outgrowths triggered in the *pin1-6 bot1-7* background. This work is in progress.

How the disruption of CMT anisotropy acts on gene expression remains unclear. The cells could sense changes in cell wall isotropy. A good candidate to fulfill as integrator between cell wall and BR signaling is the receptor-like protein (RLP)44 (Wolf et al., 2012b; Wolf et al., 2014). Presumably, the interaction of RLP44 with the BR pathway is through the BR co-receptor BAK1 (Wolf et al., 2014). Although RLP44 is not part of the BR core pathway, it is proposed that it could favor the BR receptor complex BAK1-BRI1 and in turn activate the BR signaling pathway. Since *RLP44* is expressed in the shoot apex inflorescence (Wolf et al., 2014) it would be worth testing if it could be a downstream component of the disruption of CMT anisotropy in the SAM, receiving information from the cell wall and laterally activating BR signaling. Certainly, the analyses of *rlp44* mutants and RLP44 overexpression lines would give insight to this question.

Conclusions and perspectives

In conclusion our results indicate that cellular, mechanical anisotropy at the shoot apex links together organ initiation and transcriptional regulation. We previously suggested that this regulation involved cell wall remodeling genes (chapter 2). Here we propose that this coupling mechanism also affects genes involved in organ patterning. The feedback mechanism itself remains elusive but our results support a model in which organ initiation receives multiple inputs, which opens to a myriad of possibilities. In particular, we show here the potential role of BR signaling in the regulation of organ initiation and transcriptional activation. Signal integration and crosstalk with other pathways has been documented for BR signaling. Thus, BRs might act in parallel or in synergy with auxin to activate growth anisotropy and/or transcription. Now the challenge is to reveal how this coordination between anisotropy and transcriptional regulation is modulated throughout plant development

Experimental procedures

Plant materials

Arabidopsis thaliana ecotypes Columbia-0 (Col-0) were the wild types seeds used in this study. Transgenic lines and mutants used in this work were for the most part previously described. The *pin1-6* (Vernoux et al., 2000), *bot1-7* (Uyttewaal et al., 2012), *pin1-6 bot1-7* (Sassi et al., 2014), *arf5-1* (Przemeck et al., 1996), *arf5-2* (Donner et al., 2009), *bri1-5* (Noguchi et al., 1999), *DR5::VENUS-N7* (Heisler et al., 2005), p*ANT::erGFP* and pLFY>GFP (Grandjean et al., 2004). The *arf5-1 bot1-7*, *arf5-1 PDF1::mCitrine-MBD* lines were generated by crossing and further PCR selection. Growth conditions were previously described (Sassi et al., 2014).

Growth conditions and Treatments

For napthylphtalamic acid (NPA) treatments, plants were sown in petri dishes with a medium adapted for Arabidopsis (Duchefa) containing NPA to a final concentration of 10µM. Lanolin paste for local SAM treatments was prepared as follows: 1 volume of chemical stock solution (3x concentrated) was added to 2 volumes of melted (55°C) lanolin and thoroughly mixed until the formation of a homogenous emulsion. The concentration of the stocks was 3mMfor IAA and 666 µg/ml for oryzalin. Local applications were made with a pipette tip und er a binocular. Equal amounts of DMSO were used for untreated controls. Treated meristems were imaged prior the treatment and then 24h, 48h, 72h and 96h after. For eBL induced organ formation, NPA grown plants were treated in petri dishes with 100nM eBL liquid solution for 3h after imaging the t=0 time point and again the next day after imaging the t=24h time point. No further treatment was done after the 24h time point until the completion of the experiment. *pin1-6* treated plants were sown in petri dishes with MS medium. After phenotype-based selection, homozygous *pin1-6* plants were transferred to new fresh MS medium, leaving enough space to allow the plants to develop *in vitro*. eBL treatments were performed as previously described. Plants were kept in the petri dishes for all the duration of analyses. For adventitious root formation of *arf5-1*, seeds were surface-sterilized and germinated on MS medium. After germination, homozygous *arf5-1* seedlings were identified by the rootless phenotype. Mutant plants were wounded below cotyledons as earlier described (Berleth and Jurgens, 1993), then transferred to MS medium supplemented with the synthetic auxin 1-naphthaleneacetic acid (NAA) to a final concentration of 10µM and kept on these plates for 7

days, when they were transferred to free MS medium free of NAA to allow the elongation of the root. Plants were either kept in plates or transplanted to soil after rooting, where they grew under a 16-h-light/8-h-dark photoperiod.

Confocal live Imaging and image analyses.

Confocal imaging was carried out on a Zeiss LSM700 system as previously described (Sassi et al., 2014). SEM imaging was carried out on a Hirox SE-3000 system as previously described (Sassi et al., 2014).

Histochemistry

RNA in situ hybridization assays were performed as described previously (Ferrandiz and Sessions, 2008a, b). For whole-mount RNA in situ hybridization assays, meristems from WT plants, *pin1-6*, *pin1-6 bot1-7*, *arf5-1*, *arf5-1 bot1-7* grown on soil were processed as previously described (Rozier et al., 2014). At least three independent experiments for both assays were performed for each probe tested. Primers used are listed in Table S2.

Enhanced Yeast-One-Hybrid

The eYIH assays were performed as previously described (Gaudinier et al., 2011; Taylor-Teeples et al., 2015). Briefly, gene promoters (2000bp of upstream regulatory region from the translational start site, or the next gene) were cloned and recombined to reporter vectors pMW2 (Y1H *HIS3* reporter vector) and PMW3 (YIH *LacZ* reporter vector) (Brady et al., 2011). Interactions were called for transcription factors that activated at least one reporter assay. In addition gene promoters were fused to the *mCitrine* targeted to the nucleus through an SV40 NLS using the Gateway system. Final destination vectors were obtained by using the three-fragment recombination system using the *pB7m34GW* destination vector. Constructs were transformed into *Arabidopsis Col-0* ecotype. Primers used are listed in Table S3.

Supplementary Material

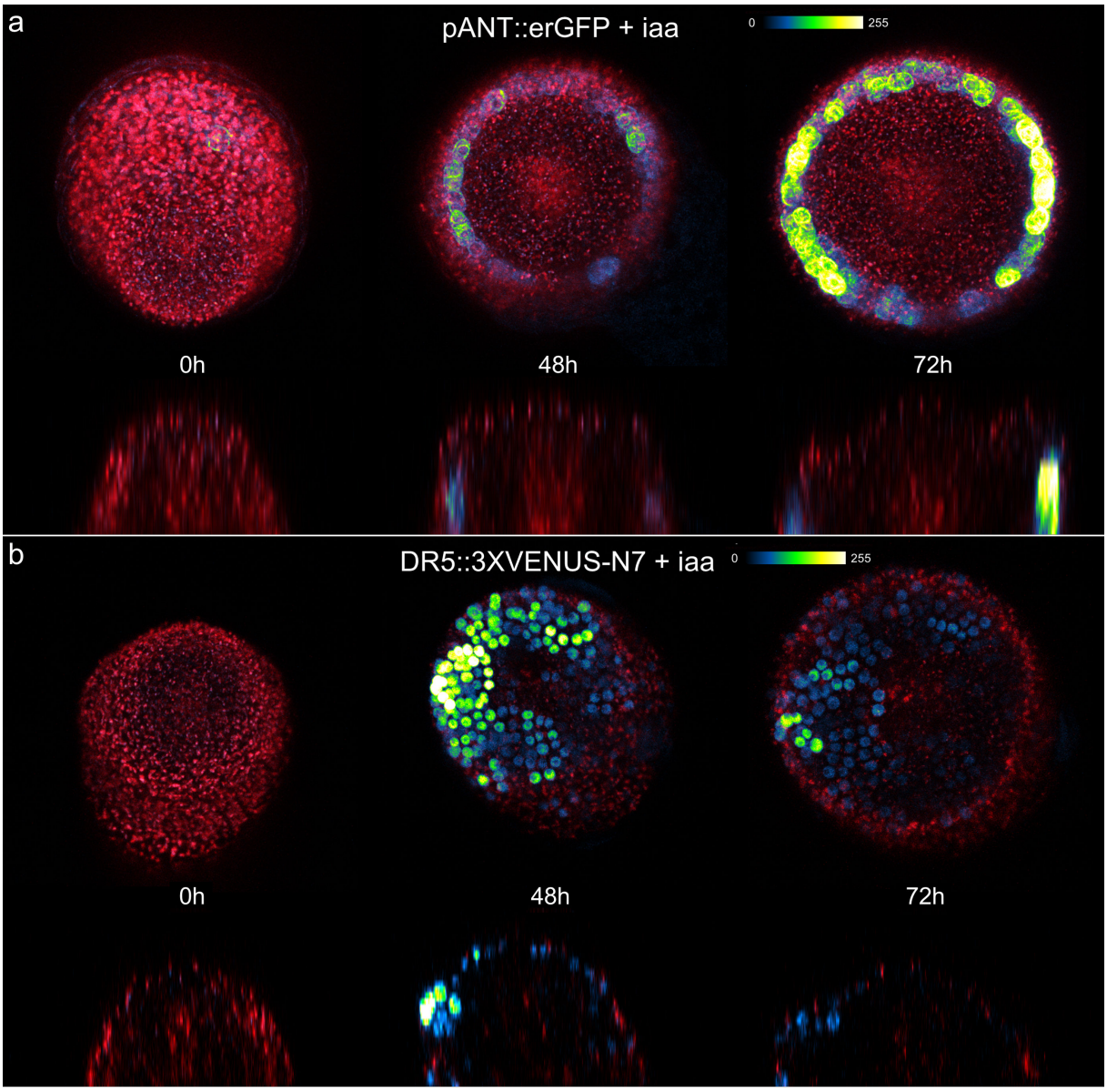

Figure S1. Auxin-induced microtubule disorganization and its correlation with *ANT* expression and auxin transcriptional activity.
(a) Expression pattern of fluorescent reporter plants pANT::erGFP showing *ANT* transcriptional activity before (0h) and after (48h) and (72h) of local treatment with auxin.
(b) Expression pattern of fluorescent synthetic reporter DR5::3XVENUS-N7 showing auxin-mediated transcriptional activity before (0h) and after (48) and (72h) of local treatment with auxin.

Table S1. Identified transcription factor-promoter interactions

TF AGI	TF Name	TF family	Target
AT5G44160	NUC	C2H2	ANT
AT1G19210	AT1G19210	AP2/EREBP	ANT
AT2G01650	PUX2	C2H2	ANT
AT1G26610	AT1G26610	C2H2	ANT
AT2G26940	AT2G26940	C2H2	ANT
AT5G05410	DREB2A	AP2/EREBP	ANT
AT1G73870	AT1G73870	C2C2-CO-LIKE	ANT
AT1G16530	LBD3		ANT
AT4G35900	FD	BZIP	ANT
AT1G19350	BZR2		ANT
AT5G61380	TOC1		ANT
AT1G32130	IWS1		ANT
AT1G67260	TCP1	TCP	ANT
AT2G44910	ATHB4	HB	ANT
AT3G20670	HTA13	CCAAT	ANT
AT2G40450	AT2G40450	TRAF	ANT
AT5G08790	anac081/ATAF2	NAC	ANT
AT5G10120	AT5G10120	EIL	ANT
AT1G74650	ATMYB31/ATY13	MYB	ANT
AT3G03660	WOX11	HB	ANT
AT1G03790	AtTZF4/SOM	C3H	ANT
AT5G07500	AtTZF6/PEI1	C3H	ANT
AT3G01030	AT3G01030	C2H2	ANT
AT5G38490	AT5G38490	REM(B3)	ANT
AT1G21780	AT1G21780	TRAF	ANT
AT1G02230	ANAC004	NAC	ANT
AT2G45420	LBD18	LOB/AS2	ANT
AT3G27650	LBD25	LOB/AS2	ANT
AT2G33550	AT2G33550	TRIHELIX	ANT
AT5G44260	AtTZF5	C3H	ANT
AT1G27370	SPL10	SBP	ANT
AT1G26590	AT1G26590	C2H2	ANT
AT3G45260	AT3G45260	C2H2	ANT
AT2G12646	AT2G12646	PLATZ	ANT
AT5G15480	AT5G15480	C2H2	ANT
AT1G02030	AT1G02030	C2H2	ANT
AT5G52830	ATWRKY27	WRKY	ANT
AT1G63030	ddf2	AP2-EREBP	ANT
AT2G45480	AtGRF9	GRF	ANT
AT3G53680	AT3G53680	PHD	ANT
AT1G24190	ATSIN3/SNL3	Orphans	ANT
AT5G15020	SNL2	Orphans	ANT
AT5G54680	ILR3	BHLH	AIL6

AT5G44210	ERF9	AP2/EREBP	AIL6
AT3G14180	AT3G14180	TRIHELIX	AIL6
AT1G47870	ATE2F2	E2F/DP	AIL6
AT5G44160	NUC	C2H2	AIL6
AT1G34190	anac017	NAC	AIL6
AT2G28510	AT2G28510	C2C2-DOF	AIL6
AT3G10500	anac053	NAC	AIL6
AT3G11580	AT3G11580	ABI3/VP1	AIL6
AT5G13330	Rap2.6L	AP2/EREBP	AIL6
AT1G71130	AT1G71130	AP2/EREBP	AIL6
AT1G43700	VIP1	BZIP	AIL6
AT3G03200	anac045	NAC	AIL6
AT2G23290	AtMYB70	MYB	AIL6
AT3G53340	NF-YB10	CCAAT-HAP3	AIL6
AT1G29160	AT1G29160	C2C2-DOF	AIL6
AT1G54060	ASIL1	TRIHELIX	AIL6
AT1G03840	MGP	C2H2	AIL6
AT1G76880	AT1G76880	TRIHELIX	AIL6
AT2G44730	AT2G44730	TRIHELIX	AIL6
AT5G15130	WRKY72	WRKY	AIL6
AT5G05410	DREB2A	AP2/EREBP	AIL6
AT4G01120	GBF2	BZIP	AIL6
AT3G14230	RAP2.2	AP2/EREBP	AIL6
AT3G61830	ARF18	ARF	AIL6
AT1G14580	AT1G14580	C2H2	AIL6
AT4G00940	AT4G00940	C2C2-Dof	AIL6
AT1G76420	CUC3	NAC	AIL6
AT5G63090	LOB		AIL6
AT5G57390	PLT5	AP2/EREBP	AIL6
AT2G24430	ANAC038/ANAC039	NAC	AIL6
AT3G18400	NAC058	NAC	AIL6
AT4G38000	DOF4.7	C2C2-DOF	AIL6
AT3G60670	AT3G60670	PLATZ	AIL6
AT3G09230	AtMYB1	MYB	AIL6
AT1G80580	AT1G80580	AP2-EREBP	AIL6
AT1G14685	ATBPC2	BBR-BPC	AIL6
AT3G01890	AT3G01890	SWI/SNF-BAF60	AIL6
AT1G02210	AT1G02210	NAC	AIL6
AT4G35700	DAZ3	C2H2	AIL6
AT3G11100	AT3G11100	TRIHELIX	AIL6
AT1G55650	AT1G55650	ARID	AIL6
AT2G02820	AtMYB88	MYB	AIL6
AT5G22890	STOP2	C2H2	AIL6
AT5G67480	ATBT4	TAZ	AIL6
AT2G18160	ATBZIP2/FTM3/GBF5	bZIP	AIL6
AT4G02670	AtIDD12	C2H2	AIL6

AT1G62120	AT1G62120	mTERF	AIL6
AT1G66370	AtMYB113	MYB	AIL6
AT3G58190	ASL16/LBD29	LOB/AS2	AIL6
AT4G03170	AT4G03170	ABI3-VP1	AIL6
AT3G12977	AT3G12977	NAC/NAM	AIL6
AT2G42380	ATBZIP34	bZIP	AIL6
AT5G66940	AT5G66940	C2C2-DOF	AIL6
AT4G04890	PDF2	HB	AIL6
AT5G65590	SCAP1	C2C2-DOF	AIL6
AT2G46670	AT2G46670	Orphans/C2C2-CO-like	AIL6
AT5G14170	BAF60/CHC1	SWI/SNF-BAF60	AIL6
AT1G65620	AS2	LOB/AS2	AIL6
AT5G60142	AT5G60142	ABI3-VP1/B3	AIL6
AT3G14740	AT3G14740	PHD	AIL6
AT2G34620	AT2G34620	mTERF	AIL6
AT2G17180	DAZ1	C2H2	AIL6
AT2G35550	ATBPC7/BBR	BBR-BPC	AIL6
AT4G00238	AT4G00238	GeBP	AIL6
AT5G51980	AT5G51980	C3H	AIL6
AT2G21400	SRS3	SRS	AIL6
AT1G05230	HDG2	HB	AIL6
AT5G18090	AT5G18090	ABI3-VP1	AIL6
AT3G27785	ATMYB118	MYB	AIL6
AT1G02230	ANAC004	NAC	AIL6
AT5G52230	MBD13	ND	AIL6
AT5G19310	AtCHR23	SNF2	AIL6
AT5G39610	ANAC092/ATNAC2/ATNAC6/ORE1	NAC	AIL6
AT3G12730	AT3G12730	G2-like	AIL6
AT5G25190	ESE3	AP2-EREBP	AIL6
AT3G57920	SPL15	SBP	AIL6
AT1G06280	LBD2	LOB/AS2	AIL6
AT1G27370	SPL10	SBP	AIL6
AT4G10240	bbx23	Orphans	AIL6
AT1G75390	AtbZIP44	bZIP	AIL6
AT2G01930	ATBPC1/BBR	BBR-BPC	AIL6
AT4G00270	AT4G00270	GeBP	AIL6
AT3G16160	AT3G16160	CPP	AIL6
AT2G01370	AT2G01370	GeBP	AIL6
AT1G72570	AT1G72570	AP2-EREBP	AIL6
AT5G65410	ATHB25/ZFHD2/ZHD1	zf-HD	AIL6
AT1G06850	AtbZIP52	bZIP	AIL6
AT2G25620	AtDBP1	DBP	AIL6
AT2G18350	AtHB24/ZHD6	zf-HD	AIL6
AT5G19790	RAP2.11	AP2-EREBP	AIL6
AT4G33280	AT4G33280	ABI3-VP1	AIL6
AT4G38910	ATBPC5BBR/BPC5	BBR-BPC	AIL6

AT5G05550	AT5G05550	TRIHELIX	AIL6
AT4G03250	AT4G03250	HB	AIL6
AT4G00390	AT4G00390	GeBP	AIL6
AT4G00250	AT4G00250	GeBP	AIL6
AT1G66420	AT1G66420	GeBP	AIL6
AT4G31615	AT4G31615	ABI3-VP1	AIL6
AT3G53680	AT3G53680	PHD	AIL6
AT4G01260	AT4G01260	GeBP	AIL6
AT2G18328	ATRL4	MYB-related	AIL6
AT5G52170	HDG7	HB	AIL6
AT2G21240	ATBPC4/BBR	BBR-BPC	AIL6

Table S2: Primers used for *in situ* hybridization

Gene ID	Primers used to amplify total cDNA sequence from TAIR cds
ANT	ANT_For : ATGAAGTCTTTTTGTGATAATGATGATAAT
	ANT_T7 Rev : TGTAATACGACTCACTATAGGGCTCAAGAATCAGCCCAAGCAG
AIL6	AIL6_For : ATGATGGCTCCGATGACGAACTGGTTAACG
	AIL6_T7 Rev : TGTAATACGACTCACTATAGGGCTTAGTAAGACTGATTAGGCC
BES1	BES1_For : CACCATGAAAAGATTCTTCTATAATTCC
	BES1_T7 Rev : TGTAATACGACTCACTATAGGGCTCAACTATGAGCTTTACCATT
LFY	LFY_For : ATGGATCCTGAAGGTTTCACGAGTGGCTTA
	LFY_T7 Rev : TGTAATACGACTCACTATAGGGCCTAGAAACGCAAGTCGTCGC
MP	MP_For : ATGATGGCTTCATTGTCTTGTGTTGAAGAC
	MP_T7 Rev : TGTAATACGACTCACTATAGGGCTTATGAAACAGAAGTCTTAA
STM	STM_For : ATGGAGAGTGGTTCCAACAGCACTTCTTGT
	STM_T7 Rev : TGTAATACGACTCACTATAGGGCTCAAAGCATGGTGGAGGAGA

Table S3. Primers used to amplify promoter regions for YIH assays

Primer name	Sequence (5'>3')	Use
ANT Y1H F 1st	CTCTCTGCTGCATACTTGCA	1st round promoter cloning Y1H
ANT Y1H R 1st	ACAAGTTGAGGTGGAACAGAAG	1st round promoter cloning Y1H
AIL6 Y1H F 1st	TGCATGTACGACAAGTGGAG	1st round promoter cloning Y1H
AIL6 Y1H R 1st	TATCGAGGAGATAAGGAGAGGAG	1st round promoter cloning Y1H
ANT Y1H F 2nd	TTTGTTATTTATGAAAAACAAATATT	2nd round promoter cloning Y1H
ANT Y1H R 2nd	GGTTTCTTTTTTTGGTTTCTG	2nd round promoter cloning Y1H
AIL6 Y1H F 2nd	GTTTTTTCCCTTTATCACTAAATC	2nd round promoter cloning Y1H
AIL6 Y1H R 2nd	AAACTTTCTTATAAAAACAATTTTACTT	2nd round promoter cloning Y1H

Discussion

The generation of biological shapes during development remains a central and open question in biology. Plants represent excellent systems to study these issues given their open, indeterminate development. This means that new shapes are generated over the course of their life times.

A case study: the initiation of lateral organs in the inflorescence meristem

The shoot apical meristem (SAM) has been a very important system for studying pattern formation and morphogenesis in plants. The shape of this structure results from differential growth of its regions. The central region, which contains the stem cell niche, grows at a slow pace compared to the surrounding periphery. Cells participating in the formation of a new primordium further increase their growth rate, while expansion in the organ boundary region between the meristem and the primordium slows down (Grandjean et al., 2004; Kwiatkowska and Dumais, 2003; Reddy et al., 2004).

When I started my thesis, the available data suggested a relatively straightforward scenario for organ initiation, where auxin accumulation would initially activate MP. MP would then directly induce the expression of LFY, ANT and AIL6. Together with at least one additional regulator, these three transcription factors would then control the plastic, turgor driven deformation of the cell wall. The work described in this thesis has revealed additional levels of regulation and poses a number of important perspectives for further research.

Auxin might control organ formation in part via a direct control of microtubule dynamics.

Previous work has suggested the existence of a mechanical feedback loop, where microtubules would align to stress patterns and reinforce the cell wall along the main force vectors. The precise mechanism by which microtubules respond to mechanical stress is still unclear. However, KTN1 severing activity is required for responding to growth-derived mechanical stress (Sampathkumar et al., 2014; Uyttewaal et al., 2012). KTN1 promotes microtubule bundling, which allows the reorganization of CMT into parallel arrays (Lin et al., 2013; Zhang et al., 2013). Normally, this behavior of the CMT would lead to the formation of a radial symmetric axis. Our results provide evidence for a scenario where auxin induced organ initiation would involve an inactivating of this feedback. In line with this, reduced

microtubule organization in the apices of *bot1-7* mutants triggers isotropic cellular growth and the formation of ectopic organs. We further show that auxin might directly act on microtubule dynamics via a ROP6/KTN1 signaling pathway. It is tempting to hypothesize that this pathway modulates microtubule ordering, thus participating in the establishment of growth patterns at the meristem. This pathway has been thoroughly studied in leaf pavement cells, where it was described to be under auxin control (Lin et al., 2013). Several important questions remain to be answered. First, the mechanism by which auxin activates the ROP6/RIC1 pathway remains to be clarified, especially in light of the controversial role of ABP1 in this process (Feng and Kim, 2015). Alternatively other ROP activators might be considered, for instance FERONIA (FER), a receptor-like kinase (RLK) of the *Catharanthus roseus* family (crRLKs). FER is required for transduction of mechanical signals in *Arabidopsis thaliana* roots (Shih et al., 2014). ROPs can act downstream of FER during mechanical stress transduction to regulate ROS production (Duan et al., 2010). The relatively weak phenotypes of ROP and RIC mutants might also indicate that other ROPs are involved. In particular ROP2, ROP9 and ROP10, which are also expressed at the meristem (Mantegazza et al., 2014). A thorough genetic analysis using multiple knockouts might further shed light on this.

Although auxin thus has the possibility to interfere directly with the cytoskeleton, we also found that the reorientation of CMT requires MP (Bhatia et al., 2016). We speculate, that MP must somehow control one of the components of the ROP signaling pathway to modulate the mechanical feedback.

Wall anisotropy acts together with cell wall remodeling to promote organ formation

Our results, confirm and further complete results obtained by others (Braybrook and Peaucelle, 2013; Peaucelle et al., 2011a; Peaucelle et al., 2008; Peaucelle et al., 2015), indicate that cell wall anisotropy does not act alone to initiate organ formation as it needs to be combined with a change in cell wall stiffness. The expression of a number of xyloglucan (XyG) and pectin remodeling genes, specific of organ outgrowth, confirms this. A small number of these genes are at least indirectly regulated by auxin. Importantly, we identified a cross talk between wall remodeling and cytoskeleton organization. As described in chapter 2 *PME3*, *XTH9*, and *EXPA15* expression is induced after CMT-driven growth isotropy, while

perturbing xyloglucan or pectin remodeling affects microtubule alignment. How cell wall properties affect the cytoskeleton remains an open question. As such this doesn't seem to involve auxin and auxin trafic. A possibility is, that the cell somehow senses wall composition. The potential cell surface signaling capacity of RLKs makes them good candidates to explore. Among them a few are binding to pectins, such as the wall-associated kinases (WAKs) (Decreux and Messiaen, 2005; Kohorn et al., 2009; Kohorn and Kohorn, 2012; Wagner and Kohorn, 2001). The previously mentioned crRLKs are other candidates to consider, especially THESEUS (THE) (Hematy et al., 2007) which is likely in charge of surveying cellulose synthesis and perceiving cellulose modification. RLKs in theory could act in synergy with other mechanosensory molecules, mechanosensitive ion channels for instance (Hamilton et al., 2015). The cellular signaling pathways could then interact with cytoskeleton organization, for example via the ROP/KTN pathway described in chapter 1 and Sassi et al., (2014).

While cell wall modifications might directly influence cytoskeleton organization, we show here that CMT arrangements affect wall remodeling via transcriptional regulation. Identifying the transcription factors involved is an important and challenging objective. The eY1H analysis has identified a range of transcription factors that potentially control XTH4, XTH9, EXPA4 and EXPA15. Some of these have been associated with auxin signaling (e.g. ARF 18 and ARF 22). However links with other hormonal pathways can also be made (e.g. LOB, involved in BR signaling and interacting with the EXPA4 promoter in the 1H assay). This would explain why the outgrowths induced by perturbing CMT organization could induce the expression of these genes in the absence of auxin transport.

Crosstalks are not only limited to the cytoskeleton and cell wall remodeling. Different components of the wall remodeling machinery itself are also interacting. Although in the past XyGs and pectins were conceived as independent mechanisms in control of plant cell growth, recent studies have shown that the two systems are mutually dependent. Several studies revisiting cell wall structure suggests that in the absence of XyGs, pectins act as load-bearing components (Cavalier et al., 2008; Park and Cosgrove, 2012a). This and other compensation mechanisms that guarantee a robust control of wall mechanics are still poorly understood.

Microtubule-driven growth isotropy promotes the expression of patterning genes

The auxin-dependent transcriptional network is also regulated by CMT-driven isotropic growth, although only at certain level. Consistently, the expression of *ANT* was activated downstream of CMT disorganization at the outgrowing cells. The nature of the mechanism coupling the changes in CMT dynamics and transcriptional activation remains to be determined. Since, the activation of this mechanism can be triggered in the absence of auxin transport or signaling, it might even act in parallel or in synergy with auxin.

Beyond ARF5/MP only a few regulators of *ANT* have been described. Here we found that *ANT* cis regulation can be broad and that it might include BR signaling as was also shown for ovule development (Huang et al., 2013). BRs play essential roles in growth control and regulate the expression of cell wall-related genes. Although there is no strong evidence for this yet, we are tempted to hypothesize that BR signaling couples CMT disorganization with the transcriptional activation of both patterning and cell wall related genes. Recently, a receptor-like protein (RLP)44 was described as an integrator of cell wall homeostasis and BR signaling (Wolf et al., 2012; Wolf et al., 2014). Therefore, we wonder about the possibility that a cell wall mediated activation of BR signaling regulates the transcriptional feed back we have described here.

References

Abad, U., Sassi, M., and Traas, J. (2017). Flower development: from morphodynamics to morphomechanics. Philos Trans R Soc Lond B Biol Sci *372*.

Abas, L., Benjamins, R., Malenica, N., Paciorek, T., Wisniewska, J., Moulinier-Anzola, J.C., Sieberer, T., Friml, J., and Luschnig, C. (2006). Intracellular trafficking and proteolysis of the Arabidopsis auxin-efflux facilitator PIN2 are involved in root gravitropism. Nat Cell Biol *8*, 249-256.

Abe, M., Kobayashi, Y., Yamamoto, S., Daimon, Y., Yamaguchi, A., Ikeda, Y., Ichinoki, H., Notaguchi, M., Goto, K., and Araki, T. (2005). FD, a bZIP protein mediating signals from the floral pathway integrator FT at the shoot apex. Science *309*, 1052-1056.

Adamowski, M., and Friml, J. (2015). PIN-dependent auxin transport: action, regulation, and evolution. Plant Cell *27*, 20-32.

Adibi, M., Yoshida, S., Weijers, D., and Fleck, C. (2016). Centering the Organizing Center in the Arabidopsis thaliana Shoot Apical Meristem by a Combination of Cytokinin Signaling and Self-Organization. PLoS One *11*, e0147830.

Aida, M., Ishida, T., Fukaki, H., Fujisawa, H., and Tasaka, M. (1997). Genes involved in organ separation in Arabidopsis: an analysis of the cup-shaped cotyledon mutant. Plant Cell *9*, 841-857.

Aida, M., Ishida, T., and Tasaka, M. (1999). Shoot apical meristem and cotyledon formation during Arabidopsis embryogenesis: interaction among the CUP-SHAPED COTYLEDON and SHOOT MERISTEMLESS genes. Development *126*, 1563-1570.

Ali, O., Mirabet, V., Godin, C., and Traas, J. (2014). Physical models of plant development. Annu Rev Cell Dev Biol *30*, 59-78.

Ali, O., and Traas, J. (2016). Force-Driven Polymerization and Turgor-Induced Wall Expansion. Trends Plant Sci *21*, 398-409.

Alim, K., and Frey, E. (2010). Quantitative predictions on auxin-induced polar distribution of PIN proteins during vein formation in leaves. Eur Phys J E Soft Matter *33*, 165-173.

Arnaud, N., and Laufs, P. (2013). Plant development: brassinosteroids go out of bounds. Curr Biol *23*, R152-154.

Ashe, H.L., and Briscoe, J. (2006). The interpretation of morphogen gradients. Development *133*, 385-394.

Atmodjo, M.A., Hao, Z., and Mohnen, D. (2013). Evolving views of pectin biosynthesis. Annu Rev Plant Biol *64*, 747-779.

Bancos, S., Nomura, T., Sato, T., Molnar, G., Bishop, G.J., Koncz, C., Yokota, T., Nagy, F., and Szekeres, M. (2002). Regulation of transcript levels of the Arabidopsis cytochrome p450 genes involved in brassinosteroid biosynthesis. Plant Physiol *130*, 504-513.

Bao, F., Shen, J., Brady, S.R., Muday, G.K., Asami, T., and Yang, Z. (2004). Brassinosteroids interact with auxin to promote lateral root development in Arabidopsis. Plant Physiol *134*, 1624-1631.

Barbez, E., Kubes, M., Rolcik, J., Beziat, C., Pencik, A., Wang, B., Rosquete, M.R., Zhu, J., Dobrev, P.I., Lee, Y., *et al*. (2012). A novel putative auxin carrier family regulates intracellular auxin homeostasis in plants. Nature *485*, 119-122.

Barkoulas, M., Galinha, C., Grigg, S.P., and Tsiantis, M. (2007). From genes to shape: regulatory interactions in leaf development. Curr Opin Plant Biol *10*, 660-666.

Barrett, T., Troup, D.B., Wilhite, S.E., Ledoux, P., Rudnev, D., Evangelista, C., Kim, I.F., Soboleva, A., Tomashevsky, M., and Edgar, R. (2007). NCBI GEO: mining tens of millions of expression profiles--database and tools update. Nucleic Acids Res *35*, D760-765.

Bashline, L., Lei, L., Li, S., and Gu, Y. (2014). Cell wall, cytoskeleton, and cell expansion in higher plants. Mol Plant *7*, 586-600.

Baskin, T.I. (2005). Anisotropic expansion of the plant cell wall. Annu Rev Cell Dev Biol *21*, 203-222.

Baskin, T.I., Beemster, G.T., Judy-March, J.E., and Marga, F. (2004). Disorganization of cortical microtubules stimulates tangential expansion and reduces the uniformity of cellulose microfibril alignment among cells in the root of Arabidopsis. Plant Physiol *135*, 2279-2290.

Baskin, T.I., and Jensen, O.E. (2013). On the role of stress anisotropy in the growth of stems. J Exp Bot *64*, 4697-4707.

Baurle, I., and Laux, T. (2005). Regulation of WUSCHEL transcription in the stem cell niche of the Arabidopsis shoot meristem. Plant Cell *17*, 2271-2280.

Bayer, E.M., Smith, R.S., Mandel, T., Nakayama, N., Sauer, M., Prusinkiewicz, P., and Kuhlemeier, C. (2009). Integration of transport-based models for phyllotaxis and midvein formation. Genes Dev *23*, 373-384.

Beauzamy, L., Louveaux, M., Hamant, O., and Boudaoud, A. (2015). Mechanically, the Shoot Apical Meristem of Arabidopsis Behaves like a Shell Inflated by a Pressure of About 1 MPa. Front Plant Sci *6*, 1038.

Bell, E.M., Lin, W.C., Husbands, A.Y., Yu, L., Jaganatha, V., Jablonska, B., Mangeon, A., Neff, M.M., Girke, T., and Springer, P.S. (2012). Arabidopsis lateral organ boundaries negatively regulates brassinosteroid accumulation to limit growth in organ boundaries. Proc Natl Acad Sci U S A *109*, 21146-21151.

Benjamins, R., Quint, A., Weijers, D., Hooykaas, P., and Offringa, R. (2001). The PINOID protein kinase regulates organ development in Arabidopsis by enhancing polar auxin transport. Development *128*, 4057-4067.

Benkova, E., Ivanchenko, M.G., Friml, J., Shishkova, S., and Dubrovsky, J.G. (2009). A morphogenetic trigger: is there an emerging concept in plant developmental biology? Trends Plant Sci *14*, 189-193.

Benkova, E., Michniewicz, M., Sauer, M., Teichmann, T., Seifertova, D., Jurgens, G., and Friml, J. (2003). Local, efflux-dependent auxin gradients as a common module for plant organ formation. Cell *115*, 591-602.

Bennett, S.R.M., Alvarez, J., Bossinger, G., and Smyth, D.R. (1995). Morphogenesis in pinoid mutants of Arabidopsis thaliana. The Plant Journal *8*, 505-520.

Bennett, T., Brockington, S.F., Rothfels, C., Graham, S.W., Stevenson, D., Kutchan, T., Rolf, M., Thomas, P., Wong, G.K., Leyser, O., *et al*. (2014). Paralogous radiations of PIN proteins with multiple origins of noncanonical PIN structure. Mol Biol Evol *31*, 2042-2060.

Bergfeld, R., Speth, V., and Schopfer, P. (1988). Reorientation of Microfibrils and Microtubules at the Outer Epidermal Wall of Maize Coleoptiles During Auxin-Mediated Growth. Botanica Acta *101*, 57-67.

Berleth, T., and Jurgens, G. (1993). The role of the monopteros gene in organising the basal body region of the Arabidopsis embryo. Development *118*, 575-587.

Besnard, F., Rozier, F., and Vernoux, T. (2014). The AHP6 cytokinin signaling inhibitor mediates an auxin-cytokinin crosstalk that regulates the timing of organ initiation at the shoot apical meristem. Plant Signal Behav *9*.

Bhalerao, R.P., and Bennett, M.J. (2003). The case for morphogens in plants. Nat Cell Biol *5*, 939-943.

Bhatia, N., Bozorg, B., Larsson, A., Ohno, C., Jonsson, H., and Heisler, M.G. (2016). Auxin Acts through MONOPTEROS to Regulate Plant Cell Polarity and Pattern Phyllotaxis. Curr Biol *26*, 3202-3208.

Bichet, A., Desnos, T., Turner, S., Grandjean, O., and Hofte, H. (2001). BOTERO1 is required for normal orientation of cortical microtubules and anisotropic cell expansion in Arabidopsis. Plant J *25*, 137-148.

Bidhendi, A.J., and Geitmann, A. (2016). Relating the mechanics of the primary plant cell wall to morphogenesis. J Exp Bot *67*, 449-461.

Bishop, G.J., Harrison, K., and Jones, J.D. (1996). The tomato Dwarf gene isolated by heterologous transposon tagging encodes the first member of a new cytochrome P450 family. Plant Cell *8*, 959-969.

Bishopp, A., Help, H., El-Showk, S., Weijers, D., Scheres, B., Friml, J., Benkova, E., Mahonen, A.P., and Helariutta, Y. (2011a). A mutually inhibitory interaction between auxin and cytokinin specifies vascular pattern in roots. Curr Biol *21*, 917-926.

Bishopp, A., Lehesranta, S., Vaten, A., Help, H., El-Showk, S., Scheres, B., Helariutta, K., Mahonen, A.P., Sakakibara, H., and Helariutta, Y. (2011b). Phloem-transported cytokinin regulates polar auxin transport and maintains vascular pattern in the root meristem. Curr Biol *21*, 927-932.

Blazquez, M.A., Soowal, L.N., Lee, I., and Weigel, D. (1997). LEAFY expression and flower initiation in Arabidopsis. Development *124*, 3835-3844.

Blilou, I., Xu, J., Wildwater, M., Willemsen, V., Paponov, I., Friml, J., Heidstra, R., Aida, M., Palme, K., and Scheres, B. (2005). The PIN auxin efflux facilitator network controls growth and patterning in Arabidopsis roots. Nature *433*, 39-44.

Borghi, L., Bureau, M., and Simon, R. (2007). Arabidopsis JAGGED LATERAL ORGANS is expressed in boundaries and coordinates KNOX and PIN activity. Plant Cell *19*, 1795-1808.

Boudon, F., Chopard, J., Ali, O., Gilles, B., Hamant, O., Boudaoud, A., Traas, J., and Godin, C. (2015). A computational framework for 3D mechanical modeling of plant morphogenesis with cellular resolution. PLoS Comput Biol *11*, e1003950.

Brady, S.M., Zhang, L., Megraw, M., Martinez, N.J., Jiang, E., Yi, C.S., Liu, W., Zeng, A., Taylor-Teeples, M., Kim, D., *et al*. (2011). A stele-enriched gene regulatory network in the Arabidopsis root. Mol Syst Biol *7*, 459.

Brand, U., Grunewald, M., Hobe, M., and Simon, R. (2002). Regulation of CLV3 expression by two homeobox genes in Arabidopsis. Plant Physiol *129*, 565-575.

Brandstatter, I., and Kieber, J.J. (1998). Two genes with similarity to bacterial response regulators are rapidly and specifically induced by cytokinin in Arabidopsis. Plant Cell *10*, 1009-1019.

Braybrook, S.A., and Jonsson, H. (2016). Shifting foundations: the mechanical cell wall and development. Curr Opin Plant Biol *29*, 115-120.

Braybrook, S.A., and Peaucelle, A. (2013). Mechano-chemical aspects of organ formation in Arabidopsis thaliana: the relationship between auxin and pectin. PLoS One *8*, e57813.

Breuil-Broyer, S., Morel, P., de Almeida-Engler, J., Coustham, V., Negrutiu, I., and Trehin, C. (2004). High-resolution boundary analysis during Arabidopsis thaliana flower development. Plant J *38*, 182-192.

Bringmann, M., Li, E., Sampathkumar, A., Kocabek, T., Hauser, M.T., and Persson, S. (2012). POM-POM2/cellulose synthase interacting1 is essential for the functional association of cellulose synthase and microtubules in Arabidopsis. Plant Cell *24*, 163-177.

Brunoud, G., Wells, D.M., Oliva, M., Larrieu, A., Mirabet, V., Burrow, A.H., Beeckman, T., Kepinski, S., Traas, J., Bennett, M.J., *et al*. (2012). A novel sensor to map auxin response and distribution at high spatio-temporal resolution. Nature *482*, 103-106.

Burian, A., Ludynia, M., Uyttewaal, M., Traas, J., Boudaoud, A., Hamant, O., and Kwiatkowska, D. (2013). A correlative microscopy approach relates microtubule behaviour, local organ geometry, and cell growth at the Arabidopsis shoot apical meristem. J Exp Bot *64*, 5753-5767.

Burk, D.H., and Ye, Z.H. (2002). Alteration of oriented deposition of cellulose microfibrils by mutation of a katanin-like microtubule-severing protein. Plant Cell *14*, 2145-2160.

Burkle, L., Cedzich, A., Dopke, C., Stransky, H., Okumoto, S., Gillissen, B., Kuhn, C., and Frommer, W.B. (2003). Transport of cytokinins mediated by purine transporters of the PUP family expressed in phloem, hydathodes, and pollen of Arabidopsis. Plant J *34*, 13-26.

Burstenbinder, K., Mitra, D., and Quegwer, J. (2017a). Functions of IQD proteins as hubs in cellular calcium and auxin signaling: A toolbox for shape formation and tissue-specification in plants? Plant Signal Behav, e1331198.

Burstenbinder, K., Moller, B., Plotner, R., Stamm, G., Hause, G., Mitra, D., and Abel, S. (2017b). The IQD Family of Calmodulin-Binding Proteins Links Calcium Signaling to Microtubules, Membrane Subdomains, and the Nucleus. Plant Physiol *173*, 1692-1708.

Busch, W., Miotk, A., Ariel, F.D., Zhao, Z., Forner, J., Daum, G., Suzaki, T., Schuster, C., Schultheiss, S.J., Leibfried, A.*, et al.* (2010). Transcriptional control of a plant stem cell niche. Dev Cell *18*, 849-861.

Byrne, M.E., Barley, R., Curtis, M., Arroyo, J.M., Dunham, M., Hudson, A., and Martienssen, R.A. (2000). Asymmetric leaves1 mediates leaf patterning and stem cell function in Arabidopsis. Nature *408*, 967-971.

Calderon Villalobos, L.I., Lee, S., De Oliveira, C., Ivetac, A., Brandt, W., Armitage, L., Sheard, L.B., Tan, X., Parry, G., Mao, H.*, et al.* (2012). A combinatorial TIR1/AFB-Aux/IAA co-receptor system for differential sensing of auxin. Nat Chem Biol *8*, 477-485.

Cantarel, B.L., Coutinho, P.M., Rancurel, C., Bernard, T., Lombard, V., and Henrissat, B. (2009). The Carbohydrate-Active EnZymes database (CAZy): an expert resource for Glycogenomics. Nucleic Acids Res *37*, D233-238.

Carabelli, M., Sessa, G., Baima, S., Morelli, G., and Ruberti, I. (1993). The Arabidopsis Athb-2 and -4 genes are strongly induced by far-red-rich light. Plant J *4*, 469-479.

Catterou, M., Dubois, F., Schaller, H., Aubanelle, L., Vilcot, B., Sangwan-Norreel, B.S., and Sangwan, R.S. (2001). Brassinosteroids, microtubules and cell elongation in Arabidopsis thaliana. II. Effects of brassinosteroids on microtubules and cell elongation in the bul1 mutant. Planta *212*, 673-683.

Causier, B., Schwarz-Sommer, Z., and Davies, B. (2010). Floral organ identity: 20 years of ABCs. Semin Cell Dev Biol *21*, 73-79.

Cavalier, D.M., and Keegstra, K. (2006). Two xyloglucan xylosyltransferases catalyze the addition of multiple xylosyl residues to cellohexaose. J Biol Chem *281*, 34197-34207.

Cavalier, D.M., Lerouxel, O., Neumetzler, L., Yamauchi, K., Reinecke, A., Freshour, G., Zabotina, O.A., Hahn, M.G., Burgert, I., Pauly, M.*, et al.* (2008). Disrupting two Arabidopsis thaliana xylosyltransferase genes results in plants deficient in xyloglucan, a major primary cell wall component. Plant Cell *20*, 1519-1537.

Chan, J., Crowell, E., Eder, M., Calder, G., Bunnewell, S., Findlay, K., Vernhettes, S., Hofte, H., and Lloyd, C. (2010). The rotation of cellulose synthase trajectories is microtubule dependent and influences the texture of epidermal cell walls in Arabidopsis hypocotyls. J Cell Sci *123*, 3490-3495.

Chandler, J.W. (2016). Auxin response factors. Plant Cell Environ *39*, 1014-1028.

Chandler, J.W., Cole, M., Flier, A., and Werr, W. (2009). BIM1, a bHLH protein involved in brassinosteroid signalling, controls Arabidopsis embryonic patterning via interaction with DORNROSCHEN and DORNROSCHEN-LIKE. Plant Mol Biol *69*, 57-68.

Chapman, E.J., and Estelle, M. (2009). Mechanism of auxin-regulated gene expression in plants. Annu Rev Genet *43*, 265-285.

Chen, D., Deng, Y., and Zhao, J. (2012a). Distribution and change patterns of free IAA, ABP 1 and PM H(+)-ATPase during ovary and ovule development of Nicotiana tabacum L. J Plant Physiol *169*, 127-136.

Chen, J., Wang, F., Zheng, S., Xu, T., and Yang, Z. (2015). Pavement cells: a model system for non-transcriptional auxin signalling and crosstalks. J Exp Bot *66*, 4957-4970.

Chen, J.G., Ullah, H., Young, J.C., Sussman, M.R., and Jones, A.M. (2001). ABP1 is required for organized cell elongation and division in Arabidopsis embryogenesis. Genes Dev *15*, 902-911.

Chen, X., Naramoto, S., Robert, S., Tejos, R., Lofke, C., Lin, D., Yang, Z., and Friml, J. (2012b). ABP1 and ROP6 GTPase signaling regulate clathrin-mediated endocytosis in Arabidopsis roots. Curr Biol *22*, 1326-1332.

Cheng, Y., Dai, X., and Zhao, Y. (2006). Auxin biosynthesis by the YUCCA flavin monooxygenases controls the formation of floral organs and vascular tissues in Arabidopsis. Genes Dev *20*, 1790-1799.

Cheng, Y., Dai, X., and Zhao, Y. (2007). Auxin synthesized by the YUCCA flavin monooxygenases is essential for embryogenesis and leaf formation in Arabidopsis. Plant Cell *19*, 2430-2439.

Chickarmane, V.S., Gordon, S.P., Tarr, P.T., Heisler, M.G., and Meyerowitz, E.M. (2012). Cytokinin signaling as a positional cue for patterning the apical-basal axis of the growing Arabidopsis shoot meristem. Proc Natl Acad Sci U S A *109*, 4002-4007.

Chitwood, D.H., and Timmermans, M.C. (2010). Small RNAs are on the move. Nature *467*, 415-419.

Choe, S., Dilkes, B.P., Fujioka, S., Takatsuto, S., Sakurai, A., and Feldmann, K.A. (1998). The DWF4 gene of Arabidopsis encodes a cytochrome P450 that mediates multiple 22alpha-hydroxylation steps in brassinosteroid biosynthesis. Plant Cell *10*, 231-243.

Chung, Y., and Choe, S. (2013). The Regulation of Brassinosteroid Biosynthesis in Arabisopsis. Critical Reviews in Plant Sciences *32*, 396-410.

Chung, Y., Maharjan, P.M., Lee, O., Fujioka, S., Jang, S., Kim, B., Takatsuto, S., Tsujimoto, M., Kim, H., Cho, S., *et al*. (2011). Auxin stimulates DWARF4 expression and brassinosteroid biosynthesis in Arabidopsis. Plant J *66*, 564-578.

Clark, S.E., Williams, R.W., and Meyerowitz, E.M. (1997). The CLAVATA1 gene encodes a putative receptor kinase that controls shoot and floral meristem size in Arabidopsis. Cell *89*, 575-585.

Clouse, S.D., Hall, A.F., Langford, M., McMorris, T.C., and Baker, M.E. (1993). Physiological and molecular effects of brassinosteroids on Arabidopsis thaliana. Journal of Plant Growth Regulation *12*, 61.

Clouse, S.D., Langford, M., and McMorris, T.C. (1996). A brassinosteroid-insensitive mutant in Arabidopsis thaliana exhibits multiple defects in growth and development. Plant Physiol *111*, 671-678.

Clouse, S.D., and Sasse, J.M. (1998). BRASSINOSTEROIDS: Essential Regulators of Plant Growth and Development. Annu Rev Plant Physiol Plant Mol Biol *49*, 427-451.

Cocuron, J.C., Lerouxel, O., Drakakaki, G., Alonso, A.P., Liepman, A.H., Keegstra, K., Raikhel, N., and Wilkerson, C.G. (2007). A gene from the cellulose synthase-like C family encodes a beta-1,4 glucan synthase. Proc Natl Acad Sci U S A *104*, 8550-8555.

Coen, E., Rolland-Lagan, A.G., Matthews, M., Bangham, J.A., and Prusinkiewicz, P. (2004). The genetics of geometry. Proc Natl Acad Sci U S A *101*, 4728-4735.

Corson, F., Hamant, O., Bohn, S., Traas, J., Boudaoud, A., and Couder, Y. (2009). Turning a plant tissue into a living cell froth through isotropic growth. Proc Natl Acad Sci U S A *106*, 8453-8458.

Cosgrove, D.J. (2005). Growth of the plant cell wall. Nat Rev Mol Cell Biol *6*, 850-861.

Cosgrove, D.J. (2014). Re-constructing our models of cellulose and primary cell wall assembly. Curr Opin Plant Biol *22*, 122-131.

Cosgrove, D.J. (2015). Plant expansins: diversity and interactions with plant cell walls. Curr Opin Plant Biol *25*, 162-172.

Cosgrove, D.J. (2016a). Catalysts of plant cell wall loosening. F1000Res *5*.

Cosgrove, D.J. (2016b). Plant cell wall extensibility: connecting plant cell growth with cell wall structure, mechanics, and the action of wall-modifying enzymes. J Exp Bot *67*, 463-476.

Cosgrove, D.J., Li, L.C., Cho, H.T., Hoffmann-Benning, S., Moore, R.C., and Blecker, D. (2002). The growing world of expansins. Plant Cell Physiol *43*, 1436-1444.

Crawford, S., Shinohara, N., Sieberer, T., Williamson, L., George, G., Hepworth, J., Muller, D., Domagalska, M.A., and Leyser, O. (2010). Strigolactones enhance competition between shoot branches by dampening auxin transport. Development *137*, 2905-2913.

Cucinotta, M., Colombo, L., and Roig-Villanova, I. (2014). Ovule development, a new model for lateral organ formation. Front Plant Sci *5*, 117.

D'Agostino, I.B., Deruere, J., and Kieber, J.J. (2000). Characterization of the response of the Arabidopsis response regulator gene family to cytokinin. Plant Physiol *124*, 1706-1717.

Dai, X., Zhang, Y., Zhang, D., Chen, J., Gao, X., Estelle, M., and Zhao, Y. (2015). Embryonic lethality of Arabidopsis abp1-1 is caused by deletion of the adjacent BSM gene. Nat Plants *1*.

Dal Bosco, C., Dovzhenko, A., Liu, X., Woerner, N., Rensch, T., Eismann, M., Eimer, S., Hegermann, J., Paponov, I.A., Ruperti, B., *et al*. (2012). The endoplasmic reticulum localized PIN8 is a pollen-specific auxin carrier involved in intracellular auxin homeostasis. Plant J *71*, 860-870.

Daum, G., Medzihradszky, A., Suzaki, T., and Lohmann, J.U. (2014). A mechanistic framework for noncell autonomous stem cell induction in Arabidopsis. Proc Natl Acad Sci U S A *111*, 14619-14624.

de Folter, S., Immink, R.G., Kieffer, M., Parenicova, L., Henz, S.R., Weigel, D., Busscher, M., Kooiker, M., Colombo, L., Kater, M.M., *et al*. (2005). Comprehensive interaction map of the Arabidopsis MADS Box transcription factors. Plant Cell *17*, 1424-1433.

de Reuille, P.B., Bohn-Courseau, I., Ljung, K., Morin, H., Carraro, N., Godin, C., and Traas, J. (2006). Computer simulations reveal properties of the cell-cell signaling network at the shoot apex in Arabidopsis. Proc Natl Acad Sci U S A *103*, 1627-1632.

De Smet, I., and Beeckman, T. (2011). Asymmetric cell division in land plants and algae: the driving force for differentiation. Nat Rev Mol Cell Biol *12*, 177-188.

Decreux, A., and Messiaen, J. (2005). Wall-associated kinase WAK1 interacts with cell wall pectins in a calcium-induced conformation. Plant Cell Physiol *46*, 268-278.

Dello Ioio, R., Nakamura, K., Moubayidin, L., Perilli, S., Taniguchi, M., Morita, M.T., Aoyama, T., Costantino, P., and Sabatini, S. (2008). A genetic framework for the control of cell division and differentiation in the root meristem. Science *322*, 1380-1384.

Deplancke, B., Dupuy, D., Vidal, M., and Walhout, A.J. (2004). A gateway-compatible yeast one-hybrid system. Genome Res *14*, 2093-2101.

Desprez, T., Juraniec, M., Crowell, E.F., Jouy, H., Pochylova, Z., Parcy, F., Hofte, H., Gonneau, M., and Vernhettes, S. (2007). Organization of cellulose synthase complexes involved in primary cell wall synthesis in Arabidopsis thaliana. Proc Natl Acad Sci U S A *104*, 15572-15577.

Dharmasiri, N., Dharmasiri, S., and Estelle, M. (2005a). The F-box protein TIR1 is an auxin receptor. Nature *435*, 441-445.

Dharmasiri, N., Dharmasiri, S., Weijers, D., Lechner, E., Yamada, M., Hobbie, L., Ehrismann, J.S., Jurgens, G., and Estelle, M. (2005b). Plant development is regulated by a family of auxin receptor F box proteins. Dev Cell *9*, 109-119.

Dhonukshe, P., Aniento, F., Hwang, I., Robinson, D.G., Mravec, J., Stierhof, Y.D., and Friml, J. (2007). Clathrin-mediated constitutive endocytosis of PIN auxin efflux carriers in Arabidopsis. Curr Biol *17*, 520-527.

Dhonukshe, P., Huang, F., Galvan-Ampudia, C.S., Mahonen, A.P., Kleine-Vehn, J., Xu, J., Quint, A., Prasad, K., Friml, J., Scheres, B., *et al*. (2010). Plasma membrane-bound AGC3 kinases phosphorylate PIN auxin carriers at TPRXS(N/S) motifs to direct apical PIN recycling. Development *137*, 3245-3255.

Dhonukshe, P., Tanaka, H., Goh, T., Ebine, K., Mahonen, A.P., Prasad, K., Blilou, I., Geldner, N., Xu, J., Uemura, T., *et al*. (2008). Generation of cell polarity in plants links endocytosis, auxin distribution and cell fate decisions. Nature *456*, 962-966.

Dick-Perez, M., Zhang, Y., Hayes, J., Salazar, A., Zabotina, O.A., and Hong, M. (2011). Structure and interactions of plant cell-wall polysaccharides by two- and three-dimensional magic-angle-spinning solid-state NMR. Biochemistry *50*, 989-1000.

Ding, Z., Galvan-Ampudia, C.S., Demarsy, E., Langowski, L., Kleine-Vehn, J., Fan, Y., Morita, M.T., Tasaka, M., Fankhauser, C., Offringa, R., *et al*. (2011). Light-mediated polarization of the PIN3 auxin transporter for the phototropic response in Arabidopsis. Nat Cell Biol *13*, 447-452.

Ding, Z., Wang, B., Moreno, I., Duplakova, N., Simon, S., Carraro, N., Reemmer, J., Pencik, A., Chen, X., Tejos, R., *et al*. (2012). ER-localized auxin transporter PIN8 regulates auxin homeostasis and male gametophyte development in Arabidopsis. Nat Commun *3*, 941.

Dinneny, J.R., and Benfey, P.N. (2008). Plant stem cell niches: standing the test of time. Cell *132*, 553-557.

Doblin, M.S., Kurek, I., Jacob-Wilk, D., and Delmer, D.P. (2002). Cellulose biosynthesis in plants: from genes to rosettes. Plant Cell Physiol *43*, 1407-1420.

Donner, T.J., Sherr, I., and Scarpella, E. (2009). Regulation of preprocambial cell state acquisition by auxin signaling in Arabidopsis leaves. Development *136*, 3235-3246.

Driever, W., and Nusslein-Volhard, C. (1988). A gradient of bicoid protein in Drosophila embryos. Cell *54*, 83-93.

Duan, Q., Kita, D., Li, C., Cheung, A.Y., and Wu, H.M. (2010). FERONIA receptor-like kinase regulates RHO GTPase signaling of root hair development. Proc Natl Acad Sci U S A *107*, 17821-17826.

Dubrovsky, J.G., Sauer, M., Napsucialy-Mendivil, S., Ivanchenko, M.G., Friml, J., Shishkova, S., Celenza, J., and Benkova, E. (2008). Auxin acts as a local morphogenetic trigger to specify lateral root founder cells. Proc Natl Acad Sci U S A *105*, 8790-8794.

Elliott, R.C., Betzner, A.S., Huttner, E., Oakes, M.P., Tucker, W.Q., Gerentes, D., Perez, P., and Smyth, D.R. (1996). AINTEGUMENTA, an APETALA2-like gene of Arabidopsis with pleiotropic roles in ovule development and floral organ growth. Plant Cell *8*, 155-168.

Emons, A.M., Hofte, H., and Mulder, B.M. (2007). Microtubules and cellulose microfibrils: how intimate is their relationship? Trends Plant Sci *12*, 279-281.

Endrizzi, K., Moussian, B., Haecker, A., Levin, J.Z., and Laux, T. (1996). The SHOOT MERISTEMLESS gene is required for maintenance of undifferentiated cells in Arabidopsis shoot and floral meristems and acts at a different regulatory level than the meristem genes WUSCHEL and ZWILLE. Plant J *10*, 967-979.

Esau, K. (1965). Plant anatomy (Wiley).

Eshed, Y., Baum, S.F., Perea, J.V., and Bowman, J.L. (2001). Establishment of polarity in lateral organs of plants. Curr Biol *11*, 1251-1260.

Faik, A., Price, N.J., Raikhel, N.V., and Keegstra, K. (2002). An Arabidopsis gene encoding an alpha-xylosyltransferase involved in xyloglucan biosynthesis. Proc Natl Acad Sci U S A *99*, 7797-7802.

Feng, M., and Kim, J.Y. (2015). Revisiting Apoplastic Auxin Signaling Mediated by AUXIN BINDING PROTEIN 1. Mol Cells *38*, 829-835.

Fernandez, R., Das, P., Mirabet, V., Moscardi, E., Traas, J., Verdeil, J.L., Malandain, G., and Godin, C. (2010). Imaging plant growth in 4D: robust tissue reconstruction and lineaging at cell resolution. Nat Methods *7*, 547-553.

Ferrandiz, C., and Sessions, A. (2008a). Nonradioactive in situ hybridization of RNA probes to sections of plant tissues. CSH Protoc *2008*, pdb prot4943.

Ferrandiz, C., and Sessions, A. (2008b). Preparation and hydrolysis of digoxygenin-labeled probes for in situ hybridization of plant tissues. CSH Protoc *2008*, pdb prot4942.

Feugier, F.G., Mochizuki, A., and Iwasa, Y. (2005). Self-organization of the vascular system in plant leaves: inter-dependent dynamics of auxin flux and carrier proteins. J Theor Biol *236*, 366-375.

Finet, C., and Jaillais, Y. (2012). Auxology: when auxin meets plant evo-devo. Dev Biol *369*, 19-31.

Fisher, D.D., and Cyr, R.J. (1998). Extending the Microtubule/Microfibril paradigm. Cellulose synthesis is required for normal cortical microtubule alignment in elongating cells. Plant Physiol *116*, 1043-1051.

Fleming, A.J., McQueen-Mason, S., Mandel, T., and Kuhlemeier, C. (1997). Induction of Leaf Primordia by the Cell Wall Protein Expansin. Science *276*, 1415-1418.

Frigerio, G., Burri, M., Bopp, D., Baumgartner, S., and Noll, M. (1986). Structure of the segmentation gene paired and the Drosophila PRD gene set as part of a gene network. Cell *47*, 735-746.

Friml, J., Benkova, E., Blilou, I., Wisniewska, J., Hamann, T., Ljung, K., Woody, S., Sandberg, G., Scheres, B., Jurgens, G., *et al*. (2002a). AtPIN4 mediates sink-driven auxin gradients and root patterning in Arabidopsis. Cell *108*, 661-673.

Friml, J., Vieten, A., Sauer, M., Weijers, D., Schwarz, H., Hamann, T., Offringa, R., and Jurgens, G. (2003). Efflux-dependent auxin gradients establish the apical-basal axis of Arabidopsis. Nature *426*, 147-153.

Friml, J., Wisniewska, J., Benkova, E., Mendgen, K., and Palme, K. (2002b). Lateral relocation of auxin efflux regulator PIN3 mediates tropism in Arabidopsis. Nature *415*, 806-809.

Fry, S.C., York, W.S., Albersheim, P., Darvill, A., Hayashi, T., Joseleau, J.-P., Kato, Y., Lorences, E.P., Maclachlan, G.A., McNeil, M., *et al*. (1993). An unambiguous nomenclature for xyloglucan-derived oligosaccharides. Physiologia Plantarum *89*, 1-3.

Fu, Y., Gu, Y., Zheng, Z., Wasteneys, G., and Yang, Z. (2005). Arabidopsis interdigitating cell growth requires two antagonistic pathways with opposing action on cell morphogenesis. Cell *120*, 687-700.

Fu, Y., Xu, T., Zhu, L., Wen, M., and Yang, Z. (2009). A ROP GTPase signaling pathway controls cortical microtubule ordering and cell expansion in Arabidopsis. Curr Biol *19*, 1827-1832.

Fujioka, S., and Yokota, T. (2003). Biosynthesis and metabolism of brassinosteroids. Annu Rev Plant Biol *54*, 137-164.

Fujita, S., Ohnishi, T., Watanabe, B., Yokota, T., Takatsuto, S., Fujioka, S., Yoshida, S., Sakata, K., and Mizutani, M. (2006). Arabidopsis CYP90B1 catalyses the early C-22 hydroxylation of C27, C28 and C29 sterols. Plant J *45*, 765-774.

Furutani, M., Vernoux, T., Traas, J., Kato, T., Tasaka, M., and Aida, M. (2004). PIN-FORMED1 and PINOID regulate boundary formation and cotyledon development in Arabidopsis embryogenesis. Development *131*, 5021-5030.

Gagnot, S., Tamby, J.P., Martin-Magniette, M.L., Bitton, F., Taconnat, L., Balzergue, S., Aubourg, S., Renou, J.P., Lecharny, A., and Brunaud, V. (2008). CATdb: a public access to Arabidopsis transcriptome data from the URGV-CATMA platform. Nucleic Acids Res *36*, D986-990.

Galbiati, F., Sinha Roy, D., Simonini, S., Cucinotta, M., Ceccato, L., Cuesta, C., Simaskova, M., Benkova, E., Kamiuchi, Y., Aida, M., *et al*. (2013). An integrative model of the control of ovule primordia formation. Plant J *76*, 446-455.

Galweiler, L., Guan, C., Muller, A., Wisman, E., Mendgen, K., Yephremov, A., and Palme, K. (1998). Regulation of polar auxin transport by AtPIN1 in Arabidopsis vascular tissue. Science *282*, 2226-2230.

Gampala, S.S., Kim, T.W., He, J.X., Tang, W., Deng, Z., Bai, M.Y., Guan, S., Lalonde, S., Sun, Y., Gendron, J.M., *et al*. (2007). An essential role for 14-3-3 proteins in brassinosteroid signal transduction in Arabidopsis. Dev Cell *13*, 177-189.

Gao, Y., Zhang, Y., Zhang, D., Dai, X., Estelle, M., and Zhao, Y. (2015). Auxin binding protein 1 (ABP1) is not required for either auxin signaling or Arabidopsis development. Proc Natl Acad Sci U S A *112*, 2275-2280.

Gaudinier, A., Zhang, L., Reece-Hoyes, J.S., Taylor-Teeples, M., Pu, L., Liu, Z., Breton, G., Pruneda-Paz, J.L., Kim, D., Kay, S.A., *et al*. (2011). Enhanced Y1H assays for Arabidopsis. Nat Methods *8*, 1053-1055.

Geldner, N., Friml, J., Stierhof, Y.D., Jurgens, G., and Palme, K. (2001). Auxin transport inhibitors block PIN1 cycling and vesicle trafficking. Nature *413*, 425-428.

Gendron, J.M., Liu, J.S., Fan, M., Bai, M.Y., Wenkel, S., Springer, P.S., Barton, M.K., and Wang, Z.Y. (2012). Brassinosteroids regulate organ boundary formation in the shoot apical meristem of Arabidopsis. Proc Natl Acad Sci U S A *109*, 21152-21157.

Gierer, A., and Meinhardt, H. (1972). A theory of biological pattern formation. Kybernetik *12*, 30-39.

Goda, H., Sawa, S., Asami, T., Fujioka, S., Shimada, Y., and Yoshida, S. (2004). Comprehensive comparison of auxin-regulated and brassinosteroid-regulated genes in Arabidopsis. Plant Physiol *134*, 1555-1573.

Goda, H., Shimada, Y., Asami, T., Fujioka, S., and Yoshida, S. (2002). Microarray analysis of brassinosteroid-regulated genes in Arabidopsis. Plant Physiol *130*, 1319-1334.

Goldsmith, M.H.M. (1977). The Polar Transport of Auxin. Annual Review of Plant Physiology *28*, 439-478.

Gordon, S.P., Chickarmane, V.S., Ohno, C., and Meyerowitz, E.M. (2009). Multiple feedback loops through cytokinin signaling control stem cell number within the Arabidopsis shoot meristem. Proc Natl Acad Sci U S A *106*, 16529-16534.

Grandjean, O., Vernoux, T., Laufs, P., Belcram, K., Mizukami, Y., and Traas, J. (2004). In vivo analysis of cell division, cell growth, and differentiation at the shoot apical meristem in Arabidopsis. Plant Cell *16*, 74-87.

Green, J.B., and Sharpe, J. (2015). Positional information and reaction-diffusion: two big ideas in developmental biology combine. Development *142*, 1203-1211.

Green, P.B. (1962). Mechanism for Plant Cellular Morphogenesis. Science *138*, 1404-1405.

Green, P.B., Erickson, R.O., and Richmond, P.A. (1970). ON THE PHYSICAL BASIS OF CELL MORPHOGENESIS*. Annals of the New York Academy of Sciences *175*, 712-731.

Gruel, J., Landrein, B., Tarr, P., Schuster, C., Refahi, Y., Sampathkumar, A., Hamant, O., Meyerowitz, E.M., and Jonsson, H. (2016). An epidermis-driven mechanism positions and scales stem cell niches in plants. Sci Adv *2*, e1500989.

Gu, Y., Kaplinsky, N., Bringmann, M., Cobb, A., Carroll, A., Sampathkumar, A., Baskin, T.I., Persson, S., and Somerville, C.R. (2010). Identification of a cellulose synthase-associated protein required for cellulose biosynthesis. Proc Natl Acad Sci U S A *107*, 12866-12871.

Guilfoyle, T.J., and Hagen, G. (2007). Auxin response factors. Curr Opin Plant Biol *10*, 453-460.

Guo, H., Li, L., Aluru, M., Aluru, S., and Yin, Y. (2013). Mechanisms and networks for brassinosteroid regulated gene expression. Curr Opin Plant Biol *16*, 545-553.

Gutierrez, R., Lindeboom, J.J., Paredez, A.R., Emons, A.M., and Ehrhardt, D.W. (2009). Arabidopsis cortical microtubules position cellulose synthase delivery to the plasma membrane and interact with cellulose synthase trafficking compartments. Nat Cell Biol *11*, 797-806.

Hacham, Y., Sela, A., Friedlander, L., and Savaldi-Goldstein, S. (2012). BRI1 activity in the root meristem involves post-transcriptional regulation of PIN auxin efflux carriers. Plant Signal Behav *7*, 68-70.

Haecker, A., Gross-Hardt, R., Geiges, B., Sarkar, A., Breuninger, H., Herrmann, M., and Laux, T. (2004). Expression dynamics of WOX genes mark cell fate decisions during early embryonic patterning in Arabidopsis thaliana. Development *131*, 657-668.

Hamant, O., Heisler, M.G., Jonsson, H., Krupinski, P., Uyttewaal, M., Bokov, P., Corson, F., Sahlin, P., Boudaoud, A., Meyerowitz, E.M., *et al.* (2008). Developmental patterning by mechanical signals in Arabidopsis. Science *322*, 1650-1655.

Hamilton, E.S., Schlegel, A.M., and Haswell, E.S. (2015). United in diversity: mechanosensitive ion channels in plants. Annu Rev Plant Biol *66*, 113-137.

Han, H., and Krizek, B.A. (2016). AINTEGUMENTA-LIKE6 can functionally replace AINTEGUMENTA but alters Arabidopsis flower development when misexpressed at high levels. Plant Mol Biol *92*, 597-612.

Hardtke, C.S. (2007). Transcriptional auxin-brassinosteroid crosstalk: who's talking? Bioessays *29*, 1115-1123.

Hardtke, C.S., and Berleth, T. (1998). The Arabidopsis gene MONOPTEROS encodes a transcription factor mediating embryo axis formation and vascular development. EMBO J *17*, 1405-1411.

Hardtke, C.S., Dorcey, E., Osmont, K.S., and Sibout, R. (2007). Phytohormone collaboration: zooming in on auxin-brassinosteroid interactions. Trends Cell Biol *17*, 485-492.

Haughn, G.W., and Somerville, C.R. (1988). Genetic control of morphogenesis in Arabidopsis. Developmental Genetics *9*, 73-89.

Hay, A., and Tsiantis, M. (2010). KNOX genes: versatile regulators of plant development and diversity. Development *137*, 3153-3165.

He, J.X., Gendron, J.M., Sun, Y., Gampala, S.S., Gendron, N., Sun, C.Q., and Wang, Z.Y. (2005). BZR1 is a transcriptional repressor with dual roles in brassinosteroid homeostasis and growth responses. Science *307*, 1634-1638.

Heisler, M.G., Ohno, C., Das, P., Sieber, P., Reddy, G.V., Long, J.A., and Meyerowitz, E.M. (2005). Patterns of auxin transport and gene expression during primordium development revealed by live imaging of the Arabidopsis inflorescence meristem. Curr Biol *15*, 1899-1911.

Hematy, K., Sado, P.E., Van Tuinen, A., Rochange, S., Desnos, T., Balzergue, S., Pelletier, S., Renou, J.P., and Hofte, H. (2007). A receptor-like kinase mediates the response of Arabidopsis cells to the inhibition of cellulose synthesis. Curr Biol *17*, 922-931.

Hempel, F.D., Weigel, D., Mandel, M.A., Ditta, G., Zambryski, P.C., Feldman, L.J., and Yanofsky, M.F. (1997). Floral determination and expression of floral regulatory genes in Arabidopsis. Development *124*, 3845-3853.

Hernandez-Hernandez, V., Niklas, K.J., Newman, S.A., and Benitez, M. (2012). Dynamical patterning modules in plant development and evolution. Int J Dev Biol *56*, 661-674.

Hervieux, N., Dumond, M., Sapala, A., Routier-Kierzkowska, A.L., Kierzkowski, D., Roeder, A.H., Smith, R.S., Boudaoud, A., and Hamant, O. (2016). A Mechanical Feedback Restricts Sepal Growth and Shape in Arabidopsis. Curr Biol.

Hesse, T., Feldwisch, J., Balshusemann, D., Bauw, G., Puype, M., Vandekerckhove, J., Lobler, M., Klambt, D., Schell, J., and Palme, K. (1989). Molecular cloning and structural analysis of a gene from Zea mays (L.) coding for a putative receptor for the plant hormone auxin. EMBO J *8*, 2453-2461.

Heyl, A., Riefler, M., Romanov, G.A., and Schmulling, T. (2012). Properties, functions and evolution of cytokinin receptors. Eur J Cell Biol *91*, 246-256.

Hibara, K., Karim, M.R., Takada, S., Taoka, K., Furutani, M., Aida, M., and Tasaka, M. (2006). Arabidopsis CUP-SHAPED COTYLEDON3 regulates postembryonic shoot meristem and organ boundary formation. Plant Cell *18*, 2946-2957.

Honma, T., and Goto, K. (2001). Complexes of MADS-box proteins are sufficient to convert leaves into floral organs. Nature *409*, 525-529.

Huang, F., Zago, M.K., Abas, L., van Marion, A., Galvan-Ampudia, C.S., and Offringa, R. (2010). Phosphorylation of conserved PIN motifs directs Arabidopsis PIN1 polarity and auxin transport. Plant Cell *22*, 1129-1142.

Huang, H.Y., Jiang, W.B., Hu, Y.W., Wu, P., Zhu, J.Y., Liang, W.Q., Wang, Z.Y., and Lin, W.H. (2013). BR signal influences Arabidopsis ovule and seed number through regulating related genes expression by BZR1. Mol Plant *6*, 456-469.

Hulskamp, M. (2004). Plant trichomes: a model for cell differentiation. Nat Rev Mol Cell Biol *5*, 471-480.

Husbands, A.Y., Benkovics, A.H., Nogueira, F.T., Lodha, M., and Timmermans, M.C. (2015). The ASYMMETRIC LEAVES Complex Employs Multiple Modes of Regulation to Affect Adaxial-Abaxial Patterning and Leaf Complexity. Plant Cell *27*, 3321-3335.

Husbands, A.Y., Chitwood, D.H., Plavskin, Y., and Timmermans, M.C. (2009). Signals and prepatterns: new insights into organ polarity in plants. Genes Dev *23*, 1986-1997.

Ivakov, A., and Persson, S. (2013). Plant cell shape: modulators and measurements. Front Plant Sci *4*, 439.

Jackson, D., Veit, B., and Hake, S. (1994). Expression of maize KNOTTED1 related homeobox genes in the shoot apical meristem predicts patterns of morphogenesis in the vegetative shoot. Development *120*, 405-413.

Jaillais, Y., Hothorn, M., Belkhadir, Y., Dabi, T., Nimchuk, Z.L., Meyerowitz, E.M., and Chory, J. (2011). Tyrosine phosphorylation controls brassinosteroid receptor activation by triggering membrane release of its kinase inhibitor. Genes Dev *25*, 232-237.

Jasinski, S., Piazza, P., Craft, J., Hay, A., Woolley, L., Rieu, I., Phillips, A., Hedden, P., and Tsiantis, M. (2005). KNOX action in Arabidopsis is mediated by coordinate regulation of cytokinin and gibberellin activities. Curr Biol *15*, 1560-1565.

Jeong, S., Trotochaud, A.E., and Clark, S.E. (1999). The Arabidopsis CLAVATA2 gene encodes a receptor-like protein required for the stability of the CLAVATA1 receptor-like kinase. Plant Cell *11*, 1925-1934.

Jonsson, H., Heisler, M.G., Shapiro, B.E., Meyerowitz, E.M., and Mjolsness, E. (2006). An auxin-driven polarized transport model for phyllotaxis. Proc Natl Acad Sci U S A *103*, 1633-1638.

Kakimoto, T. (2001). Identification of plant cytokinin biosynthetic enzymes as dimethylallyl diphosphate:ATP/ADP isopentenyltransferases. Plant Cell Physiol *42*, 677-685.

Ke, J., Ma, H., Gu, X., Thelen, A., Brunzelle, J.S., Li, J., Xu, H.E., and Melcher, K. (2015). Structural basis for recognition of diverse transcriptional repressors by the TOPLESS family of corepressors. Sci Adv *1*, e1500107.

Kempin, S.A., Savidge, B., and Yanofsky, M.F. (1995). Molecular basis of the cauliflower phenotype in Arabidopsis. Science *267*, 522-525.

Kende, H., Bradford, K., Brummell, D., Cho, H.T., Cosgrove, D., Fleming, A., Gehring, C., Lee, Y., McQueen-Mason, S., Rose, J., *et al*. (2004). Nomenclature for members of the expansin superfamily of genes and proteins. Plant Mol Biol *55*, 311-314.

Kepinski, S., and Leyser, O. (2005). The Arabidopsis F-box protein TIR1 is an auxin receptor. Nature *435*, 446-451.

Kiba, T., Aoki, K., Sakakibara, H., and Mizuno, T. (2004). Arabidopsis response regulator, ARR22, ectopic expression of which results in phenotypes similar to the wol cytokinin-receptor mutant. Plant Cell Physiol *45*, 1063-1077.

Kiba, T., Taniguchi, M., Imamura, A., Ueguchi, C., Mizuno, T., and Sugiyama, T. (1999). Differential expression of genes for response regulators in response to cytokinins and nitrate in Arabidopsis thaliana. Plant Cell Physiol *40*, 767-771.

Kicheva, A., and Briscoe, J. (2010). Limbs made to measure. PLoS Biol *8*, e1000421.

Kierzkowski, D., Nakayama, N., Routier-Kierzkowska, A.L., Weber, A., Bayer, E., Schorderet, M., Reinhardt, D., Kuhlemeier, C., and Smith, R.S. (2012). Elastic domains regulate growth and organogenesis in the plant shoot apical meristem. Science *335*, 1096-1099.

Kim, D., Kim, Y.S., and Jung, J. (1997). Involvement of soluble proteinous factors in auxin-induced modulation of P-type ATPase in rice (Oryza sativa L.) seedlings. FEBS Lett *409*, 273-276.

Kim, H.B., Kwon, M., Ryu, H., Fujioka, S., Takatsuto, S., Yoshida, S., An, C.S., Lee, I., Hwang, I., and Choe, S. (2006). The regulation of DWARF4 expression is likely a critical mechanism in maintaining the homeostasis of bioactive brassinosteroids in Arabidopsis. Plant Physiol *140*, 548-557.

Kim, T.W., Guan, S., Burlingame, A.L., and Wang, Z.Y. (2011). The CDG1 kinase mediates brassinosteroid signal transduction from BRI1 receptor kinase to BSU1 phosphatase and GSK3-like kinase BIN2. Mol Cell *43*, 561-571.

Kim, T.W., Guan, S., Sun, Y., Deng, Z., Tang, W., Shang, J.X., Sun, Y., Burlingame, A.L., and Wang, Z.Y. (2009). Brassinosteroid signal transduction from cell-surface receptor kinases to nuclear transcription factors. Nat Cell Biol *11*, 1254-1260.

Kim, T.W., Lee, S.M., Joo, S.H., Yun, H.S., Lee, Y., Kaufman, P.B., Kirakosyan, A., Kim, S.H., Nam, K.H., Lee, J.S., *et al*. (2007). Elongation and gravitropic responses of Arabidopsis roots are regulated by brassinolide and IAA. Plant Cell Environ *30*, 679-689.

Kim, T.W., and Wang, Z.Y. (2010). Brassinosteroid signal transduction from receptor kinases to transcription factors. Annu Rev Plant Biol *61*, 681-704.

Kinoshita, T., Cano-Delgado, A., Seto, H., Hiranuma, S., Fujioka, S., Yoshida, S., and Chory, J. (2005). Binding of brassinosteroids to the extracellular domain of plant receptor kinase BRI1. Nature *433*, 167-171.

Kleine-Vehn, J., Dhonukshe, P., Sauer, M., Brewer, P.B., Wisniewska, J., Paciorek, T., Benkova, E., and Friml, J. (2008). ARF GEF-dependent transcytosis and polar delivery of PIN auxin carriers in Arabidopsis. Curr Biol *18*, 526-531.

Kleine-Vehn, J., Wabnik, K., Martiniere, A., Langowski, L., Willig, K., Naramoto, S., Leitner, J., Tanaka, H., Jakobs, S., Robert, S., *et al*. (2011). Recycling, clustering, and endocytosis jointly maintain PIN auxin carrier polarity at the plasma membrane. Mol Syst Biol *7*, 540.

Knauer, S., Holt, A.L., Rubio-Somoza, I., Tucker, E.J., Hinze, A., Pisch, M., Javelle, M., Timmermans, M.C., Tucker, M.R., and Laux, T. (2013). A protodermal miR394 signal defines a region of stem cell competence in the Arabidopsis shoot meristem. Dev Cell *24*, 125-132.

Kohorn, B.D., Johansen, S., Shishido, A., Todorova, T., Martinez, R., Defeo, E., and Obregon, P. (2009). Pectin activation of MAP kinase and gene expression is WAK2 dependent. Plant J *60*, 974-982.

Kohorn, B.D., and Kohorn, S.L. (2012). The cell wall-associated kinases, WAKs, as pectin receptors. Front Plant Sci *3*, 88.

Kondo, S., Iwashita, M., and Yamaguchi, M. (2009). How animals get their skin patterns: fish pigment pattern as a live Turing wave. Int J Dev Biol *53*, 851-856.

Kondo, S., and Miura, T. (2010). Reaction-diffusion model as a framework for understanding biological pattern formation. Science *329*, 1616-1620.

Krecek, P., Skupa, P., Libus, J., Naramoto, S., Tejos, R., Friml, J., and Zazimalova, E. (2009). The PIN-FORMED (PIN) protein family of auxin transporters. Genome Biol *10*, 249.

Krizek, B. (2009). AINTEGUMENTA and AINTEGUMENTA-LIKE6 act redundantly to regulate Arabidopsis floral growth and patterning. Plant Physiol *150*, 1916-1929.

Krizek, B.A. (1999). Ectopic expression of AINTEGUMENTA in Arabidopsis plants results in increased growth of floral organs. Dev Genet *25*, 224-236.

Krizek, B.A. (2015). AINTEGUMENTA-LIKE genes have partly overlapping functions with AINTEGUMENTA but make distinct contributions to Arabidopsis thaliana flower development. J Exp Bot *66*, 4537-4549.

Krizek, B.A., Bequette, C.J., Xu, K., Blakley, I.C., Fu, Z.Q., Stratmann, J.W., and Loraine, A.E. (2016). RNA-Seq Links the Transcription Factors AINTEGUMENTA and AINTEGUMENTA-LIKE6 to Cell Wall Remodeling and Plant Defense Pathways. Plant Physiol *171*, 2069-2084.

Kuhlemeier, C. (2017). Phyllotaxis. Curr Biol *27*, R882-R887.

Kuhlemeier, C., and Timmermans, M.C. (2016). The Sussex signal: insights into leaf dorsiventrality. Development *143*, 3230-3237.

Kurakawa, T., Ueda, N., Maekawa, M., Kobayashi, K., Kojima, M., Nagato, Y., Sakakibara, H., and Kyozuka, J. (2007). Direct control of shoot meristem activity by a cytokinin-activating enzyme. Nature *445*, 652-655.

Kuroha, T., Tokunaga, H., Kojima, M., Ueda, N., Ishida, T., Nagawa, S., Fukuda, H., Sugimoto, K., and Sakakibara, H. (2009). Functional analyses of LONELY GUY cytokinin-activating enzymes reveal the importance of the direct activation pathway in Arabidopsis. Plant Cell *21*, 3152-3169.

Kwiatkowska, D. (2004). Surface growth at the reproductive shoot apex of Arabidopsis thaliana pin-formed 1 and wild type. J Exp Bot *55*, 1021-1032.

Kwiatkowska, D. (2006). Flower primordium formation at the Arabidopsis shoot apex: quantitative analysis of surface geometry and growth. J Exp Bot *57*, 571-580.

Kwiatkowska, D., and Dumais, J. (2003). Growth and morphogenesis at the vegetative shoot apex of Anagallis arvensis L. J Exp Bot *54*, 1585-1595.

Landrein, B., and Hamant, O. (2013). How mechanical stress controls microtubule behavior and morphogenesis in plants: history, experiments and revisited theories. Plant J *75*, 324-338.

Landrein, B., and Vernoux, T. (2014). Auxin, Chief Architect of the Shoot Apex. In Auxin and Its Role in Plant Development, E. Zažímalová, J. Petrášek, and E. Benková, eds. (Vienna: Springer Vienna), pp. 191-212.

Lau, S., Slane, D., Herud, O., Kong, J., and Jurgens, G. (2012). Early embryogenesis in flowering plants: setting up the basic body pattern. Annu Rev Plant Biol *63*, 483-506.

Laux, T., Mayer, K.F., Berger, J., and Jurgens, G. (1996). The WUSCHEL gene is required for shoot and floral meristem integrity in Arabidopsis. Development *122*, 87-96.

Lazzaro, M.D., Donohue, J.M., and Soodavar, F.M. (2003). Disruption of cellulose synthesis by isoxaben causes tip swelling and disorganizes cortical microtubules in elongating conifer pollen tubes. Protoplasma *220*, 201-207.

Leibfried, A., To, J.P., Busch, W., Stehling, S., Kehle, A., Demar, M., Kieber, J.J., and Lohmann, J.U. (2005). WUSCHEL controls meristem function by direct regulation of cytokinin-inducible response regulators. Nature *438*, 1172-1175.

Leitner, J., Retzer, K., Korbei, B., and Luschnig, C. (2012). Dynamics in PIN2 auxin carrier ubiquitylation in gravity-responding Arabidopsis roots. Plant Signal Behav *7*, 1271-1273.

Lenhard, M., Jurgens, G., and Laux, T. (2002). The WUSCHEL and SHOOTMERISTEMLESS genes fulfil complementary roles in Arabidopsis shoot meristem regulation. Development *129*, 3195-3206.

Levesque-Tremblay, G., Pelloux, J., Braybrook, S.A., and Muller, K. (2015). Tuning of pectin methylesterification: consequences for cell wall biomechanics and development. Planta *242*, 791-811.

Levy, S., York, W.S., Stuike-Prill, R., Meyer, B., and Staehelin, L.A. (1991). Simulations of the static and dynamic molecular conformations of xyloglucan. The role of the fucosylated sidechain in surface-specific sidechain folding. Plant J *1*, 195-215.

Li, J., and Chory, J. (1997). A putative leucine-rich repeat receptor kinase involved in brassinosteroid signal transduction. Cell *90*, 929-938.

Li, J., Nagpal, P., Vitart, V., McMorris, T.C., and Chory, J. (1996). A role for brassinosteroids in light-dependent development of Arabidopsis. Science *272*, 398-401.

Li, L., Ye, H., Guo, H., and Yin, Y. (2010). Arabidopsis IWS1 interacts with transcription factor BES1 and is involved in plant steroid hormone brassinosteroid regulated gene expression. Proc Natl Acad Sci U S A *107*, 3918-3923.

Li, S., Lei, L., Somerville, C.R., and Gu, Y. (2012). Cellulose synthase interactive protein 1 (CSI1) links microtubules and cellulose synthase complexes. Proc Natl Acad Sci U S A *109*, 185-190.

Li, W., Zhou, Y., Liu, X., Yu, P., Cohen, J.D., and Meyerowitz, E.M. (2013). LEAFY controls auxin response pathways in floral primordium formation. Sci Signal *6*, ra23.

Lin, D., Cao, L., Zhou, Z., Zhu, L., Ehrhardt, D., Yang, Z., and Fu, Y. (2013). Rho GTPase signaling activates microtubule severing to promote microtubule ordering in Arabidopsis. Curr Biol *23*, 290-297.

Lin, D., Nagawa, S., Chen, J., Cao, L., Chen, X., Xu, T., Li, H., Dhonukshe, P., Yamamuro, C., Friml, J., *et al*. (2012). A ROP GTPase-dependent auxin signaling pathway regulates the subcellular distribution of PIN2 in Arabidopsis roots. Curr Biol *22*, 1319-1325.

Lin, W.C., Shuai, B., and Springer, P.S. (2003). The Arabidopsis LATERAL ORGAN BOUNDARIES-domain gene ASYMMETRIC LEAVES2 functions in the repression of KNOX gene expression and in adaxial-abaxial patterning. Plant Cell *15*, 2241-2252.

Liu, C., Thong, Z., and Yu, H. (2009a). Coming into bloom: the specification of floral meristems. Development *136*, 3379-3391.

Liu, J., Mehdi, S., Topping, J., Friml, J., and Lindsey, K. (2013). Interaction of PLS and PIN and hormonal crosstalk in Arabidopsis root development. Front Plant Sci *4*, 75.

Liu, Q., Kasuga, M., Sakuma, Y., Abe, H., Miura, S., Yamaguchi-Shinozaki, K., and Shinozaki, K. (1998). Two transcription factors, DREB1 and DREB2, with an EREBP/AP2 DNA binding domain separate two cellular signal transduction pathways in drought- and low-temperature-responsive gene expression, respectively, in Arabidopsis. Plant Cell *10*, 1391-1406.

Liu, Q., Yao, X., Pi, L., Wang, H., Cui, X., and Huang, H. (2009b). The ARGONAUTE10 gene modulates shoot apical meristem maintenance and establishment of leaf polarity by repressing miR165/166 in Arabidopsis. Plant J *58*, 27-40.

Lodha, M., Marco, C.F., and Timmermans, M.C. (2013). The ASYMMETRIC LEAVES complex maintains repression of KNOX homeobox genes via direct recruitment of Polycomb-repressive complex2. Genes Dev *27*, 596-601.

Long, J., and Barton, M.K. (2000). Initiation of axillary and floral meristems in Arabidopsis. Dev Biol *218*, 341-353.

Long, J.A., Moan, E.I., Medford, J.I., and Barton, M.K. (1996). A member of the KNOTTED class of homeodomain proteins encoded by the STM gene of Arabidopsis. Nature *379*, 66-69.

Long, J.A., Ohno, C., Smith, Z.R., and Meyerowitz, E.M. (2006). TOPLESS regulates apical embryonic fate in Arabidopsis. Science *312*, 1520-1523.

Madson, M., Dunand, C., Li, X., Verma, R., Vanzin, G.F., Caplan, J., Shoue, D.A., Carpita, N.C., and Reiter, W.D. (2003). The MUR3 gene of Arabidopsis encodes a xyloglucan galactosyltransferase that is evolutionarily related to animal exostosins. Plant Cell *15*, 1662-1670.

Mahonen, A.P., Bishopp, A., Higuchi, M., Nieminen, K.M., Kinoshita, K., Tormakangas, K., Ikeda, Y., Oka, A., Kakimoto, T., and Helariutta, Y. (2006). Cytokinin signaling and its inhibitor AHP6 regulate cell fate during vascular development. Science *311*, 94-98.

Mantegazza, O., Gregis, V., Chiara, M., Selva, C., Leo, G., Horner, D.S., and Kater, M.M. (2014). Gene coexpression patterns during early development of the native Arabidopsis reproductive meristem: novel candidate developmental regulators and patterns of functional redundancy. Plant J *79*, 861-877.

Marc, J., Granger, C.L., Brincat, J., Fisher, D.D., Kao, T., McCubbin, A.G., and Cyr, R.J. (1998). A GFP-MAP4 reporter gene for visualizing cortical microtubule rearrangements in living epidermal cells. Plant Cell *10*, 1927-1940.

Marhavy, P., Bielach, A., Abas, L., Abuzeineh, A., Duclercq, J., Tanaka, H., Parezova, M., Petrasek, J., Friml, J., Kleine-Vehn, J.*, et al.* (2011). Cytokinin modulates endocytic trafficking of PIN1 auxin efflux carrier to control plant organogenesis. Dev Cell *21*, 796-804.

Mason, M.G., Li, J., Mathews, D.E., Kieber, J.J., and Schaller, G.E. (2004). Type-B response regulators display overlapping expression patterns in Arabidopsis. Plant Physiol *135*, 927-937.

Matheson, L.A., Hanton, S.L., and Brandizzi, F. (2006). Traffic between the plant endoplasmic reticulum and Golgi apparatus: to the Golgi and beyond. Curr Opin Plant Biol *9*, 601-609.

Mathur, J., Molnar, G., Fujioka, S., Takatsuto, S., Sakurai, A., Yokota, T., Adam, G., Voigt, B., Nagy, F., Maas, C., *et al*. (1998). Transcription of the Arabidopsis CPD gene, encoding a steroidogenic cytochrome P450, is negatively controlled by brassinosteroids. Plant J *14*, 593-602.

Mayer, K.F., Schoof, H., Haecker, A., Lenhard, M., Jurgens, G., and Laux, T. (1998). Role of WUSCHEL in regulating stem cell fate in the Arabidopsis shoot meristem. Cell *95*, 805-815.

McClung, C.E. (1942). Growth and Form. Science *96*, 471-473.

McConnell, J.R., Emery, J., Eshed, Y., Bao, N., Bowman, J., and Barton, M.K. (2001). Role of PHABULOSA and PHAVOLUTA in determining radial patterning in shoots. Nature *411*, 709-713.

McQueen-Mason, S., Durachko, D.M., and Cosgrove, D.J. (1992). Two endogenous proteins that induce cell wall extension in plants. Plant Cell *4*, 1425-1433.

McQueen-Mason, S.J., and Cosgrove, D.J. (1995). Expansin mode of action on cell walls. Analysis of wall hydrolysis, stress relaxation, and binding. Plant Physiol *107*, 87-100.

Meinhardt, H. (1994). Models of pattern formation and their application to plant development In Positional Controls in Plant Development, P.W. Barlow, and D.J. Carr, eds. (UK: Cambridge University Press), pp. 1-32.

Meinhardt, H. (1996). Models of biological pattern formation: common mechanism in plant and animal development. Int J Dev Biol *40*, 123-134.

Meinhardt, H. (2003). Complex pattern formation by a self-destabilization of established patterns: chemotactic orientation and phyllotaxis as examples. C R Biol *326*, 223-237.

Meinhardt, H., and Gierer, A. (2000). Pattern formation by local self-activation and lateral inhibition. Bioessays *22*, 753-760.

Merks, R.M., Van de Peer, Y., Inze, D., and Beemster, G.T. (2007). Canalization without flux sensors: a traveling-wave hypothesis. Trends Plant Sci *12*, 384-390.

Michalko, J., Dravecka, M., Bollenbach, T., and Friml, J. (2015). Embryo-lethal phenotypes in early abp1 mutants are due to disruption of the neighboring BSM gene. F1000Res *4*, 1104.

Michalko, J., Glanc, M., Perrot-Rechenmann, C., and Friml, J. (2016). Strong morphological defects in conditional Arabidopsis abp1 knock-down mutants generated in absence of functional ABP1 protein. F1000Res *5*, 86.

Michniewicz, M., Zago, M.K., Abas, L., Weijers, D., Schweighofer, A., Meskiene, I., Heisler, M.G., Ohno, C., Zhang, J., Huang, F., *et al*. (2007). Antagonistic regulation of PIN phosphorylation by PP2A and PINOID directs auxin flux. Cell *130*, 1044-1056.

Milani, P., Gholamirad, M., Traas, J., Arneodo, A., Boudaoud, A., Argoul, F., and Hamant, O. (2011). In vivo analysis of local wall stiffness at the shoot apical meristem in Arabidopsis using atomic force microscopy. Plant J *67*, 1116-1123.

Mizukami, Y., and Fischer, R.L. (2000). Plant organ size control: AINTEGUMENTA regulates growth and cell numbers during organogenesis. Proc Natl Acad Sci U S A *97*, 942-947.

Mohnen, D. (2008). Pectin structure and biosynthesis. Curr Opin Plant Biol *11*, 266-277.

Mok, D.W., and Mok, M.C. (2001). Cytokinin Metabolism and Action. Annu Rev Plant Physiol Plant Mol Biol *52*, 89-118.

Moller, B.K., Ten Hove, C.A., Xiang, D., Williams, N., Lopez, L.G., Yoshida, S., Smit, M., Datla, R., and Weijers, D. (2017). Auxin response cell-autonomously controls ground tissue initiation in the early Arabidopsis embryo. Proc Natl Acad Sci U S A *114*, E2533-E2539.

Mouchel, C.F., Osmont, K.S., and Hardtke, C.S. (2006). BRX mediates feedback between brassinosteroid levels and auxin signalling in root growth. Nature *443*, 458-461.

Mravec, J., Skupa, P., Bailly, A., Hoyerova, K., Krecek, P., Bielach, A., Petrasek, J., Zhang, J., Gaykova, V., Stierhof, Y.D., *et al*. (2009). Subcellular homeostasis of phytohormone auxin is mediated by the ER-localized PIN5 transporter. Nature *459*, 1136-1140.

Muller, B., and Sheen, J. (2007). Advances in cytokinin signaling. Science *318*, 68-69.

Muller, B., and Sheen, J. (2008). Cytokinin and auxin interaction in root stem-cell specification during early embryogenesis. Nature *453*, 1094-1097.

Muller, R., Bleckmann, A., and Simon, R. (2008). The receptor kinase CORYNE of Arabidopsis transmits the stem cell-limiting signal CLAVATA3 independently of CLAVATA1. Plant Cell *20*, 934-946.

Mundy, J., Nielsen, H.B., and Brodersen, P. (2006). Crosstalk. Trends Plant Sci *11*, 63-64.

Murray, J.A., Jones, A., Godin, C., and Traas, J. (2012). Systems analysis of shoot apical meristem growth and development: integrating hormonal and mechanical signaling. Plant Cell *24*, 3907-3919.

Mussig, C., Fischer, S., and Altmann, T. (2002). Brassinosteroid-regulated gene expression. Plant Physiol *129*, 1241-1251.

Mutwil, M., Debolt, S., and Persson, S. (2008). Cellulose synthesis: a complex complex. Curr Opin Plant Biol *11*, 252-257.

Nagawa, S., Xu, T., Lin, D., Dhonukshe, P., Zhang, X., Friml, J., Scheres, B., Fu, Y., and Yang, Z. (2012). ROP GTPase-dependent actin microfilaments promote PIN1 polarization by localized inhibition of clathrin-dependent endocytosis. PLoS Biol *10*, e1001299.

Nakamura, A., Fujioka, S., Sunohara, H., Kamiya, N., Hong, Z., Inukai, Y., Miura, K., Takatsuto, S., Yoshida, S., Ueguchi-Tanaka, M., *et al*. (2006a). The role of OsBRI1 and its homologous genes, OsBRL1 and OsBRL3, in rice. Plant Physiol *140*, 580-590.

Nakamura, A., Goda, H., Shimada, Y., and Yoshida, S. (2004). Brassinosteroid selectively regulates PIN gene expression in Arabidopsis. Biosci Biotechnol Biochem *68*, 952-954.

Nakamura, A., Nakajima, N., Goda, H., Shimada, Y., Hayashi, K., Nozaki, H., Asami, T., Yoshida, S., and Fujioka, S. (2006b). Arabidopsis Aux/IAA genes are involved in brassinosteroid-mediated growth responses in a manner dependent on organ type. Plant J *45*, 193-205.

Nakashima, K., Shinwari, Z.K., Sakuma, Y., Seki, M., Miura, S., Shinozaki, K., and Yamaguchi-Shinozaki, K. (2000). Organization and expression of two Arabidopsis DREB2 genes encoding DRE-binding proteins involved in dehydration- and high-salinity-responsive gene expression. Plant Mol Biol *42*, 657-665.

Nakaya, M., Tsukaya, H., Murakami, N., and Kato, M. (2002). Brassinosteroids control the proliferation of leaf cells of Arabidopsis thaliana. Plant Cell Physiol *43*, 239-244.

Nam, K.H., and Li, J. (2002). BRI1/BAK1, a receptor kinase pair mediating brassinosteroid signaling. Cell *110*, 203-212.

Nemhauser, J.L., Hong, F., and Chory, J. (2006). Different plant hormones regulate similar processes through largely nonoverlapping transcriptional responses. Cell *126*, 467-475.

Nemhauser, J.L., Mockler, T.C., and Chory, J. (2004). Interdependency of brassinosteroid and auxin signaling in Arabidopsis. PLoS Biol *2*, E258.

Newman, S.A., and Frisch, H.L. (1979). Dynamics of skeletal pattern formation in developing chick limb. Science *205*, 662-668.

Nick, P., Bergfeld, R., Schafer, E., and Schopfer, P. (1990). Unilateral reorientation of microtubules at the outer epidermal wall during photo- and gravitropic curvature of maize coleoptiles and sunflower hypocotyls. Planta *181*, 162-168.

Niklas, K. (2000). The Evolution of Plant Body Plans—A Biomechanical Perspective. Annals of Botany *85*, 411-438.

Niklas, K., and Kutschera, U. (2009). The evolutionary development of plant body plans. Functional Plant Biology *36*, 682-695.

Nisar, N., Cuttriss, A.J., Pogson, B.J., and Cazzonelli, C.I. (2014). The promoter of the Arabidopsis PIN6 auxin transporter enabled strong expression in the vasculature of roots, leaves, floral stems and reproductive organs. Plant Signal Behav *9*, e27898.

Noguchi, T., Fujioka, S., Choe, S., Takatsuto, S., Yoshida, S., Yuan, H., Feldmann, K.A., and Tax, F.E. (1999). Brassinosteroid-insensitive dwarf mutants of Arabidopsis accumulate brassinosteroids. Plant Physiol *121*, 743-752.

Nordstrom, A., Tarkowski, P., Tarkowska, D., Norbaek, R., Astot, C., Dolezal, K., and Sandberg, G. (2004). Auxin regulation of cytokinin biosynthesis in Arabidopsis thaliana: a factor of potential importance for auxin-cytokinin-regulated development. Proc Natl Acad Sci U S A *101*, 8039-8044.

O'Maoileidigh, D.S., Graciet, E., and Wellmer, F. (2014). Gene networks controlling Arabidopsis thaliana flower development. New Phytol *201*, 16-30.

Odat, O., Gardiner, J., Sawchuk, M.G., Verna, C., Donner, T.J., and Scarpella, E. (2014). Characterization of an allelic series in the MONOPTEROS gene of Arabidopsis. Genesis *52*, 127-133.

Ogawa, M., Shinohara, H., Sakagami, Y., and Matsubayashi, Y. (2008). Arabidopsis CLV3 peptide directly binds CLV1 ectodomain. Science *319*, 294.

Ohnishi, T., Godza, B., Watanabe, B., Fujioka, S., Hategan, L., Ide, K., Shibata, K., Yokota, T., Szekeres, M., and Mizutani, M. (2012). CYP90A1/CPD, a brassinosteroid biosynthetic cytochrome P450 of Arabidopsis, catalyzes C-3 oxidation. J Biol Chem *287*, 31551-31560.

Ohnishi, T., Yokota, T., and Mizutani, M. (2009). Insights into the function and evolution of P450s in plant steroid metabolism. Phytochemistry *70*, 1918-1929.

Okada, K., Ueda, J., Komaki, M.K., Bell, C.J., and Shimura, Y. (1991). Requirement of the Auxin Polar Transport System in Early Stages of Arabidopsis Floral Bud Formation. Plant Cell *3*, 677-684.

Paponov, I.A., Teale, W.D., Trebar, M., Blilou, I., and Palme, K. (2005). The PIN auxin efflux facilitators: evolutionary and functional perspectives. Trends Plant Sci *10*, 170-177.

Parcy, F., Nilsson, O., Busch, M.A., Lee, I., and Weigel, D. (1998). A genetic framework for floral patterning. Nature *395*, 561-566.

Paredez, A.R., Somerville, C.R., and Ehrhardt, D.W. (2006). Visualization of cellulose synthase demonstrates functional association with microtubules. Science *312*, 1491-1495.

Park, Y.B., and Cosgrove, D.J. (2012a). Changes in cell wall biomechanical properties in the xyloglucan-deficient xxt1/xxt2 mutant of Arabidopsis. Plant Physiol *158*, 465-475.

Park, Y.B., and Cosgrove, D.J. (2012b). A revised architecture of primary cell walls based on biomechanical changes induced by substrate-specific endoglucanases. Plant Physiol *158*, 1933-1943.

Park, Y.B., and Cosgrove, D.J. (2015). Xyloglucan and its interactions with other components of the growing cell wall. Plant Cell Physiol *56*, 180-194.

Parry, G., Calderon-Villalobos, L.I., Prigge, M., Peret, B., Dharmasiri, S., Itoh, H., Lechner, E., Gray, W.M., Bennett, M., and Estelle, M. (2009). Complex regulation of the TIR1/AFB family of auxin receptors. Proc Natl Acad Sci U S A *106*, 22540-22545.

Peaucelle, A., Braybrook, S.A., Le Guillou, L., Bron, E., Kuhlemeier, C., and Hofte, H. (2011a). Pectin-induced changes in cell wall mechanics underlie organ initiation in Arabidopsis. Curr Biol *21*, 1720-1726.

Peaucelle, A., Louvet, R., Johansen, J.N., Hofte, H., Laufs, P., Pelloux, J., and Mouille, G. (2008). Arabidopsis phyllotaxis is controlled by the methyl-esterification status of cell-wall pectins. Curr Biol *18*, 1943-1948.

Peaucelle, A., Louvet, R., Johansen, J.N., Salsac, F., Morin, H., Fournet, F., Belcram, K., Gillet, F., Hofte, H., Laufs, P., *et al*. (2011b). The transcription factor BELLRINGER modulates phyllotaxis by regulating the expression of a pectin methylesterase in Arabidopsis. Development *138*, 4733-4741.

Peaucelle, A., Wightman, R., and Hofte, H. (2015). The Control of Growth Symmetry Breaking in the Arabidopsis Hypocotyl. Curr Biol *25*, 1746-1752.

Peer, W.A., Blakeslee, J.J., Yang, H., and Murphy, A.S. (2011). Seven things we think we know about auxin transport. Mol Plant *4*, 487-504.

Perrin, R.M., DeRocher, A.E., Bar-Peled, M., Zeng, W., Norambuena, L., Orellana, A., Raikhel, N.V., and Keegstra, K. (1999). Xyloglucan fucosyltransferase, an enzyme involved in plant cell wall biosynthesis. Science *284*, 1976-1979.

Persson, S., Paredez, A., Carroll, A., Palsdottir, H., Doblin, M., Poindexter, P., Khitrov, N., Auer, M., and Somerville, C.R. (2007). Genetic evidence for three unique components in primary cell-wall cellulose synthase complexes in Arabidopsis. Proc Natl Acad Sci U S A *104*, 15566-15571.

Petrasek, J., and Friml, J. (2009). Auxin transport routes in plant development. Development *136*, 2675-2688.

Petrasek, J., Mravec, J., Bouchard, R., Blakeslee, J.J., Abas, M., Seifertova, D., Wisniewska, J., Tadele, Z., Kubes, M., Covanova, M., *et al*. (2006). PIN proteins perform a rate-limiting function in cellular auxin efflux. Science *312*, 914-918.

Pfaffl, M.W. (2001). A new mathematical model for relative quantification in real-time RT-PCR. Nucleic Acids Res *29*, e45.

Pinon, V., Prasad, K., Grigg, S.P., Sanchez-Perez, G.F., and Scheres, B. (2013). Local auxin biosynthesis regulation by PLETHORA transcription factors controls phyllotaxis in Arabidopsis. Proc Natl Acad Sci U S A *110*, 1107-1112.

Prasad, K., Grigg, S.P., Barkoulas, M., Yadav, R.K., Sanchez-Perez, G.F., Pinon, V., Blilou, I., Hofhuis, H., Dhonukshe, P., Galinha, C., *et al*. (2011). Arabidopsis PLETHORA transcription factors control phyllotaxis. Curr Biol *21*, 1123-1128.

Pruneda-Paz, J.L., Breton, G., Nagel, D.H., Kang, S.E., Bonaldi, K., Doherty, C.J., Ravelo, S., Galli, M., Ecker, J.R., and Kay, S.A. (2014). A genome-scale resource for the functional characterization of Arabidopsis transcription factors. Cell Rep *8*, 622-632.

Przemeck, G.K., Mattsson, J., Hardtke, C.S., Sung, Z.R., and Berleth, T. (1996). Studies on the role of the Arabidopsis gene MONOPTEROS in vascular development and plant cell axialization. Planta *200*, 229-237.

Qi, J.Y., Wu, B.B., Feng, S.L., Lu, S.Q., Guan, C.M., Zhang, X., Qiu, D.L., Hu, Y.C., Zhou, Y.H., Li, C.Y., *et al*. (2017). Mechanical regulation of organ asymmetry in leaves. Nature Plants *3*, 724-733.

Rashotte, A.M., Carson, S.D., To, J.P., and Kieber, J.J. (2003). Expression profiling of cytokinin action in Arabidopsis. Plant Physiol *132*, 1998-2011.

Rashotte, A.M., Mason, M.G., Hutchison, C.E., Ferreira, F.J., Schaller, G.E., and Kieber, J.J. (2006). A subset of Arabidopsis AP2 transcription factors mediates cytokinin responses in concert with a two-component pathway. Proc Natl Acad Sci U S A *103*, 11081-11085.

Raspopovic, J., Marcon, L., Russo, L., and Sharpe, J. (2014). Modeling digits. Digit patterning is controlled by a Bmp-Sox9-Wnt Turing network modulated by morphogen gradients. Science *345*, 566-570.

Rast, M.I., and Simon, R. (2012). Arabidopsis JAGGED LATERAL ORGANS acts with ASYMMETRIC LEAVES2 to coordinate KNOX and PIN expression in shoot and root meristems. Plant Cell *24*, 2917-2933.

Raven, J.A. (1975). TRANSPORT OF INDOLEACETIC ACID IN PLANT CELLS IN RELATION TO pH AND ELECTRICAL POTENTIAL GRADIENTS, AND ITS SIGNIFICANCE FOR POLAR IAA TRANSPORT. New Phytologist *74*, 163-172.

Reddy, G.V., Heisler, M.G., Ehrhardt, D.W., and Meyerowitz, E.M. (2004). Real-time lineage analysis reveals oriented cell divisions associated with morphogenesis at the shoot apex of Arabidopsis thaliana. Development *131*, 4225-4237.

Reece-Hoyes, J.S., Barutcu, A.R., McCord, R.P., Jeong, J.S., Jiang, L., MacWilliams, A., Yang, X., Salehi-Ashtiani, K., Hill, D.E., Blackshaw, S., *et al*. (2011a). Yeast one-hybrid assays for gene-centered human gene regulatory network mapping. Nat Methods *8*, 1050-1052.

Reece-Hoyes, J.S., Diallo, A., Lajoie, B., Kent, A., Shrestha, S., Kadreppa, S., Pesyna, C., Dekker, J., Myers, C.L., and Walhout, A.J. (2011b). Enhanced yeast one-hybrid assays for high-throughput gene-centered regulatory network mapping. Nat Methods *8*, 1059-1064.

Reinhardt, D., Mandel, T., and Kuhlemeier, C. (2000). Auxin regulates the initiation and radial position of plant lateral organs. Plant Cell *12*, 507-518.

Reinhardt, D., Pesce, E.R., Stieger, P., Mandel, T., Baltensperger, K., Bennett, M., Traas, J., Friml, J., and Kuhlemeier, C. (2003). Regulation of phyllotaxis by polar auxin transport. Nature *426*, 255-260.

Reinhardt, D., Wittwer, F., Mandel, T., and Kuhlemeier, C. (1998). Localized upregulation of a new expansin gene predicts the site of leaf formation in the tomato meristem. Plant Cell *10*, 1427-1437.

Richmond, T.A., and Somerville, C.R. (2000). The cellulose synthase superfamily. Plant Physiol *124*, 495-498.

Robert, S., Kleine-Vehn, J., Barbez, E., Sauer, M., Paciorek, T., Baster, P., Vanneste, S., Zhang, J., Simon, S., Covanova, M., *et al*. (2010). ABP1 mediates auxin inhibition of clathrin-dependent endocytosis in Arabidopsis. Cell *143*, 111-121.

Rolland-Lagan, A.G., and Prusinkiewicz, P. (2005). Reviewing models of auxin canalization in the context of leaf vein pattern formation in Arabidopsis. Plant J *44*, 854-865.

Rozier, F., Mirabet, V., Vernoux, T., and Das, P. (2014). Analysis of 3D gene expression patterns in plants using whole-mount RNA in situ hybridization. Nat Protoc *9*, 2464-2475.

Rubery, P.H., and Sheldrake, A.R. (1974). Carrier-mediated auxin transport. Planta *118*, 101-121.

Sabatini, S., Beis, D., Wolkenfelt, H., Murfett, J., Guilfoyle, T., Malamy, J., Benfey, P., Leyser, O., Bechtold, N., Weisbeek, P., *et al*. (1999). An auxin-dependent distal organizer of pattern and polarity in the Arabidopsis root. Cell *99*, 463-472.

Sachs, T. (1981). The Control of the Patterned Differentiation of Vascular Tissues. Advances in Botanical Researcch *9*, 151-262.

Sakakibara, H., Takei, K., and Hirose, N. (2006). Interactions between nitrogen and cytokinin in the regulation of metabolism and development. Trends Plant Sci *11*, 440-448.

Sakamoto, T., Morinaka, Y., Inukai, Y., Kitano, H., and Fujioka, S. (2013). Auxin signal transcription factor regulates expression of the brassinosteroid receptor gene in rice. Plant J *73*, 676-688.

Sampathkumar, A., Krupinski, P., Wightman, R., Milani, P., Berquand, A., Boudaoud, A., Hamant, O., Jonsson, H., and Meyerowitz, E.M. (2014). Subcellular and supracellular mechanical stress prescribes cytoskeleton behavior in Arabidopsis cotyledon pavement cells. Elife *3*, e01967.

Sampedro, J., and Cosgrove, D.J. (2005). The expansin superfamily. Genome Biol *6*, 242.

Sanchez-Rodriguez, C., Bauer, S., Hematy, K., Saxe, F., Ibanez, A.B., Vodermaier, V., Konlechner, C., Sampathkumar, A., Ruggeberg, M., Aichinger, E., *et al*. (2012). Chitinase-like1/pom-pom1 and its homolog CTL2 are glucan-interacting proteins important for cellulose biosynthesis in Arabidopsis. Plant Cell *24*, 589-607.

Sanchez-Rodriguez, C., Ketelaar, K., Schneider, R., Villalobos, J.A., Somerville, C.R., Persson, S., and Wallace, I.S. (2017). BRASSINOSTEROID INSENSITIVE2 negatively regulates cellulose synthesis in Arabidopsis by phosphorylating cellulose synthase 1. Proc Natl Acad Sci U S A *114*, 3533-3538.

Santner, A., Calderon-Villalobos, L.I., and Estelle, M. (2009). Plant hormones are versatile chemical regulators of plant growth. Nat Chem Biol *5*, 301-307.

Santner, A., and Estelle, M. (2009). Recent advances and emerging trends in plant hormone signalling. Nature *459*, 1071-1078.

Sarkar, A.K., Luijten, M., Miyashima, S., Lenhard, M., Hashimoto, T., Nakajima, K., Scheres, B., Heidstra, R., and Laux, T. (2007). Conserved factors regulate signalling in Arabidopsis thaliana shoot and root stem cell organizers. Nature *446*, 811-814.

Sasidharan, R., Keuskamp, D.H., Kooke, R., Voesenek, L.A., and Pierik, R. (2014). Interactions between auxin, microtubules and XTHs mediate green shade- induced petiole elongation in arabidopsis. PLoS One *9*, e90587.

Sassi, M., Ali, O., Boudon, F., Cloarec, G., Abad, U., Cellier, C., Chen, X., Gilles, B., Milani, P., Friml, J., *et al*. (2014). An auxin-mediated shift toward growth isotropy promotes organ formation at the shoot meristem in Arabidopsis. Curr Biol *24*, 2335-2342.

Sassi, M., Lu, Y., Zhang, Y., Wang, J., Dhonukshe, P., Blilou, I., Dai, M., Li, J., Gong, X., Jaillais, Y., *et al*. (2012). COP1 mediates the coordination of root and shoot growth by light through modulation of PIN1- and PIN2-dependent auxin transport in Arabidopsis. Development *139*, 3402-3412.

Sassi, M., and Vernoux, T. (2013). Auxin and self-organization at the shoot apical meristem. J Exp Bot *64*, 2579-2592.

Sauer, M., and Kleine-Vehn, J. (2011). AUXIN BINDING PROTEIN1: the outsider. Plant Cell *23*, 2033-2043.

Savaldi-Goldstein, S., Peto, C., and Chory, J. (2007). The epidermis both drives and restricts plant shoot growth. Nature *446*, 199-202.

Scacchi, E., Osmont, K.S., Beuchat, J., Salinas, P., Navarrete-Gomez, M., Trigueros, M., Ferrandiz, C., and Hardtke, C.S. (2009). Dynamic, auxin-responsive plasma membrane-to-nucleus movement of Arabidopsis BRX. Development *136*, 2059-2067.

Scheible, W.R., Eshed, R., Richmond, T., Delmer, D., and Somerville, C. (2001). Modifications of cellulose synthase confer resistance to isoxaben and thiazolidinone herbicides in Arabidopsis Ixr1 mutants. Proc Natl Acad Sci U S A *98*, 10079-10084.

Scheller, H.V., and Ulvskov, P. (2010). Hemicelluloses. Annu Rev Plant Biol *61*, 263-289.

Schlereth, A., Moller, B., Liu, W., Kientz, M., Flipse, J., Rademacher, E.H., Schmid, M., Jurgens, G., and Weijers, D. (2010). MONOPTEROS controls embryonic root initiation by regulating a mobile transcription factor. Nature *464*, 913-916.

Schneider, R., Hanak, T., Persson, S., and Voigt, C.A. (2016). Cellulose and callose synthesis and organization in focus, what's new? Curr Opin Plant Biol *34*, 9-16.

Schuster, C., Gaillochet, C., Medzihradszky, A., Busch, W., Daum, G., Krebs, M., Kehle, A., and Lohmann, J.U. (2014). A regulatory framework for shoot stem cell control integrating metabolic, transcriptional, and phytohormone signals. Dev Cell *28*, 438-449.

Shani, E., Yanai, O., and Ori, N. (2006). The role of hormones in shoot apical meristem function. Curr Opin Plant Biol *9*, 484-489.

Shih, H.W., Miller, N.D., Dai, C., Spalding, E.P., and Monshausen, G.B. (2014). The receptor-like kinase FERONIA is required for mechanical signal transduction in Arabidopsis seedlings. Curr Biol *24*, 1887-1892.

Shikata, M., Koyama, T., Mitsuda, N., and Ohme-Takagi, M. (2009). Arabidopsis SBP-box genes SPL10, SPL11 and SPL2 control morphological change in association with shoot maturation in the reproductive phase. Plant Cell Physiol *50*, 2133-2145.

Shimada, Y., Goda, H., Nakamura, A., Takatsuto, S., Fujioka, S., and Yoshida, S. (2003). Organ-specific expression of brassinosteroid-biosynthetic genes and distribution of endogenous brassinosteroids in Arabidopsis. Plant Physiol *131*, 287-297.

Shuai, B., Reynaga-Pena, C.G., and Springer, P.S. (2002). The lateral organ boundaries gene defines a novel, plant-specific gene family. Plant Physiol *129*, 747-761.

Siegfried, K.R., Eshed, Y., Baum, S.F., Otsuga, D., Drews, G.N., and Bowman, J.L. (1999). Members of the YABBY gene family specify abaxial cell fate in Arabidopsis. Development *126*, 4117-4128.

Smith, R.S., Guyomarc'h, S., Mandel, T., Reinhardt, D., Kuhlemeier, C., and Prusinkiewicz, P. (2006). A plausible model of phyllotaxis. Proc Natl Acad Sci U S A *103*, 1301-1306.

Sorin, C., Salla-Martret, M., Bou-Torrent, J., Roig-Villanova, I., and Martinez-Garcia, J.F. (2009). ATHB4, a regulator of shade avoidance, modulates hormone response in Arabidopsis seedlings. Plant J *59*, 266-277.

Souer, E., van Houwelingen, A., Kloos, D., Mol, J., and Koes, R. (1996). The no apical meristem gene of Petunia is required for pattern formation in embryos and flowers and is expressed at meristem and primordia boundaries. Cell *85*, 159-170.

Soyars, C.L., James, S.R., and Nimchuk, Z.L. (2016). Ready, aim, shoot: stem cell regulation of the shoot apical meristem. Curr Opin Plant Biol *29*, 163-168.

Sparks, E.E., Drapek, C., Gaudinier, A., Li, S., Ansariola, M., Shen, N., Hennacy, J.H., Zhang, J., Turco, G., Petricka, J.J., *et al*. (2016). Establishment of Expression in the SHORTROOT-SCARECROW Transcriptional Cascade through Opposing Activities of Both Activators and Repressors. Dev Cell *39*, 585-596.

Spinelli, S.V., Martin, A.P., Viola, I.L., Gonzalez, D.H., and Palatnik, J.F. (2011). A mechanistic link between STM and CUC1 during Arabidopsis development. Plant Physiol *156*, 1894-1904.

Steeves, T.A., and Sussex, I.M. (1989). Patterns in Plant Development (Cambridge: Cambridge University Press).

Stepanova, A.N., Robertson-Hoyt, J., Yun, J., Benavente, L.M., Xie, D.Y., Dolezal, K., Schlereth, A., Jurgens, G., and Alonso, J.M. (2008). TAA1-mediated auxin biosynthesis is essential for hormone crosstalk and plant development. Cell *133*, 177-191.

Stoma, S., Lucas, M., Chopard, J., Schaedel, M., Traas, J., and Godin, C. (2008). Flux-based transport enhancement as a plausible unifying mechanism for auxin transport in meristem development. PLoS Comput Biol *4*, e1000207.

Stoppin-Mellet, V., Gaillard, J., and Vantard, M. (2006). Katanin's severing activity favors bundling of cortical microtubules in plants. Plant J *46*, 1009-1017.

Strayer, C., Oyama, T., Schultz, T.F., Raman, R., Somers, D.E., Mas, P., Panda, S., Kreps, J.A., and Kay, S.A. (2000). Cloning of the Arabidopsis clock gene TOC1, an autoregulatory response regulator homolog. Science *289*, 768-771.

Sun, Y., Fan, X.Y., Cao, D.M., Tang, W., He, K., Zhu, J.Y., He, J.X., Bai, M.Y., Zhu, S., Oh, E., *et al*. (2010). Integration of brassinosteroid signal transduction with the transcription network for plant growth regulation in Arabidopsis. Dev Cell *19*, 765-777.

Symons, G.M., and Reid, J.B. (2008). Brassinosteroids, de-etiolation and the re-emerging art of plant hormone quantification. Plant Signal Behav *3*, 868-870.

Szekeres, M., Nemeth, K., Koncz-Kalman, Z., Mathur, J., Kauschmann, A., Altmann, T., Redei, G.P., Nagy, F., Schell, J., and Koncz, C. (1996). Brassinosteroids rescue the deficiency of CYP90, a cytochrome P450, controlling cell elongation and de-etiolation in Arabidopsis. Cell *85*, 171-182.

Szemenyei, H., Hannon, M., and Long, J.A. (2008). TOPLESS mediates auxin-dependent transcriptional repression during Arabidopsis embryogenesis. Science *319*, 1384-1386.

Takada, S., Hibara, K., Ishida, T., and Tasaka, M. (2001). The CUP-SHAPED COTYLEDON1 gene of Arabidopsis regulates shoot apical meristem formation. Development *128*, 1127-1135.

Takahashi, T., Gasch, A., Nishizawa, N., and Chua, N.H. (1995). The DIMINUTO gene of Arabidopsis is involved in regulating cell elongation. Genes Dev *9*, 97-107.

Takeda, S., Hanano, K., Kariya, A., Shimizu, S., Zhao, L., Matsui, M., Tasaka, M., and Aida, M. (2011). CUP-SHAPED COTYLEDON1 transcription factor activates the expression of LSH4 and LSH3, two members of the ALOG gene family, in shoot organ boundary cells. Plant J *66*, 1066-1077.

Takei, K., Sakakibara, H., and Sugiyama, T. (2001). Identification of genes encoding adenylate isopentenyltransferase, a cytokinin biosynthesis enzyme, in Arabidopsis thaliana. J Biol Chem *276*, 26405-26410.

Tang, W., Kim, T.W., Oses-Prieto, J.A., Sun, Y., Deng, Z., Zhu, S., Wang, R., Burlingame, A.L., and Wang, Z.Y. (2008). BSKs mediate signal transduction from the receptor kinase BRI1 in Arabidopsis. Science *321*, 557-560.

Tang, W., Yuan, M., Wang, R., Yang, Y., Wang, C., Oses-Prieto, J.A., Kim, T.W., Zhou, H.W., Deng, Z., Gampala, S.S., *et al*. (2011). PP2A activates brassinosteroid-responsive gene expression and plant growth by dephosphorylating BZR1. Nat Cell Biol *13*, 124-131.

Taylor, N.G., Howells, R.M., Huttly, A.K., Vickers, K., and Turner, S.R. (2003). Interactions among three distinct CesA proteins essential for cellulose synthesis. Proc Natl Acad Sci U S A *100*, 1450-1455.

Taylor, N.G., Laurie, S., and Turner, S.R. (2000). Multiple cellulose synthase catalytic subunits are required for cellulose synthesis in Arabidopsis. Plant Cell *12*, 2529-2540.

Taylor-Teeples, M., Lin, L., de Lucas, M., Turco, G., Toal, T.W., Gaudinier, A., Young, N.F., Trabucco, G.M., Veling, M.T., Lamothe, R., *et al*. (2015). An Arabidopsis gene regulatory network for secondary cell wall synthesis. Nature *517*, 571-575.

Teale, W.D., Paponov, I.A., and Palme, K. (2006). Auxin in action: signalling, transport and the control of plant growth and development. Nat Rev Mol Cell Biol *7*, 847-859.

ten Hove, C.A., Lu, K.J., and Weijers, D. (2015). Building a plant: cell fate specification in the early Arabidopsis embryo. Development *142*, 420-430.

Thompson, D.A.W. (1917). On Growth and Form (Cambrige: Cambridge University Press).

Thompson, J.E., and Fry, S.C. (2001). Restructuring of wall-bound xyloglucan by transglycosylation in living plant cells. Plant J *26*, 23-34.

Tokunaga, H., Kojima, M., Kuroha, T., Ishida, T., Sugimoto, K., Kiba, T., and Sakakibara, H. (2012). Arabidopsis lonely guy (LOG) multiple mutants reveal a central role of the LOG-dependent pathway in cytokinin activation. Plant J *69*, 355-365.

Tromas, A., Braun, N., Muller, P., Khodus, T., Paponov, I.A., Palme, K., Ljung, K., Lee, J.Y., Benfey, P., Murray, J.A., *et al*. (2009). The AUXIN BINDING PROTEIN 1 is required for differential auxin responses mediating root growth. PLoS One *4*, e6648.

Tsuda, K., Kurata, N., Ohyanagi, H., and Hake, S. (2014). Genome-wide study of KNOX regulatory network reveals brassinosteroid catabolic genes important for shoot meristem function in rice. Plant Cell *26*, 3488-3500.

Tsugama, D., Liu, S., and Takano, T. (2016a). The bZIP Protein VIP1 Is Involved in Touch Responses in Arabidopsis Roots. Plant Physiol *171*, 1355-1365.

Tsugama, D., Liu, S., and Takano, T. (2016b). VIP1 is very important/interesting protein 1 regulating touch responses of Arabidopsis. Plant Signal Behav *11*, e1187358.

Tucker, M.R., Roodbarkelari, F., Truernit, E., Adamski, N.M., Hinze, A., Lohmuller, B., Wurschum, T., and Laux, T. (2013). Accession-specific modifiers act with ZWILLE/ARGONAUTE10 to maintain shoot meristem stem cells during embryogenesis in Arabidopsis. BMC Genomics *14*, 809.

Turchi, L., Carabelli, M., Ruzza, V., Possenti, M., Sassi, M., Penalosa, A., Sessa, G., Salvi, S., Forte, V., Morelli, G., *et al*. (2013). Arabidopsis HD-Zip II transcription factors control apical embryo development and meristem function. Development *140*, 2118-2129.

Turing, A.M. (1952). The chemical basis of morphogenesis. Philosophical Transactions of the Royal Society of London Series B, Biological Sciences *237*, 37-72.

Tzafrir, I., Pena-Muralla, R., Dickerman, A., Berg, M., Rogers, R., Hutchens, S., Sweeney, T.C., McElver, J., Aux, G., Patton, D., *et al*. (2004). Identification of genes required for embryo development in Arabidopsis. Plant Physiol *135*, 1206-1220.

Uchida, N., Shimada, M., and Tasaka, M. (2013). ERECTA-family receptor kinases regulate stem cell homeostasis via buffering its cytokinin responsiveness in the shoot apical meristem. Plant Cell Physiol *54*, 343-351.

Uyttewaal, M., Burian, A., Alim, K., Landrein, B., Borowska-Wykret, D., Dedieu, A., Peaucelle, A., Ludynia, M., Traas, J., Boudaoud, A., *et al*. (2012). Mechanical stress acts via katanin to amplify differences in growth rate between adjacent cells in Arabidopsis. Cell *149*, 439-451.

Vain, T., Crowell, E.F., Timpano, H., Biot, E., Desprez, T., Mansoori, N., Trindade, L.M., Pagant, S., Robert, S., Hofte, H., *et al*. (2014). The Cellulase KORRIGAN Is Part of the Cellulose Synthase Complex. Plant Physiol *165*, 1521-1532.

van Berkel, K., de Boer, R.J., Scheres, B., and ten Tusscher, K. (2013). Polar auxin transport: models and mechanisms. Development *140*, 2253-2268.

Van Hautegem, T., Waters, A.J., Goodrich, J., and Nowack, M.K. (2015). Only in dying, life: programmed cell death during plant development. Trends Plant Sci *20*, 102-113.

Van Speybroeck, L. (2002). From epigenesis to epigenetics: the case of C. H. Waddington. Ann N Y Acad Sci *981*, 61-81.

Vernoux, T., Brunoud, G., Farcot, E., Morin, V., Van den Daele, H., Legrand, J., Oliva, M., Das, P., Larrieu, A., Wells, D., *et al*. (2011). The auxin signalling network translates dynamic input into robust patterning at the shoot apex. Mol Syst Biol *7*, 508.

Vernoux, T., Kronenberger, J., Grandjean, O., Laufs, P., and Traas, J. (2000). PIN-FORMED 1 regulates cell fate at the periphery of the shoot apical meristem. Development *127*, 5157-5165.

Vert, G., and Chory, J. (2006). Downstream nuclear events in brassinosteroid signalling. Nature *441*, 96-100.

Vert, G., Walcher, C.L., Chory, J., and Nemhauser, J.L. (2008). Integration of auxin and brassinosteroid pathways by Auxin Response Factor 2. Proc Natl Acad Sci U S A *105*, 9829-9834.

Vroemen, C.W. (2003). The CUP-SHAPED COTYLEDON3 Gene Is Required for Boundary and Shoot Meristem Formation in Arabidopsis. The Plant Cell Online *15*, 1563-1577.

Waddington, C.H. (1956). Principles of embryology (Allen & Unwin).

Waddington, C.H. (1957). The strategy of the genes: a discussion of some aspects of theoretical biology (Allen & Unwin).

Wagner, T.A., and Kohorn, B.D. (2001). Wall-associated kinases are expressed throughout plant development and are required for cell expansion. Plant Cell *13*, 303-318.

Walcher, C.L., and Nemhauser, J.L. (2012). Bipartite promoter element required for auxin response. Plant Physiol *158*, 273-282.

Wang, Q., Kohlen, W., Rossmann, S., Vernoux, T., and Theres, K. (2014). Auxin Depletion from the Leaf Axil Conditions Competence for Axillary Meristem Formation in Arabidopsis and Tomato. Plant Cell *26*, 2068-2079.

Wang, T., Zabotina, O., and Hong, M. (2012). Pectin-cellulose interactions in the Arabidopsis primary cell wall from two-dimensional magic-angle-spinning solid-state nuclear magnetic resonance. Biochemistry *51*, 9846-9856.

Wang, X., and Chory, J. (2006). Brassinosteroids regulate dissociation of BKI1, a negative regulator of BRI1 signaling, from the plasma membrane. Science *313*, 1118-1122.

Wang, X., Kota, U., He, K., Blackburn, K., Li, J., Goshe, M.B., Huber, S.C., and Clouse, S.D. (2008). Sequential transphosphorylation of the BRI1/BAK1 receptor kinase complex impacts early events in brassinosteroid signaling. Dev Cell *15*, 220-235.

Wang, Z.Y., Nakano, T., Gendron, J., He, J., Chen, M., Vafeados, D., Yang, Y., Fujioka, S., Yoshida, S., Asami, T., *et al*. (2002). Nuclear-localized BZR1 mediates brassinosteroid-

induced growth and feedback suppression of brassinosteroid biosynthesis. Dev Cell *2*, 505-513.

Wang, Z.Y., Seto, H., Fujioka, S., Yoshida, S., and Chory, J. (2001). BRI1 is a critical component of a plasma-membrane receptor for plant steroids. Nature *410*, 380-383.

Weigel, D., Alvarez, J., Smyth, D.R., Yanofsky, M.F., and Meyerowitz, E.M. (1992). LEAFY controls floral meristem identity in Arabidopsis. Cell *69*, 843-859.

Weijers, D., Sauer, M., Meurette, O., Friml, J., Ljung, K., Sandberg, G., Hooykaas, P., and Offringa, R. (2005). Maintenance of embryonic auxin distribution for apical-basal patterning by PIN-FORMED-dependent auxin transport in Arabidopsis. Plant Cell *17*, 2517-2526.

Willige, B.C., Ahlers, S., Zourelidou, M., Barbosa, I.C., Demarsy, E., Trevisan, M., Davis, P.A., Roelfsema, M.R., Hangarter, R., Fankhauser, C., *et al*. (2013). D6PK AGCVIII kinases are required for auxin transport and phototropic hypocotyl bending in Arabidopsis. Plant Cell *25*, 1674-1688.

Willige, B.C., Isono, E., Richter, R., Zourelidou, M., and Schwechheimer, C. (2011). Gibberellin regulates PIN-FORMED abundance and is required for auxin transport-dependent growth and development in Arabidopsis thaliana. Plant Cell *23*, 2184-2195.

Wils, C.R., and Kaufmann, K. (2017). Gene-regulatory networks controlling inflorescence and flower development in Arabidopsis thaliana. Biochim Biophys Acta *1860*, 95-105.

Winter, D., Vinegar, B., Nahal, H., Ammar, R., Wilson, G.V., and Provart, N.J. (2007). An "Electronic Fluorescent Pictograph" browser for exploring and analyzing large-scale biological data sets. PLoS One *2*, e718.

Wisniewska, J., Xu, J., Seifertova, D., Brewer, P.B., Ruzicka, K., Blilou, I., Rouquie, D., Benkova, E., Scheres, B., and Friml, J. (2006). Polar PIN localization directs auxin flow in plants. Science *312*, 883.

Wolf, S., Hematy, K., and Hofte, H. (2012a). Growth control and cell wall signaling in plants. Annu Rev Plant Biol *63*, 381-407.

Wolf, S., Mravec, J., Greiner, S., Mouille, G., and Hofte, H. (2012b). Plant cell wall homeostasis is mediated by brassinosteroid feedback signaling. Curr Biol *22*, 1732-1737.

Wolf, S., van der Does, D., Ladwig, F., Sticht, C., Kolbeck, A., Schurholz, A.K., Augustin, S., Keinath, N., Rausch, T., Greiner, S., *et al*. (2014). A receptor-like protein mediates the response to pectin modification by activating brassinosteroid signaling. Proc Natl Acad Sci U S A *111*, 15261-15266.

Wolpert, L. (1969). Positional information and the spatial pattern of cellular differentiation. J Theor Biol *25*, 1-47.

Wolpert, L. (1971). Positional information and pattern formation. Curr Top Dev Biol *6*, 183-224.

Wolpert, L. (2011). Principles of Development (OUP Oxford).

Wolters, H., and Jurgens, G. (2009). Survival of the flexible: hormonal growth control and adaptation in plant development. Nat Rev Genet *10*, 305-317.

Woo, E.J., Marshall, J., Bauly, J., Chen, J.G., Venis, M., Napier, R.M., and Pickersgill, R.W. (2002). Crystal structure of auxin-binding protein 1 in complex with auxin. EMBO J *21*, 2877-2885.

Woodward, A.W., and Bartel, B. (2005). Auxin: regulation, action, and interaction. Ann Bot *95*, 707-735.

Wu, H.M., Hazak, O., Cheung, A.Y., and Yalovsky, S. (2011). RAC/ROP GTPases and auxin signaling. Plant Cell *23*, 1208-1218.

Wu, M.F., Yamaguchi, N., Xiao, J., Bargmann, B., Estelle, M., Sang, Y., and Wagner, D. (2015). Auxin-regulated chromatin switch directs acquisition of flower primordium founder fate. Elife *4*, e09269.

Xiao, C., Zhang, T., Zheng, Y., Cosgrove, D.J., and Anderson, C.T. (2016). Xyloglucan Deficiency Disrupts Microtubule Stability and Cellulose Biosynthesis in Arabidopsis, Altering Cell Growth and Morphogenesis. Plant Physiol *170*, 234-249.

Xie, L., Yang, C., and Wang, X. (2011). Brassinosteroids can regulate cellulose biosynthesis by controlling the expression of CESA genes in Arabidopsis. J Exp Bot *62*, 4495-4506.

Xu, T., Dai, N., Chen, J., Nagawa, S., Cao, M., Li, H., Zhou, Z., Chen, X., De Rycke, R., Rakusova, H., *et al*. (2014). Cell surface ABP1-TMK auxin-sensing complex activates ROP GTPase signaling. Science *343*, 1025-1028.

Xu, T., Wen, M., Nagawa, S., Fu, Y., Chen, J.G., Wu, M.J., Perrot-Rechenmann, C., Friml, J., Jones, A.M., and Yang, Z. (2010). Cell surface- and rho GTPase-based auxin signaling controls cellular interdigitation in Arabidopsis. Cell *143*, 99-110.

Yadav, R.K., Girke, T., Pasala, S., Xie, M., and Reddy, G.V. (2009). Gene expression map of the Arabidopsis shoot apical meristem stem cell niche. Proc Natl Acad Sci U S A *106*, 4941-4946.

Yadav, R.K., Perales, M., Gruel, J., Girke, T., Jonsson, H., and Reddy, G.V. (2011). WUSCHEL protein movement mediates stem cell homeostasis in the Arabidopsis shoot apex. Genes Dev *25*, 2025-2030.

Yadav, R.K., Perales, M., Gruel, J., Ohno, C., Heisler, M., Girke, T., Jonsson, H., and Reddy, G.V. (2013). Plant stem cell maintenance involves direct transcriptional repression of differentiation program. Mol Syst Biol *9*, 654.

Yadav, R.K., and Reddy, G.V. (2012). WUSCHEL protein movement and stem cell homeostasis. Plant Signal Behav *7*, 592-594.

Yamaguchi, N., Jeong, C.W., Nole-Wilson, S., Krizek, B.A., and Wagner, D. (2016). AINTEGUMENTA and AINTEGUMENTA-LIKE6/PLETHORA3 Induce LEAFY Expression in Response to Auxin to Promote the Onset of Flower Formation in Arabidopsis. Plant Physiol *170*, 283-293.

Yamaguchi, N., Wu, M.F., Winter, C.M., Berns, M.C., Nole-Wilson, S., Yamaguchi, A., Coupland, G., Krizek, B.A., and Wagner, D. (2013). A molecular framework for auxin-mediated initiation of flower primordia. Dev Cell *24*, 271-282.

Yamaguchi, N., Wu, M.F., Winter, C.M., and Wagner, D. (2014). LEAFY and Polar Auxin Transport Coordinately Regulate Arabidopsis Flower Development. Plants (Basel) *3*, 251-265.

Yang, H., and Murphy, A.S. (2009). Functional expression and characterization of Arabidopsis ABCB, AUX 1 and PIN auxin transporters in Schizosaccharomyces pombe. Plant J *59*, 179-191.

Yang, W., Schuster, C., Beahan, C.T., Charoensawan, V., Peaucelle, A., Bacic, A., Doblin, M.S., Wightman, R., and Meyerowitz, E.M. (2016). Regulation of Meristem Morphogenesis by Cell Wall Synthases in Arabidopsis. Curr Biol *26*, 1404-1415.

Yao, X., Wang, H., Li, H., Yuan, Z., Li, F., Yang, L., and Huang, H. (2009). Two types of cis-acting elements control the abaxial epidermis-specific transcription of the MIR165a and MIR166a genes. FEBS Lett *583*, 3711-3717.

Yin, Y., Vafeados, D., Tao, Y., Yoshida, S., Asami, T., and Chory, J. (2005). A new class of transcription factors mediates brassinosteroid-regulated gene expression in Arabidopsis. Cell *120*, 249-259.

Yin, Y., Wang, Z.Y., Mora-Garcia, S., Li, J., Yoshida, S., Asami, T., and Chory, J. (2002). BES1 accumulates in the nucleus in response to brassinosteroids to regulate gene expression and promote stem elongation. Cell *109*, 181-191.

Yu, X., Li, L., Li, L., Guo, M., Chory, J., and Yin, Y. (2008). Modulation of brassinosteroid-regulated gene expression by Jumonji domain-containing proteins ELF6 and REF6 in Arabidopsis. Proc Natl Acad Sci U S A *105*, 7618-7623.

Yu, X., Li, L., Zola, J., Aluru, M., Ye, H., Foudree, A., Guo, H., Anderson, S., Aluru, S., Liu, P., *et al*. (2011). A brassinosteroid transcriptional network revealed by genome-wide identification of BESI target genes in Arabidopsis thaliana. Plant J *65*, 634-646.

Zabotina, O.A. (2012). Xyloglucan and its biosynthesis. Front Plant Sci *3*, 134.

Zabotina, O.A., van de Ven, W.T., Freshour, G., Drakakaki, G., Cavalier, D., Mouille, G., Hahn, M.G., Keegstra, K., and Raikhel, N.V. (2008). Arabidopsis XXT5 gene encodes a putative alpha-1,6-xylosyltransferase that is involved in xyloglucan biosynthesis. Plant J *56*, 101-115.

Zazimalova, E., Murphy, A.S., Yang, H., Hoyerova, K., and Hosek, P. (2010). Auxin transporters--why so many? Cold Spring Harb Perspect Biol *2*, a001552.

Zhang, F., May, A., and Irish, V.F. (2017). Type-B ARABIDOPSIS RESPONSE REGULATORs Directly Activate WUSCHEL. Trends Plant Sci.

Zhang, Q., Fishel, E., Bertroche, T., and Dixit, R. (2013). Microtubule severing at crossover sites by katanin generates ordered cortical microtubule arrays in Arabidopsis. Curr Biol *23*, 2191-2195.

Zhang, W., To, J.P., Cheng, C.Y., Schaller, G.E., and Kieber, J.J. (2011). Type-A response regulators are required for proper root apical meristem function through post-transcriptional regulation of PIN auxin efflux carriers. Plant J *68*, 1-10.

Zhao, Z., Andersen, S.U., Ljung, K., Dolezal, K., Miotk, A., Schultheiss, S.J., and Lohmann, J.U. (2010). Hormonal control of the shoot stem-cell niche. Nature *465*, 1089-1092.

Zhu, H., Hu, F., Wang, R., Zhou, X., Sze, S.H., Liou, L.W., Barefoot, A., Dickman, M., and Zhang, X. (2011). Arabidopsis Argonaute10 specifically sequesters miR166/165 to regulate shoot apical meristem development. Cell *145*, 242-256.

Zhu, J.Y., Sae-Seaw, J., and Wang, Z.Y. (2013). Brassinosteroid signalling. Development *140*, 1615-1620.

Zourelidou, M., Absmanner, B., Weller, B., Barbosa, I.C., Willige, B.C., Fastner, A., Streit, V., Port, S.A., Colcombet, J., de la Fuente van Bentem, S., *et al*. (2014). Auxin efflux by PIN-FORMED proteins is activated by two different protein kinases, D6 PROTEIN KINASE and PINOID. Elife *3*.

Zurcher, E., and Muller, B. (2016). Cytokinin Synthesis, Signaling, and Function--Advances and New Insights. Int Rev Cell Mol Biol *324*, 1-38.

Zurcher, E., Tavor-Deslex, D., Lituiev, D., Enkerli, K., Tarr, P.T., and Muller, B. (2013). A robust and sensitive synthetic sensor to monitor the transcriptional output of the cytokinin signaling network in planta. Plant Physiol *161*, 1066-1075.

Zurek, D.M., Rayle, D.L., McMorris, T.C., and Clouse, S.D. (1994). Investigation of Gene Expression, Growth Kinetics, and Wall Extensibility during Brassinosteroid-Regulated Stem Elongation. Plant Physiol *104*, 505-513.

Annexes

Annex 1

An auxin-mediated shift toward growth isotropy promotes organ formation at the shoot meristem in Arabidopsis.

Sassi M, Ali O, Boudon F, Cloarec G, Abad U, Cellier C, Chen X, Gilles B, Milani P, Friml J, Vernoux T, Godin C, Hamant O, Traas J.

Curr Biol. 2014 Oct 6;24(19):2335-42. doi: 10.1016/j.cub.2014.08.036.

Annex 2

Supplementary information: Modelling methods

Modus operandi

We use a segmented Pin-like meristem as shown on figure (2) in the main text. Following the "pressurized tissue "hypothesis [2], only the outermost anticlinal cell walls are taken into consideration for the mechanical simulations. Each one of them is tiled with triangular first order finite elements (FEs). All the FEs belonging to the same cell feature the same values for their mechanical and growth characteristics which correspond to seven independent parameters listed in table 1 hereafter.

Depending on the case, cells are either regrouped in three or four zones, see figure 1-**A, B** : The central zone (blue), the periphery (green), the initium (red) and the border zone (white). All cells in a given zone feature the same mechanical and growth characteristics.

Mechanical parameters	
α	Angular aperture of the fiber distribution.
ρ_0	fibers mean angular density.
$^{\Delta\rho}/_{\rho_0}$	Relative increase of fibers density within the reenforced direction.
Y_0	The elastic modulus of cellulose-based fibers within the cell wall.
μ_{iso}	Poisson's ratio of the cell wall.
Growth parameters	
γ	Extensibility of the cell wall.
ε_{th}	Strain threshold above with growth occurs.

Table 1: Mechanical and growth parameters used in our simulations.

1 Mechanical description of the cell wall

We consider the cell walls as a linearly elastic continuum with transverse isotropy. This means that they feature a direction of higher rigidity. Their elastic behavior is characterized by the corresponding Hooke's tensor ($\boldsymbol{H}$ in equation (1)).

$$\boldsymbol{\sigma} = \boldsymbol{H} \cdot \boldsymbol{\varepsilon} \quad with: \quad \boldsymbol{H} = \begin{bmatrix} Y_{x\ eff} & Y_{x\ eff}\mu_{xy} & 0 \\ Y_{y\ eff}\mu_{yx} & Y_{y\ eff} & 0 \\ 0 & 0 & G \end{bmatrix} \quad and \quad \begin{cases} Y_{i\ eff} = \frac{Y_i}{1-\mu_{xy}\mu_{yx}} \\ Y_{x\ eff}\mu_{xy} = Y_{y\ eff}\mu_{yx} \end{cases} \tag{1}$$

Where Voigt notation is used (*i.e.* $\boldsymbol{\sigma}^t = \begin{bmatrix} \sigma_{xx} & \sigma_{yy} & \sigma_{xy} \end{bmatrix}$ and $\boldsymbol{\varepsilon}^t = \begin{bmatrix} \varepsilon_{xx} & \varepsilon_{yy} & 2\varepsilon_{xy} \end{bmatrix}$).

1.1 Structural considerations

From a structural perspective, the cell wall is considered as a fiber reinforced linear elastic continuum. Its structural anisotropy is quantified by its constituting fibers angular distribution $\rho(\theta)$, a $\pi-$periodic function for the fibers are not oriented, see figure 1-**E, H & J**. Note that by construction we choose $\rho(\theta)$ to be even, meaning that its maximum is along the $x-$axis (*i.e.* $max(\rho) = \rho(0)$).

By assuming that each fiber has the same linear elastic behavior, characterized by the stiffness coefficient k and their resting length l_0, we can relate the elastic coefficients displayed in Hooke's matrix ($\boldsymbol{H}$ in equation (1)) to the fibers angular distribution, as exposed hereafter in equation (2).

$$\begin{array}{ll} Y_{xeff} = \frac{\pi}{16} Y_0 (6\tilde{\rho}_0 + 4\tilde{\rho}_1 + \tilde{\rho}_2) & \mu_{xy} = \frac{2\tilde{\rho}_0 - \tilde{\rho}_2}{6\tilde{\rho}_0 + 4\tilde{\rho}_1 + \tilde{\rho}_2} \\ Y_{yeff} = \frac{\pi}{16} Y_0 (6\tilde{\rho}_0 - 4\tilde{\rho}_1 + \tilde{\rho}_2) & \\ G = \frac{\pi}{8} Y_0 (2\tilde{\rho}_0 - \tilde{\rho}_2) & \mu_{yx} = \frac{2\tilde{\rho}_0 - \tilde{\rho}_2}{6\tilde{\rho}_0 - 4\tilde{\rho}_1 + \tilde{\rho}_2} \end{array} \tag{2}$$

Where $Y_0 = {}^{kl_0}/_2$ and the $\tilde{\rho}_k$ are the k^{th} Fourier's coefficients of $\rho(\theta)$:

$$\tilde{\rho}_0 = \frac{1}{\pi}\int_\pi d\theta\rho(\theta) \quad and \quad \tilde{\rho}_k = \frac{2}{\pi}\int_\pi d\theta\rho(\theta)cos(2k\theta) \quad for \quad k \geq 1 \tag{3}$$

For the sake of simplicity we considered in our simulations the simplest angular distribution possible, the unit step function:

$$\rho(\theta) = \rho_0\left(1 - \frac{\alpha\Delta\rho}{\pi\rho_0} + \frac{\Delta\rho}{\rho_0}\Pi_\alpha(\theta - \theta_0)\right) \quad with: \quad \Pi_\alpha(\theta) = \begin{cases} 1 & \theta_0 - \alpha/2 \leq \theta \leq \theta_0 + \alpha/2 \\ 0 & elsewhere \end{cases} \tag{4}$$

With this parametrization ρ_0 stands for the fibers mean angular density ($\frac{1}{\pi}\int_\pi \rho d\theta = \rho_0$), $\Delta\rho$ stands for the amplitude step between the directions of low ($\rho_{low} = \rho_0 - \Delta\rho\alpha/\pi$) and high ($\rho_{high} = \rho_0 + \Delta\rho(1 - \alpha/\pi)$) density and α stands for the angular aperture of the distribution, see figure 1-**J** . This specific expression for $\rho(\theta)$ yields the following expressions for Hooke's matrix coefficients:

$$\begin{aligned} Y_{xeff} &= \frac{3\pi}{16}Y_0\rho_0\left(1 + \frac{\Delta\rho}{6\pi\rho_0}(8sin(\alpha) + sin(2\alpha))\right) \\ Y_{yeff} &= \frac{3\pi}{16}Y_0\rho_0\left(1 - \frac{\Delta\rho}{6\pi\rho_0}(8sin(\alpha) - sin(2\alpha))\right) \\ G &= \frac{\pi}{4}Y_0\rho_0\left(1 - \frac{\Delta\rho}{2\pi\rho_0}sin(2\alpha)\right) \\ \mu_{xy} &= \frac{1}{3}\frac{1 - \frac{\Delta\rho}{2\pi\rho_0}sin(2\alpha)}{1 + \frac{\Delta\rho}{6\pi\rho_0}(4sin(\alpha) + sin(2\alpha))} \\ \mu_{yx} &= \frac{1}{3}\frac{1 - \frac{\Delta\rho}{2\pi\rho_0}sin(2\alpha)}{1 - \frac{\Delta\rho}{6\pi\rho_0}(4sin(\alpha) - sin(2\alpha))} \end{aligned} \tag{5}$$

To visualize the corresponding rigidity tensor, we plotted the norm of its projection in every angular directions (named angular rigidity and noted $Y(\theta)$ hereafter):

$$Y(\theta) = \|\mathbb{H} : \boldsymbol{P}_\theta\| \tag{6}$$

where $\boldsymbol{P}_\theta = \hat{\boldsymbol{e}}_\theta \otimes \hat{\boldsymbol{e}}_\theta$ is the projector in the direction given by the unit vector $\hat{\boldsymbol{e}}_\theta = \begin{bmatrix} cos(\theta) & sin(\theta) \end{bmatrix}^t$ and $\|\cdot\|$ depicts the second order tensorial norm defined as follow: $\|\boldsymbol{M}\| = \sqrt{\frac{1}{2}\sum_{i,j} M_{ij}^2}$, see 1.

1.2 Numerical implementation

We implemented the mechanical model with the numerical framework described in [1] .To implement the mechanical behavior prescribed by expressions (5) in the simulations, we use the Sofa module *HookeOrthotropicForceField* with specific definitions for the various coefficients as exposed in the python code below.

```
Yiso  =   150
muiso =   1./3.
Giso  =  Yiso * (1 + muiso)


fx    = 1 + d/(6*np.pi) * (8*np.sin(a) + np.sin(2*a))
fy    = 1 - d/(6*np.pi) * (8*np.sin(a) - np.sin(2*a))
fxy   = 1 - d/(2*np.pi) * np.sin(2*a)

Yx    = Yiso*fx
Yy    = Yiso*fy
Gani  = Giso*fxy
mu    = muiso*fxy/fx

Hooke_matrix = np.array([[Yx      , Yx * mu,     0],
                         [Yx * mu,       Yy,     0],
                         [      0,        0, Gani]])
```

In the previous code the parameters "a" and "d" correspond respectively to the angular aperture (α) of the microfibrils distribution $\rho(\theta)$ and its relative directional enrichment ($\Delta\rho/\rho_0$). We changed the aperture value to to simulate a change in the anisotropy of the fibers angular distribution. The complete list of parameters used in the various simulations are given in Tabs.2 to 4.

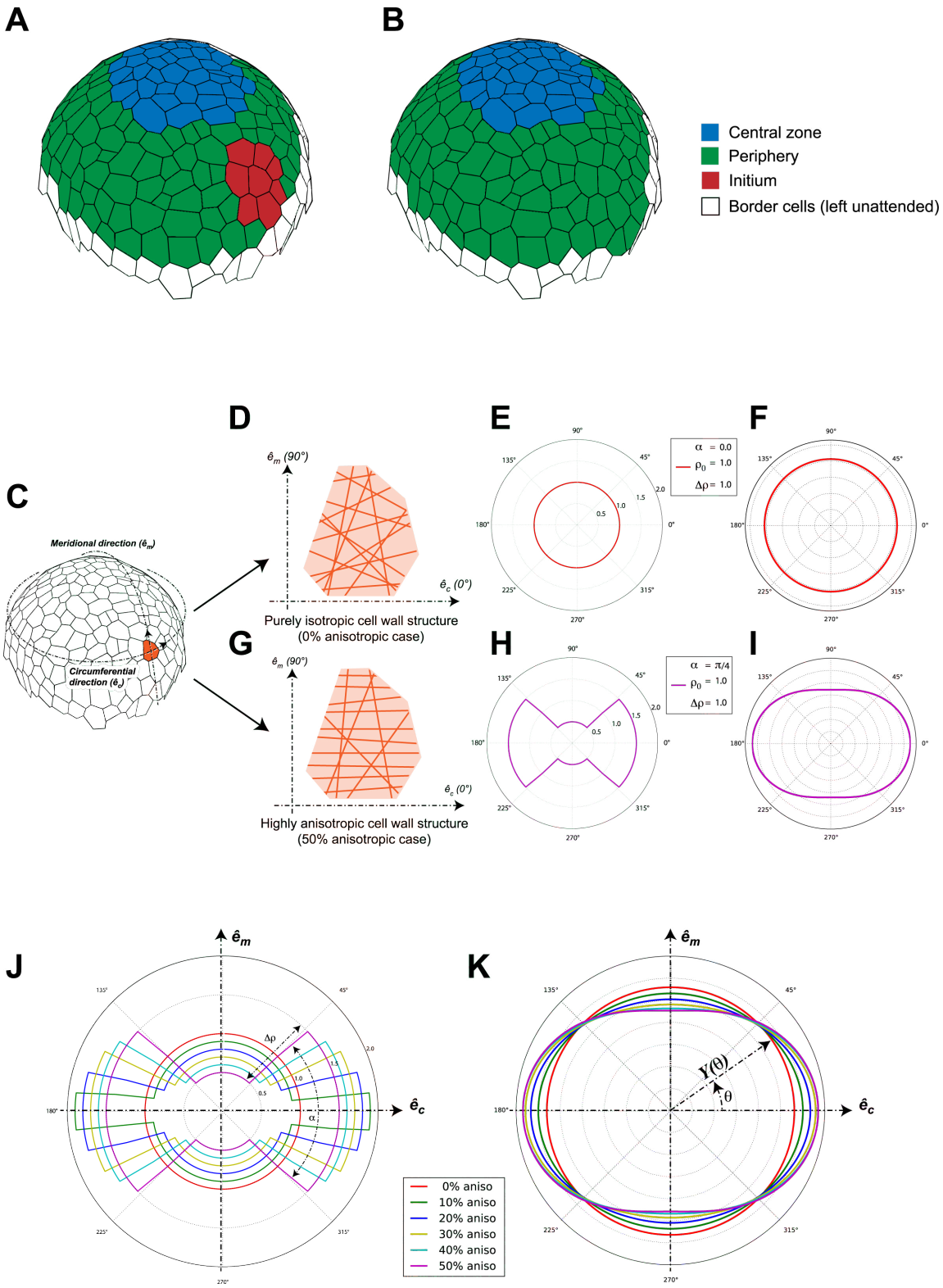

Figure 1: **Zoning, structural anisotropy & cell wall rigidity of the simulated structure**. **A & B:** Zoning used to perform the various simulations. In case **A** we defined an initium zone with different mechanical properties than its surrounding *(i.e.* the peripheral zone). In case **B**, we modified the structural anisotropy of the whole peripheral zone. **C:** Parametrization of the structure, we can attribute specific mechanical properties to every single cell of the structure, we depict here two extreme cases. **D, E & F:** The purely isotropic case and **G, H & I:** The highly anisotropic one. **D & G:** schematic representation of fibers distribution within the cell wall in each case. **E & H:** polar plots of the corresponding fiber angular density function ($\rho(\theta)$ in the text). **F & I:** polar plot of the corresponding angular rigidity ($Y(\theta)$ in equation (6)). **J:** polar plots of all the fibers angular density functions used in the various simulations ($\rho(\theta)$). **K:** polar plots of the corresponding angular rigidity functions ($Y(\theta)$).

2 Growth of the structure

The elastic response of the structure is coupled with a plastic one, depicting growth. Following a commonly accepted idea ([2]) we assumed this irreversible part of the deformation to be controlled by a viscoelastic, strain-based, constitutive equation:

$$\boldsymbol{L}_g = \gamma \cdot \boldsymbol{\Theta}\left(\boldsymbol{\varepsilon} - \boldsymbol{\varepsilon}_{th}\right) \quad with: \quad \boldsymbol{\Theta}\left(\boldsymbol{A}\right)_{ij} = \begin{cases} 0 \ if \ A_{ij} \leq 0 \\ A_{ij} \ if \ A_{ij} > 0 \end{cases} \tag{7}$$

where $\boldsymbol{L}_g$ stands for the deformation velocity gradient, $\boldsymbol{\varepsilon}$for the Green-Lagrangian strain field, γ and $\boldsymbol{\varepsilon}_{th}$ are two parameters exposed in Tab.1.

From an initial resting configuration, the structure is put under constrains and mechanical equilibrium is computed. If the resulting strain field ($\boldsymbol{\varepsilon}$) overshoot the threshold parameter ($\boldsymbol{\varepsilon}_{th}$) the resting configuration is updated, simulating the irreversible deformation due to growth. Once this update applied, the previously computed mechanical equilibrium is no longer valid and a new equilibrium is computed, initiating a second step of the growth process. More detail on this approach and its implemanation are available in [1].

3 Details about the various simulation produced

In the case of the present study, we performed three main sets of simulations:

Case#1: We study the influence of the structural anisotropy of the cell wall on a spatially limited zone (the *initium*) on its growth dynamics.

Case#2: We study the influence of the stiffness of the cell walls of the initium on its growth dynamics, in the case the structure of these walls is isotropic.

Case#3: We study the influence of the structural anisotropy of the cell wall on a large zone (the whole *periphery*) on the growth dynamics of the meristem.

Each of these sets consisted in a series of six simulations in which we slightly modified one mechanical parameter of the studied zone. To investigate the influence of the structural anisotropy of the cell wall, we modified the values of the angular aperture of the fibers distribution (variable α in equation (4) and/or parameter "a" in the code). To investigate the influence of the stiffness, we modified the overall Young's modulus (variable Y_0 in equation (5) and/or parameter "Yiso" in the code).

Numerical values of the various parameters (elastic, growth-related and solver-related) are given in TAB.BLABLA.

4 Quantification of cellular expansion

From the simulations, we could compute $S_i\left(t_n\right)$, the surface area of cell number i at growth step t_n. By dividing this surface area by the initial surface area of the considered cell ($S_i\left(t_0\right)$), we defined the relative surface area increase at growth step t_n: $r_i\left(t_n\right) = {}^{S_i(t_n)}/_{S_i(t_0)}$ .Finally we averaged this ratio over all cells belonging to the same zone, examples of its evolution for various zones of interest are given on figure 2 and figure 3 .

References

[1] Frédéric Boudon, Jérôme Chopard, Olivier Ali, Benjamin Gilles, Olivier Hamant, Arezki Boudaoud, Jan Traas, and Christophe Godin. A computational framework for 3D mechanical modeling of plant morphogenesis with cellular resolution. *PLoS Computational Biology*, 11(1):e1003950, January 2015.

[2] Behruz Bozorg, Pawel Krupinski, and Henrik Jönsson. Stress and Strain Provide Positional and Directional Cues in Development. *PLoS Computational Biology*, 10(1):e1003410, January 2014.

Mechanical parameters							Growth parameters			Numerical parameters			
zones	α	ρ_0	$\frac{\Delta\rho}{\rho_0}$	Y_{iso}	μ_{iso}	$\begin{bmatrix} Y_{x\ eff} & Y_{y\ eff} & \mu_{xy} & G \end{bmatrix}$	γ	ε_{th}	N_g	Solver type	N_{stp}	Δt_{stp}	n_i
$\begin{Bmatrix} Bottom \\ Periphery \\ Initium \\ Central\ Zone \end{Bmatrix}$	$\begin{Bmatrix} .5 \\ .5 \\ 0 \\ 0 \end{Bmatrix}$	1	1	150	1/3	$\begin{Bmatrix} 214 & 86.3 & 0.23, & 56.2 \\ 214 & 86.3 & 0.23, & 56.2 \\ 150 & 150 & 0.33, & 56.3 \\ 150 & 150 & 0.33, & 56.3 \end{Bmatrix}$	$\begin{Bmatrix} 1 \\ 1 \\ 1 \\ 2 \end{Bmatrix}$	$4 \cdot 10^{-3}$	10^2	Euler implicit	50	10^{-2}	$3 \cdot 10^2$
	$\begin{Bmatrix} .5 \\ .5 \\ .1 \\ 0 \end{Bmatrix}$					$\begin{Bmatrix} 214 & 86.3 & 0.23, & 56.2 \\ 214 & 86.3 & 0.23, & 56.2 \\ 174 & 135 & 0.26, & 51.0 \\ 150 & 150 & 0.33, & 56.3 \end{Bmatrix}$							
	$\begin{Bmatrix} .5 \\ .5 \\ .2 \\ 0 \end{Bmatrix}$					$\begin{Bmatrix} 214 & 86.3 & 0.23, & 56.2 \\ 214 & 86.3 & 0.23, & 56.2 \\ 195 & 120 & 0.22, & 47.7 \\ 150 & 150 & 0.33, & 56.3 \end{Bmatrix}$							
	$\begin{Bmatrix} .5 \\ .5 \\ .3 \\ 0 \end{Bmatrix}$					$\begin{Bmatrix} 214 & 86.3 & 0.23, & 56.2 \\ 214 & 86.3 & 0.23, & 56.2 \\ 195 & 120 & 0.22, & 47.7 \\ 150 & 150 & 0.33, & 56.3 \end{Bmatrix}$							
	$\begin{Bmatrix} .5 \\ .5 \\ .4 \\ 0 \end{Bmatrix}$					$\begin{Bmatrix} 214 & 86.3 & 0.23, & 56.2 \\ 214 & 86.3 & 0.23, & 56.2 \\ 215 & 94.1 & 0.21, & 50.1 \\ 150 & 150 & 0.33, & 56.3 \end{Bmatrix}$							
	$\begin{Bmatrix} .5 \\ .5 \\ .5 \\ 0 \end{Bmatrix}$					$\begin{Bmatrix} 214 & 86.3 & 0.23, & 56.2 \\ 214 & 86.3 & 0.23, & 56.2 \\ 214 & 86.3 & 0.23, & 56.1 \\ 150 & 150 & 0.33, & 56.3 \end{Bmatrix}$							

Table 2: Numerical values of the parameters used in the simulations of **Case #1**.

Mechanical parameters							Growth parameters			Numerical parameters			
zones	α	ρ_0	$\frac{\Delta\rho}{\rho_0}$	Y_{iso}	μ_{iso}	$\begin{bmatrix} Y_{x\ eff} & Y_{y\ eff} & \mu_{xy} & G \end{bmatrix}$	γ	ε_{th}	N_g	Solver type	N_{stp}	Δt_{stp}	n_i
$\begin{Bmatrix} Bottom \\ Periphery \\ Initium \\ Central\ Zone \end{Bmatrix}$	$\begin{Bmatrix} .5 \\ .5 \\ 0 \\ 0 \end{Bmatrix}$	1	1	$\begin{Bmatrix} 1 \\ 1 \\ 1 \\ 1 \end{Bmatrix} \cdot 150$	1/3	$\left\{ \begin{bmatrix} 214 & 86.3 & 0.23, & 56.2 \\ 214 & 86.3 & 0.23, & 56.2 \\ 150 & 150 & 0.33, & 56.3 \\ 150 & 150 & 0.33, & 56.3 \end{bmatrix} \right\}$	$\begin{Bmatrix} 1 \\ 1 \\ 1 \\ 2 \end{Bmatrix}$	$4 \cdot 10^{-3}$	10^2	Euler implicit	50	10^{-2}	$3 \cdot 10^2$
				$\begin{Bmatrix} 1 \\ 1 \\ .9 \\ 1 \end{Bmatrix} \cdot 150$		$\left\{ \begin{bmatrix} 214 & 86.3 & 0.23, & 56.2 \\ 214 & 86.3 & 0.23, & 56.2 \\ 135 & 135 & 0.33, & 50.6 \\ 150 & 150 & 0.33, & 56.3 \end{bmatrix} \right\}$						
				$\begin{Bmatrix} 1 \\ 1 \\ .8 \\ 1 \end{Bmatrix} \cdot 150$		$\left\{ \begin{bmatrix} 214 & 86.3 & 0.23, & 56.2 \\ 214 & 86.3 & 0.23, & 56.2 \\ 120 & 120 & 0.33, & 45.0 \\ 150 & 150 & 0.33, & 56.3 \end{bmatrix} \right\}$						
				$\begin{Bmatrix} 1 \\ 1 \\ .7 \\ 1 \end{Bmatrix} \cdot 150$		$\left\{ \begin{bmatrix} 214 & 86.3 & 0.23, & 56.2 \\ 214 & 86.3 & 0.23, & 56.2 \\ 105 & 105 & 0.33, & 39.4 \\ 150 & 150 & 0.33, & 56.3 \end{bmatrix} \right\}$						
				$\begin{Bmatrix} 1 \\ 1 \\ .6 \\ 1 \end{Bmatrix} \cdot 150$		$\left\{ \begin{bmatrix} 214 & 86.3 & 0.23, & 56.2 \\ 214 & 86.3 & 0.23, & 56.2 \\ 90.0 & 90.0 & 0.33, & 33.7 \\ 150 & 150 & 0.33, & 56.3 \end{bmatrix} \right\}$						
				$\begin{Bmatrix} 1 \\ 1 \\ .5 \\ 1 \end{Bmatrix} \cdot 150$		$\left\{ \begin{bmatrix} 214 & 86.3 & 0.23, & 56.2 \\ 214 & 86.3 & 0.23, & 56.2 \\ 75.0 & 75.0 & 0.33, & 28.1 \\ 150 & 150 & 0.33, & 56.3 \end{bmatrix} \right\}$						

Table 3: Numerical values of the parameters used in the simulations of **Case #2**.

Mechanical parameters							Growth parameters			Numerical parameters			
zones	α	ρ_0	$\frac{\Delta\rho}{\rho_0}$	Y_{iso}	μ_{iso}	$\begin{bmatrix} Y_{x\ eff} & Y_{y\ eff} & \mu_{xy} & G \end{bmatrix}$	γ	ε_{th}	N_g	Solver type	N_{stp}	Δt_{stp}	n_i
$\begin{Bmatrix} Bottom \\ Periphery \\ Central\ Zone \end{Bmatrix}$	$\begin{Bmatrix} .5 \\ 0 \\ 0 \end{Bmatrix}$	1	1	150	1/3	$\begin{Bmatrix} 214 & 86.3 & 0.23, & 56.2 \\ 150 & 150 & 0.33, & 56.3 \\ 150 & 150 & 0.33, & 56.3 \end{Bmatrix}$	$\begin{Bmatrix} 1 \\ 1 \\ 2 \end{Bmatrix}$	$4 \cdot 10^{-3}$	10^2	Euler implicit	50	10^{-2}	$3 \cdot 10^2$
	$\begin{Bmatrix} .5 \\ .1 \\ 0 \end{Bmatrix}$					$\begin{Bmatrix} 214 & 86.3 & 0.23, & 56.2 \\ 174 & 135 & 0.26, & 51.0 \\ 150 & 150 & 0.33, & 56.3 \end{Bmatrix}$							
	$\begin{Bmatrix} .5 \\ .2 \\ 0 \end{Bmatrix}$					$\begin{Bmatrix} 214 & 86.3 & 0.23, & 56.2 \\ 195 & 120 & 0.22, & 47.7 \\ 150 & 150 & 0.33, & 56.3 \end{Bmatrix}$							
	$\begin{Bmatrix} .5 \\ .3 \\ 0 \end{Bmatrix}$					$\begin{Bmatrix} 214 & 86.3 & 0.23, & 56.2 \\ 195 & 120 & 0.22, & 47.7 \\ 150 & 150 & 0.33, & 56.3 \end{Bmatrix}$							
	$\begin{Bmatrix} .5 \\ .4 \\ 0 \end{Bmatrix}$					$\begin{Bmatrix} 214 & 86.3 & 0.23, & 56.2 \\ 215 & 94.1 & 0.21, & 50.1 \\ 150 & 150 & 0.33, & 56.3 \end{Bmatrix}$							
	$\begin{Bmatrix} .5 \\ .5 \\ 0 \end{Bmatrix}$					$\begin{Bmatrix} 214 & 86.3 & 0.23, & 56.2 \\ 214 & 86.3 & 0.23, & 56.1 \\ 150 & 150 & 0.33, & 56.3 \end{Bmatrix}$							

Table 4: Numerical values of the parameters used in the simulations of **Case #**3.

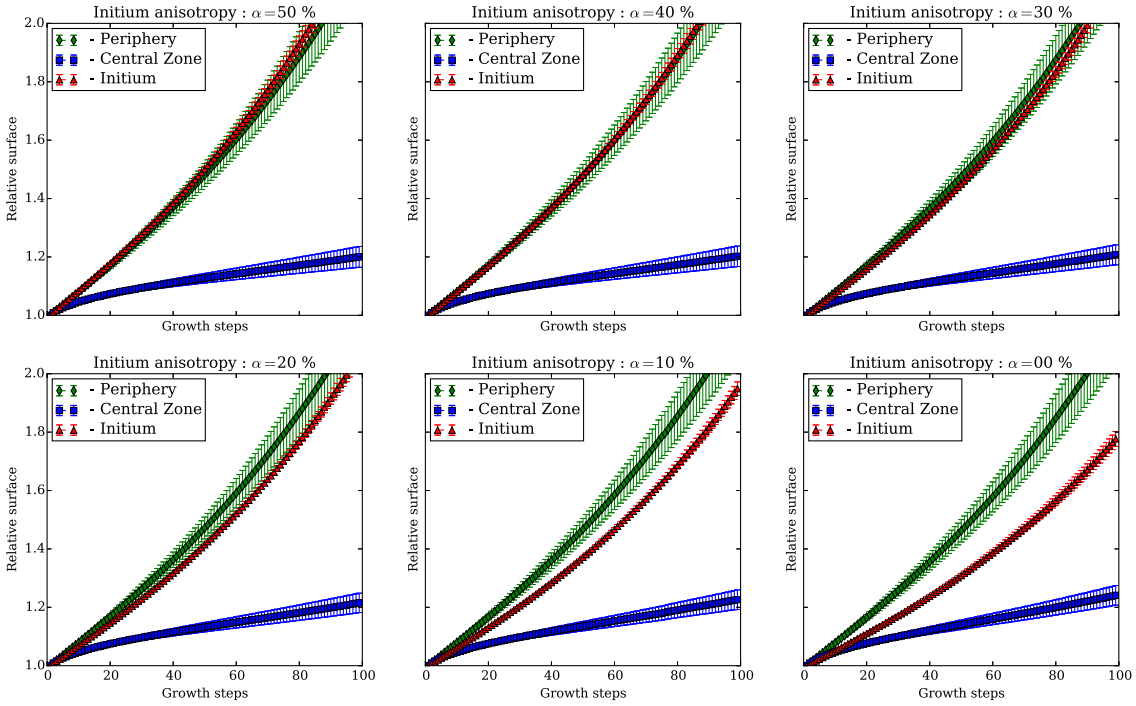

Figure 2: Time evolution of the mean surface area of cells in each zone for different values of the structural anisotropy in the initium. Error bars represent the standard deviation.

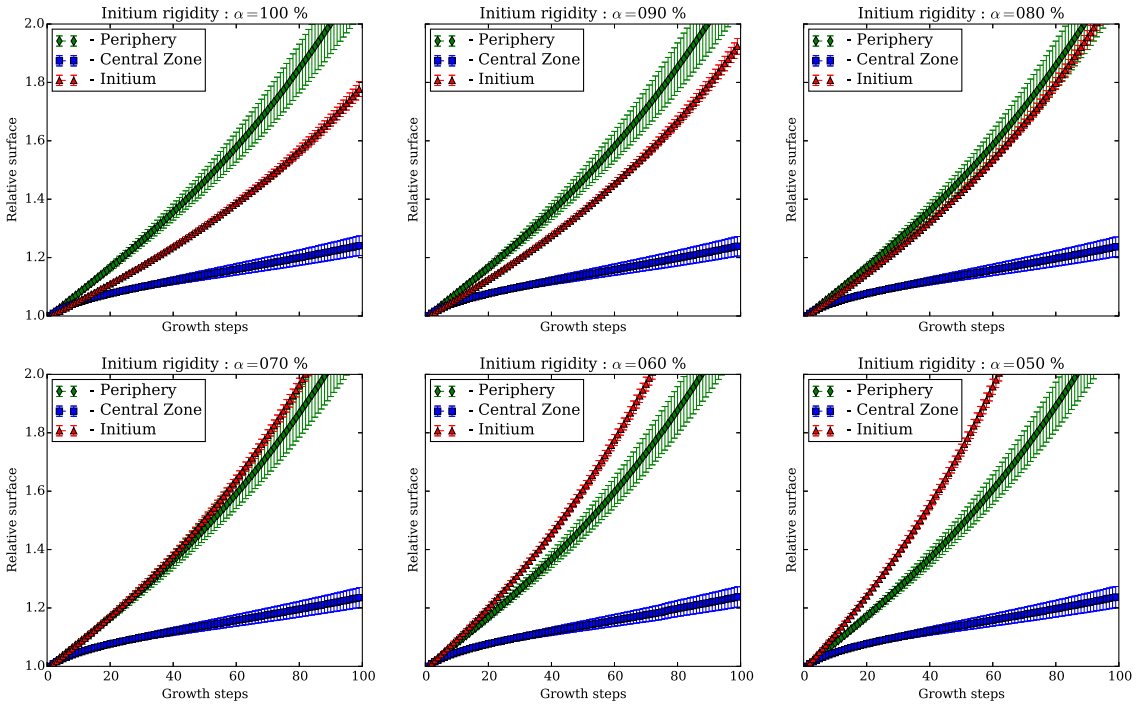

Figure 3: Time evolution of the relative mean surface area of cells in each zone ($\langle r_i(t_n)\rangle_Z$) for different zones when we decrease the rigidity amplitude in the initium, in the fully isotropic case. Error bars represent the standard deviation.

Annex 3

Flower development: from morphodynamics to morphomechanics.
Abad U, Sassi M, Traas J.
Philos Trans R Soc Lond B Biol Sci. 2017 May 19;372(1720). doi: 10.1098/rstb.2015.0545.